USNRDL-TR-67-83
18 July 1967

RADIATION EFFECTS IN THERMOELECTRICS

2. PERMANENT AND QUASI-PERMANENT EFFECTS OF PILE BOMBARDMENT ON SEVERAL COMPOUND SEMICONDUCTORS

by

J. W. Winslow *

U.S. NAVAL RADIOLOGICAL DEFENSE LABORATORY

SAN FRANCISCO · CALIFORNIA · 94135

THERMAL RADIATION BRANCH
R. S. Alger, Head

RADIATION PHYSICS DIVISION
C. S. Cook, Head

ADMINISTRATIVE INFORMATION

This report covers a portion of the work authorized by the Naval Ship Systems Command under Subproject SR007 1101, Task 10254.

*Present address: Northrop Nortronics, 2323 Teller Road, Newbury Park, California 91320.

ACKNOWLEDGMENT

Thanks are due to J. C. Boteler and R. R. Hart for their contributions to development of the test equipment and procedures, to R. L. Rudkin for the thermal diffusivity measurements, and to L. A. Webb for production of all the samples of these generally untractable materials. In addition, thanks are due all four of these gentlemen for their assistance in taking and processing the large amounts of data required for this report.

DDC AVAILABILITY NOTICE

This document has been approved for public release and sale; its distribution is unlimited.

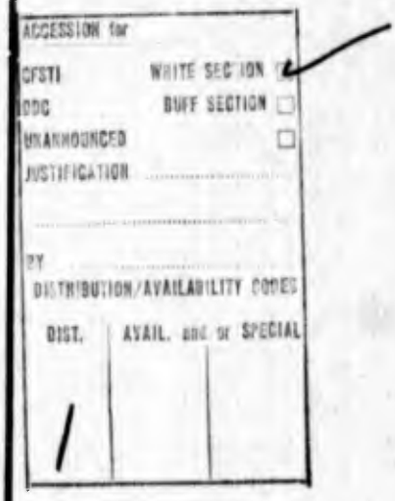

Eugene P. Cooper
Eugene P. Cooper
Technical Director

D. C. Campbell, CAPT USN
Commanding Officer and Director

ABSTRACT

The effects of reactor bombardment on the thermoelectric properties of several compound semiconductors have been observed experimentally for exposure doses up to 2.3×10^{19} fast ($E > 1$ MeV) neutrons/cm^2. Results are reported for the following materials: PbTe; $Ge_{.95}Bi_{.05}Te$; Ag_2Se; n- and p-types of a Ge-Si alloy whose exact composition is classified; $(GeTe)_{90\%}(AgSbTe_2)_{10\%}$; CoSi; n- and p-types of commercial grade Bi_2Te_3; and single-crystal, stoichiometric Bi_2Te_3. Properties measured were Seebeck coefficient (S), electrical resistivity (ρ), and thermal diffusivity (α). The effects observed ranged from an apparently simple case of change in majority charge carrier concentration due to transmutations, to rather complicated cases in which the behavior of the variables was strongly influenced, both for the better and for the worse, by post-irradiation, thermally activated processes, e.g., annealing. In some cases, no effects at all were found.

Post-annealing values of the radiation-induced changes found in the observed variables were used to calculate the corresponding changes to be expected in the thermoelectric figure of merit (z) of each material, using the relationship

$$Z = \frac{S^2}{\rho\alpha\, c_p \delta} ,$$

where c_p is specific heat and δ is density, under the assumption that the product $c_p\,\delta$ remained constant. These changes in z ranged from a decrease of about an order of magnitude, to about a four-fold increase, in the pre-irradiation value of z.

Some indications that substantial improvements in z for the Ge-Si alloys may be possible through appropriate sequences of irradiation and post-irradiation thermal treatment, were seen. A brief review of the field, aimed at providing suitable background for non-specialist readers, and recommendations for future Navy activity in this technological area, are given.

SUMMARY

Problem

The Navy, for obvious reasons, has a continuing interest in the development of new sources of energy, especially in electrical form. Thus, the use of thermoelectric materials to convert heat generated by a nuclear pile directly into electricity, without intervening mechanical equipment, is a matter of some interest. Prior to the work reported here, very little reliable information describing the effects of pile bombardment upon the thermoelectric properties of promising materials, was available. Without such information it was not possible to predict, with reasonable assurance, the performance or lifetime of a thermoelectric generator operating within the biological shield of a pile, and the design of such generators would have to rely upon speculations in this area.

Findings

A number of high-precision determinations of the effects of pile bombardment and subsequent thermal treatments upon the thermoelectric properties of several thermoelectric materials, have been made. These determinations substantiate previous opinions to the effect that such effects can be based upon a wide range of mechanisms, in different materials, and that some materials may be improved by the bombardment, while others are worsened, and still others left essentially unchanged. The principal finding is that promising materials must be examined as individual materials, and not lumped together as a single class, when the effects of irradiation are to be considered. A minor finding indicates that a particular material, an alloy of germanium and silicon, merits further investigation, because of hints that a substantial improvement in thermoelectric properties may be possible.

CONTENTS

FIGURES

INTRODUCTION AND BACKGROUND DISCUSSION

DIRECT CONVERSION

General

The interesting feature of the so-called "direct energy conversion" class of techniques, which includes thermoelectric power generation, is that they generate electricity by processes which avoid intermediate mechanical stages. Consequently, direct energy converters are characterized by a lack of moving parts, and thus comprise a technological area which merits close attention wherever such design goals as long equipment life, unattended operation, infrequent parts replacement, ease of maintenance, increased conversion efficiency, or silent operation are important.

A Specific Case

As a case in point, consider the generation of electrical power from nuclear energy aboard ship. The reactions taking place within a nuclear pile can generate extremely large amounts of energy from almost negligibly small amounts of fuel. It is this property which makes the nuclear pile an attractive power source for mobile units, such as ships. Unfortunately, almost all of the energy released is available only as heat, an energy-form which is of limited utility. For most uses, from operating bilge pumps and driving radar to lighting binacles and propelling ships, it is necessary to convert this thermal energy into a more convenient form.

At present, standard shipboard practice for making this conversion is fairly complicated. First the heat is transported from the pile to a heat exchanger located outside the pile. This is done using a heat transfer fluid of some sort, which is circulated through an intermediate heat exchange loop connected between the pile and the exchanger. The fluid is fairly expensive, and replacement supplies are not readily available in most parts of the world.

The exchanger transfers the heat to water, which becomes steam. The resulting steam is then fed to a conventional steam turbine, which in turn converts the thermal energy into mechanical energy, part of which is used in this form to propel the ship.

Finally, the turbine drives an electric generator, which converts the rest of the mechanical energy into electricity. In this form it can be distributed to distant shipboard points as desired, with relative ease.

A direct conversion system, if one were feasible, would permit a marked simplification of this system. Here, the direct conversion generator would be located contiguous with, or even within, the pile, and would convert the heat into electricity at that point, bypassing the mechanical stage entirely. Such a system would eliminate the intermediate heat exchange loop and its transfer fluid, the heat exchanger, the electrical generator, and the steam turbine, requiring in their stead only a set of electric motors for propelling the ship. The resulting reduction of noise by itself is sufficient to make the prospect of such a system of considerable interest with respect to power generation aboard submarines.

Current Status

1. General

In recent years a number of direct conversion schemes, including thermoelectric power generation, have been given close study. In general, two common findings have emerged: (i) the discovery of certain roadblocks which prevent immediate practical exploitation of the scheme at hand; and (ii) the realization that the underlying theory is only partially developed, usually in such a way as to shed little, if any, theoretical light on the question of practical feasibility of the scheme at hand. In other words, the roadblocks appear to be only technological difficulties, rather than fundamental limitations of the scheme, but no one can either prove or disprove it.

2. A Specific Case: Thermoelectricity

a. Experimental

Thermoelectric power generation is a typical example. In this case the roadblocks all relate to physical properties of the thermoelectric material. For example, conversion efficiencies are marginally low, while specific gravities and costs are rather high. As a result, today's thermoelectric generators are too heavy to be useful in propelling ships, and too costly to compete economically with mechanically generated power on land. One widespread problem has been with mechanical properties, i.e., many thermoelectric materials tend to break or

crumble too easily. Another problem frequently encountered has been difficulty in forming good thermal and electrical contacts with electrodes, and in keeping them from opening up in operation, having once been formed. Typically, these seem all to be merely technological difficulties, with no theoretical basis to suspect them of being insurmountable.

b. Theoretical

With respect to the theoretical situation, the thermoelectric scheme is typical, too. Macroscopic understanding, i.e., the thermodynamics of the situation, is reasonably well advanced, but microscopic understanding, i.e., the development of models for the underlying mechanism(s) is just beginning.

For homogeneous materials, the descriptive phase of macroscopic theory is essentially complete. The principal remaining gap in understanding lies in the more abstruse region of the principles underlying general, non-equilibrium thermodynamics. To be more specific, there is general agreement that the observed macroscopic behavior of these materials can be explained as a special case of a rather general, mathematical model of transport processes, and that the model therefore is an adequate one. Why, and to what extent this general model is valid, however, is not completely understood.

The question of the departures from homogeneous thermoelectric material behavior resulting from material inhomogeneities has been the subject of a moderate amount of attention. It is as yet too early for a consensus of opinion to have been formed. To date, however, none of the findings have indicated any reason to suspect the existence of any fundamental limitations that would make thermoelectric power generation impractical. This, again, is typical.

From the microscopic viewpoint, thermoelectric theory is in a state of flux. Several models, each purporting to describe a portion of the observed behavior, have been suggested, each accompanied by experimental observations tending to support its claim. No claims, however, have been made on behalf of any comprehensive model, and available data, taken all together, do not suggest any simple representation.

Whether this situation requires a new, more complicated model, or perhaps just more careful experimenters, is not clear. In any event, more effort in this area will be required before comprehensive microscopic understanding can be acheived. It is, of course, just this area in which one would expect to find fundamental limitations on material

parameters such as conversion efficiency and mechanical properties, i.e., just those which currently prevent practical exploitation of this scheme.

THERMOELECTRICITY

Definitions

Over 160 years ago, in Prussia, one T. J. Seebeck reported the observation of an electric current in a circuit consisting of merely a simple closed loop, made from two wires of dissimilar materials, providing that the two junctions thus formed were kept at different temperatures. This is the first recorded observation of the THERMOELECTRIC EFFECT, which consequently also is known as the SEEBECK EFFECT. Modern thermoelectric generators are but modifications of Seebeck's simple circuit.

If one of the wires comprising a thermoelectric loop is broken, the current disappears and the broken ends assume different electric potentials. This potential difference is called the THERMOELECTRIC EMF, or SEEBECK VOLTAGE, and in this report will be represented by the symbol V_S. This voltage is a function of the temperature difference between the two dissimilar-metal junctions, and consequently provides a measure of that temperature difference. When used in this fashion the thermoelectric loop is called a THERMOCOUPLE. Figure 1 shows such a configuration.

The slope of the curve giving V_S as a function of the temperature difference, $T_1 - T_2$, where T_1 and T_2 are the temperatures of the hot and cold junctions, respectively, as shown in Fig. 1, is known as the THERMOELECTRIC POWER, or SEEBECK COEFFICIENT, of the couple. At a given temperature the Seebeck coefficient is characteristic of the given pair of materials. Consequently, it is necessary to indicate which pair is meant, when discussing thermoelectric power. In the case illustrated in Fig. 1 we shall speak of the SEEBECK COEFFICIENT (or THERMOELECTRIC POWER) of A with respect to B, and will use the symbol S_{AB} for the same meaning. In cases where the identity of material A is unambiguous, we will speak of the SEEBECK COEFFICIENT with respect to B, and use the symbol $S_{w/r\ B}$. In most cases the Seebeck coefficient changes slowly with temperature, so that for small temperature differences the Seebeck coefficient may be taken as

NRDL-451-67

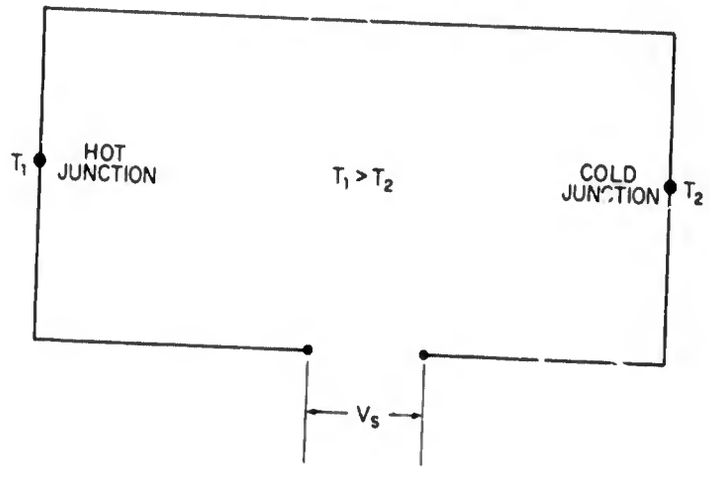

Fig. 1 Seebeck Circuit

$$S_{AB} = V_S/\Delta T , \quad (\Delta T \equiv T_1 - T_2)$$

with only negligible error.

Unfortunately, an ambiguity can be encountered in the discussion of thermoelectric powers. It arises from the fact that it is possible to derive, from thermodynamic considerations, a meaningful and useful quantity known as the ABSOLUTE THERMOELECTRIC POWER, or ABSOLUTE SEEBECK COEFFICIENT. This quantity is a property of the material in question alone, rather than a pair of materials. In referring to the absolute Seebeck coefficient of materials A and B, we shall use the symbols S_A and S_B, respectively. In theoretical discussions we shall represent the absolute Seebeck coefficient by the symbol S, without subscript, since there will be no particularly relevant material in such cases. We will attempt to distinguish clearly between relative and absolute Seebeck coefficients whenever a possibility of ambiguity arises. In general, the term SEEBECK COEFFICIENT will be taken to mean the absolute Seebeck coefficient, unless the context clearly indicates otherwise.

It can be shown that

$$S_{AB} = S_A - S_B ,$$

so that if the absolute Seebeck coefficient of one material is known, experimentation with a thermocouple made from that material and any other will reveal the absolute Seebeck coefficient of that other material. Further, it is rather well established experimentally that the absolute Seebeck coefficient of a superconductor, below its transition temperature, is zero. Thus it has been possible to determine within experimental limits of accuracy, the absolute Seebeck coefficients of many materials. Likewise, it is possible to subject various models to quantitative tests, through experimental verification of their theoretical predictions. From the viewpoint of power generation, the interesting fundamental property of a thermoelectric material is the efficiency, η , with which it converts heat into electricity, i.e., the ratio of electrical energy output to thermal energy input. This CONVERSION EFFICIENCY is critical in that it strongly influences the amount of thermoelectric material required to make a generator which will meet the specifications at hand, and hence is important in determining the cost and weight of the resulting generator.

It can be shown that η increases as the THERMOELECTRIC FIGURE OF MERIT, z, of the material is increased, and that for a homogeneous material z is given by

$$z = S^2/K\rho \quad , \tag{1}$$

where S is the absolute Seebeck coefficient of the material, and K and ρ are its thermal conductivity and electrical resistivity, respectively. Materials developed in recent years display figures of merit on the order of 10^{-3} per degree Celsius, leading to conversion efficiencies on the order of a few percent. These efficiencies are within an order of magnitude of being competitive economically with modern mechanical generators, which accounts for the current widespread interest in thermoelectric materials development.

Fundamental Assumption

Having suggested a potential use for thermoelectric materials which would subject them to intense fluxes of nuclear radiation, namely for direct conversion within or immediately adjacent to a nuclear pile, and having indicated the importance of the thermoelectric figure of merit, z, we next will consider the question of what effects the former may have upon the latter. In doing so we will assume that equation (1) holds throughout, i.e., that we may determine the response of z to irradiation by observing separately the individual responses of S, K, and ρ, and then combining them by means of this equation.

That this assumption is valid is by no means obvious. Indeed, there is theoretical reason to question its validity on the ground that most materials to be examined are not homogeneous in S, while the quantity S is defined (and measurable) only for materials which are homogeneous. Further, certain experimental evidence[1] suggests that, at least in cases where the temperature gradient varies substantially throughout the material, this assumption may be grossly in error.

It generally is assumed, however, that an inhomogeneous material in which the variations of S from point to point are not too large, may be assigned an average value for S, and that the relations developed for homogeneous materials hold, at least approximately, when this average value is used. Intuitively this argument is quite attractive, and seems reasonable, providing that the temperature gradient is reasonably constant throughout the material. That such an approximation is valid, however, has not been shown as yet, either by theoretical

analysis or by experiment.

It would be possible to check the error introduced by this assumption, in any given case, by measuring directly the conversion efficiency of the specific device, and comparing this to the value predicted via equation (1). This would be a fairly difficult experiment to perform, however, since it would involve accurate measurement of heat input and heat output, and strict control of heat losses to the environment along the device. At the present stage of development, i.e., where general trends and qualitative descriptions of behavior are sought, such an extra effort does not seem justified, and reliance upon our fundamental assumption is permissible. When quantitative evaluation becomes important, however, e.g., should a material of competitively high z be found, it would seem highly desirable that this question be given close examination.

PILE BOMBARDMENT EFFECTS

Current Status of Research

1. Theory

The question of the effects of nuclear pile radiation upon thermoelectric properties has received little attention. On the theoretical side, a number of generalized, "hand-waving" type arguments have been advanced to suggest that such effects should be relatively small, should require quite large exposures before becoming noticeable, and "probably" ought to anneal to insignificant levels at normal operating temperatures. In view of the incomplete state of thermoelectric theory, however, these conclusions are more nearly pious hopes than reliable predictions.

2. Experimental

a. General Status

On the experimental side, only a handful of studies have examined the effects of pile irradiation on thermoelectric properties, most of them involving only commercially available thermocouple wires. These materials are metallic in nature and have low values of z, and consequently are of little interest from the viewpoint of power generation.

Two teams of investigators,[3,4], however, working independently and at different laboratories, have reported observations of pile bombardment effects in some nine different, high-z materials. In general, observations were made on only a few samples of any given material (usually only one or two), and little attention was paid to thermal conductivity, the chief effort being directed instead toward observing the Seebeck coefficient and electrical resistivity. Consequently, these studies and their conclusions must be considered as only preliminary in nature, subject to revision as further information becomes available.

b. First Study

The first team conducted a fairly detailed, careful study of three materials. Their data show quite clearly that for two of these materials, PbTe and Bi_2Te_3, (i) pile bombardment tends to increase S and ρ, and to decrease κ; (ii) these effects are caused by high-energy neutrons rather than thermal neutrons; (iii) post-irradiation heating to temperatures in the range 350 to 500°C permits both S and ρ to recover almost completely to their pre-irradiation levels; and (iv) for ρ the recovery is a single-temperature process, taking place at about 150°C in PbTe, and about 200°C in Bi_2Te_3.

Data taken in-piles for all three materials (the two tellurides plus ZnSb), operating at average temperatures of about 150°C, show that (i) large, sharply discontinuous increases in ρ can occur when large thermal shocks are administered by reactor scrams; (ii) aside from these discontinuous changes, both S and ρ tend to increase slightly as total exposure accumulates; and (iii) these smaller effects appear to saturate, reaching constant values by the time the total fast ($E > 1$ MeV) neutron exposure reaches the order of 4×10^{19} n/cm^2.

c. Second Study

The second team subjected some nine materials to a less painstaking study, which partially overlapped the first study. This second study was characterized by inconsistencies, both qualitative and quantitative, and both internal and external. Where the two studies overlap, their results disagree in most respects . Where the second team has observed two samples of the same material, the results are more often in opposition to each other than in harmony. Even where this team has measured the same sample from time to time, large and discontinuous differences have been noted.

Such gross inconsistency is typical of situations where the measurement technique has left an influential variable uncontrolled.

consequently, it seems only prudent to look for possible flaws in the measurement technique involved, and to interpret the results of this second study with considerable caution.

The second team concluded that, for "typical" thermoelectric materials: (i) pile bombardment tends to raise both S and ρ, while depressing the ratio S^2/ρ; (ii) radiation damage anneals out at "relatively low" temperatures; and (iii) for each material there appears to be some temperature above which pile bombardment would effect no net change in z. A close examination of the data reported, however, suggests that this team either had other data available as bases for these conclusions, or else indulged in a considerable amount of wishful thinking and/or clairvoyance.

For example, no obserbations of the behavior of thermal conductivity, K, are reported. Thus, any conclusions expressed about the behavior of z must assume a given behavior for K, and hence can only be speculative. Further, the reported data for S is rather evenly split, pile bombardment apparently causing this variable to increase in eight cases, and to decrease in six cases. In some cases the so-called "annealing" not only removed the change allegedly induced in the variable in question by pile bombardment, it further "removed" an additional fraction of its pre-irradiation value. In other cases, the observed "annealing" acted to increase the alleged radiation-induced change, i.e., "reverse" annealing occurred. And finally, in some cases the changes observed between the end of one post-irradiation measurement run and the beginning of the next, were comparable to those found between the pre- and post-irradiation runs.

In view of these discrepancies, it is difficult to avoid suspecting the second team of reaching its conclusions while unduly influenced by external factors, such as the results reported by the first team. A more rigorous appraisal of the second team's reported data suggests that only the following, more limited set of generalizations is experimentally justified: (i) quantitative conclusions cannot be drawn, probably because of a defect in the measurement technique which leaves an unknown influential variable not completely controlled; (ii) qualitatively speaking, in the materials studied, ρ showed a general tendency to increase as a result of pile bombardment, while no such general trend was displayed by S; and (iii) in some of the materials the observed changes in both S and ρ were at least partially removed during post-irradiation heating.

We note that these more limited conclusions do not preclude the possibility that the second team's speculations may be found to provide an accurate description of the general behavior of thermoelectric materials, by future studies. Indeed, in the absence of

information to the contrary, the results reported by the first team tilt the probabilities slightly in favor of such an eventual verification. We must recognize, however, that the amount of reliable information presently available is extremely small, and that consequently the amount of such tilting is also very small. The immediate need in this technological area is for a larger supply of solid information.

Simple Solid State Model

1. Particles

In the modern view, any solid material consists of a very large number of very small particles. For our purposes we may consider the particles comprising a thermoelectric material as divisible into two loosely defined classes: ELECTRONS; and NUCLEI.

2. General Array of Nuclei

The nuclei are comparatively massive particles which are rather firmly bound in positions which are fixed with respect to each other. Thus, they form a fairly rigid array, which largely determines the material's mechanical properties. Alteration of this array, e.g., removing a nucleus from its site and transporting it to some other location, requires a comparatively large expenditure of energy. It is characteristic of the array that removal of a single nucleus causes significant readjustments in position by only those nuclei in the immediate vicinity of the removed nucleus' sites, and that even these readjustments are minor. The chief effect is the creation of a VACANCY, i.e., an empty site.

At any given temperature, a given solid body contains a certain amount of heat, i.e., thermal energy. According to kinetic theory the particles comprising the body share this thermal energy, but in a statistical fashion, rather than in strict equality. Thus it is possible for a given nucleus to acquire enough kinetic energy to escape from its site and move to another location. The fact that the body is a solid, however, implies that such displacements are relatively rare events.

Displaced nuclei are eligible to share still further in the body's thermal energy, and thus may be bumped about from place to place within the volume bounded by the array. One would not expect this process to continue indefinitely, however, as the displaced nucleus eventually will encounter a site from which another nucleus has been displaced. In this event, the wandering nucleus will occupy the empty site, giving up its energy of displacement in the process.

It frequently is convenient to represent this situation in terms of a ficticious spatial array of mathematical points, called the LATTICE*. For the most part, each lattice point has a nucleus associated with it, each nucleus being constrained to remain within a short distance of its lattice site. A few of the lattice sites are empty, however, the associated nuclei having been removed to other locations by virtue of the statistical fluctuations of the lattice thermal energy.

3. General Array of Electrons

The electrons, on the other hand, are relatively light particles, being several orders of magnitude less massive than the nuclei. Like the nuclei, they also form a spatial array, but this array is determined largely by that of the nuclei, the electrons tending to form a cloud-like structure surrounding each nucleus. It is the details of this array that determine the electrical properties of the material.

Most of the electrons making up the cloud surrounding a given nucleus are rather tightly bound to that nucleus, and would require substantial amounts of thermal energy in order to be freed from it. These electrons may be thought of as occupying the inner portions of the cloud, closest to the nucleus, and as being more or less permanently associated with it†.

The remaining electrons, which may be thought of as occupying the outer portions of the cloud, may be rather weakly bound to the nucleus and hence easily detached from it by thermal energies. In some cases the attraction of the nucleus for the outermost electron may be completely overcome by the forces exerted by the rest of the body's particles. Thus, some electrons may be free to move about throughout the body even without the assistance of thermal energy. These electrons may be considered as associated with the entire body, rather than with any particular nucleus.

---

* We note that this definition of lattice is much looser than that usually used by crystallographers and workers in the solid state field in general, the latter implying some sort of geometric regularity in the location of the lattice sites. We do not wish to limit this discussion to regular crystals, but want to include non-crystalline solids, as well. Hence, the broader definition.

† We ignore here the "exchange" processes on the grounds that these depend upon the essential indistinguishability of electrons, and for our purposes, one bound electron is as good as another. Hence, these processes are irrelevant to our discussion.

4. Electronic Energy Level Structure

It frequently is convenient to represent this situation in terms of a ficticious spatial structure which plays much the same role for the electrons as does the lattice for the nuclei. In the electronic case, however, the basic element of the structure is not a point, but rather is a continuous set of points called a STATE. Each state is characterized by the energy which an electron must have in order to occupy that state. Hence, these states also are known as ENERGY LEVELS.

The energy level structure of a solid may be thought of as consisting of four types of states: (i) BOUND states, which have the lowest characteristic energies and are very limited in spatial extent; (ii) VALENCE states, which have the next highest range of characteristic energies and have considerable spatial extent; (iii) TRAPPING states, which are next highest in characteristic energies, but are very limited in spatial extent; and (iv) CONDUCTION states, which are the highest in characteristic energies, and have considerable spatial extent.

The states occupied by the inner, tightly bound electrons are typical bound states. They can be visualized, crudely, as a set of concentric shells, not necessarily regular in shape, surrounding the nucleus. As one goes outward from the nucleus, the characteristic electronic energy associated with the shell increases in discontinuous jumps, from shell to shell.

Valence states are occupied by electrons which are shared among adjacent nuclei. They form what are known as covalent bonds between adjoining nuclei. These bonds can contribute significantly, and in some cases, predominantly, to the forces which maintain the lattice structure. Valence states can be visualized, again crudely, as a connected set of sticks or bridges connecting adjoining nuclei.

Trapping states generally are associated with irregularities in the lattice structure, e.g., impurity nuclei. They occupy regions in the inter-nuclear space not already enclosed by the bound states or the valence states. There is no particularly appropriate visualization for these states.

The states occupied by free electrons are typical conduction states. They may be visualized, very roughly, as highly warped planes or networks extending through large regions of the inter-nuclear space not already enclosed by the other states. Conduction states are characterized by the fact that motion of the conduction electrons can be observed externally, as electric current.

5. Model Complications

a. Vacancies and Foreign Atoms

Up to this point, our model of the solid state has been quite simple, consisting of arrays of two types of particles, electrons and nuclei, which can be discussed in terms of two ficticious structures, the lattice, and the electronic energy levels. Now we must introduce complicating factors. We will treat the nuclei first, as this case is the simpler, and can be of some use in discussing the electronic picture.

It was pointed out earlier that if a nucleus were removed from its lattice point, a vacancy would be introduced into the array. The ways in which that vacancy might be filled, however, were not discussed, beyond pointing out that a nucleus displaced from some other lattice point might happen by and fall into it, much as the stereotyped drunken sailor might fall into an open manhole.

Another possibility would be for a nucleus occupying a lattice point immediately adjacent to the vacancy to move over to the empty site. There are two possible mechanisms for such a happening: (i) the nucleus could acquire enough energy to become a displaced nucleus and then proceed to fall into the vacancy, a process somewhat akin to jumping out of one manhole, running down the street, and jumping into the next one; and (ii) the nucleus could "tunnel" through the force barrier separating the two sites, which would be something like crawling through the underground pipe connecting the two manholes. In either case, the final result would be that the nucleus and the vacancy had exchanged places.

If several such vacancy, nearest-neighbor exchanges were to take place in sequence, the corresponding events could be described in terms of a chain of nuclei playing follow the leader. A somewhat simpler view, however, would be to treat the vacancy as though it were a different kind of nucleus (a sort of non-nucleus-where-a-nucleus-ought-to-be), moving through the lattice. From this viewpoint, a lattice consists of two kinds of particles, nuclei and vacancies, each having its own set of properties, and each able to move through the lattice according to its own set of rules.

Now the previous discussion stated that each lattice point was either occupied by a nucleus, or else corresponded to a displaced nucleus which was wandering about the lattice at the moment. That is, the number of nuclei was exactly matched by the number of lattice points. This is true only in the ideal case. In practice, the number of lattice points will be somewhat greater than the number of nuclei, i.e., the vacancies will outnumber the displaced nuclei.

The excess vacancies may have been introduced through a number of sources. For example, when the material froze, the solidification process may have failed to fill some of the lattice sites. This can happen for any of a number of reasons. Even had the original solid been perfect, it is surrounded by empty space which, from our new viewpoint, is nothing but a "perfect lattice" of vacancies. In time, one would expect a number of vacancies to diffuse into the solid, utilizing their ability to move through the lattice as described above.

In addition, a number of foreign nuclei generally will be present, introduced either accidentally, as contaminants, or deliberately, in order to influence the electronic energy level structure. The array of nuclei can still be considered in terms of the lattice, but the treatment has been made more complicated by the necessity of allowing for several types of nuclei, including the vacancies, each able to move about through the lattice under its own set of rules.

b. Holes

The previous discussion of electronic states ignored the question of requirements for occupancy of a given state, except to observe that the energy of the tenant electron must equal that associated with the state. Two additional requirements now will be discussed.

First, every electron must occupy some state, but multiple occupancy is banned. Thus, only two conditions are possible for any given state: it is occupied by a single electron of the proper energy; or it is empty. Second, the filling of empty states is a statistical process, which occurs preferentially according to energy, those of lowest energy being filled first. That is, if a state is empty, while other nearby states of higher energy are filled, an electron occupying one of the higher states eventually will transfer residence to the lower state. The liklihood of this transition occurring usually increases as the difference between the two states' energies increases, as the distance between the two states decreases, and as time increases.

One of the several interesting consequences of these restrictions is a strong tendency toward complete filling of the bound and valence states. The same mechanisms which displace nuclei from their lattice sites, of course, also can deliver excess energy to the tenant of one of these electronic states, thereby raising it to a higher state and leaving behind an empty state.

Because of the strong filling tendency, the bound and valence states surrounding the empty state (both those associated with its own nucleus and those associated with adjoining nuclei) are filled. The

resemblance of such an empty state amongst a sea of filled states, to an empty lattice site surrounded by its sea of occupied lattice points, seems obvious. This condition of emptiness is very much like a vacancy, and can be treated as a new kind of charged particle, called a HOLE.

During the time before it is refilled, a hole acts like a positively charged particle having a mass on the same order as the electron, and able to move from nucleus to adjoining nucleus in much the same manner as a vacancy can move from lattice site to adjoining lattice site. This motion is equivalent to a follow the leader type of motion by a chain of bound and/or valence electrons, and can be observed externally as an electric current, since it constitutes a displacement of charge within the solid.

c. Ideal Materials

We consider now a hypothetical material which contains no trapping states, and which has a number of electrons exactly equal to the sum of the number of bound states plus the number of valence states. If disturbing influences such as thermal energy were excluded, the material would adopt a configuration in which all the bound and valence states were filled, and all the conduction states were empty. In this configuration no net charge transport could take place in the material, and it would not be an electrical conductor.

If we now were to add an appreciable number of electrons to our material (and to maintain charge neutrality, an equal number of protons) in such a way as to leave the energy level structure unchanged, they would have to occupy conduction states, since all the non-conduction states would already be filled. These conduction electrons could carry an externally observable electric current, and the material would be an electronic, or n-type, conductor.

If, instead of adding electrons, a few were taken away (along with an equal number of protons, of course), again in such a way as to leave the electronic energy level structure unchanged, the uppermost valence states would be only partially filled. The resulting holes could move about, to the extent of the valence states, and the material again could conduct. This time, however, the charge carriers would be holes, rather than electrons, and the material would be a hole, or p-type, conductor.

d. Real Materials

If, instead of changing the number of electrons, we were to admit momentarily the influence of disturbing forces such as thermal

energy, a number of electrons would be transferred from the lower states into the conduction states, leaving empty states behind. In due time, of course, these conduction electrons would pass close enough to the recently emptied states to recombine with them, and the original, non-conducting situation would be restored. During the intervening time, however, both the conduction electrons and the holes they left behind them would carry current. If the disturbing element were maintained at a constant level, rather than promptly removed, a dynamic balance eventually would be established between the activating and recombining processes, and steady state concentrations of conducting electrons and holes would result.

In either case, the effect of the disturbing element would be to create charge carriers of both types. Assuming that the two types of charge carrier encountered about the same resistance to motion through the lattice, both types would carry significant amounts of current, and the material would be an AMBIPOLAR conductor.

If, to our ambipolar conductor, we now were to add a large number of trapping states, many conduction electrons would fall into them, instead of recombining with holes. Once in a trap, an electron could have a rather lengthy visit, for it would remain there until it were reexcited into a conduction state, or until a hole came close enough to the trap site that the electron could make the trap-to-hole transition. Thus the effect of adding traps is to decrease the ratio of conduction electrons to holes. Since the trapped electrons cannot carry current, the introduction of enough trapping states would leave only holes to carry current, and our material would again have become a p-type conductor.

It was noted previously that the energy level structure can be influenced by the presence of impurity atoms, which are called DOPANTS. Dopants are available in two main types. The ACCEPTORS are those whose net effect, when used in place of a relatively small fraction of the original atoms, is to add trapping states to the material's energy level structure. The results of this dopant are described immediately above.

The other type of dopant is the DONOR, whose net effect is to add electrons to the material. If enough nuclei were replaced by donors, the supply of electrons would exceed the number of non-conducting states, and the conduction electron concentration would be increased. This would drive the hole concentration down somewhat, and if enough donors were added, the conductive electrons would dominate the externally observable current. In this case, the material would again have become an n-type conductor.

e. Thermoelectric Materials

This discussion has treated the electronic energy level structure from the viewpoing of the electron. It seems obvious, however, that the resulting system has a certain amount of symmetry with respect to charge carrier sign. The bound and valence states, for example, play the same role for holes that the conduction states play for electrons. Similarly, electron acceptors can be thought of as hole donors, and vice versa. Consequently, in many cases it is possible to describe the behavior of both p-type and n-type conductors simultaneously, by describing charge carriers in terms of their functional roles, i.e., MAJORITY CARRIERS, or MINORITY CARRIERS, rather than the associated electrical charge sign.

Thermoelectric materials, for example, may be either p-type or n-type materials. For some purposes, however, it is less important to know the type of material at hand than it is to know the concentration of the majority carrier. It so happens that for both types, the highest values of z, as deduced from equation (1), correspond to majority carrier concentrations on the order of 10^{19} carriers/cm^3. Typical semiconductors, on the other hand, are characterized by majority carrier concentrations on the order of 10^{16} carriers/cm^3. Consequently, from the viewpoint of typical semiconductors, thermoelectric materials of high z are quite heavily doped.

In most cases the base material for a thermoelectric is a compound, rather than a single element, so that the addition of impurity atoms may not be necessary, the required doping being provided through control of the relative concentrations of the base constituents. In other cases, however, foreign atoms must be added in order to attain the desired level for the majority charge carrier concentration.

6. Important Features

Despite the complications introduced in the preceeding discussions, the basic structure of the simple model still applies. Whatever illumination is to be derived from the discussions to follow will be based upon that simple basic structure.

For our purposes, it is important to note that the nuclei comprise a dynamic system, with all its members in motion. The bound nuclei execute oscillatory motions about their respective lattice points, while the displaced nuclei migrate through the lattice. In addition, a continuing exchange between bound and displaced nuclei takes place, with some of the bound nuclei acquiring enough thermal energy to escape from their lattice sites, while some of the previously displaced nuclei attach themselves to empty lattice

sites, thus becoming bound nuclei. Thus, the equilibrium number of lattice sites depends upon a dynamic balance between the displacement, or activating process, and the deactivating, or rebinding process.

It is especially important to note that when a material is in thermal equilibrium with its surroundings at a temperature T, a unit volume of the material will contain a given number of vacancies. Further, this equilibrium concentration of vacancies is a function of T, increasing as T becomes larger. If T became large enough, the number of vacancies would become so large that the material could no longer maintain the lattice structure, and the material would melt. We shall concern ourselves here, however, with vacancy concentrations that will remain orders of magnitude less than those corresponding to the melting process.

The electronic array also is a dynamic system. The bound electrons may be thought of as executing oscillatory motions around their respective nuclei, the valence electrons as crossing back and forth between pairs of nuclei, the trapped electrons as vibrating about their traps, and the conduction electrons as migrating through the solid. Further, the continuing exchange between bound and displaced nuclei is paralleled by similar exchanges between the various types of electrons. Thus, the two arrays have much in common.

The two arrays also display a number of differences. For our purposes the significant differences are three in number; (i) the energy required to activate a nucleus is much greater than that required to activate a majority charge carrier; (ii) the resistance to migration through the lattice is much greater for a displaced nucleus than it is for an activated majority charge carrier; and (iii) the number of nuclei in a thermoelectric material is significantly less than the number of lattice sites, while the number of majority charge carriers is significantly more than the number of non-conducting states for that carrier.

Observable Parameters

1. Macroscopic-Microscopic Linkage

In theory, the observable properties of a solid are deduced from knowledge of its microscopic structure. In fact, however, details of microscopic structure cannot be measured directly. Consequently, the process is reversed, with microscopic structure being induced from observation of the ways in which macroscopic variables behave.

As a result, the amount of information about microscopic structure which is available for predicting the effects of radiation on a given observable parameter varies considerably from a parameter to parameter, depending upon the efforts previously devoted to establishing the corresponding microscopic details and their linkage to the observable macroscopic parameter.

To date, a great deal of attention has been devoted to electrical resistivity, ρ, consequently a widely accepted, fairly complete microscopic model, a simplified version of which is discussed above, has been developed. Thus, there is one parameter for which the macroscopic-microscopic relationship, while not yet entirely complete, is sufficiently well-developed that it should be quite useful in predicting radiation effects.

The behavior of thermal conductivity, κ, also has been subjected to considerable examination in detail, and a partially complete microscopic model has been constructed. The linkage between microscopic structure and macroscopic behavior, while not so well-developed as in the case of ρ, still is sufficiently advanced that some reasonably reliable, conditional predictions of the effects of radiation on κ should be possible.

And finally, the attention devoted to the study of the Seebeck coefficient, S, has been rather small, in comparison to that spent on ρ and κ. Consequently, the macroscopic-microscopic relationship here is considerably less well-developed than that for κ. Certain tentative, qualified predictions can be advanced, however. Consequently, we shall now proceed to outline the three linkages, as a basis for discussing what radiation effects might be anticipated.

2. Electrical Resistivity

The microscopic model developed to account for observed electric charge transport properties assumed the existence of a number of particles, called charge carriers, each having associated with it a certain amount of electric charge. Each particle is viewed as drifting through the solid in response to externally applied, electromagnetic forces and internally supplied, dissipative forces, the latter arising out of the particle's motion. The observed charge transport then is taken to be the sum over all charge carriers of the charge transport contributed by a single carrier.

In mathematical terms, a group of n identical carriers, each carrying charge e, will produce a total conductivity*, σ, given by

$$\sigma \equiv ne\mu \quad , \tag{2}$$

where μ is the mobility of the charge carrier, a measure of the dissipative forces developed per unit of applied electric field. Thus, there are three potential routes by which irradiation could lead to changes in σ : by changing the number of charge carriers; by changing the amount of charge carried by each carrier; and by changing the mobility.

We dismiss the second of these routes from further consideration on two counts: (i) the only such changes permitted by fundamental particle theory are those which involve integral multiples of e, and thus, are equivalent to and indistinguishable from changes in n; and (ii) experiment unanimously supports theory on this point. Thus, we are left with two routes: changing n; and changing μ. The background for a discussion of the first of these routes has been provided in our previous discussion. Mobility, however, has not been discussed in any detail. Thus, we now proceed to such considerations.

An electron in a conduction state may be visualized as following a more or less random path, much like a die being rattled about in a throwing cup. Collisions with other particles in the body will be frequent, owing to the relatively high speeds (on the order of 10^5 or 10^6 cm/sec) engendered by the electron's thermal energy. Application of an external electric field will superimpose upon this motion a slow (on the order of 10^{-3} to 1 cm/sec) drift of the carrier along the field's gradient. It is with this drift, and the opposition it encounters, that we are concerned here.

It is convenient to think of the electron as drifting along in the direction dictated by the externally applied field until it encounters an obstacle of some kind. The electron is thought of as suffering some sort of collision with the obstacle, and as being diverted from the field-dictated course, i.e., SCATTERED, as a result of that collision. The mobility, of course, will decrease as the amount of scattering increases.

---

*For some purposes the electrical resistivity is an awkward quantity to manipulate. In these cases it is frequently much more convenient to think in terms of the inverse quantity the conductivity, σ , and then put the results in terms of ρ via the defining relationship $\rho \equiv 1/\sigma$. Here is one such case.

The amount of scattering suffered by the typical electron will be a product of the frequency of scattering collisions and the amount of scattering experienced at the typical collision. The frequency will depend upon scatterer concentration and the thermal (rather than the drift) speed of the electron. Because thermal speeds are rather high, the frequency also can be rather high.

The amount of scattering introduced by the typical scattering collision will depend primarily upon the characteristics of the scatterer. In the event these are sensitive to direction, it may be necessary to take into account the distribution of pre-collision velocities of the electrons, the lattice orientation of the bombarded material, the direction of the externally applied electric field, and perhaps even the net direction of the radiation field. In the first approximation, fortunately, it often is adequate to assume the scattering characteristics of the scatterer to be insensitive to direction, and it is possible to express them as a scalar quantity.

The microscopic picture related to mobility, then, comprises in large part a compilation of various sorts of scattering obstacles and processes. To date, a number of scatterers have been identified, including vacancies, foreign atoms, several types of defects in regular crystal lattices, phonons*, and even other electrons. There is no assurance that the present list is complete, so current research in this area includes a continuing search for new scatterers and scattering mechanisms.

The above discussion of mobility has been based upon the properties and activities of electrons. We assert without further discussion that holes behave in a similar fashion, and that by referring to charge carriers in place of electrons, our picture of scattering and mobility provides an adequate representation of the situation obtaining in both p-type and n-type conductors.

3. Thermal Conductivity

By definition, thermal conductivity is the rate at which heat, i.e., kinetic energy, is transported through a body, under the driving force supplied by a temperature gradient imposed across that body.

---

*Phonon: a ficticious particle associated with certain heat transport processes. See next section for further definition.

Clearly, if a charge carrier is excited to a conduction state at the hot side of the body and drifts over to the cold side, it carries with it its activation energy, in kinetic form. If it then gives up some of that kinetic energy, e.g., by falling into a trapping state, it will have contributed to the total thermal conductivity according to the amount of kinetic energy it released. This constituent of the total thermal conductivity, K , is called the electronic thermal conductivity, and will be represented here by the symbol K_e .

The second means of transporting kinetic energy through a body involves a transmission of the energy along the lattice. This may be thought of roughly as comparable to the transmission of motion along an elastic string of widely separated beads, the transmission being facilitated if the beads are of equal masses and spaced evenly along the string. Uneven spacing and irregularities in the bead masses hamper the transmission. This process is called the lattice thermal conductivity, and will be represented here by the symbol K_L .

An alternative view is to consider lattice conduction as the transport of packets of kinetic energy by ficticious particles called PHONONS. The phonons are thought of as traveling through the solid in much the same manner as do electrons, and being scattered in similar fashion by lattice irregularities, charge carriers, and even other phonons.

Whichever view is taken, the total thermal conductivity is given by the relation

$$K = K_L + K_e \quad .$$

If $K_e >> K_L$, the heat is carried primarily by charge carriers, and one would expect to find the ratio K/σ constant. In the case of metals, which are characterized by very large concentrations of majority charge carriers, such indeed is the case (Wiedemann-Franz Law). Since freezing this ratio would reduce the number of independently adjustable parameters in equation (1), such a material would not seem very promising as a high-z thermoelectric. Consequently, thermoelectric materials are designed so that $K_L >> K_e$.

4. Seebeck Coefficient

If one assumes the electric charge associated with a single charge carrier to be the same for all carriers, then the existence of a Seebeck voltage in a given body shows beyond all reasonable doubt that the local concentration of conduction-state charge carriers differs between the body's hot and cold regions. Since this is a non-equilibrium situation, it follows that the applied temperature gradient has induced driving forces which have established the concentration gradients. The steady state condition clearly represents a dynamic balance between these driving forces and those counterforces, e.g., electrical repulsion between like charges, which tend to reduce these concentration gradients.

Unfortunately the details of this dynamic balance are only partially understood. Further, those which are understood require for their description models which are beyond our simplified discussion.† Hence we must assert without support of analogy certain relationships which are generally accepted as valid for commercial thermoelectric materials. For a more complete discussion of these models the reader is referred to reference (2).

The most successful theory to date‡ suggests that S is determined by three fundamental material parameters: charge carrier effective mass, m^*; charge carrier concentration, n; and charge carrier scattering. The mathematical relationship developed from this theory takes the form:

$$S = A \left\{ B + \ln C \frac{(m^* T)^{3/2}}{n} \right\} , \qquad (3)$$

where A and C are combinations of fundamental physical constants, T is absolute temperature, and B is a measure of charge carrier scattering.

In particular, B is determined by the form of the relationship between kinetic energy and mean free path length for charge carriers. Since this form in turn depends principally upon the body's lattice structural characteristics, any significant change in B corresponds to a major change in the body's structure. Thus, any process or treatment which influenced S significantly through B necessarily would convert a substantial portion of the base material into a different form.

---

† For a more complete discussion of these models the reader is referred to Reference 2.

‡ See Reference 2, pp 28 ff.

Similarly, m^* is primarily a function of the material's electronic energy level structure, which in turn also depends mostly upon lattice structure. Thus, changes of B and m^* are expected to contribute only small changes in S, providing that the basic structure of the material in question is not substantially altered.

The remaining material parameter n, however, depends strongly upon the concentration of defects in the lattice structure, particularly upon the concentration of trapping states. In commercial thermoelectrics the latter may be present in concentrations on the order of hundredths of a percent of the number of lattice sites, so substantial variations are possible while the material's lattice structure remains substantially unchanged.

In a number of cases† S has been found experimentally to vary proportionally with the logarithm of the inverse of n, thus verifying this aspect of equation (3). It is generally agreed that this expression describes the dependence of S on n adequately for thermoelectrics, and that variation of n is the major cause of variations in S.

Simple Radiation Effects Model

1. Field-Target Interaction

a. In General

A radiation field can be considered as a collection of energetic particles, each traveling along its own, more or less straight-line path. Correspondingly, the interaction between the field and an exposed material can be thought of in terms of collisions between the field particles and the particles making up the target material, the chief characteristics of a collision being the transfer of energy from field to target particle. The ensuing behavior of the target particles depends upon both collision type(s) and constraints imposed by the target material itself. The effects of irradiation upon a given observable parameter of the target material then are explicable in terms of this target particle behavior.

---

†See Reference 2, pp 31 ff, for example.

b. Reactor Fields

The radiation field produced by a nuclear reactor consists primarily of two particle types: photons; and neutrons. The photon is a quantum of electromagnetic energy having energy proportional to its frequency, and which can be treated as a particle having zero rest mass and zero electric charge. The neutron also has no electric charge, but has a rest mass roughly 1800 times that of an electron. The entire energy of a photon is available for transfer to the target particle during any collision. For the neutron, on the other hand, with few exceptions only the kinetic energy is available for transfer, as long as this kinetic energy is large. When this energy becomes low, however, its rest mass also may become available for transfer.

2. Transient Mechanisms

a. Imposition of the Field

The amount of energy transferred in a primary collision usually is much larger than the thermal energy available to the target particle. Thus, one effect of irradiation is to increase the rates at which disarrangements are introduced into the nuclear and electronic arrays, beyond those already established thermally.

One might expect the deactivation rates for activated particles also to be affected directly by irradiation, through collisions between field and activated target particles. The number of activated particles at any instant, however, usually is very small compared to the number of deactivated particles, for any given type. Thus, the direct effect of irradiation upon deactivation rates usually is negligible.

With the activation rate for any given type of particle increased much more than the corresponding deactivation rate, it follows that the instantaneous concentration, c, of activated particles of that type, must increase. Since the deactivation rate generally is proportional to c, however, the process eventually will reach a steady state at a new, larger value of c, provided that the intensity of irradiation is held constant. Thus, a second effect of irradiation is to raise the instantaneous concentration of activated particles, for all particle types.

A substantial part of the energy transferred from field to target contributes, via one route or another, to increased mechanical motion by the non-activated target particles. Thus, a third effect of irradiation is to raise the target's temperature above that already established by normal heat transfer mechanisms.

b. Removal of Field

When the radiation field is removed, the heating processes induced by the irradiation will stop and the target will cool, more or less gradually, until its pre-irradiation temperature distribution is regained. Simultaneously, each activation rate will undergo a two-step fall toward its pre-irradiation value: the first at a rate corresponding to that at which the field is removed; and the second corresponding to the target's cooling rate. In addition, it follows that for each particle type the previously defined, instantaneous concentration, c, must also fall towards its pre-irradiation value.

The rate, $\dot{c}$, at which c decreases may follow first the rate of removal of the radiation field, and then the cooling rate. On the other hand, e.g., if complicated trapping processes are involved, c may be substantially slower than this in its return toward its pre-irradiation value. In either case, this transition stage is an unstable situation, which eventually will terminate. From a practical point of view, however, the rate may be so slow that the unstable transition state appears unchanging. In the case of displaced nuclei, for example, return to the pre-irradiation state may require years, or centuries, if temperatures are low.

3. Irreversible Mechanisms

a. Chemical Effects

In some materials, it is possible for an unoccupied valence state to change its location. Thus, a state which connects two nuclei when occupied, may disconnect itself from one of them when its electron is activated, and connect its loose end to a different neighboring nucleus when it is refilled. Such a CHEMICAL CHANGE will not reverse itself when the radiation field is removed, but will remain in effect until the new valence state is emptied. In effect, one chemical bond has been destroyed, and a new one has been established.

In a more complicated kind of chemical change, the primary collision can completely detach a nucleus from its neighbors and move it out of their influence. In this case, the neighbors are obliged to make other arrangements for their valence electrons. If the displaced nucleus does not return, e.g., it may undergo a chemical combination with another displaced nucleus, the rebounding arrangement taken on by

the remaining neighbors assumes a more permanent existence.† One result of such chemical change might be to alter the scattering mechanisms, thus influencing both μ and B, of equations (2) and (3), respectively. Another might be to alter the electronic energy level structure, thus influencing both n and m^*. Since such changes would be more or less permanent, they are known as PERMANENT EFFECTS.

Fortunately, chemical effects generally are not very common in thermoelectric materials. When exposed to reactor radiation, however, another type of permanent change known as TRANSMUTATION, can be encountered in sufficient strength to cause concern. We now direct our attention to this matter.

b. Transmutation

Photons interact primarily with the target material's electrons, in the general manner described in the preceding paragraphs, and with the same general results. Neutrons, on the other hand, interact primarily with the target materials' nuclei, and in two rather different ways.

The first type of interaction occurs when the incident neutron's kinetic energy is large, and produces about the same kind of effects as described in the preceding paragraphs. Here the primary collision is much like that between billiard balls of unequal masses. The incident neutron imparts some of its energy to the struck nucleus, rebounds to strike another nucleus where the process is repeated, and so on, until the incident neutron's kinetic energy is reduced to thermal levels. The struck nucleus is displaced from its original site, usually as a charged particle, since it seldom can take all its electrons with it. Being a charged particle, the struck nucleus interacts with the electrons of other nuclei, as though it were an incident charged particle.

The second type of interaction usually occurs when the incident neutron's kinetic energy is in the thermal range, i.e., in the neighborhood of 0.025 electron volts. Here the incident neutron is completely absorbed by the struck nucleus. In general, such a NUCLEAR REACTION produces a COMPOUND NUCLEUS which eventually decays into a stable state, emitting a number of energetic particles in the process.

† If the rebonding arrangement constitutes a state of lower energy than the original situation, it of course is not necessary that the displaced nucleus be prevented from returning to its original site, for the new arrangement to be permanent.

These secondary particles may be photons, charged particles, or even neutrons, all of which can interact with other target particles just as though they were incident field particles.

In general the daughter nucleus differs from the original both in atomic weight and in atomic number. Thus the nuclear reaction transmutes the target nucleus into a different element, and the process is called TRANSMUTATION.

Transmutation affects both the scattering mechanisms and the electronic energy level structure, and thus can introduce permanent changes in all the significant parameters: μ, B, n, and m^*.

4. Combined Effects

Both temporary and permanent effects occur simultaneously. Thus the value of a given observable variable at any instant differs from its pre-irradiation value not only by the amount due to instantaneous changes resulting from transient effects, but also by an additional amount due to the permanent changes accrued since the pre-irradiation value was determined.

General Predictions for Thermoelectrics

1. Ionization Effects

When a material is exposed to a reactor's field, its array of electrons suffers disarrangements as a result of primary collisions with incident photons, as described previously, and as a result of collisions with the energetic, charged, secondary particles generated by both types of primary collision, i.e., those involving either incident photons or incident neutrons. Those disarrangements which constitute excitation of an electron into a higher level bound or valence state of its parent nucleus generally have only trivial effects, so much so that workers in the field of radiation effects have not developed any generally accepted class name for them. Those which constitute excitation to a conduction state, however, frequently are of great importance. Since these disarrangements constitute ionization of the parent nucleus, their results are called IONIZATION EFFECTS.

The importance of ionization effects results primarily from the corresponding changes in the instantaneous concentrations of majority and minority charge carriers. Since thermoelectrics are characterized by majority carrier concentrations on the order of 10^{19} carriers/cm^3, an incident radiation field would have to produce a change on the order of 10^{17} carriers /cm^3 to be noticeable. Assuming a lifetime on the order of a microsecond for an activated carrier, an activation rate on the order of 10^{33} carriers/cm^3/sec would be required to effect the 1% change.

The radiation field required to produce so large an activation rate would be several orders of magnitude greater than those found in modern nuclear piles. Further, the rate at which such a field would deposit thermal energy in the target would be far greater than thermoelectric materials, which are characterized by low thermal conductivities, could dissipate without melting. Hence, one would not expect ionization effects to be noticeable in thermoelectrics located inside nuclear piles. Further, one would not expect ionization effects to become noticeable until the incident field became intense enough to melt the material. Both of these expectations have been given experimental verification in specific cases[1][3][4].

2. Displacement Effects

a. Definition

When a material is exposed to a reactor's field, its array of nuclei suffers disarrangements as a result of primary collisions with incident neutrons. The principal result is the removal of the nucleus from its site in the lattice to some other location, usually not a lattice site. The results of such nuclear displacements are called DISPLACEMENT EFFECTS.

b. Temperature Dependence

As was pointed out previously, both the displacement process for nuclei and the ionization process for electrons are dynamic in nature, and thus have much in common. In each case the history of a single particle can be considered as a combination of six general steps: the original activation; motion through the lattice while activated; partial deactivation (e.g., falling into trap); reactivation; motion while reactivated; and final deactivation, (i.e., return to a site at the original energy level). The trapping-untrapping pair can, of course, be repeated several times before the final deactivation takes place,

or may be skipped entirely.

In both cases the energy required to accomplish the original activation is supplied by the incident field particle, or by a secondary charged particle. In both cases the activated particle is subjected to strong electrical interaction forces by unactivated target material electrons. In both cases energy is transferred to the unactivated electrons, and at least partial deactivation takes place. At this point, however, significant differences develop between the two particle histories.

Since a rather large number of electrons occupied conduction states even prior to irradiation, it follows that most of the electron traps, and particularly most of the deeper ones, already were filled. Thus the only trapping states that were available in any significant concentrations for our activated electron to fall into were those which had recently been emptied by thermal energy, i.e., those located close to the conduction level. Hence, our trapped electron soon is reactivated by thermal energy, too, and it can move about through the lattice relatively easily, until it encounters an empty bound or valence state, and undergoes final deactivation.

In this case the only step exhibiting anything other than a weak dependence upon temperature is the reactivation. So long as this step does not become the slowest, and therefore the rate-determiner, the entire process will be relatively independent of temperature changes. Thus, as long as cryogenic temperatures are avoided, we should expect to find the ionization process exhibiting a fast, temperature independent response to changes in radiation field intensity.

In the case of the displaced nuclei, on the other hand, relatively few trapping states were occupied prior to irradiation. Further, activated nuclei are so massive that frequently they force their new neighbors to adjust to their presence somewhat. As a result of both factors, our trapped nucleus requires considerably more energy for reactivation than would a trapped electron. Thus, if the temperature is low enough, the reactivation step becomes the dominant step in the process. Consequently, if the target is maintained at sufficiently low temperatures, we should expect to find the displacement process exhibiting a slow, temperature-dependent response to changes in radiation field intensity.

If the temperature is maintained low enough, it seems clear that the displacement process can be very much one-sided, i.e., all displacement and no return. In such a case, the last three steps of the

process are "frozen out", and after the irradiation has been completed, the target will be in a non-equilibrium state, so far as the nuclei are concerned. If the sample is examined at this temperature, the effects resulting from the displaced nuclei will appear to be permanent in nature. If the temperature is raised, however, the system will return to its equilibrium state, and the quasi-permanent nature of the effects will be revealed.

It also seems clear that if several kinds of trapping states are involved, the temperature chosen for irradiation may permit some of them to empty rapidly, during irradiation or after, while others will be frozen in. Thus, the behavior of the target after irradiation may depend not only quantitatively, but qualitatively as well, upon the temperature chosen. And finally, it also seems clear that if the irradiation temperature is chosen low enough, post-irradiation annealing studies should provide considerable insight into the nature of the traps.

c. Effects

Given that the irradiation temperature has been set low enough to freeze in a significant number of the displaced nuclei, the next item of consideration is the effects these nuclei might be expected to produce.

The first of these effects would occur if the displaced nuclei introduced significant changes in the concentration of trapping states for the majority charge carriers, thus changing the value of n. The sense of this change would depend upon whether the displacement increased or decreased the number of traps. In either case, however, this effect should not become noticeable until displacement concentrations on the order of $10^{17}/cm^3$ were achieved, since the charge carrier concentration in thermoelectrics characteristically is on the order of $10^{19}/cm^3$.

A second effect should be to increase the scattering suffered by charge carriers and by phonons. This should produce an increase in B, and decreases in μ, K_e , and K_l . As noted before, scattering is determined largely by the lattice, which has scattering center concentrations on the order of $10^{23}/cm^3$. Thus, displacement induced scattering should not become appreciable until enough nuclei have been displaced to constitute a substantial change in the base material, i.e., until displacement concentrations become on the order of $10^{21}/cm^3$ or so.

In the immediate vicinity of a displaced nucleus one might expect to find the effective mass of a charge carrier somewhat different than elsewhere in the material. This again is a local effect, somewhat akin to scattering, and most likely also will not be noticeable until

displacement concentrations become so high that a substantial change in the base material has been achieved.

3. Transmutation Effects

As discussed previously, transmutation converts target nuclei into the nuclei of new elements. Since for all practical purposes the probability of the reverse of a transmutation occuring is negligibly small, transmutation effects are true permanent effects, and hence are accumulative. Thus, the concentration of transmuted nuclei, along with the size of the corresponding change in observable variables, will continue to grow with increasing time of exposure, regardless of the temperature at which the exposure takes place.

The probability of a transmutation occuring depend strongly upon on which target elements are present. For many elements this probability is quite small, hence in many cases transmutation effects are negligible.

In cases where the probability is not negligibly small, the types of secondary particles generated by the nuclear reaction, and the resulting effects, depend strongly upon which element the original nucleus was. In the most common case, the only secondary charged particle is an electron. Here, the effect is to increase the number of electrons. If the material is n-type, this will increase the concentration, n, of the majority charge carriers. If it is p-type, n will be reduced.

In a significant number of other cases, however, the charged secondary particles are positively charged. This has the effect of reducing n for n-type materials, and increasing n for p-type materials. Thus, it is necessary to make specific predictions for each thermoelectric material, based upon the type of nuclear reaction known to occur in its nuclei.

In either type of case, one would not expect such effects to become noticeable, in view of the original charge carrier concentration level in thermoelectrics, until the concentration of transmuted nuclei approached the order of $10^{17}/cm^3$.

As in the case of a displaced nucleus, a transmuted nucleus constitutes a new irregularity in the lattice. Consequently, it also should increase the scattering suffered by both charge carriers and phonons, thereby increasing B and decreasing μ, K_e , and K_L . The size of such effects, however, should be rather small when compared to the effects on n, for the same reasons as were discussed previously in the section treating displacement effects. Consequently, transmutation induced scattering should not become appreciable until enough nuclei have been

transmuted to constitute a substantial change in the base material, i.e., until transmutation concentrations become on the order of $10^{21}/cm^3$ or so.

Also as in the case of a displaced nucleus, a transmuted nucleus might be expected to have some local effect upon m^*. Again, however, the observable effect should be negligible until transmutation concentrations became so high that a substantial change in the base material were achieved.

It should be noted that, while the mechanisms by which transmutations and displacements affect the fundamental parameters may have many similarities, they differ with respect to temperature dependence, and that this difference can be important. Specifically, it is possible that the upper limit for concentration of displacements can be determined by the temperature of irradiation, rather than the accumulated dose. Such is not possible for transmutations. Thus, if the irradiation temperature is properly chosen, the effects of displacements upon observable parameters can saturate, i.e., become constant, as the exposure progresses. Further, the value at which saturation takes place should be a function of temperature. Observable effects which are caused by transmutations, however, should increase more or less continuously with continued exposure, and no such temperature-dependent saturation should be seen.

4. Thermal Effects

As remarked previously, most of the energy deposited in a target by high-energy radiation eventually appears as heat. Since thermoelectric materials are characterized by low thermal conductivities, this deposited heat can pose serious problems.

If the designer has not made adequate provision for removing this heat, the temperature can rise to values substantially above those to be expected in the absence of the radiation field, especially at interior points. Since thermoelectric properties generally vary with temperature, and the designer presumably has designed his generator for optimum performance, the net effect of these unexpectedly high temperatures should be sub-optimal performance of the device, while in the presence of the radiation field.

In especially severe cases, the interior temperatures may rise above the melting point. In this event, the mechanical forces generated within the target can be very large indeed, and permanent deformation of the device, e.g., bulging of the walls, cracking, or electrode separation, can result.

A second type of thermal effect arises with many thermoelectric materials because they are not spatially homogeneous in S, i.e., the value of the absolute Seebeck coefficient varies from point to point. In this event, the Seebeck voltage measured in a circuit such as that shown in Fig. 1 is not merely a function of the junction temperatures, but rather is a function of temperature distribution throughout the entire region of inhomogeniety.†

While there is a certain amount of professional controversy in this area, it seems highly likely that if a generator made of materials which are inhomogeneous in S is exposed to a reactor field, the non-uniform temperature gradient resulting from the radiation-deposited heat will lead to a reduction of the device's conversion efficiency below that to be expected from equation (1), even when allowance has been made for the temperature variation of the thermoelectric parameters.

5. Predicted Behavior of Observables

a. Electrical Resistivity, ρ

When a thermoelectric material first is exposed to a reactor's radiation field, the immediate response is readjustment in the generation rate of both the minority and majority charge carriers. The direction of the net effect upon ρ will depend upon a number of factors. These are only of academic interest, however, since the amount of change to be expected from this source is negligible, owing to the relatively large excess of majority charge carriers characterizing unirradiated thermoelectric materials.

The second response is a slower, but still fairly prompt, change in the material's internal temperature distribution. This will drive ρ along the ρ -T curve in the higher temperature direction. Whether this results in an increase or decrease in ρ, and the size of the change resulting, depend upon the details of this curve and the size of the temperature increase involved. Given the physical details of the sample, mounting arrangement, etc., and the pre-determined details of the ρ -T curve, however, this change should be predictable for given cases.

---

† This problem is discussed briefly in the earlier section treating the Fundamental Assumption, and is discussed at some length elsewhere[1][5].

Both of these effects are of the transient variety, and should disappear fairly quickly upon removal of the radiation field, i.e., by the time the material cools to its pre-irradiation temperature distribution.

After the exposure has continued for some time, at temperatures low enough to permit their accumulation, the accumulative, permanent effects should start to appear. The first of these should be those involving changes in concentration of the majority charge carrier, n. They should be identifiable by means of combined resistivity and Hall coefficient measurement determination of n, and may be either displacement effects or transmutation effects, or both.

Those which are transmutation effects should be identifiable as such by the absence of thermal annealing and by chemical analysis. They may tend to either increase or decrease ρ according to the particular nuclear reaction involved. Both direction and amount of these changes should be predictable for specific cases.

Most, but not necessarily all, displacement effects should display thermal annealing, and thus should be identifiable as such by thermal analysis. These effects may tend either to increase or decrease ρ, according to the type of trapping level produced. In cases where the trap production process is known, prediction of both direction and size of the effect on ρ should be possible. In most cases, however, these details are not known, and hence prediction usually is not possible.

Finally, after further exposure, the effects involving change of charge carrier mobility should appear. These should appear only after very large radiation doses have been administered, i.e., only after the base material has been changed quite substantially. Combined resistivity and Hall coefficient measurement determination of μ should identify these effects, which might result from any combination of chemical, displacement, and transmutation effects.

In general, the relatively large concentration of majority charge carriers in thermoelectric materials suggests rather strongly that the electronic population of the material is fairly active, i.e., that activations and deactivations are fairly frequent. This in turn suggests that the material has a high probability of already being in the lowest possible energy configuration, and that consequently chemical changes after the onset of irradiation are unlikely, since any such changes possible should already have taken place prior to irradiation.

Consequently, the only types of effect involving change of μ are likely to occur as a result of the exposure are, as in the case of those affecting n, transmutation effects and displacement effects. If we assume such to be the case, we can identify those belonging to each class by the methods described previously, i.e., for the case of those effects involving change of n.

For the case of those effects involving change of μ, the direction of the effect on ρ is to increase it, at all times. Prediction of the size of such a change, however, is quite difficult, and will not be attempted here.

To summarize with respect to ρ, then, we see that the overall response of ρ to reactor bombardment is, in general, a sum of various types of response, some of which can be predicted and some of which cannot. In some of the simpler cases, reliable, detailed prediction of both direction and magnitude of change may be possible. In others, however, a considerable amount of knowledge concerning the trapping structure introduced by reactor bombardment will be required, before reliable predictions can be made. At the present state of the art, the quickest procedure is direct experimentation. If done properly, this approach not only will answer direct questions concerning the response of particular materials, but also can shed light on the microscopic processes involved.

b. Thermal Conductivity

As in the case of ρ, the first prompt adjustment of the generation rates for charge carriers should have some effect upon the electronic component of κ, i.e., κ_e, since the instantaneous value of n is changed. Since this change is expected to be negligible, however, the effect upon κ_e, and hence upon κ, should also be negligible, since $\kappa \gg \kappa_e$, prior to irradiation.

The second prompt response, the change of temperature, should drive κ along its temperature curve, in the direction of higher temperature. Since κ usually is a rather weak function of T, however, this change also should be negligible.

Even if either of these effects were perceptible, they both would disappear when the reactor field was removed, and so would be noticed only when in-pile instrumentation was available.

Those permanent effects depending upon change of n can involve only κ_e, and not κ_l. Since $\kappa \gg \kappa_e$, it follows that in order for one of these effects to produce a noticeable change in κ, the corresponding change in n should be much larger, say by an order of magnitude

at least. Hence the changes in κ resulting from this type of event should require concentrations of displacements and/or transmutations on the order of $10^{20}/cm^3$ or larger. Thus κ should be much less sensitive to effects of this type than is ρ, with the onset of perceptible change in κ corresponding to doses some two or three orders of magnitude larger than that required for ρ.

Effects corresponding to change of n should be identifiable as such by the technique mentioned previously, and the magnitude of the change in n should be measurable. Given this information and the original values of κ and κ_e, the effect on κ should be predictable, at least in the first approximation. In cases where the increase in n can be predicted without the post-irradiation measurements, reasonably complete prediction should be possible.

Effects involving change of μ can influence both κ_e and κ_l. As in the case with ρ, these would not be expected to appear until very large doses were administered. Because of the uncertainty as to the strength of the inequality $\kappa \gg \kappa_e$, however, it is not clear in general whether these effects should appear before, with, or after the appearance of those depending upon changes in n. In cases where κ/κ_e were less than 10, prior to irradiation, one would expect the latter to appear first. For all other cases, however, the situation is not so clear.

In any case it should be possible to separate those effects involving change of n from those involving change of μ by combined conductivity and Hall coefficient measurement. As is the case with ρ, however, calculation of the scattering processes is quite difficult, and impossible where the details of the scattering centers expected to result from the exposure are unknown. Thus prediction of the amount of change to be expected from the latter usually is not possible, and we can only expect that in all cases, they will lead to a decrease in κ, since scattering will be increased.

To summarize with respect to κ, then, we see that the overall response of κ, like that of ρ, is a sum of various types of response, some of which can be predicted in detail, but most of which cannot. With regard to sensitivity, κ should be no more susceptible to irradiation than is ρ, and in some cases should be considerably more resistant. Unlike ρ, however, κ should respond to irradiation in only one direction, toward smaller values. At the present state of the art, the quickest route to reliable knowledge of a particular material's behavior is direct experimentation.

c. Seeback Coefficient, S

As is the case with ρ and κ, the first prompt adjustment of the generation rates for charge carriers should have some effect upon S, but this effect should be negligible, and for the same reason.

The second prompt response, the temperature change, can affect S through two routes. The first of these is similar to those described for ρ and κ, namely a translation of S along the S-T curve toward higher temperatures. This curve usually is a much stronger function of T than is the case for ρ and κ, so that in this case the effect can be substantial. As a rule, the effect is to decrease S, but in some cases a noticeable increase may result. Since the S-T curve can be determined prior to irradiation, this effect is predictable.

The second route depends upon the target material being inhomogeneous in S. This effect, which has been described previously in this report* and elsewhere†, can be very large, and in either direction, depending upon the details of the ways in which S and T are distributed in the given case. These seldom are known, so prediction of this effect usually is not possible.

Both of these responses are transient effects, which disappear upon removal of the radiation field. Consequently, they will be detected only by in-pile instrumentation, and will not be seen in pre- and post-irradiation type studies.

According to equation (3), S should vary according to the logarithm of the inverse of n. Thus the first perceptible response of S to prolonged reactor irradiation should appear at a substantially higher total exposure than does the corresponding response of ρ, but at a lower exposure than that required to produce a similar response in κ. Further, the sensitivity to irradiation, i.e., the additional response per unit exposure, for S should lie between those for ρ and κ.

Since n may be either increased or decreased by displacement and transmutation effects, S may be changed in either direction by those effects which involve change of n. Because of the inverse relationship, however, S should change in the direction opposite to that of

---

* See pp ff.

† See reference 1.

n, and consequently σ , and in the same direction as does ρ . Since the change in n resulting from transmutation effects can be predicted, the amount of the change in S to be expected from such effects also should be predictable for specific cases. As is the case with ρ , however, prediction generally is not possible for displacement effects.

After very large exposures, effects on S which depend upon changing the scattering properties of the material should appear. Since details of the scattering centers expected to be introduced by irradiation are not known, detailed prediction of these effects usually is not possible. Referring to equation (3), one would expect an increase in the scattering center concentration to increase m^*, and thus S, provided that the scattering centers introduced by the irradiation were of the same type as dominated the pre-irradiation material, thus leaving B unchanged. If this latter condition is not maintained, however, the change of B could be dominant, in which case the direction taken by the change in S would depend upon which type of center were being introduced.

To summarize with respect to S, then, S is unlike ρ and κ in that large transient effects may arise, through radiation-induced changes in the material's temperature distribution. This is particularly true in the case where the unirradiated material is inhomogeneous in S.

With respect to permanent effects, S is rather like ρ and κ , in that the total response is a sum of various types of response, a few of which are predictable in detail, but most of which are not. Where effects dependent upon changes in n dominate, S should be less sensitive to radiation than is ρ, but more so than is κ . Where effects dependent upon changes in scattering center concentration dominate, S should be roughly equal in sensitivity to ρ and κ.

Unlike κ , S may be changed in either direction, i.e., toward larger or toward smaller values, by irradiation. In cases in which effects dependent upon changes in n are dominant, S should change in the same direction as does ρ. In cases where effects dependent upon changes in μ dominate, however, ρ can only increase, and κ can only decrease, while the possibility of change in either direction exists for S.

As is the case with the other two observable variables, the present state of the art with respect to S is such that the quickest route to reliable information concerning a particular material's behavior under irradiation is direct experimentation.

d. Thermoelectric Figure of Merit, z

It should be clear by this time that detailed prediction of the effects of reactor bombardment upon z is a fairly complicated matter. In special cases, specific predictions may be possible. In most cases, however, such will not be possible until much more is known about the trapping levels and the scattering processes introduced by the displacements and transmutations resulting from the bombardment.

Referring to equation (1), we see that the influence of changes in κ, which can only decrease as a result of the bombardment, can only be to increase z. It also is apparent, however, that this effect can be outweighed by either a corresponding increase in ρ or a corresponding decrease in S, both of which are expected to be at least as sensitive to the bombardment as is κ. Further, S enters into equation (1) as a squared factor. When we note also that under certain circumstances both S and ρ can change in either direction as a result of the bombardment, the true complexity of the situation begins to make itself felt.

Under these circumstances it would not be surprising to find different thermoelectric materials behaving differently from one another, and the existence of three sub-classes, namely those in which reactor bombardment increased z, those in which it lowered z, and those in which it left z essentially unchanged, would seem quite reasonable. Clearly the information presently available is not sufficient to justify treatment of all thermoelectric materials as a single class.

EXPERIMENTAL PROCEDURE

GENERAL

The experimental effort reported here was an exploratory study, aimed at mapping out roughly the range of variation of the thermoelectric figure of merit, z, to be expected in commercial grade thermoelectric materials, as a result of prolonged exposure to the radiation field of a nuclear reactor. The general procedure was as outlined below.

For the purposes of this study, z was assumed to be related to the observable variables through equation (1). These variables were measured as functions of temperature for samples of a number of commercial grade thermoelectric materials. These samples then were exposed to reactor bombardment. The post-irradiation values of the observable variables then were measured as functions of temperature, and the results were compared to the pre-irradiation behavior via simple computer techniques. The more prominent details of these procedures now are presented.

OBSERVABLE PARAMETERS & THEIR MEASUREMENT

Seebeck Coefficient and Electrical Resistivity

The Seebeck Coefficient, S, and the electrical resistivity, ρ, of each of several samples of each material studied were determined simultaneously as functions of the sample's "average" temperature. The essentials of the system used for these measurements are shown in Figure 2.

Referring to this figure, if the cross-sectional dimensions of the sample, the separation of the two thermocouples, and the resistance R_s, of the standard resistor are known, measurement of V_+ , V_- , and V_R , with the polarity reversing switch first in one position and then in the other, and of the thermocouple outputs, provides ample data to permit the application of a simple algebraic treatment which provides virtually simultaneous values of S and ρ , with enough redundancy to provide at least one internal check on the measurement technique. Details of this technique and treatment are given in a previous report.(6)

The equipment used for these measurements was a high-precision apparatus which was designed, and to a large extent fabricated, at this laboratory*. The precision of this apparatus depends to some extent upon the material being examined. For the present it will suffice to note that for the materials covered in this report, measurements made on successive remountings of at least one unirradiated sample of each material, reproduced each other within variations ranging from

---

* This apparatus also is described at length in Reference 6.

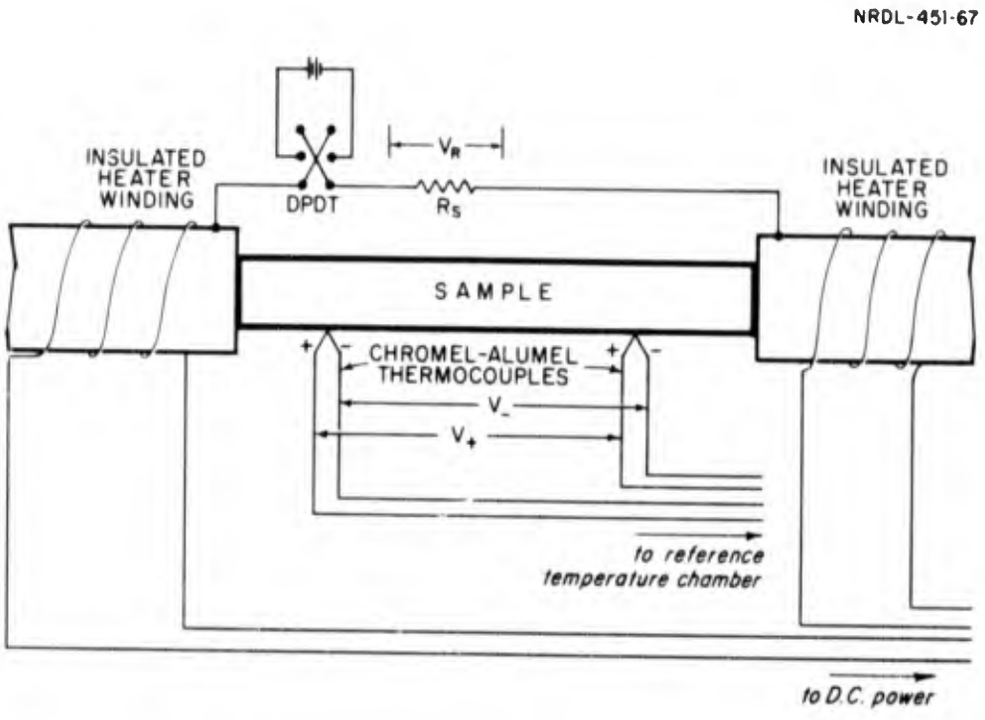

Fig. 2 Concurrent Measurement Equipment

± 1% to ± 8%, depending upon the material.

Measurement runs began at room temperature and usually proceeded through rising temperatures, with measurements being taken as the temperature rose, until a peak temperature in the neighborhood of 450°C was reached. Generally speaking, this phase of the run took about 90 minutes. The temperature then was reduced at a faster pace, reaching room temperature in about 30 minutes, with the rate of change being slowed sharply, at intervals, to permit taking of data*.

In one case the material under test was found to soften at about 125°C. For the rest of the samples of this material a peak temperature of about 120°C was used.

In some cases a preliminary examination of annealing processes was made, the first phase of the run involving lowering the temperature to the liquid nitrogen region. It then was raised to the peak value, reduced to the liquid nitrogen region again, and finally raised to room temperature. In these cases the rate of change throughout approximated the slower of those mentioned above, i.e., about 5°C/min.

Thermal Conductivity and Diffusivity

Thermal conductivity was not measured directly. Instead, thermal diffusivity, α, was observed, using a flash technique developed at this laboratory and described in detail in a previous report.(7)

The essential arrangement of this technique is shown in Fig. 3. The thermocouple output is observed as a function of time. After the lamp is flashed, the energy absorbed by the black coating on the sample's exposed face will heat the sample, diffusing through to the shielded back surface according to the properties of the material. As the energy arrives at the shielded face, the thermocouple output will rise to a peak, and then decay, as the back surface cools.

If the sample dimensions are chosen so that cooling losses are not too severe, α can be determined from the time required for the thermocouple output to rise to a given fraction of its maximum value. If calibration of the flash lamp can be achieved, the material's specific

---

* This technique requires that the signals observed remain substantially unchanged during the 15 seconds or so required to record the data for a single point.

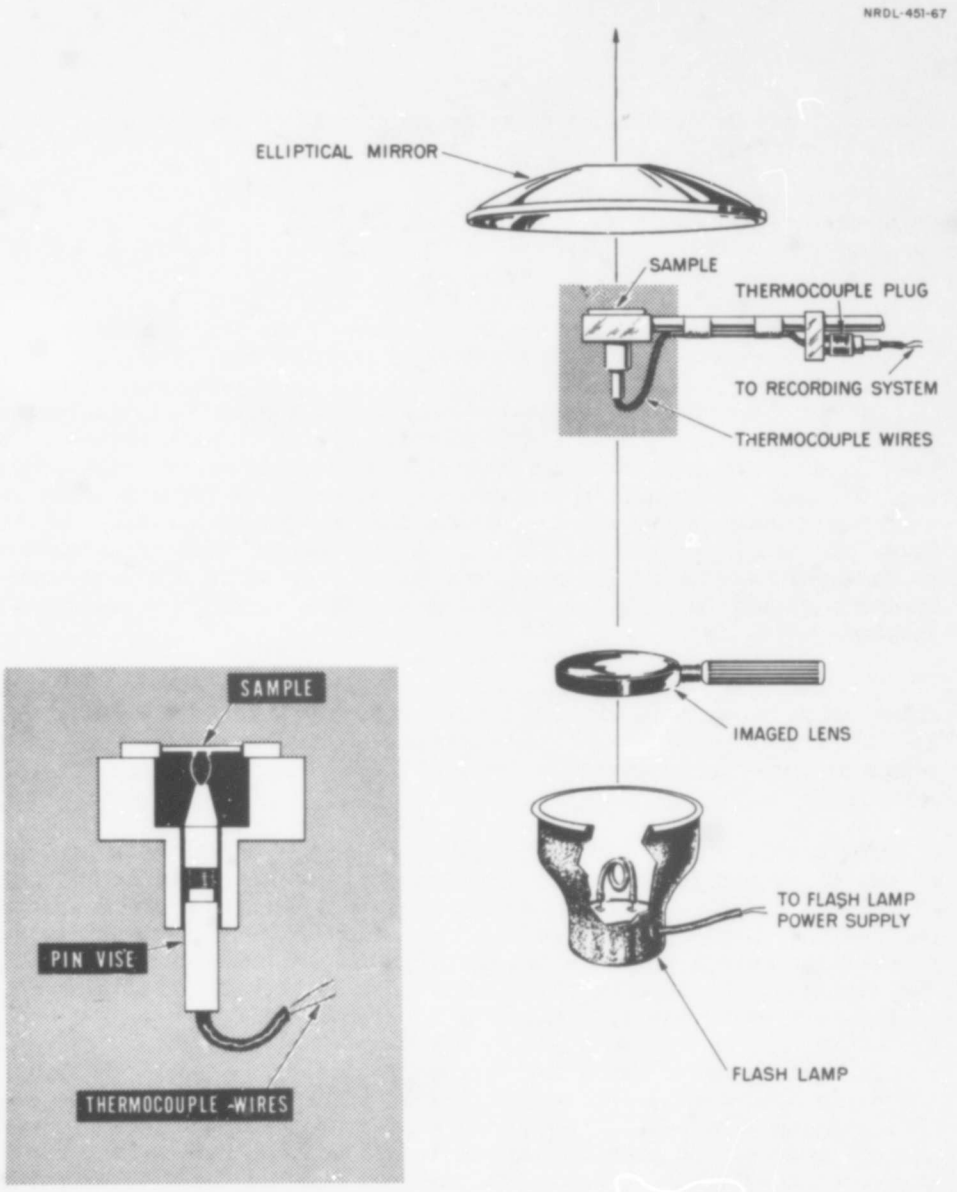

Fig. 3 Thermal Diffusivity Measurement Equipment

heat, c_p, can be determined from the magnitude of the maximum. Since these quantities are related to κ by the equation

$$\kappa = \alpha C_p \delta \quad , \tag{4}$$

where δ is mass density, κ can be calculated from the data gathered by this technique, plus a simple density measurement.

In the case where c_p and δ are constants, a given relative change in α must be matched by an equal relative change in κ. In view of the heavily doped nature of thermoelectrics, one would expect pile bombardment of these materials to be such a case, at least for exposures less than those required to effect substantial changes in the basic material. Thus, for the purpose of determining the effect of reactor bombardment on z, determination of the relative change induced in α by pile bombardment should be equivalent to determination of the correspondingly induced change in κ.

The equipment used for these measurements utilized a type 524 xenon flash lamp, through which 1600 joules were discharged to produce the radiant energy pulse. Heat for controlling the sample's average temperature (pre-flash) was supplied by a commercially available hot air gun.

The sample holder was of a type which gripped the sample by its edges, so as not to interfere with the incident energy pulse. The leads of a 3-mil alumel-chromel thermocouple were brought up to the shielded face of the sample and pressed against it separately, with sufficient pressure to make a good electrical contact, but not enough to fracture the sample. With some of the more fragile materials the attainment of this proper pressure involved considerable skill.

In most cases it was found necessary to electro-deposit a thin (on the order of one mil) layer of nickel on the back surface of the sample. This coating ensured a good thermal contact between thermocouple wires and the sample, and provided an electrical contact between the two thermocouple wires. Without this coating, the thermocouple output displayed a large amount of noise, which probably was generated by small thermal imbalances in the sample resulting from air current eddies. The principal function of the nickel coating, from this point of view, was to short out the voltage fluctuations generated by the room air currents.

The sample holder had a sufficiently large heat capacity that the heat gun could be turned off for the few seconds required to make a single observation. Even with the nickel plating, the signals generated by the heat gun's air stream were large enough to interfere with the thermocouple's output. Thus, the large heat capacity was an important property of the sample holder.

The thermocouple output was amplified by a transistorized differential amplifier, and displayed on an oscilloscope. A photograph of the scope trace, taken with a Polaroid Land Camera, formed the permanent record of the results.

Limitations imposed by other duties assigned to the personnel making the thermal diffusivity measurements precluded a thorough exploration of the influence of temperature on the pile bombardment effects on α. Instead, thermal diffusivity measurements on most materials were made at only two temperatures, room temperature and in the region of 100 to 120°C.

IRRADIATION

General

Irradiation services were obtained at the General Electric Test Reactor (GETR), at Vallecitos, California. Three sets of samples were irradiated in GETR, one each to a total fluence of approximately 10^{17}, 10^{18}, and 2×10^{19} fast ($E > 1$ MeV) neutrons/cm^2, respectively. A listing of samples according to exposure dose is included in Table I.

Capsules

For irradiation, each set of samples was mounted in its own sealed, aluminum capsule, which contained an atomsphere of helium at a pressure somewhat greater than one atmosphere. Capsule construction details are shown in Fig. 4.

Exposure doses as calculated by GETR personnel were verified by either nickel or iron dosimeters, or both, located at several places within each capsule. Average fluences determined for each capsule in this manner were 1.0×10^{17}, 1.6×10^{18}, and 2.3×10^{19} fast ($E > 1$ MeV) neutrons/cm^2, respectively.

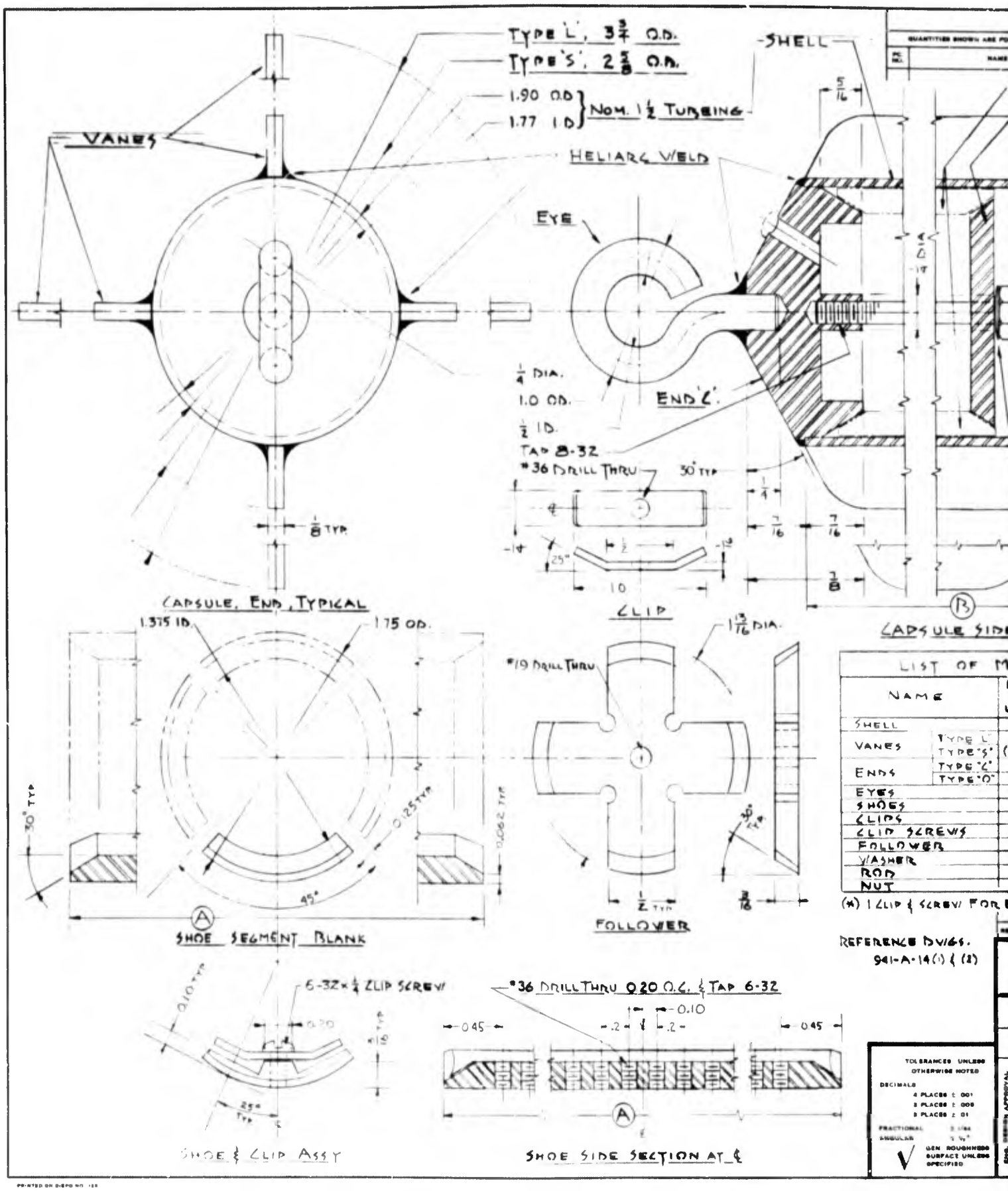

Fig. 4 Irradiation Capsule Construction Details

A

NRDL-461-67

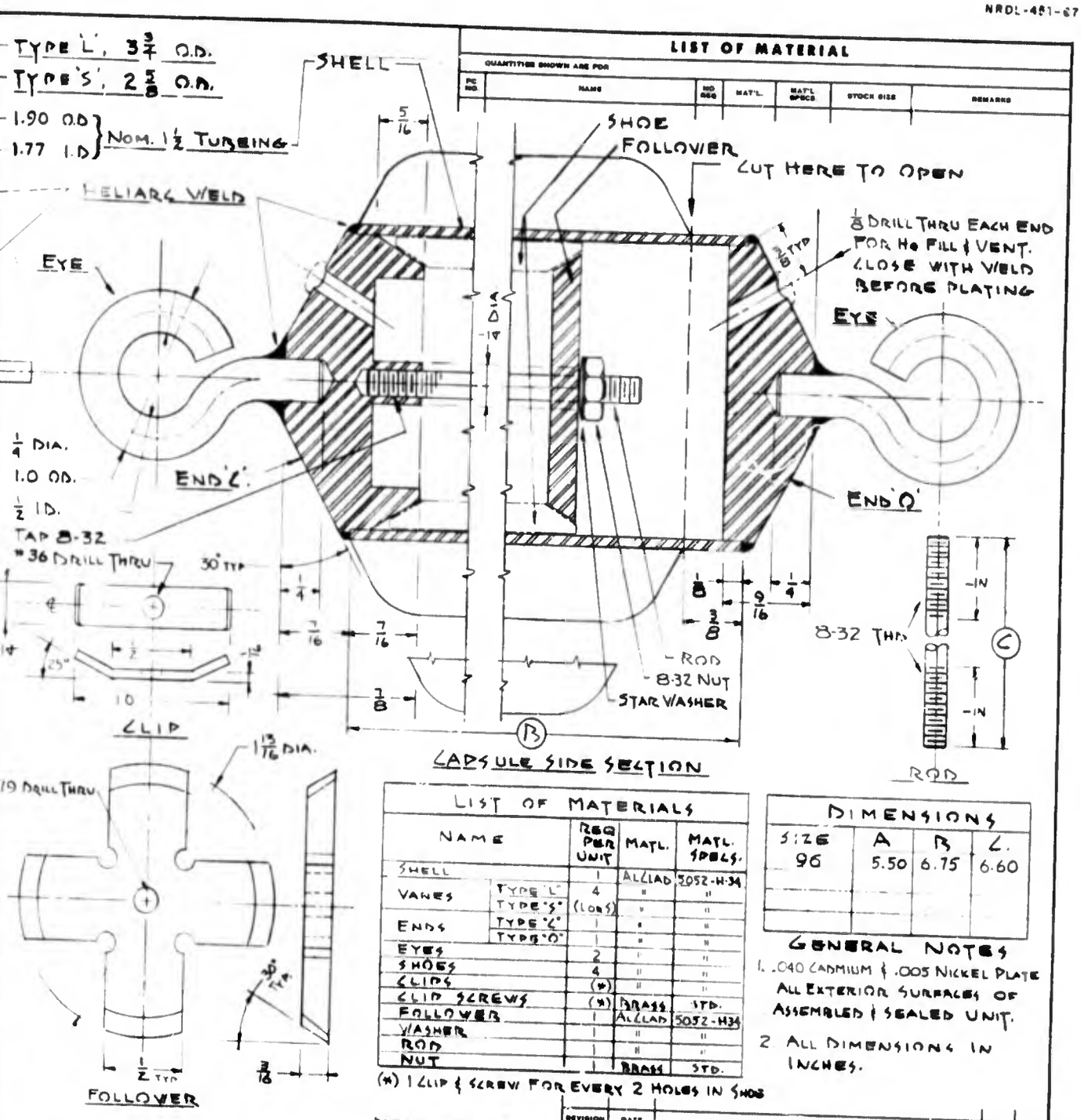

LIST OF MATERIAL						
QUANTITIES SHOWN ARE FOR						
PC NO.	NAME	NO REQ	MAT'L	MAT'L SPECS	STOCK SIZE	REMARKS

LIST OF MATERIALS				
NAME		REQ PER UNIT	MATL.	MATL. SPECS.
SHELL		1	ALCLAD	3052-H34
VANES	TYPE 'L'	4	"	"
	TYPE 'S'	(LONG)	"	"
ENDS	TYPE 'L'	1	"	"
	TYPE 'O'	1	"	"
EYES		2	"	"
SHOES		4	"	"
CLIPS		(*)	"	"
CLIP SCREWS		(*)	BRASS	STD.
FOLLOWER		1	ALCLAD	3052-H34
WASHER		1	"	"
ROD		1	"	"
NUT		1	BRASS	STD.

(*) 1 CLIP & SCREW FOR EVERY 2 HOLES IN SHOE

DIMENSIONS			
SIZE	A	B	C
96	5.50	6.75	6.60

GENERAL NOTES

1. .040 CADMIUM & .005 NICKEL PLATE ALL EXTERIOR SURFACES OF ASSEMBLED & SEALED UNIT.
2. ALL DIMENSIONS IN INCHES.

REFERENCE DWGS. 941-A-14(1) & (2)

REVISION	DATE	DESCRIPTION	BY	APP

UNITED STATES
NAVAL RADIOLOGICAL DEFENSE LABORATORY
SAN FRANCISCO 24, CALIFORNIA

DRAWN	NICHOLS	7-19-62
SCALE	DOUBLE	
PROJECT		
TECH MEMO		
DRAWING NUMBER	941-A-18	
SHEET	1 OF 1	
ALT	0	

CAPSULE UNIT FOR SPECIMEN IRRADIATION IN NUCLEAR REACTORS

TOLERANCES UNLESS OTHERWISE NOTED
DECIMALS
4 PLACES ± .001
3 PLACES ± .005
2 PLACES ± .01
FRACTIONAL ± 1/64
ANGULAR ± ½°
GEN. ROUGHNESS SURFACE UNLESS SPECIFIED.

ENG. DESIGN APPROVAL

After being sealed, each capsule was given a complete exterior coating of cadmium, using a flame-deposition technique developed by a contractor*. This layer was about 40 mils thick, which in most cases was enough to reduce the thermal neutron fluence experienced by the samples to negligible levels.

Temperature Monitoring

Temperatures experienced by the samples during the mounting, sealing, coating, irradiation, and capsule opening procedures, were monitored by wafers of fusible-link alloys. These established that the peak temperatures during these operations did not exceed 120°C.

Induced Radioactivity

The only samples exhibiting appreciable levels of induced radioactivity were some of these exposed to the highest dose, where the effectiveness of the cadmium was reduced by the burn-up factor. These samples required a cooling-off period of about two months after termination of irradiation, in order for the personnel making the post-irradiation measurements to avoid over-exposure. In all cases a sufficient waiting period was observed, and personnel exposures all were substantially below the existing permissible limits.

MATERIALS AND SAMPLE DETAILS

List of Materials

Some seven different, commercial grade, base materials, obtained from four different sources, were examined in this study. These were: (i) lead telluride, (ii) bismuth telluride, and (iii) an alloy of 90% germanium telluride and 10% silver antimony telluride, all provided by the Bureau of Ships; (iv) cobalt silicide, and (v) an alloy of germanium and bismuth tellurides, both supplied by the Naval Research Laboratory; (vi) a germanium-silicon alloy of classified proportions, obtained from the Marine Engineering Laboratory; and (vii) silver selenide, supplied by the manufacturer.

---

* Advanced Materials and Processes Corporation, Los Altos, California.

In addition, a number of samples cut from a specially-grown ingot of stoichiometric, single-crystal bismuth telluride, were examined, and the germanium-silicon alloy and the commercial grade bismuth telluride were provided in both n- and p-types. Thus a total of ten different kinds of thermoelectric materials were studied.

Sample Geometry and Construction

Samples were of two substantially different shapes. Equipment used to measure S and ρ was designed to measure Hall coefficients as well. Restrictions associated with the latter led to a rectangular bar sample, with nominal dimensions of 10 x 2-1/2 x 1 mm. These samples are referred to as HALL SAMPLES.

For measurement of α, on the other hand, the dominant consideration was to avoid excessive cooling losses in the directions transverse to the direction travelled by the wave-front intercepted by the measuring thermocouple. Consequently, the optimum shape for this case was a thin wafer. For the materials at hand, nominal dimensions were 10 mm diameter (or square) in the transverse direction, and 1 mm in thickness. These samples are referred to as THERMAL SAMPLES.

Both Hall and thermal samples were sliced from their ingots and trimmed to shape, where necessary, with a high-speed carborundum or diamond wheel. Surfaces were ground flat and polished on a lapping wheel. These processes, and the various precautions associated with the various materials, are described in further detail in a previous report.(8)

Hall samples received no further treatment. As described previously, however, it was necessary to nickel-plate the shielded face of the thermal samples, and to coat the exposed faces with a thin layer of platinum black.

A description of the individual samples is given in Table I, p 65 . At least one sample of each material was measured after exposure to the largest dose, to detecto any possible change in sample dimensions due to the Wigner effect. In all cases no change in dimensions was seen.

DATA REDUCTION

Because of the rather large number of S and ρ test runs made in this study (about 150), and the consequent large amounts of routine data reduction required, personnel of NRDL Code 905X have programmed the simple algebraic treatment discussed in Reference 6 for processing by digital computer.

The first section of this program accepts as input, punched cards containing the observed raw data. From these, the various Seebeck voltages and Seebeck Coefficients of the sample with respect to both constituents of the thermocouple, the sample's resistivity, the corresponding average sample temperature, and temperature difference between the two thermocouples, are calculated and stored.

The second section produces an instruction tape for a commercially available drawing machine, specifying details for producing linear plots of any of the calculated variables as a function of any other, the plot descriptions being provided by the investigator in the form of punched cards. This section also has the option of calculating the best-fit polynomial for the given plot, of any degree up to nine. The plots of S and ρ presented in this report were produced by this technique.

A number of peripheral routines, providing the facility for identifying mispunched input cards, for example, have been written. These, as well as the main routines are on file at NRDL, and presumably can be made available upon request.

OBSERVATIONS

GENERAL

Calibration

The reproducibility of the equipment for measuring S and ρ was determined experimentally for at least one sample of each material studied.

In general, the calibration samples were mounted in the equipment three times, with three runs made on one mounting, and one run each on the other two mountings. The data observed during these calibration runs are presented in Appendix I, in the form of plots of S and ρ as functions of sample temperature. These plots were machine drawn, by the method indicated in the previous section.

In these calibration plots, data points are indicated by numeric symbols. The numeric order of the symbols indicates the chronological order in which the corresponding portions of the runs were made. In general, odd numbers indicate points taken while temperature was rising and even symbols those taken while the sample was cooling. A gap in the numeric sequence indicates a portion of a run which was made, but produced no usable data. These usually resulted from equipment malfunctions of the types discussed in Reference 6.

Because of these malfunctions, the data taken while temperature was increasing are less reliable than those taken while the sample was cooling. Consequently, experimental limits of precision were estimated from the cooling data only. These limits are listed for each material tested in Table I, p 65 .

Pre- and Post-Irradiation Data

The pre- and post-irradiation observations made on all samples examined are presented in Appendix II, in the form of plots of S, ρ, and α as functions of sample temperature. The S- and ρ -plots were machine drawn, while the α - plots were drawn by hand.

Data points taken for samples which eventually were irradiated to the 2×10^{19} fluence are indicated by numeric symbols. Those taken for samples which were irradiated only to lesser fluences are indicated by alphabetic symbols. In both cases, the natural sequence of the symbols indicates the chronological order of the data, and missing symbols indicate measurement runs which did not produce usable data.

Quantitative estimates of the changes induced in the three parameters by irradiation have been made, and are tabulated in Table 1. Using equation (1), the corresponding changes to be expected in z have been calculated, and also tabulated in Table I. These estimates are representative approximations, made visually from the plots of Appendix II, and are not to be taken as precise evaluations. They are adequate, however, for rough determination of the order of change in z to be expected.

BLANK PAGE

It should be noted here that in many cases, the first heating portion of the S- ρ run immediately following irradiation was complicated by the presence of annealing processes. In general, sample heating was not delayed to permit completion of these processes. As a result, the observed signals may have, and in some cases almost certainly did, change appreciably during the fifteen seconds or so required to take the readings for a single data point. Since our treatment rests upon the assumption of constant signals during this period, the data taken while heating the sample are somewhat less reliable than those taken while the sample was cooling, and quantitative estimates have been confined to use of the latter.

RESULTS BY INDIVIDUAL MATERIALS

Lead Telluride

Data on the behavior of S and ρ are available for three samples of this material, numbers 136A and B, which were exposed to approximately 10^{18} n_f/cm^2, and number 130B, which was exposed to a fluence of approximately 10^{19} n_f/cm^2. In addition, data on the behavior of α are available for one sample, number 135, which was exposed first to a fluence of approximately 10^{17} n_f/cm^2, and then to a fluence of about 10^{19} n_f/cm^2. These data are presented in Appendix II, Figs. II/1 through II/7.

It will be noted that the data for S and ρ show no significant changes arising from any of the exposures. Thermal diffusivity also shows no change as a result of exposure to the lower fluence, but does show a significant decrease after the exposure to 2.3×10^{19} n_f/cm^2. This decrease does not appear to anneal out to any great extent at the higher temperature of which α was measured, i.e., about 100°C.

Calculations of z indicate that a modest improvement might be expected to result from pile bombardment. For fluences in the region of 10^{19} n_f/cm^2 this increase might be as much as 50% of the pre-irradiation value, or as little as 10%, depending upon how much of the radiation induced change in α is annealed out.

Alloy: Germanium and Bismuth Tellurides

Data on the behavior of S and ρ are available for three samples of this material, numbers 145B and 147A, which were exposed to fluences of about 10^{18} n_f/cm^2, and number 147B, which was exposed to a fluence of about 10^{19} n_f/cm^2. In addition, data on α are available from two samples, numbers 142 and 148, which were both exposed to a fluence of about 10^{17} n_f/cm^2. After this exposure, number 148 was exposed to the 10^{19} fluence, while number 142 was exposed to the 10^{18} fluence. These data are presented in Appendix II, Figs. II/8 through II/15.

Some difficulty was experienced in measuring S in these samples, particularly at the higher temperatures. Whether this is due to some inherent property of this material, or is merely the result of chance failure of the measuring equipment, is not clear.

In either event, enough credible data were accumulated to permit assertion with reasonable confidence that the 10^{18} fluence introduced increases in S on the order of 10% of the pre-irradiated value, while the 10^{19} fluence increased this parameter on the order of 20%, these figures representing the changes remaining after brief heating to temperatures in the region of 300°C above room temperature.

Electrical resistivity data are more regular, and show a radiation-induced increase in ρ, after the brief, post-irradiation heating to temperatures in the region of 300°C above room temperatures, on the order of ten percent, at both fluences. The data for sample 147B are of special interest because the post-irradiation heating curve displays a classic example of the cusp we attribute to measurement errors arising out of annealing processes, in the region of 250°C above room temperature.

Interpretation of the thermal diffusivity data for this material is somewhat uncertain. The observations displayed in Figs. II/14 and II/15 may result from sizable variations in α from region to region in the unirradiated samples, thus producing poor precision of measurement when remounting of the sample is involved. On the other hand, there may actually be an increase of α at low doses, followed by a larger decrease at higher doses, complicated in some samples by thermally induced increases without irradiation. The only resolution of this dilemma requires further data.

For the purposes of computing Table I, we have assumed the latter to be the case, since this gives us a maximum upper limit for the range of z. Under this assumption, we can expect fluences on the order of 10^{19} n_f/cm^2 to induce modest increases in z for this material, these

increases ranging from as much as 100% to as little as about 30%, of the pre-irradiation value, depending upon how much of the radiation-induced change of α is annealed out at the operating temperature. For fluences on the order of 10^{18} n_f/cm^2, the corresponding increases in z are roughly 50% and 15% respectively.

Silver Selenide

Data describing the behavior of S and ρ are available for three samples of this material, number 178A, which was exposed to the 10^{19} fluence, and numbers 181A and 181B, which both were exposed to the 10^{19} fluence. In addition, one thermal sample, number 180, produced data describing the behavior of thermal diffusivity. This sample was first exposed to the 10^{17} fluence and then to the 10^{19} fluence. These data are presented in Appendix II, Figs. II/16 through II/22.

Interpretation of the data for sample 178A is made unclear by an inadvertent extension of the measurement temperature into the range above this material's softening temperature. Judging by the fact that the data were observed at these higher temperatures, despite the lack of any containment of the sample, it would seem plausible that the observed softening point corresponds to a change of phase from one solid to another. It is certain that the material did not melt, at any rate, and the observed discontinuities in S and ρ would not be inconsistent with a change of phase.

Despite the phase uncertainties, it is clear that the neutron bombardment reduced both S and ρ for all three samples, and that little, if any, annealing occurs in either parameter at temperatures below 100°C above room temperature. The data for sample 178A suggest that heating this material further does not reduce these changes, but rather acts to increase them. When the temperature is restricted to the lower range, the 10^{19} fluence reduces S by about 50% of its pre-irradiation value, and ρ by about 70%. The 178A data suggest that fluences on the order of 10^{18} n_f/cm^2 reduce these quantities by about 25% and 40%, respectively.

The data for sample 180 also show discontinuous behavior in the neighborhood of 100°C above room temperature. In addition, the effect of the neutron bombardment clearly was to increase the thermal diffusivity by about 35% of its pre-irradiation value.

In terms of calculated z, the effect of the 10^{19} exposure was to reduce this parameter by about 40%, if the thermal diffusivity change does not anneal out, and by about half that much if all of the change

of α is annealed out. The corresponding calculated changes for the 10^{18} exposure were about -10% and -1% respectively*.

The observed changes for all three parameters in this material suggest a radiation-induced increase in the majority charge carrier concentration. The persistence of these changes despite an apparent change of phase in sample 178A argues strongly against a displacement mechanism as their cause. Consequently, it seems most likely that this material has undergone changes due to transmutation effects. When time becomes available, a few speculative calculations of the effects of this type to be expected for the possible transmutations in this material, should be quite interesting.

Germanium-Silicon Alloy (n)

Data describing the behavior of S and ρ are available for four samples of this material. Samples 224A and 224B were exposed to approximately 10^{18} n_f/cm^2, while sample 224C and 224D were exposed to the 10^{19} n_f/cm^2 fluence. In addition, data describing the behavior of α are available for two samples, both of which were exposed to the 10^{17} n_f/cm^2 fluence. Sample 225 then was exposed to the 10^{18} fluence, while sample 226 was then exposed to the 10^{19} fluence. These data are presented in Appendix II, Figs. II/23 through II/32.

Despite a certain amount of irregularity in the measurements of S in this material, it is clear that reactor bombardment introduced moderate increases in this parameter, and that post-irradiation heating tended to increase the size of these changes, rather than to anneal them out. It is clear that the microscopic behavior in this material is quite complicated.

Assignment of quantitative values to radiation-induced changes in this situation is rather difficult, and ambiguity is not easily avoided. For the purposes of the ball-park type of values reported in Table I, however, we have somewhat arbitrarily assigned values of about + 33% to the change in S induced by the 10^{18} fluence, and about + 10% for that induced by the 10^{19} fluence.

* This calculation is based upon the assumption that α would change by about + 7% (i.e., the precision limit) for an exposure to the 10^{18} fluence. This interpolation admittedly is speculative, and no great reliance should be placed upon the 10% figure.

In contrast, the electrical resistivity data present a considerably simpler picutre. These data behave as though the entities produced by reactor bombardment, which increase the room temperature resistivity by several orders of magnitude over its pre-irradiation value, gradually anneal out in the temperature range above room temperature. The data from 224A and 224B suggest the existence of an annealing temperature somewhere between 100 and 200°C above room temperature. In addition, comparison of the residual changes after heating in samples 224C and 224D suggest the existence of at least one additional annealing temperature, or perhaps a distribution of annealing temperatures, in the region between 300 and 500°C above room temperature. For both fluences, the amount of the radiation-induced increase in ρ remaining after suitable annealing was about 500%.

The thermal diffusivity data for the higher fluences show substantial radiation-induced reductions of α, which show no signs whatever of annealing out over the measurement temperature range, i.e., up to about 120°C. These changes are on the order of -10% at the 10^{17} fluence, -40% at the 10^{18} fluence, and -60% at the 10^{19} fluence.

The calculated values of radiation-induced changes in z obtained from these data range from about -50% to -70% at the 10^{18} fluence, depending upon how much of the radiation-induced change of α anneals out at higher temperatures. For the 10^{19} fluence, these values are + 80% to -30%, respectively.

The most interesting feature of these data lies in a comparison between the observations for the two higher fluences. Note that in going from the 10^{18} fluence to the 10^{19} fluence, the radiation-induced change in S was roughly doubled, while the corresponding change in ρ was held to essentially zero by the use of a higher annealing temperature. If higher annealing temperatures yet could reduce the radiation-induced change in ρ still further, while leaving the change in S fixed, substantial increases in z would seem possible. This area should be explored further.

Germanium-Silicon Alloy (p)

Data describing the behavior of S and ρ are available for four samples of this material. Samples 230A and 230B were exposed to the 10^{18} n_f/cm^2 fluence, while samples 232A and 232B were exposed to the 10^{19} n_f cm^2 fluence. In addition, data describing the behavior of thermal diffusivity are available for two samples, both of which were exposed first to the 10^{17} n_f/cm^2 fluence. Sample 234 then was exposed

to the 10^{18} fluence, while sample 236 was exposed to the 10^{19} fluence. These data are presented in Appendix II, Figs. II/33 through II/42.

Relatively well-behaved data for S in this material show that reactor bombardment introduced moderate increases in this parameter. The data taken for the two samples exposed to the 10^{18} fluence show no signs of annealing anywhere in the temperature range extending up to about 300°C above room temperature. Those taken for the samples exposed to the 10^{19} fluence, however, show definite annealing behavior, with one annealing range in the region from 100 to 200°C above room temperature, and at least one more in the range between 300 and 500°C above room temperature.

Samples 230A and 230B are in agreement that the 10^{18} fluence introduces an increase in S of about 25% of its pre-irradiation value. The amount of post-annealing change left after the 10^{19} exposure depends upon the peak temperature of the post-irradiation examination. We have somewhat arbitrarily taken this to be about +75% of the pre-irradiation value.

The resistivity data for this material bear a qualitative resemblance to those found for the n-type alloy. The effect in the p-type material seems not quite so strong, however, with pre-annealing values of the radiation-indiced increase at room temperature on the order of two orders of magnitude, rather than three, for the 10^{19} fluence.

The amount of change observed after annealing again depends upon the peak temperature of the annealing run. Applying the same arbitrary procedure used previously, we have taken the amount of change remaining after annealing to be + 100% for the 10^{18} exposure, and + 375% for the 10^{19} exposure.

The thermal diffusivity data also resemble their counterparts from the n-type alloy rather closely, although again the amount of change is a bit smaller for the p-type samples. Up to the same temperature, i.e., 120°C, no signs of annealing are seen. The changes found in α for this material were -25% for the 10^{18} fluence, and -55% for the 10^{19} fluence.

In terms of calculated z, these data correspond to a radiation-induced change somewhere between about + 10% and -20% for the 10^{18} fluence, depending upon how much of the radiation-induced change in α anneals out at the operating temperature. For the 10^{19} fluence, the corresponding figures are about + 40% and - 40%.

Again, comparison of selected portions of the observed data hint at the possibility of achieving substantial improvements in z, through judicious choice of a combination of irradiation, and post-irradiation thermal treatments. This material seems worth further attention.

Bismuth Telluride (n)

Data describing the behavior of S and ρ are available for three samples of this material. Sample 245B was exposed to the 10^{18} n_f/cm^2 fluence, while samples 245C and 245D were exposed to the 10^{19} fluence. In addition, thermal diffusivity data are available for two samples, both of which were first exposed to the 10^{17} fluence. Sample 239 then was exposed to the 10^{18} fluence, while sample 206A was exposed to the 10^{19} fluence. These data are presented in Appendix II, Figs. II/43 through II/50.

The results for S and ρ in this material display several confusing facets which make interpretation difficult. No two samples responded in exactly the same way. Definite signs of modest, radiation-induced changes are present. So are signs of thermal annealing, both before and after irradiation. Some of the data appear to indicate negative annealing in the irradiated material, while others are sufficiently irregular to raise at least a suspicion of equipment malfunction. In view of these difficulties, the quantitative analysis presented below must be considered as only tentative, pending further investigations into this material's behavior, and the conclusions based upon those calculations are best labeled speculations.

With this caution in mind, we note that the radiation-induced change in S remaining after annealing is an increase of the order of 10%, after exposure to the 10^{18} fluence, and about 45% after the 10^{19} fluence. The corresponding figures for ρ are about - 20% and zero, respectively.

The thermal diffusivity data for this material are somewhat less confused. The radiation-induced changes in α are decreases of about 20% and 45% for the 10^{18} and 2×10^{19} fluences, respectively.

Speculative values of radiation-induced change in z can be calculated from these results. In all cases these appear to be modest increases, ranging from about 80% to 45% for the 10^{18} fluence, and from 290% to 110% for the 10^{19} fluence. In both cases the former figure is calculated for the observed change in α, i.e., under the assumption that no further annealing of α takes place, while the latter figure is that calculated under the assumption that all of the observed radiation induced change in α will anneal out at the

operating temperature. The fact that all of these figures are increases in z is of some interest.

Alloy: Germanium Telluride-Silver Antimony Telluride

Data describing the behavior of S and ρ are available for four samples of this material. Samples 251A and 251E were exposed to the 10^{18} fluence, while samples 251B and 251D were exposed to the 10^{19} fluence. In addition, thermal diffusivity data are available for two samples, numbers A and C, both of which were exposed first to the 10^{17} fluence, and then to the 10^{19} fluence. These data are presented in Appendix II, Figs. II/51 through II/60.

The data for this material indicate quite strongly that reactor bombardment up to 2 x 10^{19} nγ/cm² introduce no significant changes in any of the three thermoelectric parameters, even before post-irradiation heating. An upper limit of about + 10% is calculated for radiation-induced change in z.

Cobalt Silicide

Data describing the behavior of S and ρ are available for three samples of this material. Sample 252C was exposed to the 10^{18} fluence, while samples 252A and 252B were exposed to the 10^{19} fluence. In addition, thermal diffusivity data are available for one sample, sample CoSiI, which was exposed first to the 10^{17} fluence and then to the 10^{19} fluence. These data are presented in Appendix II, Figs. II/61 through II/67.

The data describing S for this material consistently show a radiation-induced decrease, amounting to about 4% for the 10^{18} fluence, and about 40% of the pre-irradiation value, for the 10^{19} fluence. There is no indication of any annealing over the temperature range up to about 300°C above room temperature.

The elctrical resistivity data, on the other hand, consistently show a rather substantial, radiation-induced increase, ranging from about 33% at the 10^{18} fluence, to about 165% at the 10^{19} fluence. Again, there is no sign of any significant annealing during post-irradiation heating up to about 300°C above room temperature.

The thermal diffusivity data indicate a radiation-induced decrease in α of about 75% at the 10^{19} fluence. If this value is assumed not to anneal out at the operating temperature, the calculated value of z

undergoes a decrease of about 30%, at the $\equiv 10^{19}$ fluence. If this value is assumed not to anneal out at the operating temperature, the calculated value of z undergoes a decrease of about 30%, at the $\equiv 10^{19}$ fluence. If all radiation-induced change in α is assumed to anneal out at the operating temperature, an exposure to 10^{18} n_f/cm^2 would be expected to reduce z by about 50%, while exposure to $\equiv 10^{19}$ n_f/cm^2 would be expected to reduce z by about 90%.

Bismuth Telluride (p)

Data describing the behavior of S and ρ are available for four samples of this material. Samples 254B and 254C were exposed to the 10^{18} fluence, while samples 254D and 254E were exposed to the $\equiv 10^{19}$ fluence. In addition, data describing the behavior of α are available for one sample of this material, number 254, which was exposed to the $\equiv 10^{19}$ fluence. These data are presented in Appendix II, Figs. II/68 through II/76.

Reactor bombardment affects S in this material most dramatically, driving its room temperature value toward negative values until it actually changes sign. In the case of the largest exposure, the pre-annealing value for the irradiated material is as large in the n-direction as the pre-irradiation value was in the p-.

In all samples, however, the changes annealed out almost completely, with only trivial departures from the pre-irradiation behavior remaining after the annealing run. For both fluences these post-annealing changes were on the order of +5%, or less, with the return to the pre-irradiation values taking place in what appears to be a single annealing process occurring at about 100 to 200°C above room temperature.

The room-temperature value of electrical resistivity increased rather sharply as a result of reactor bombardment, although the 10^{18} exposure appeared to have produced a considerably larger change than did the 10^{19} exposure. In all cases, however, heating the irradiated sample removed substantially all of the radiation-induced changes, the annealing having been completed by the time a temperature in the region of 200°C above room temperature was reached. In two samples, one for each exposure, the post-annealing value of ρ was slightly less (on the order of 10%) than the pre-irradiation value.

The thermal diffusivity data show a remarkable increase in value as a result of the 10^{19} exposure, which does not appear to anneal at all at temperatures up to about 120°C. These data do not represent the behavior of thermal conductivity, however, since the specific heat of

the material apparently undergoes a complementary change which counterbalances the observed change in α, leaving κ substantially unchanged.

The calculated post-annealing value of the radiation-induced change in z for this material is a small increase , on the order of 10%, for both fluences.

Bismuth Telluride (single crystal)

Data describing the behavior of S and ρ are available for three samples of this material. Sample 255C was exposed to the 10^{18} fluence, while samples 255E and 255F were exposed to the 10^{19} fluence. In addition, data describing the behavior of thermal diffusivity are available for one sample, number 255, which was exposed to the 10^{19} fluence. These data are presented in Appendix II, Figs. II/77 through II/83.

With respect to S and ρ, this material responded to reactor bombardment in essentially the same fashion as did the commercial grade, p-type bismuth telluride. The room-temperature value of S was driven negative, becoming about as large in magnitude as the pre-irradiation value was. At the same time, large increases in ρ were observed.

Upon heating, both parameters returned to their pre-irradiation behavior, the annealing taking place over the same general range as for the commercial material, i.e., about 100 to 200 ^{o}C above room temperature. Post-annealing values of the radiation-induced changes in these two parameters were negligible, in all cases.

The principal difference between the single crystal material and the commercial material, as far as S and ρ are concerned, was in measurement precision, that for the single crystal material being noticably better for the commercial material.

The thermal diffusivity data for this material show a marked difference between it and the commercial material. Since data are available for only one sample in each case, this difference must be considered as only tentative, pending more investigations, rather than as an established fact. However, within this restriction, there can be no doubt that the thermal diffusivity of the single crystal material was reduced on the order of 20% by the 10^{19} fluence, while it was increased for the commercial material. This interesting difference should be pursued in future studies.

Post-annealing, radiation-induced changes in z can be calculated for only the 10^{19} fluence, in this material. That calculated change amounts to an increase of about 25%, if the change of α is assumed to be unaffected by the annealing process, and to essentially no change at all, if the radiation-induced change of α is assumed to anneal out entirely.

CONCLUSIONS

GENERAL COMMENTS

The most obvious conclusion to be drawn from this preliminary study is confirmation of our previously expressed opinion that the influence of reactor bombardment on the thermoelectric figure of merit (z) is a complicated matter. In some of the materials examined, reactor bombardment increased z, while in others it decreased z, and in still others z remained relatively fixed, despite rather large exposures. In these results we find no obvious suggestion of criteria which would permit the pre-irradiation sorting of new materials into these three classes, much less any prediction of the amount of change that should be expected. Consequently, each new material will have to be examined separately, if its response to irradiation is to be known.

In this study, the largest value calculated for radiation induced increase of z was some 287% of the pre-irradiation value, which obtained for n-type Bi_2Te_3 under the assumption that the change in thermal diffusivity induced by exposure to the 10^{19} fluence would not anneal out. The largest decrease in calculated z, obtained for CoSi exposed to the 10^{19} fluence and under the assumption that all of the radiation-induced change in thermal diffusivity would anneal out, was 87% of the pre-irradiation value. In terms of factors rather than additive corrections, these establish an experimental range of from about one-tenth to about four times the pre-irradiation value, a range of about 1-1/2 orders of magnitude. Since there is no particular reason to suspect that the materials chosen for this study include the extremes of all possible high-z materials, this range must be taken as an established minimum, rather than a maximum

Our results suggest that there need not be a correlation between pre- and post-irradiation values of z, and that consequently materials should not be excluded from future examinations merely because their pre-irradiation values of z fall short of the highest known values by factors of two or three, or so.

The principal limitations on this study were imposed by the lack of available effort to pursue investigation of the thermal diffusivity, and the related quantities of specific heat and density, in a more thorough fashion. The severity of these limitations is obvious from comparison of the alternative sets of figures for calculated radiation-induced change in z, in Table 1. In view of the importance of the contributions of thermal conductivity changes to the calculated changes in z, it seem obvious that future investigations in this area should pay special attention to expanding both the range of temperatures over which the thermal properties are measured, and to expanding the number of thermally related quantities examined. For the present we must bear in mind that a great many of the conclusions suggested by this study are only tentative, and will remain so until such future attention can be devoted to these factors.

A great deal of the complication in this field arises from the availability of a number of post-irradiation, thermally activated interactions to the entities introduced by irradiation. From the experimenter's viewpoint, these complicate the job of identifying and evaluating the effects of radiation, since the post-irradiation state is not necessarily stable. From the materials engineer's viewpoint, however, these offer the possibility of added independent variables which might be controlled in such a way as to produce materials having record high values of z.

One example of such a possibility developed in this study, is given in the data for the two germanium-silicon alloys. We note the existence of one case in each type where additional irradiation apparently introduced at least two kinds of entity, one which annealed out and the other which did not, the former associated with the radiation-induced increase in electrical resistivity, and the latter with Seebeck coefficient. The net result of the irradiation, followed by heating, was a substantial increase in S, accompanied by a negligible increase in ρ. The possibilities here are quite exciting, and this material seems well worth considerable future attention, especially in view of its unusually low density.

TABLE I

Summary of reactor-bombardment induced changes in Seebeck coefficient (S), electrical resistivity (ρ), and thermal diffusivity (α) observed in ten materials, with estimates of measurement precision, and calculated values of the corresponding changes in thermoelectric figure of merit (z) to be expected in view of Equation (1).

Material & Type	Shape	Exposure[1]	Sample	Estimated Precision Limits (%)			Radiation-Induced Change (%)				No Further Anneal[2]		100% α-anneal[2]	
				S	ρ	α	S	ρ	α	K_{calc}	1.6×10^{18}	2.3×10^{18}	1.6×10^{18}	2.3×10^{18}
PbTe (p)	Hall	C	136A	± 1 to 5	± 1 to 5									
		II					< 1	+ 5						
			136B				+ 3	+ 1						
		III	130B				+ 6	+ 4						
	Thermal	I	135			± 5			< 1	< 1				
		III	↓						-28	-28				
		↓									+ 4	+50	+ 1	+ 8
$Ge_{.96}Bi_{.08}Te$ (p)	Hall	C	145A	± 1	± 4									
		II	145B				+13	+ 6						
		↓					+11	+10						
		III	147B				+19	+ 8						
	Thermal	I	148			± 3			+12	+12				
		II	↓						-20	-20				
		I	142						+ 4	+ 4				
		III							-35	-35				
											+45	+102	+16	+31
Ag_2Te (n)	Hall	C	178A	± 2	± 3									
		II					-25	-43						
		III	181A				-50	-69						
		↓	181B				-53	-70						
	Thermal	I	180			± 7			< 7	< 7				
		III	↓			↓			+35	+35				
											- 8[4]	-38	- 1	-17
Ge-Si Alloy (n)	Hall	C	222A	± 1	± 3									
		II	224A				+25	+425						
		↓	224B				+42	+500						
		III	224C				+102	+4570						
		↓	224D				+106	+480						
	Thermal	I	225			± 3			-10	-10				
		II	↓			↓			-40	-40				
		I	226			± 6			- 9	- 9				
		III	↓			↓			-60	-60				
											-46	-79	-67	-28
Ge-Si Alloy (p)	Hall	C	229A	± 8	± 2									
		II	230A				+28	+91						
		↓	230B				+27	+104						
		III	232A				+54	+107						
		↓	232B				+123	+635						
	Thermal	I	234			±20			<20	<20				
		II	↓			↓			-25	-25				
		I	236			±10			<10	<10				
		III	↓			↓			-55	-55				
											+ 9	+43	-18	-36
Bi_2Te_3 (z)	Hall	C	246A	± 1	± 1									
		II	245B				+ 8	-19						
		III	245C				+34	- 5						
		↓	245D				+59	+ 8						
	Thermal	I	239			± 3			< 3	< 3				
		II	↓			↓			-20	-20				
		I	206A			±30			<30	<30				
		III												

		II	230A				+28	+91							
		↓	230B				+27	+104							
		III	232A				-54	+107							
		↓	232B				+123	+635							
	Thermal	I	234			±20			<20	<20					
		II	↓			↓			-25	-25					
		I	236			±10			<10	<10					
		III	↓			↓			-55	-55					
											+ 9	+43	-18	-36	
Bi_2Te_3 (n)	Hall	C	246A	± 1	± 1										
		II	245B				+ 8	-19							
		III	245C				+34	- 5							
		↓	245D				+59	+ 8							
	Thermal	I	239			± 3			< 3	< 3					
		II	↓			↓			-20	-20					
		I	206A			±30			<30	<30					
		III	↓			↓			-45	-45					
											-81	+287	+45	+113	
GeTe-$AgSbTe_2$	Hall	C	251E	± 1	± 3										
		II	↓				+ 2	< 3							
Alloy (p)		↓	251A				+ 7	↓							
		III	251B				+ 5								
	Thermal	I	A			± 3			- 4	- 4					
		III	↓			↓			-15	-15					
		I	C			± 4			< 4	< 4					
											+12	+15	+10	+ 6	
CoSi (n)	Hall	C	252C	± 1	± 1										
		II	↓				- 4	+33							
		III	252A				-40	+170							
		↓	252B				-44	-160							
	Thermal	I	CoSi I			±16			≤16	≤16					
		III	↓						-75	-75					
											-	-49	-31	-87	
Bi_2Te_3 (p)	Hall	C	254A	± 4[5]	± 2										
		II	254B				< 4	< 2							
		↓	254C				+ 6	- 9							
		III	254D				+ 5	-12							
		↓	254E				< 4	< 2							
	Thermal		254			± 5			+310	0[6]	-	+13	+10	+13	
Bi_2Te_3 (single	Hall	C	255A	< 1[5]	± 3										
		II	255C			- 3	< 3								
		III	255E			< 1	↓								
			255F			↓									
	Thermal		255			± 7			-20	-20	-	+25	-6	0	

[1] Key: C ~ pre-irradiation calibration runs, exposure dose = 0.
I ~ exposure dose = 1.0×10^{17} fast (E > 1 MeV) neutrons/cm².
II ~ exposure dose = 1.6×10^{18} fast (E > 1 MeV) neutrons/cm².
III ~ exposure dose = 2.3×10^{19} fast (E > 1 MeV) neutrons/cm².

[3] Calculations based on assumption no further annealing occurs in α.

[4] Calculations based on assumption that all observed radiation-induced change in α anneals out completely.

[5] Calculations based on assumption that change in α equals precision limit.

[6] Given in % of room-temperature value.

[7] Effect of specific heat dominates.

RECOMMENDATIONS

Within the limits imposed by a short supply of data concerning thermal diffusivity and related quantities, this study has shown that the possibility of modifying the thermoelectric figure of merit through a combination of reactor bombardment and post-irradiation heating treatments, is not negligible. Consequently, we recommend that of the effort devoted to developing new power sources for Navy use, a portion be devoted to further exploration of radiation effects on thermoelectric properties.

Part of the effort devoted to this particular exploration should be aimed at extending measurement capability in two ways: first, to increase the supply of data concerning thermal diffusivity and related quantities by adding the capability of measuring specific heat and density of the thermal samples, and extending the range of temperatures over which these quantities and thermal diffusivity can be measured; and second, by adding the capability of measuring thermal conversion efficiency directly. These measurements would contribute useful engineering data to the field.

A second part of the effort devoted to this particular exploration should be spent gathering more data, both on new materials, and on certain materials already examined. A specific example of the latter suggested by the results of the current study is the germanium-silicon alloy class of materials, a suggestion acquiring extra support by virtue of its low mass density. Thus, a continuing, relatively low level, program of materials investigations is recommended. Such a program also would be expected to contribute useful engineering data to the field.

Finally, the remainder of the effort devoted to this particular exploration should be devoted to extending understanding of the mechanisms by which the observed changes occur. This area is sufficiently complicated that the likelihood of stumbling merely by chance onto the right combination of materials constituents, and irradiation and post-irradiation treatments, to produce optimal materials, is negligibly small. Thus, a continuing, relatively low level, program of investigating basic properties of the high-z materials, e.g., Hall mobility, and the effects of reactor bombardment on these properties, is also recommended.

Current personnel limitations preclude this laboratory from conducting such further exploration as an in-house effort. Consequently, it is recommended that such exploration be conducted either at other Navy laboratories, or by contract to non-Navy research organizations.

REFERENCES

1. J. W. Winslow and R. R. Hart, "Radiation Effects in Thermoelectrics 1. Techniques for Detection of Transient Effects and Their Application for Detection of Transient Effects and Their Application to Commercial Grade Bismuth Telluride," USNRDL-TR-581, September 1962.

2. A. F. Ioffe, "Semiconductor Thermoelements and Thermoelectric Cooling," Infosearch, Ltd., London, 1957.

3. J. C. Corelli and R. T. Frost, "Effects of Reactor Irradiation on the Thermoelectric Properties of Lead and Bismuth Tellurides," Knolls Atomic Power Laboratory, KAPL-201, April 1960.

4. G. R. Kilp and P. V. Mitchell, "Radiation Effects on Thermoelectric Materials," Westinghouse Electric Corporation, WCAP-1680, May 1961.

5. A. G. Samilovich and L. L. Korenbilt, "Thermoelectric Eddy Currents in an Anisotropic Medium,"Sov. Phys. Solid State 3, 1494(1962).

6. J. W. Winslow, R. R. Hart and J. C. Boteler, "A High Precision System for Measuring Seebeck Coefficient Electrical Resistivity, and Hall Coefficient in Inhomogeneous Thermoelectric Materials," USNRDL-TR-850, May 1965.

7. W. J. Parker, et al., "Flash Method of Determining Thermal Diffusivity, Heat Capacity, and Thermal Conductivity," USNRDL-TR-424, May 1960.

8. L. A. Webb, "Techniques for Shaping and Polishing a Number of Compound Semi-Conductors," USNRDL-TR-882, August 1965.

BLANK PAGE

APPENDIX I: CALIBRATION PLOTS

APPENDIX I: CALIBRATION PLOTS

APPENDIX I - CALIBRATION PLOTS

ORDER OF PRESENTATION

This appendix presents the calibration data, from which estimates of the precision with which Seebeck coefficient and electrical resistivity could be measured, were made. These calibration data are presented for one sample of each material studied, namely PbTe, $Ge_{.95}Bi_{.05}Te$, Ag_2Se, n- and p-type Ge-Si alloys, Bi_2Te_3 (n-type), $(GeTe)_{90\%}(AgSbTe_2)_{10\%}$, CoSi, Bi_2Te_3 (p-type), and single crystal Bi_2Te_3, in that order.

The data are grouped by sample, with four plots presented for each. In each case the first and second plots show the temperature dependence of apparent Seebeck coefficient, while the third and fourth show the temperature dependence of electrical resistivity. The first and third plots present the data taken on both the heating and cooling portions of the calibration runs, while the second and fourth present only the cooling data, the estimates of precision being made from the latter.

COORDINATES, SYMBOLS AND LABELS

The data are presented in terms of apparent Seebeck coefficient and electrical resistivity, plotted as functions of the average sample temperature. These variables are the same quantities presented in Appendix II, and are defined in further detail there.

The symbols used for the calibration data are taken from the numeric system, augmented by the symbol - to represent 11 and by + to represent 12. In one case it was necessary to use two geometric symbols as well. Odd numbers are used to indicate data taken while the sample was heating, and even for those taken while the sample was cooling. Detailed identifications of the symbols used, including segregation by mounting, are given in Table I/1.

In some cases a power of ten is shown following an axis label. In these cases the numbers shown along the corresponding axis are to be multiplied by that power of ten. For example, in Fig. I/1, the abscissa ranges from -50 to +350°C above room temperature.

DATA ACCEPTANCE-REJECTION

The data presented are complete except for those removed by a gross editing process, largely visual. Points obviously falling many standard deviations away from the main trace have been rejected summarily. In addition, those taken during periods when the equipment is known to have been malfunctioning* have been rejected. The remaining data presumably include a number of points which a more sophisticated editing process would have rejected. Limitations on time available, however, have precluded application of such processes, and some questionable points have been included.

---

*Certain malfunctioning of the equipment is discussed in reference number 6.

Table I/1

Symbols used in calibration plots. (↑ = sample heating. ↓ = sample cooling.)

Sample	Material (and type)	I ↑ : ↓	II ↑ : ↓	III ↑ : ↓	IV ↑ : ↓	V ↑ : ↓	VI ↑ : ↓
136A	PbTe (p)	1,3,5:2,4,6	7:8	9:0	None	None	None
145A	$Ge_{.95}Bi_{.05}Te$(p)	1:2	3:4	5,7,9:6,8,0			
178A	Ag_2Se (n)	1,3,5:2,4,6	7:8	9:0			
222A	Ge-Si Alloy (n)	1:2	3,5,.4,6 7,9,:8,0	-:+			
229A	Ge-Si Alloy (p)	1,3,5:2,4,6	7:8	9:0	-:+	No data	□:◇
246A	Bi_2Te_3 (n)	1:2	3:4	5:6	7:8	None	None
251E	$(GeTe)_{90\%}(AgSbTe_2)_{10\%}$ (p)	1:2	3:4	5,7,9:6,8,0	None		
252C	CoSi (n)	1:2	3,5,7:4,6,8	9:0			
254A	Bi_2Te_3 (p)	1,3,5:2,4,6	7:8	9:0			
255A	Bi_2Te_3 (single crystal)(p)	1:2	3,5,7:4,6,8	9:0			

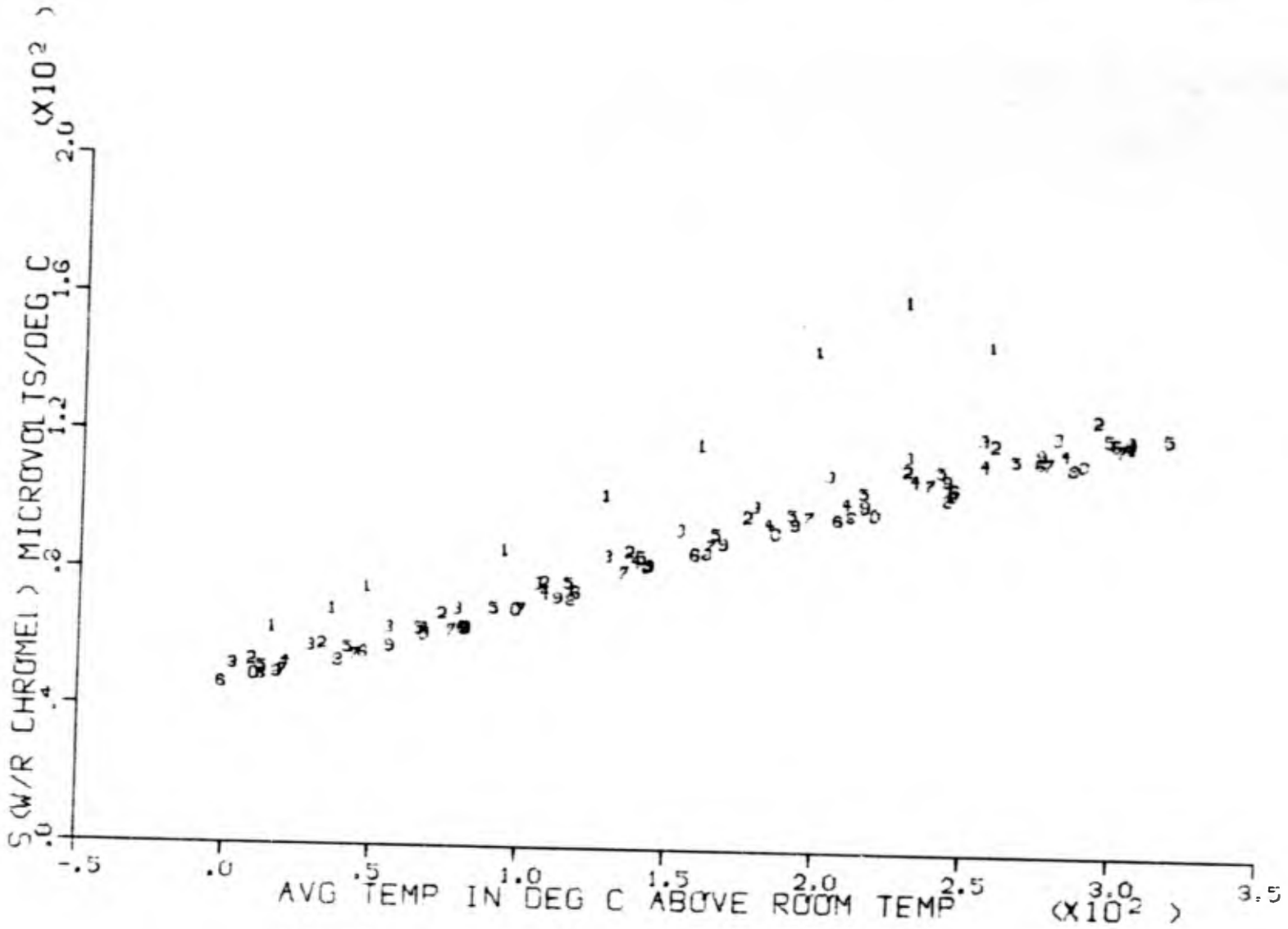

Fig. I/1. Temperature dependence of apparent Seebeck coefficient (with respect to chromel) of sample 136A (PbTe) (unirradiated), mounted three different times in the same measuring equipment. For key to symbols see Table I/1.

Fig. I/2. Temperature dependence (cooling runs only) of apparent Seebeck coefficient (with respect to chromel) of sample 136A (PbTe) (unirradiated), mounted three different times in the same measuring equipment. For key to symbols see Table I/1.

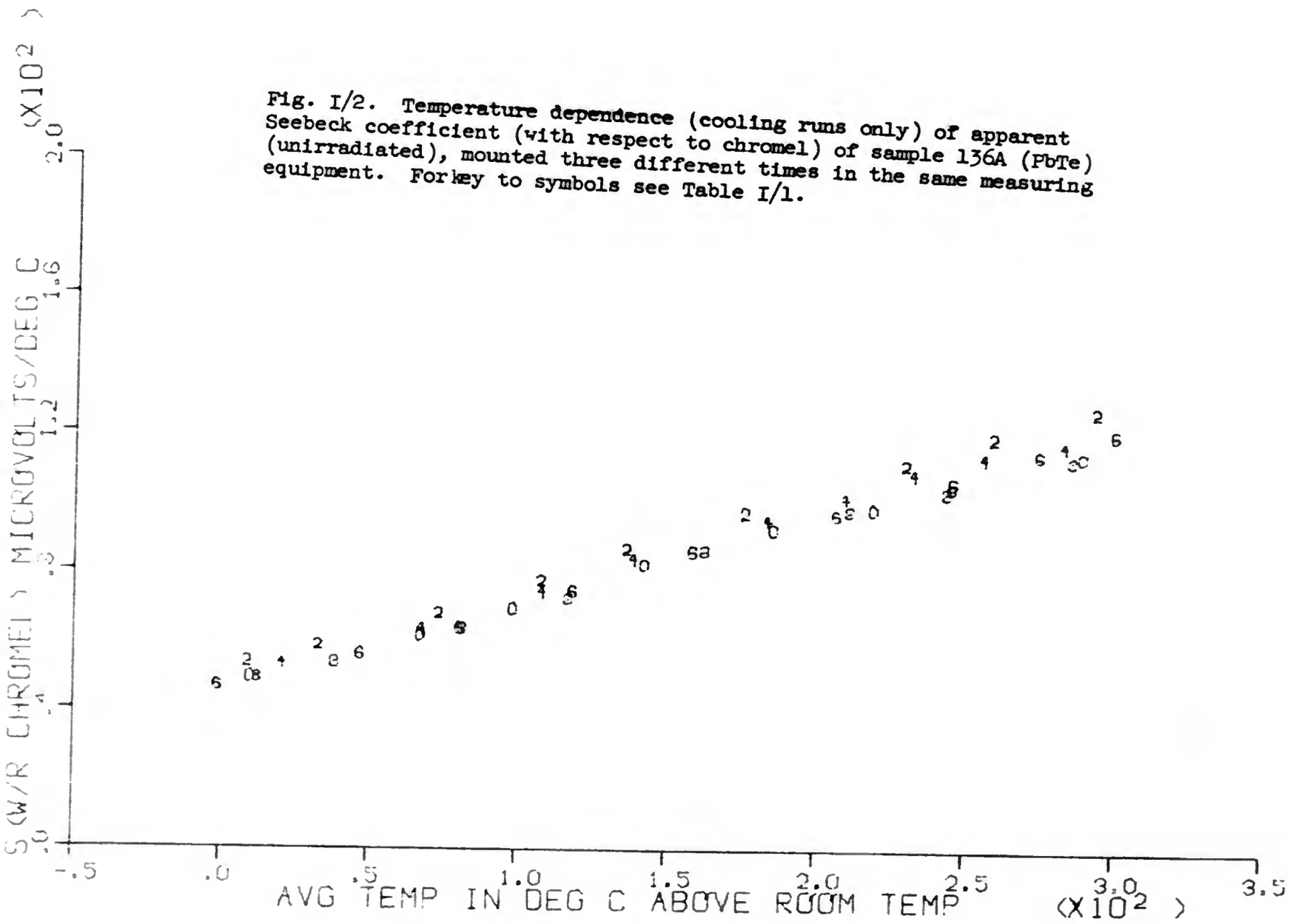

Fig. I/3. Temperature dependence of electrical resistivity of sample 136A (PbTe) (unirradiated), mounted three different times in the same measuring equipment. For key to symbols see Table I/1.

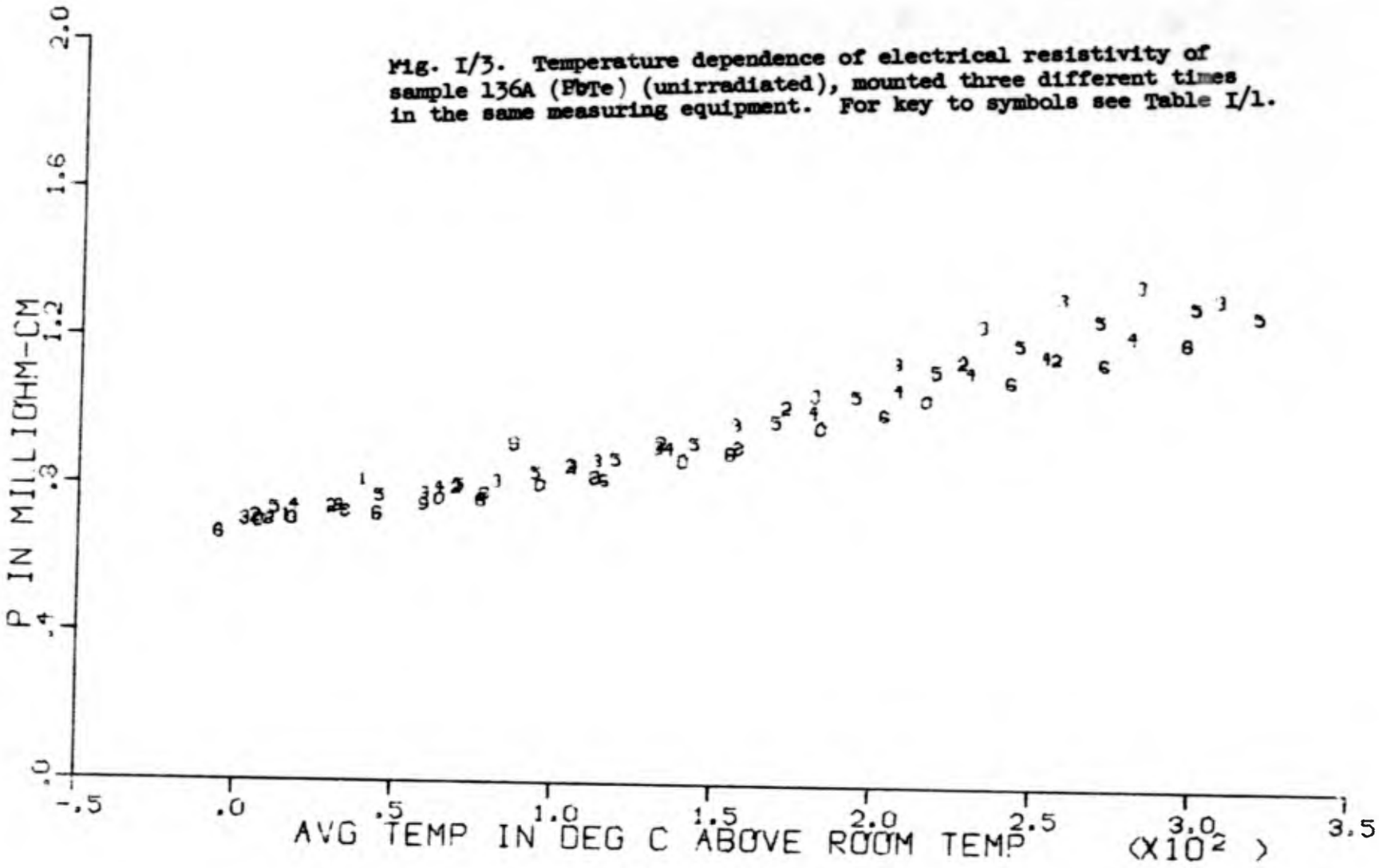

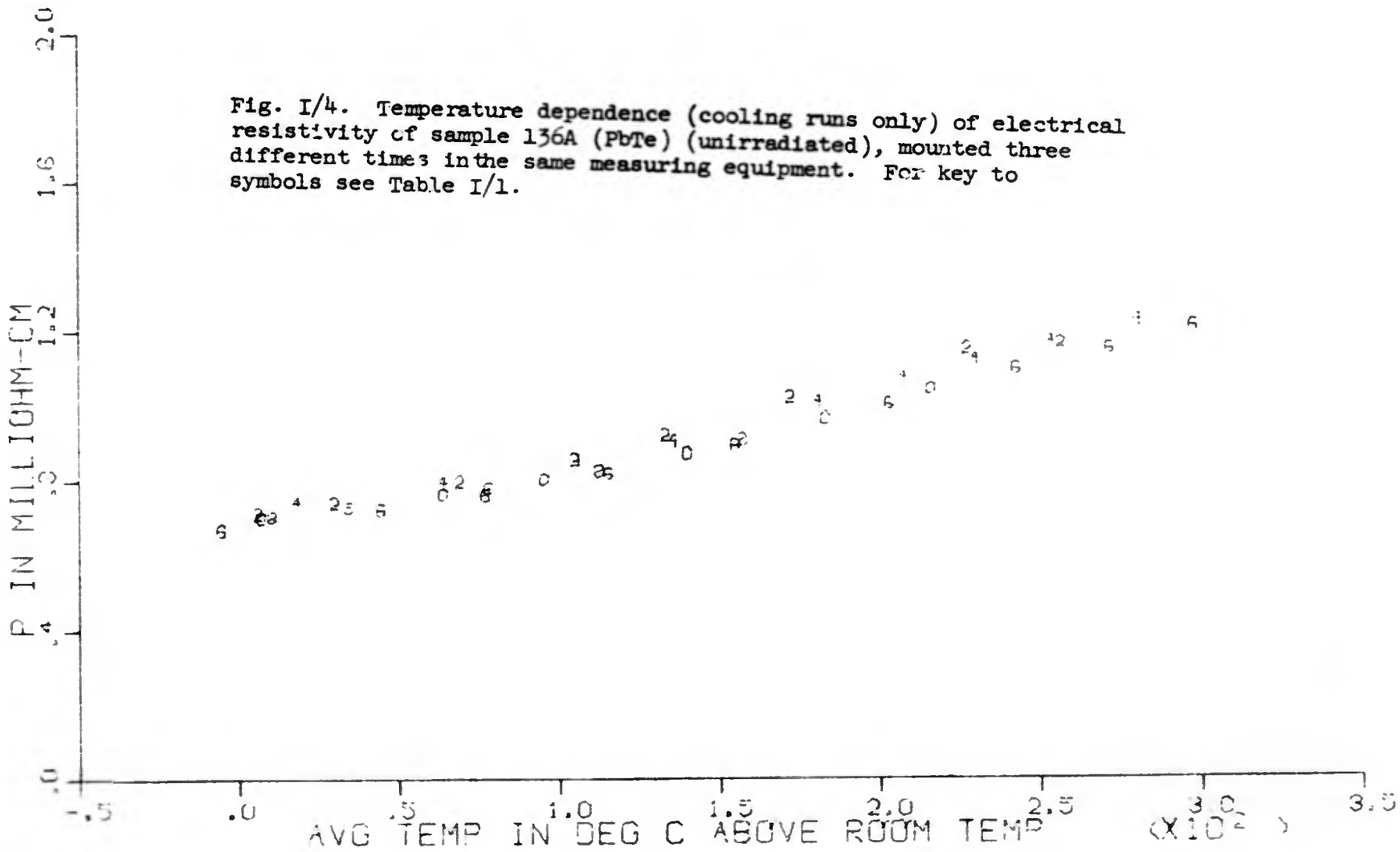

Fig. I/4. Temperature dependence (cooling runs only) of electrical resistivity of sample 136A (PbTe) (unirradiated), mounted three different times in the same measuring equipment. For key to symbols see Table I/1.

Fig. I/5. Temperature dependence of apparent Seebeck coefficient (with respect to chromel) of sample 145A ($Ge_{.95}Bi_{.05}Te$) (unirradiated), mounted three different times in the same measuring equipment. For key to symbols see Table I/1.

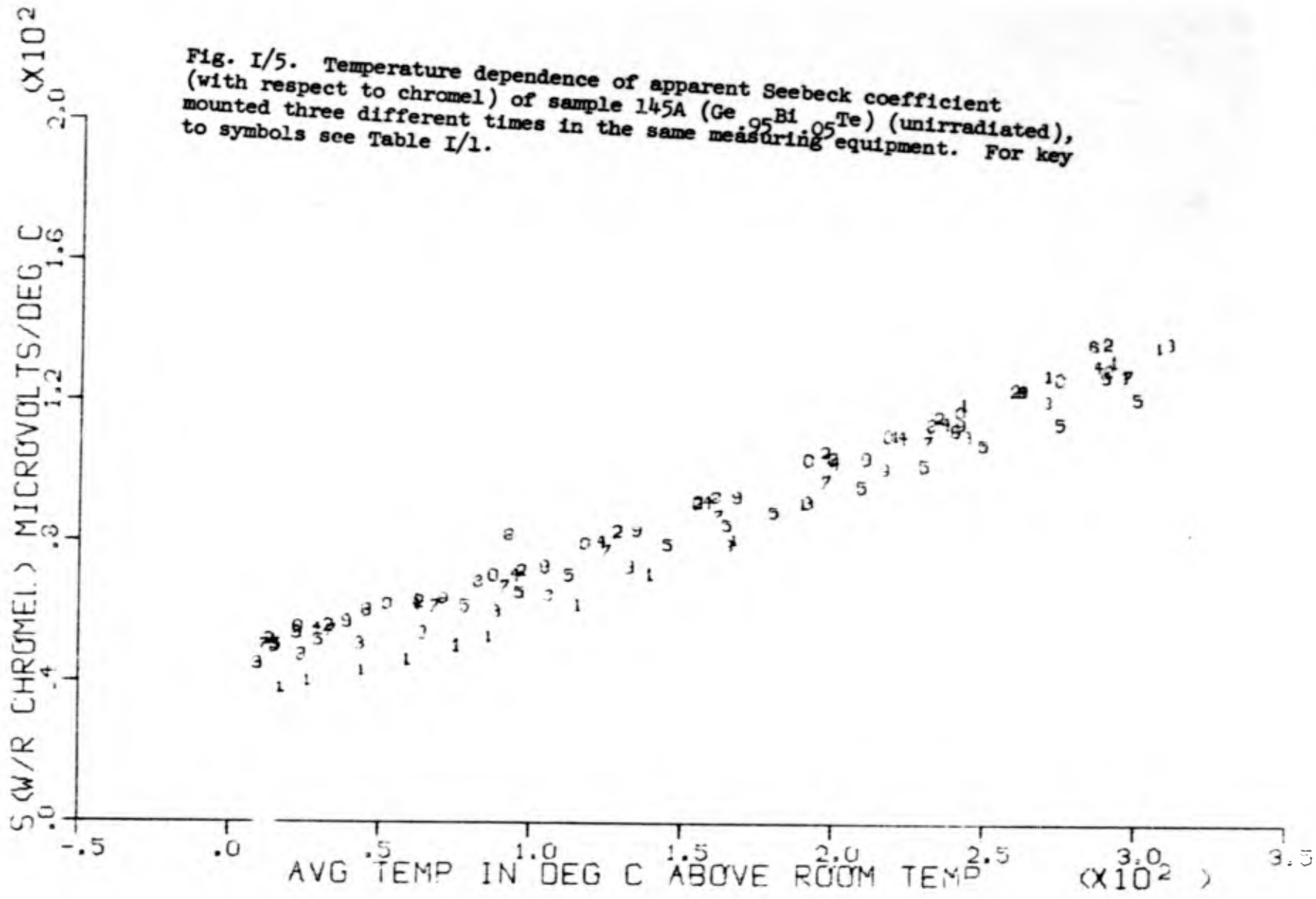

Fig. I/6. Temperature dependence (cooling runs only) of apparent Seebeck coefficient (with respect to chromel) of sample 145A ($Ge_{.95}Bi_{.05}Te$) (Unirradiated), mounted three different times in the same measuring equipment. For key to symbols see Table I/1.

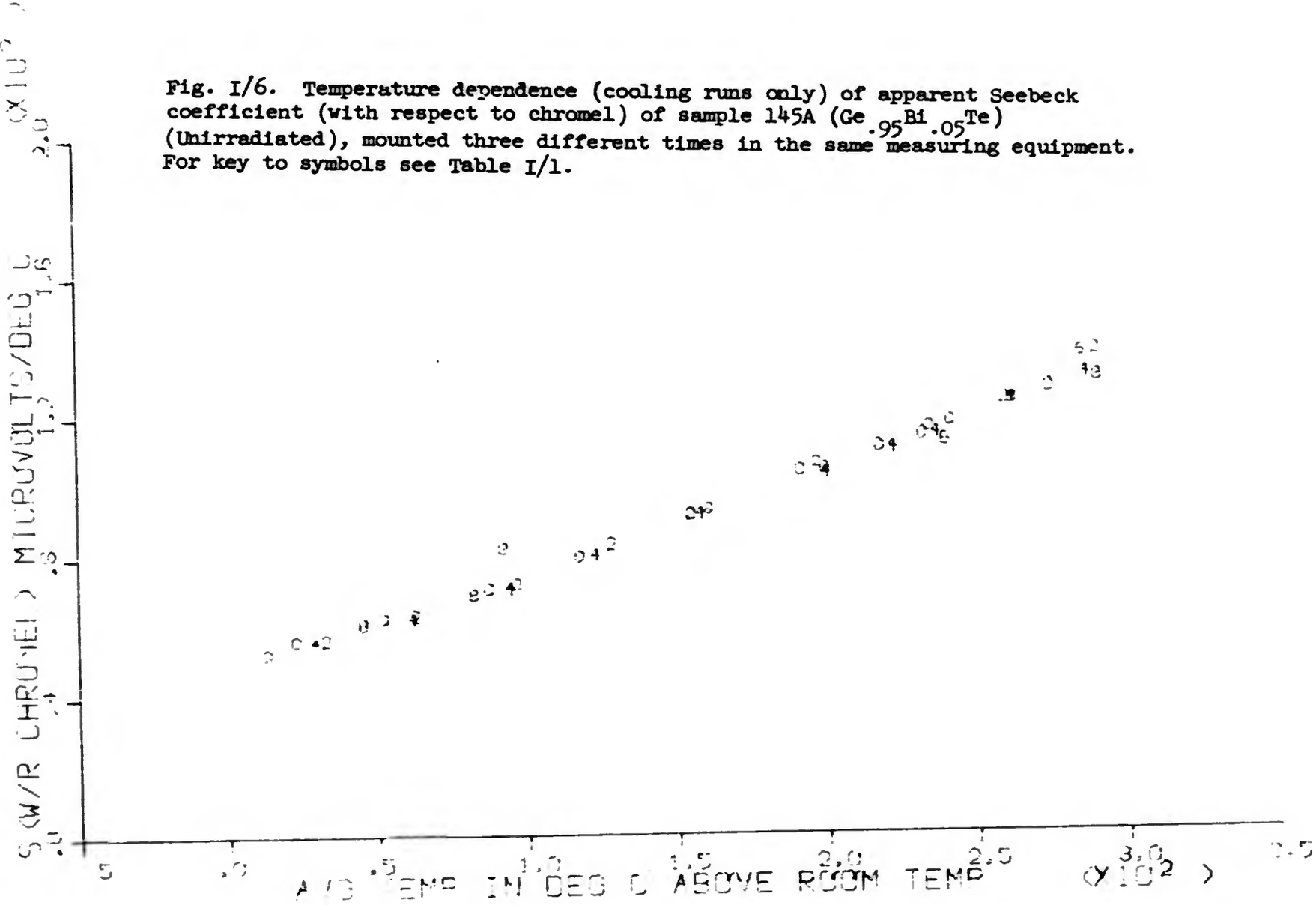

Fig. I/7. Temperature dependence of electrical resistivity of sample 145A ($Ge_{.95}Bi_{.05}Te$) (unirradiated), mounted three different times in the same measuring equipment. For key to symbols see Table I/1.

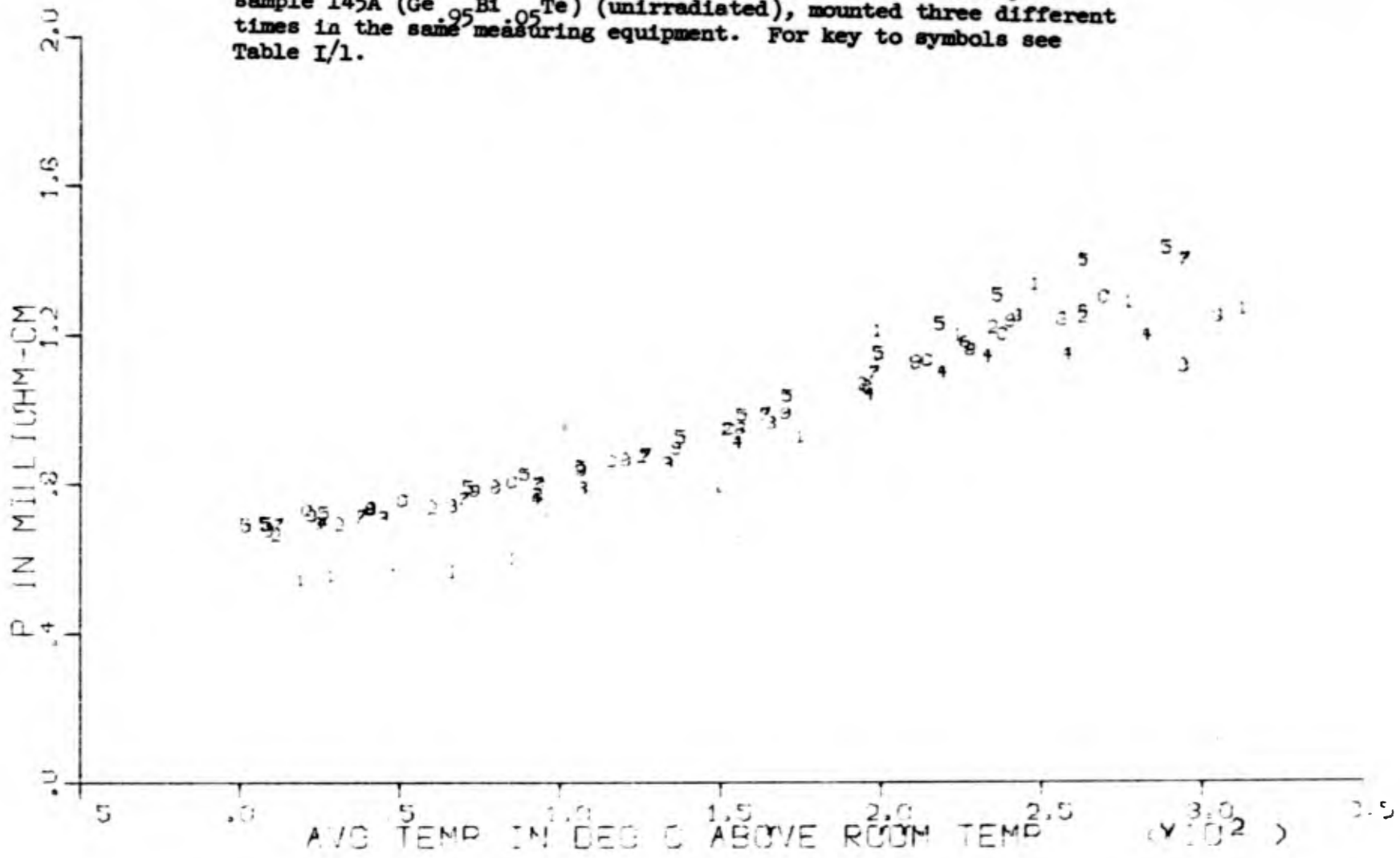

Fig. I/8. Temperature dependence (cooling runs only) of electrical resistivity of sample 145A ($Ge_{.95}Bi_{.05}Te$) (unirradiated), mounted three different times in the same measuring equipment. For key to symbols see Table I/1.

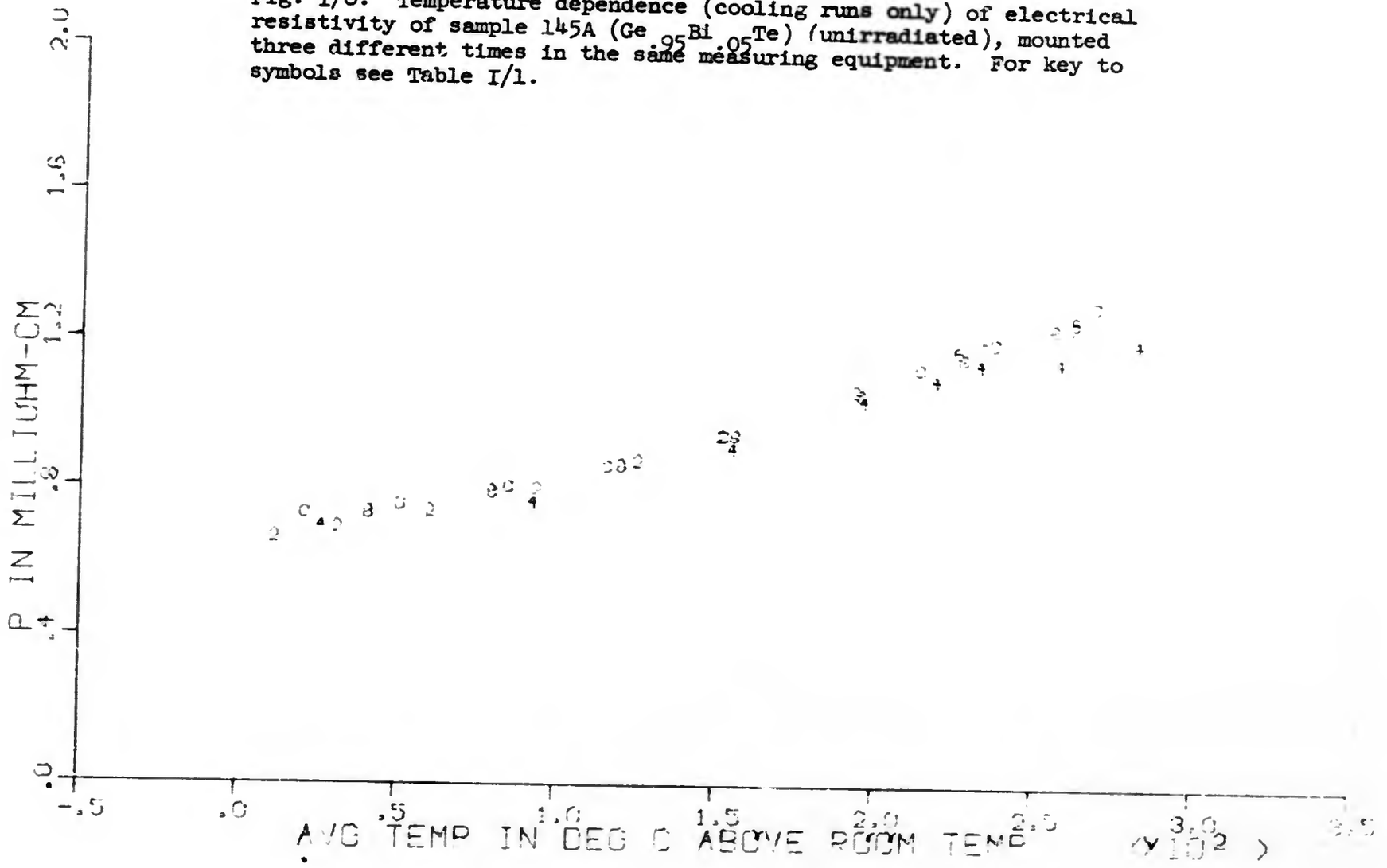

Fig. I/9. Temperature dependence of apparent Seebeck coefficient (with respect to chromel) of sample 178A (Ag_2Se) (unirradiated), mounted three different times in the same measuring equipment. For key to symbols see Table I/1.

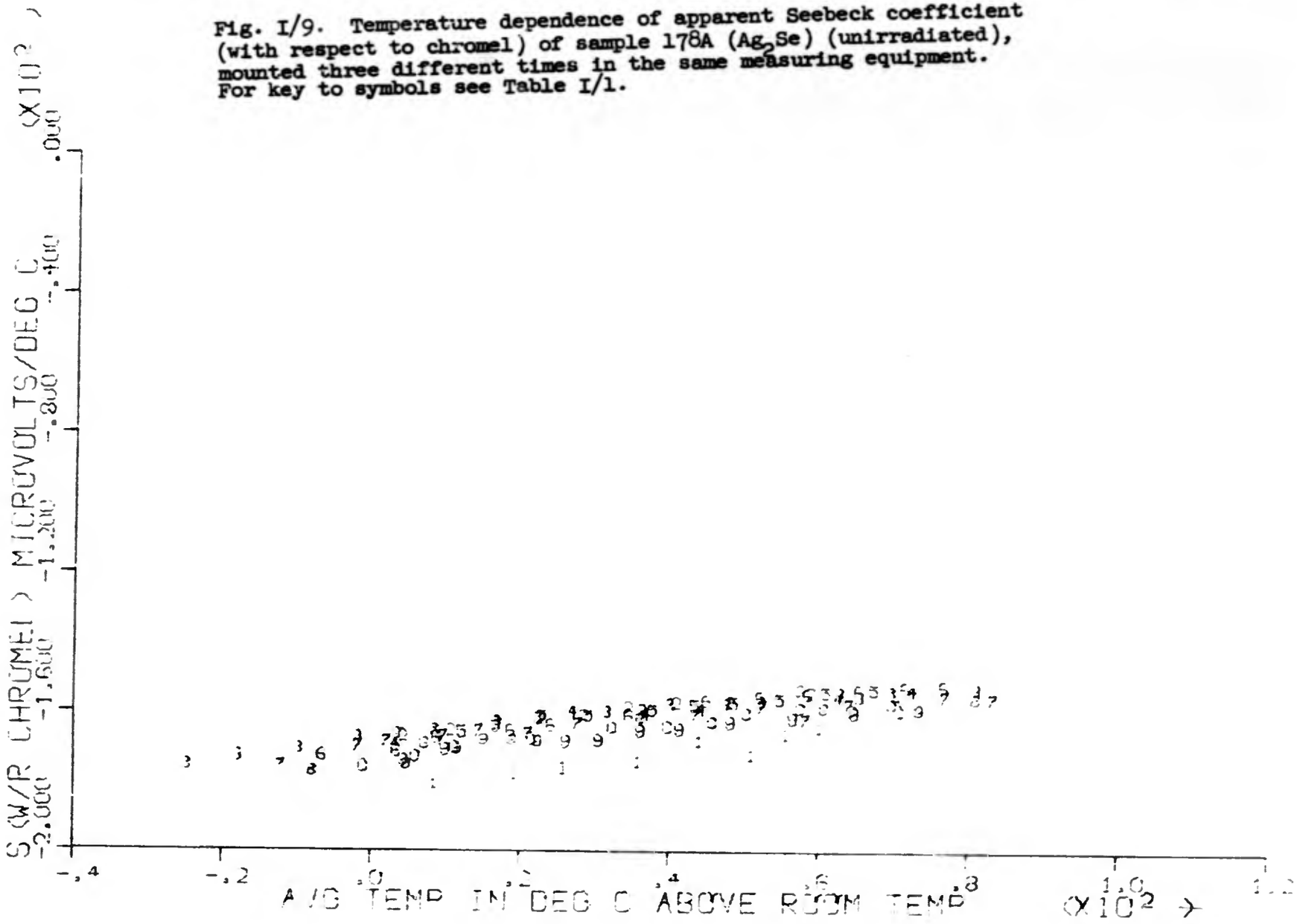

Fig. I/10. Temperature dependence (cooling runs only) of apparent Seebeck coefficient (with respect to chromel) of sample 178A (Ag_2Se) (unirradiated), mounted three different times in the same measuring equipment. For key to symbols see Table I/1.

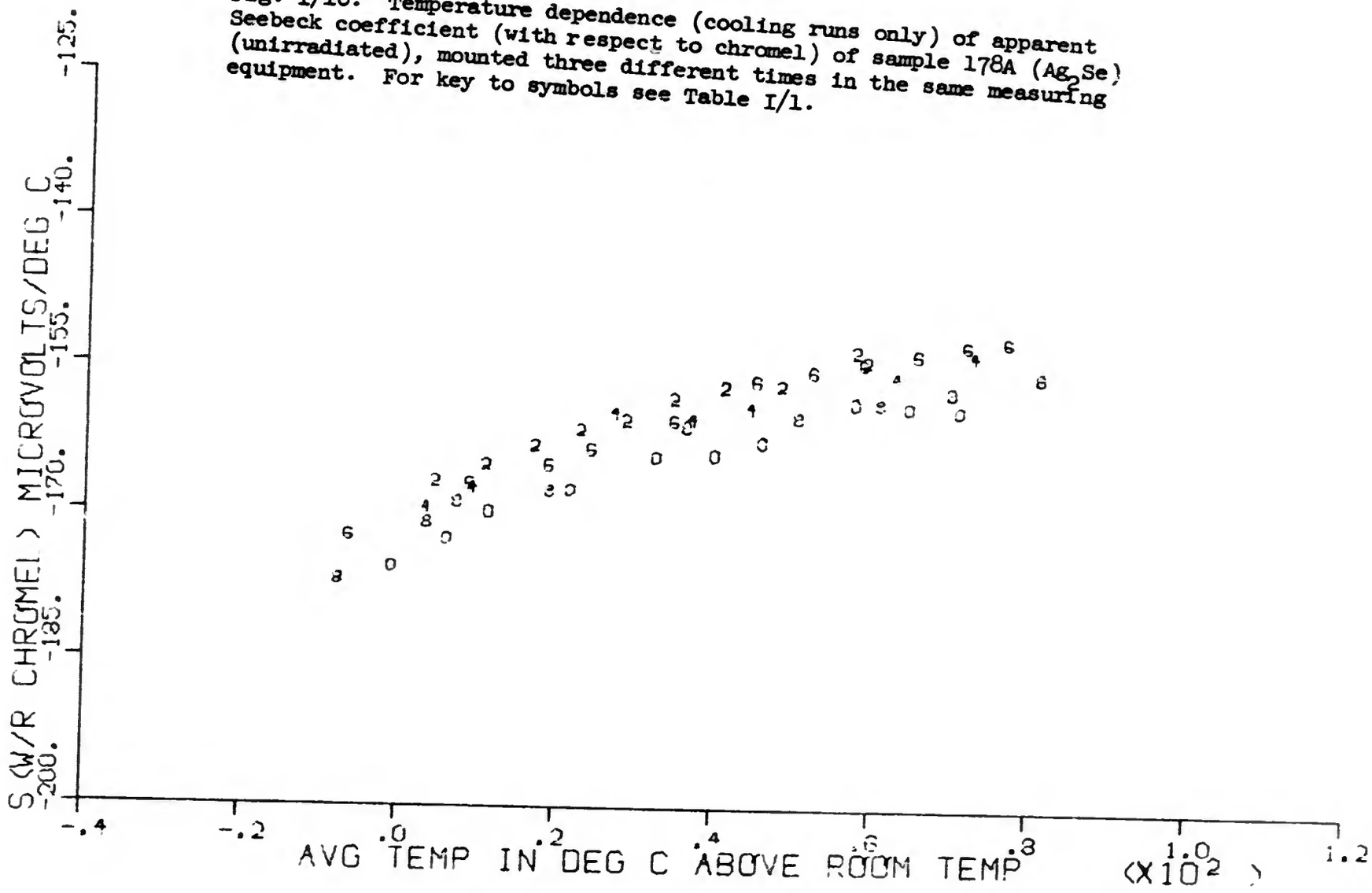

Fig. I/11. Temperature dependence of electrical resistivity of sample (Ag_2Se)(unirradiated), mounted three different times in the same measuring equipment. For key to symbols see Table I/1.

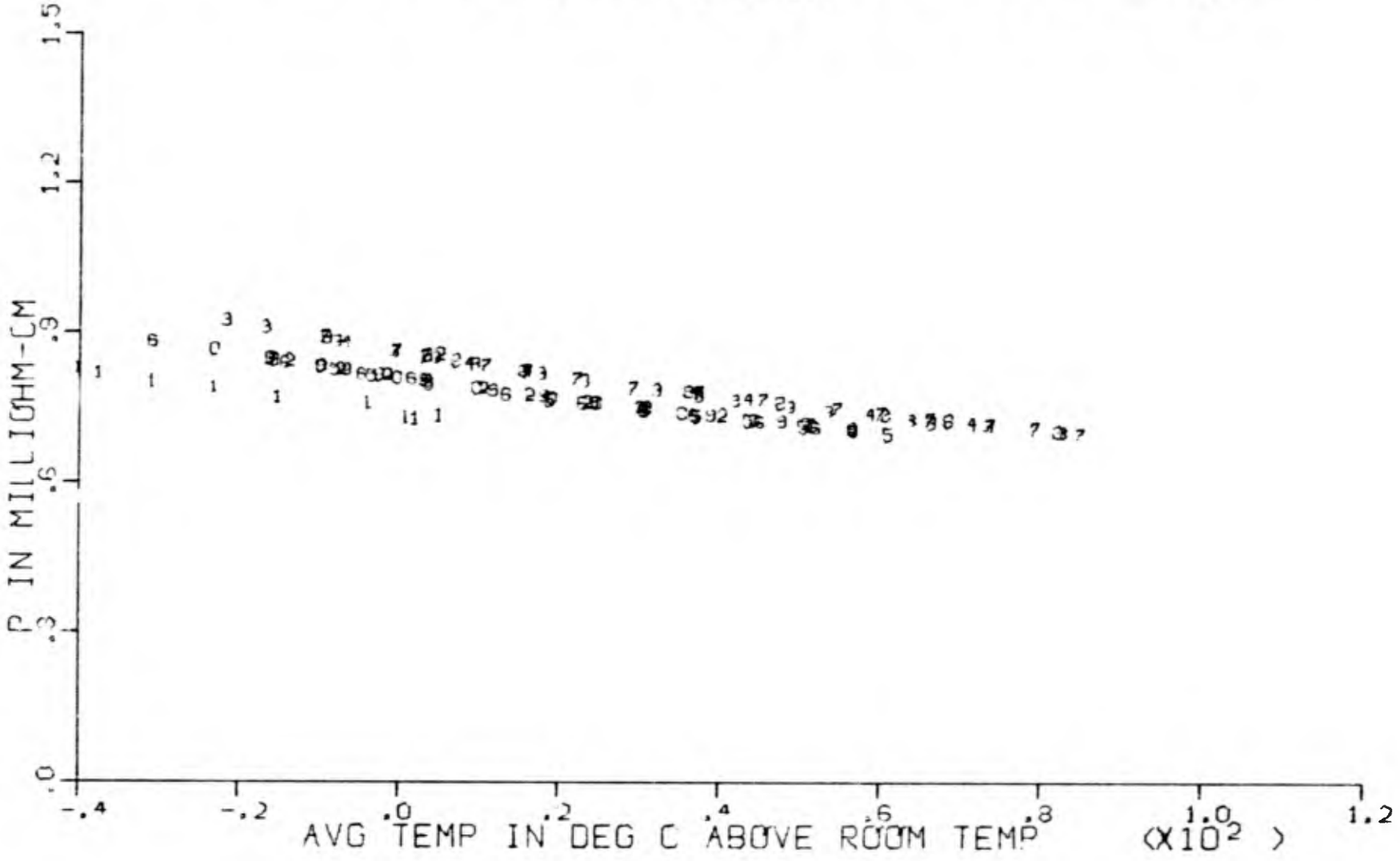

Fig. I/12. Temperature dependence (cooling runs only) of electrical resistivity of sample 178A (Ag_2Se) (unirradiated), mounted three different times in the same equipment. For key to symbols see Table I/1.

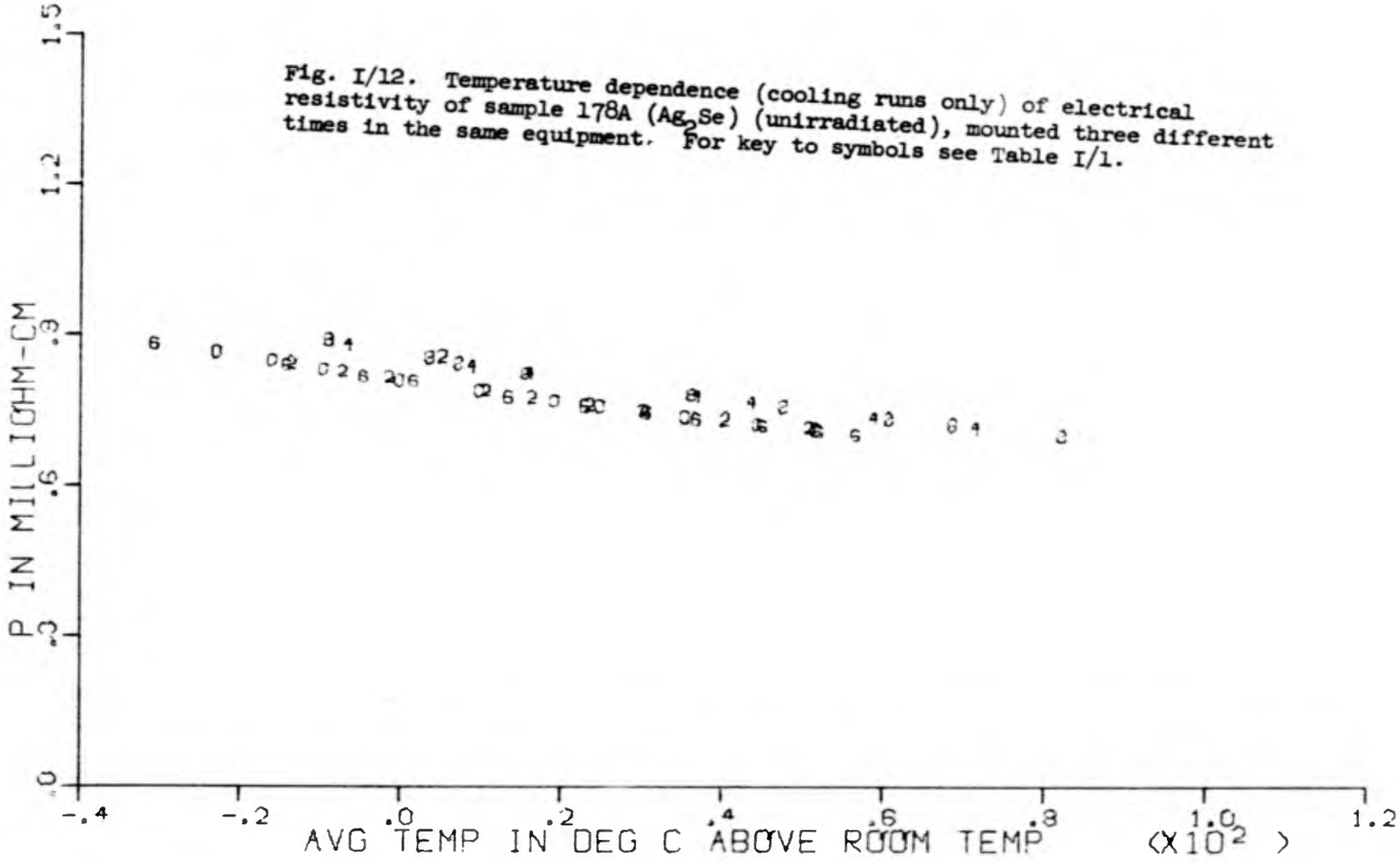

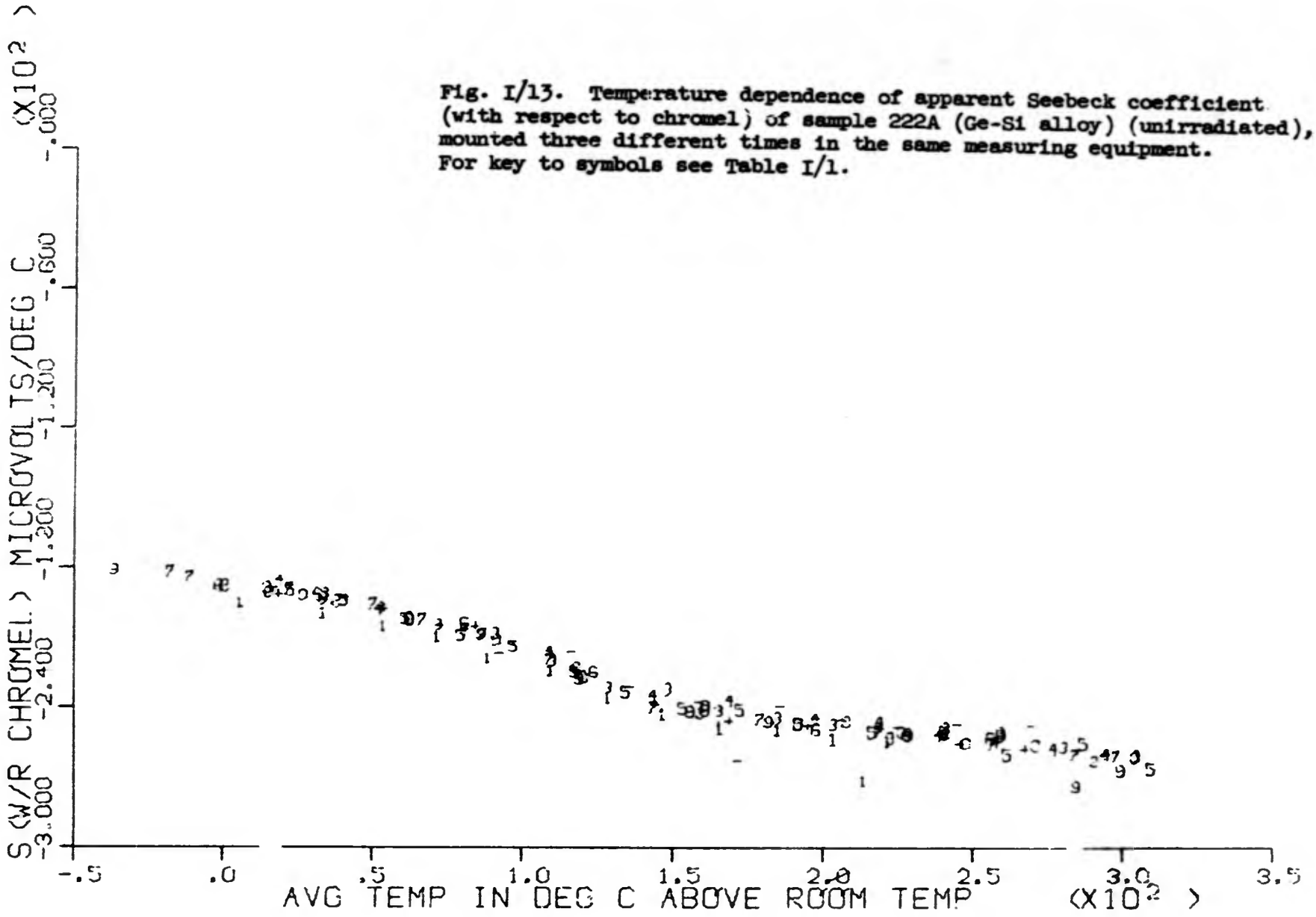

Fig. I/13. Temperature dependence of apparent Seebeck coefficient (with respect to chromel) of sample 222A (Ge-Si alloy) (unirradiated), mounted three different times in the same measuring equipment. For key to symbols see Table I/1.

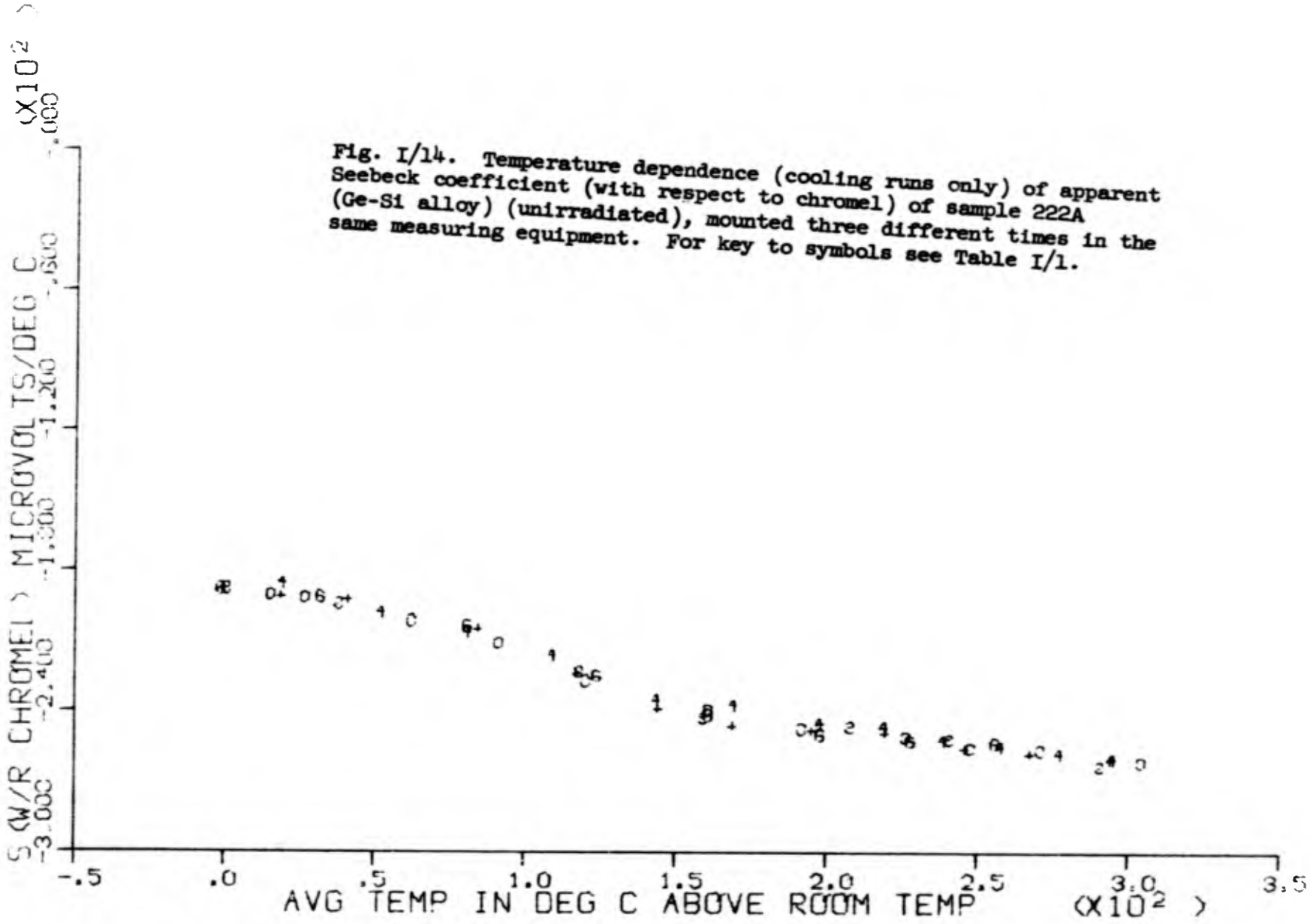

Fig. I/14. Temperature dependence (cooling runs only) of apparent Seebeck coefficient (with respect to chromel) of sample 222A (Ge-Si alloy) (unirradiated), mounted three different times in the same measuring equipment. For key to symbols see Table I/1.

Fig. I/15. Temperature dependence of electrical resistivity of sample 222A (Ge-Si alloy) (unirradiated), mounted three different times in the same measuring equipment. For key to symbols see Table I/1.

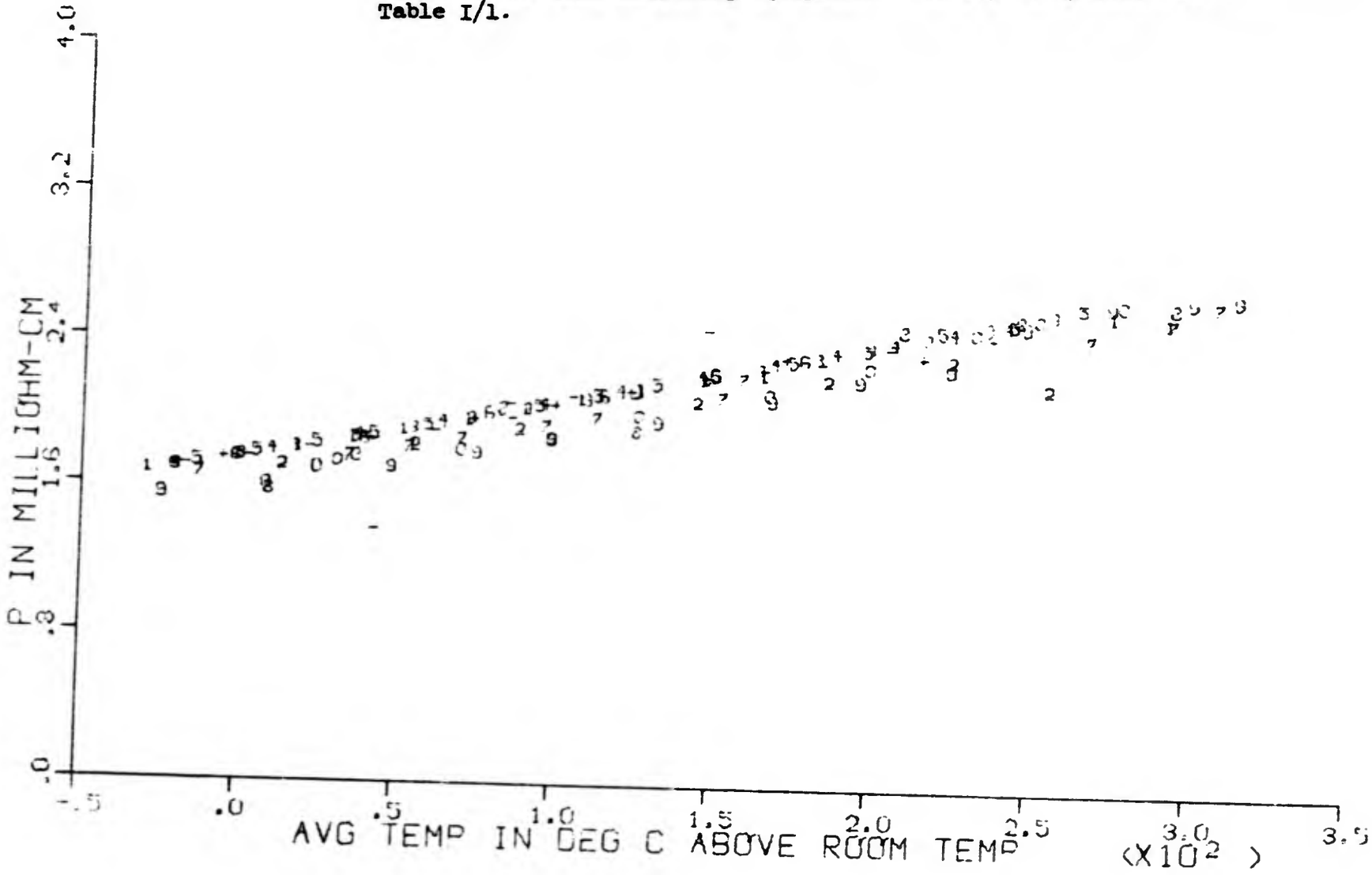

Fig. I/16. Temperat re dependence (cooling curves only) of electrical resistivity of sample 222A (Ge-Si alloy) (unirradiated), mounted three different times in the same mounting. For key to symbols see Table I/1.

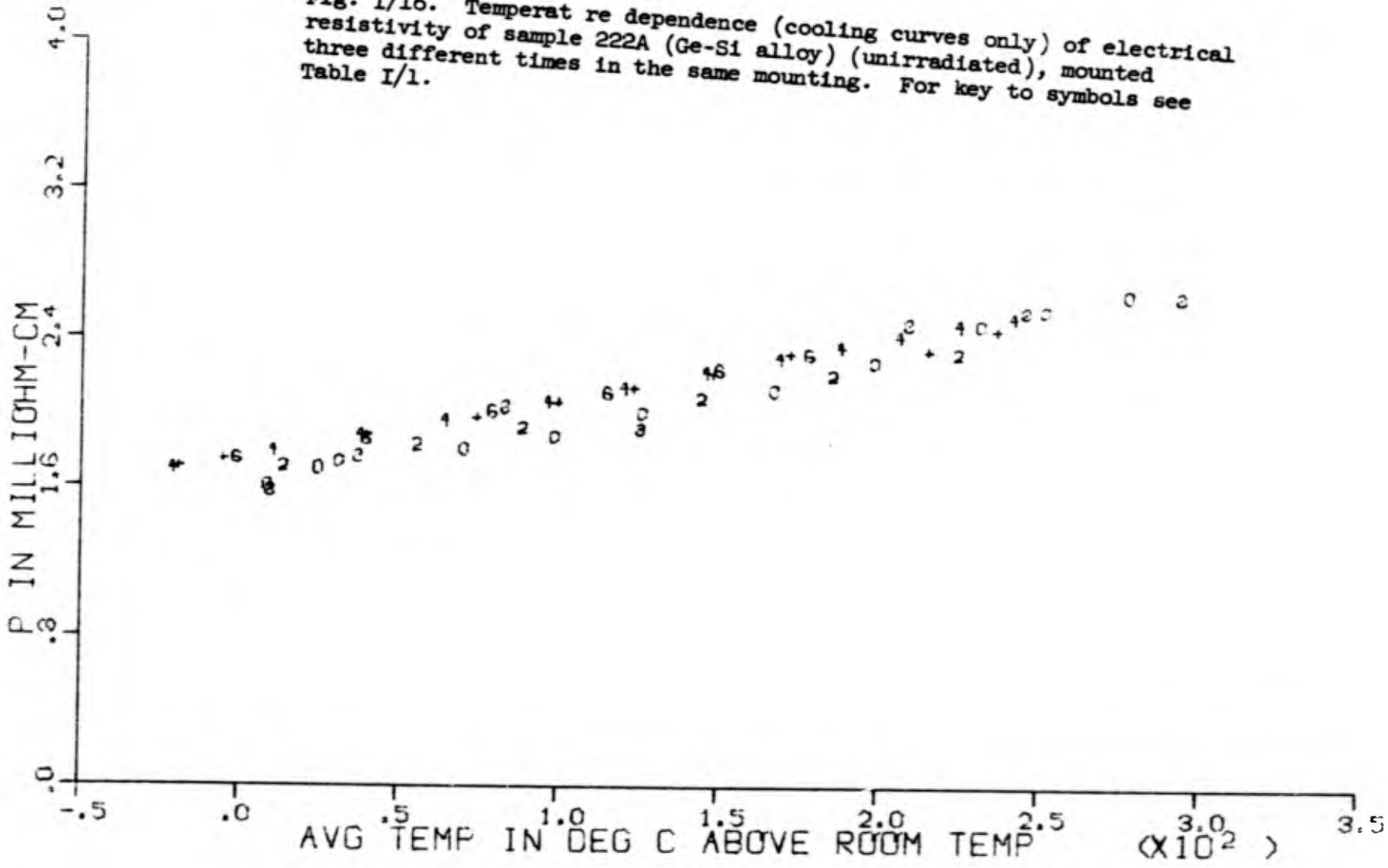

Fig. I/17. Temperature dependence of apparent Seebeck coefficient (with respect to chromel) of sample 229A (Ge-Si alloy) (unirradiated), mounted six different times in the same measuring equipment. For key to symbols see Table I/1.

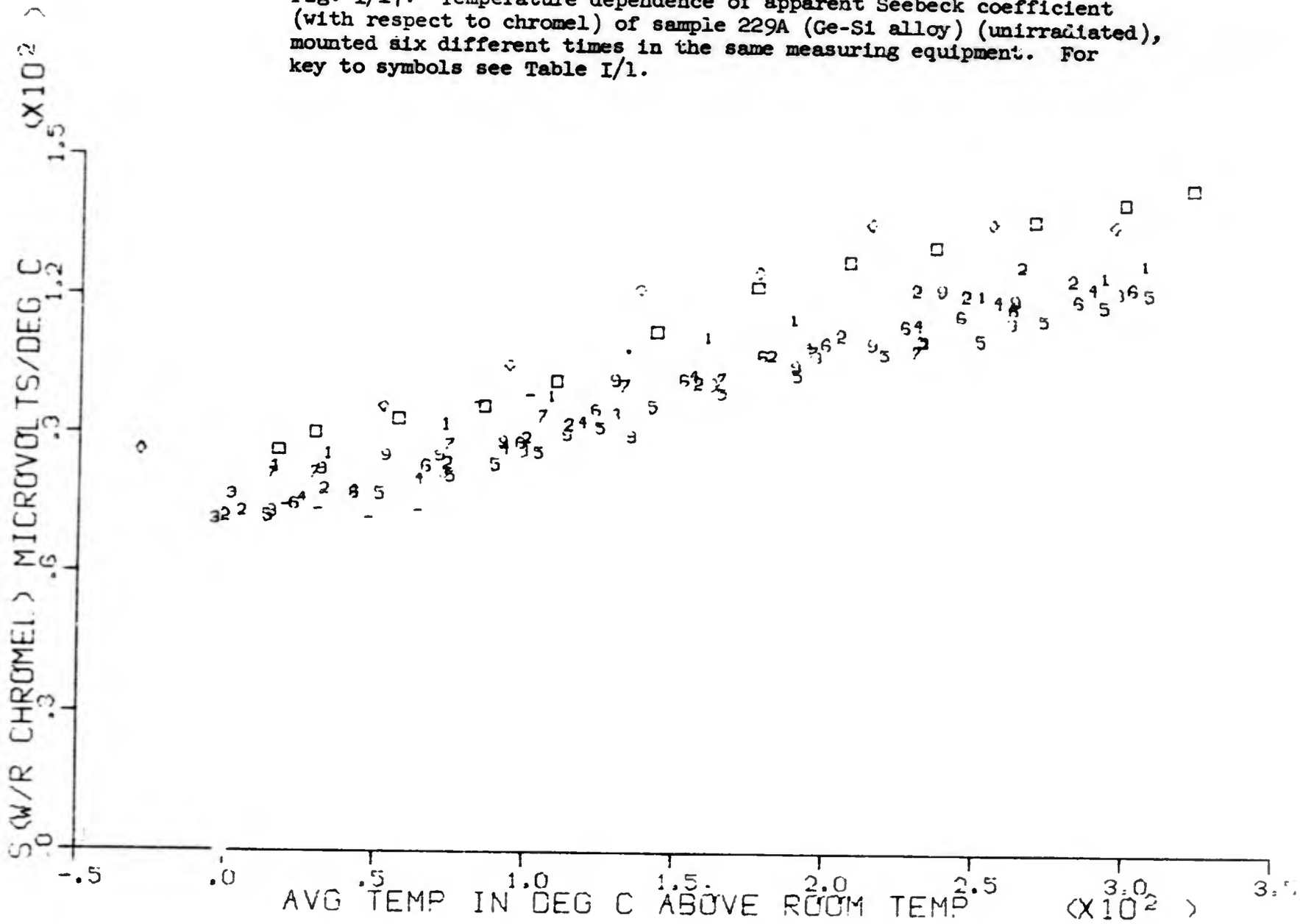

Fig. I/18. Temperature dependence (cooling runs only) of apparent Seebeck coeffient (with respect to chromel) of sample 229A (Ge-Si alloy) (unirradiated), mounted six different times in the same measuring equipment. For key to symbols see Table I/1.

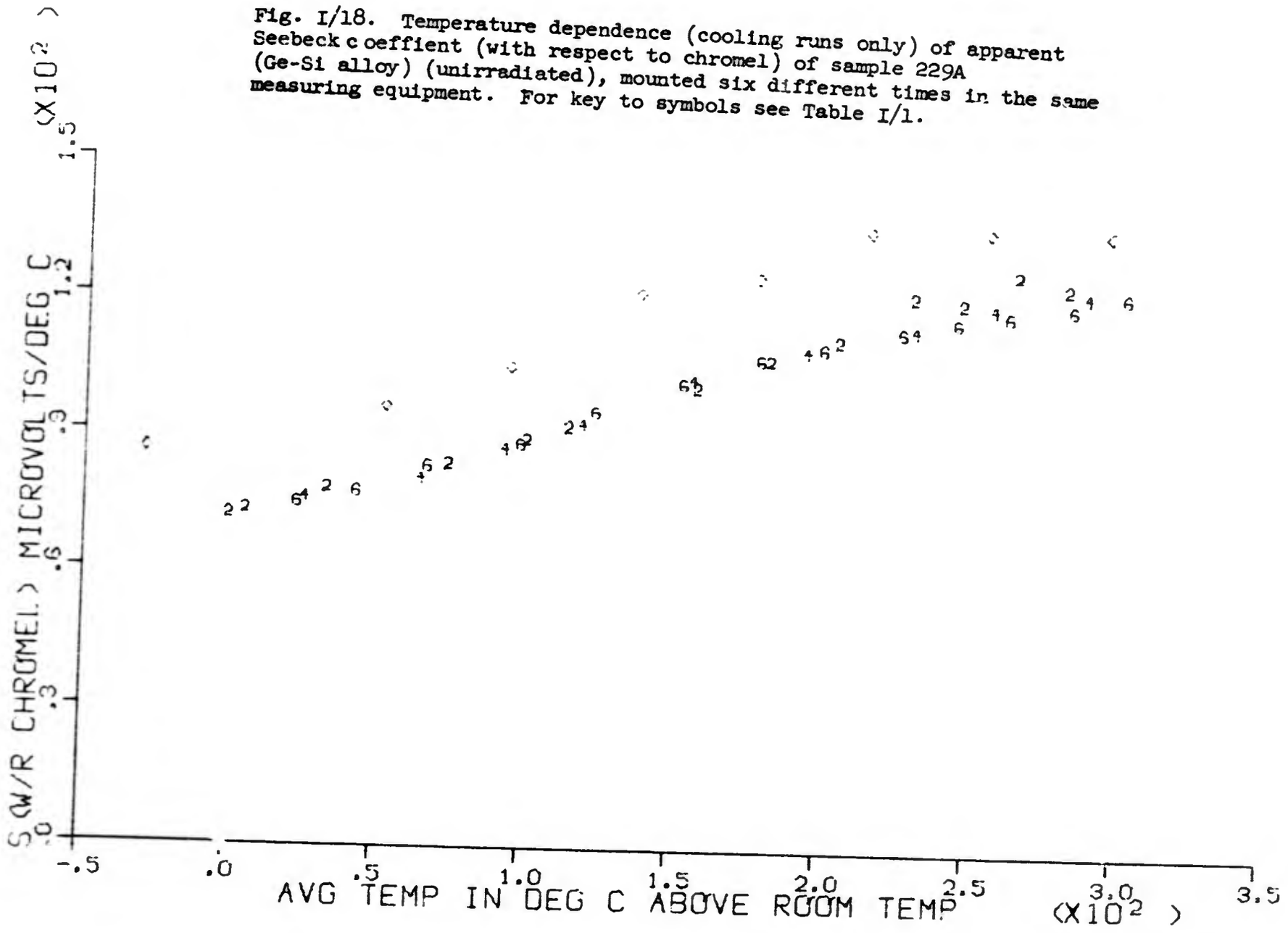

Fig. I/19. Temperature dependence of electrical resistivity of sample 22[illegible]A (Ge-Si alloy) (unirradiated), mounted six different times in the same measuring equipment. For key to symbols see Table I/1.

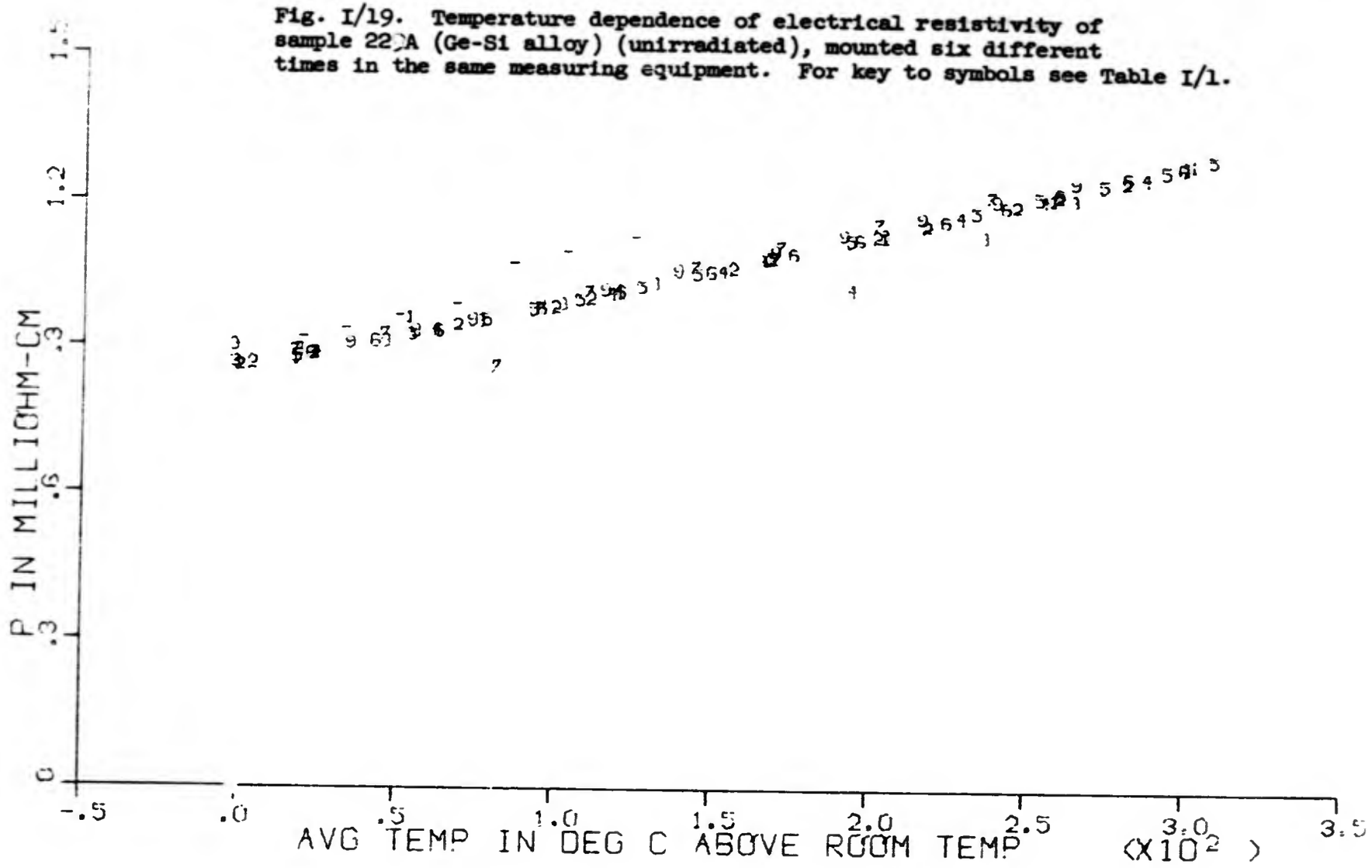

Fig. I/20. Temperature dependence (cooling runs only) of electrical resistivity of sample 229A (Ge-Si alloy) (unirradiated), mounted six times in the same measuring equipment. For key to symbols see Table I/1.

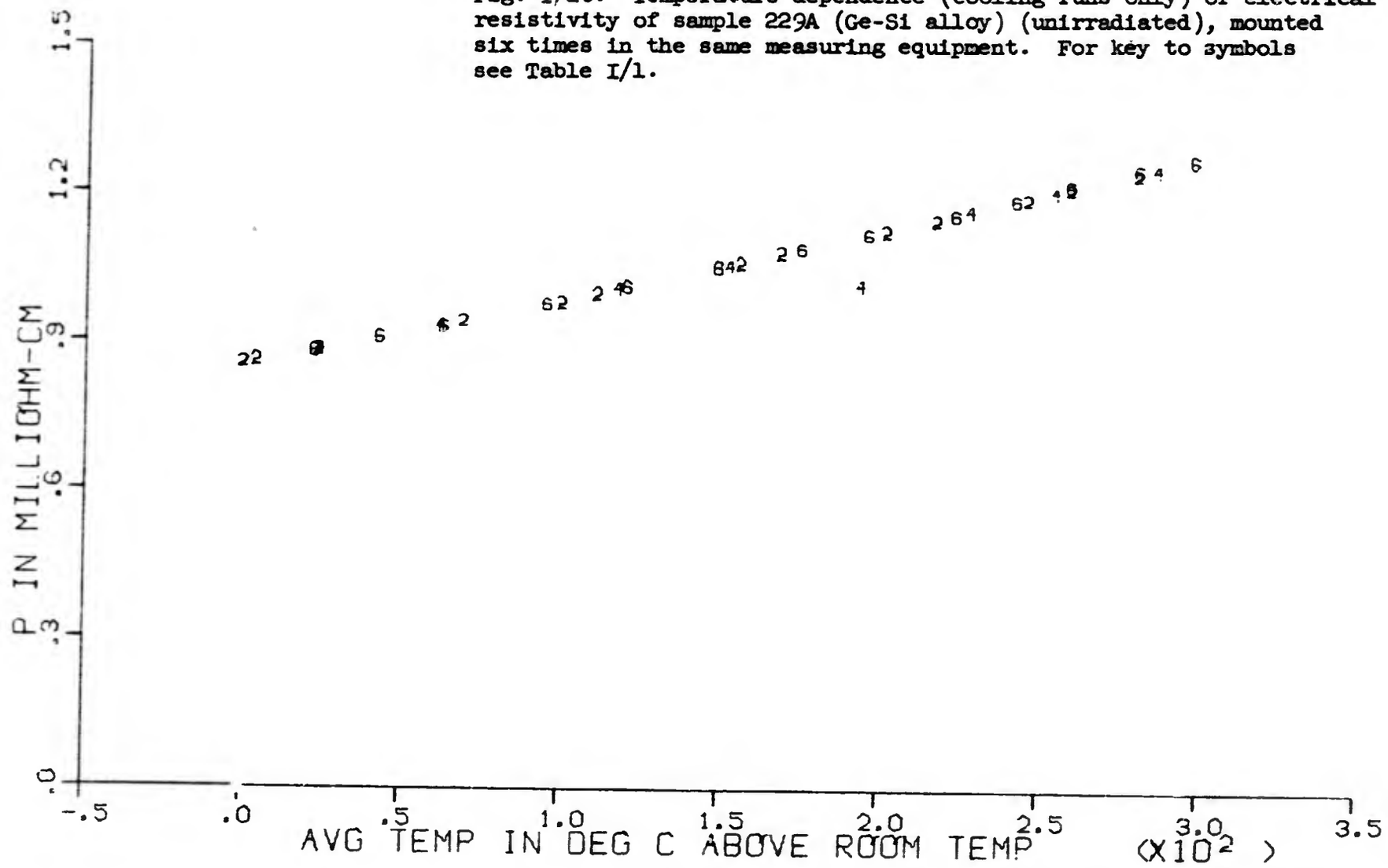

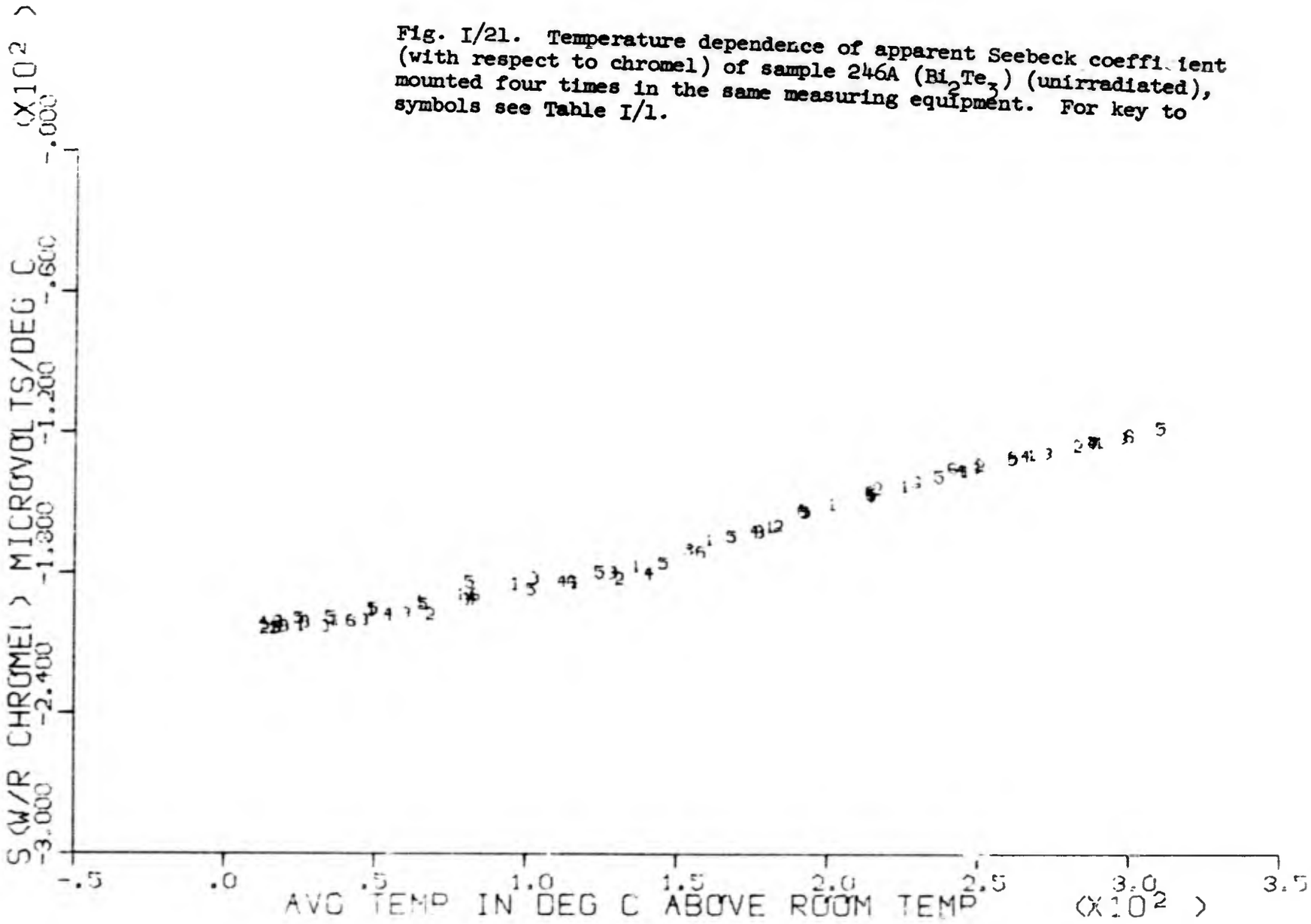

Fig. I/21. Temperature dependence of apparent Seebeck coefficient (with respect to chromel) of sample 246A (Bi_2Te_3) (unirradiated), mounted four times in the same measuring equipment. For key to symbols see Table I/1.

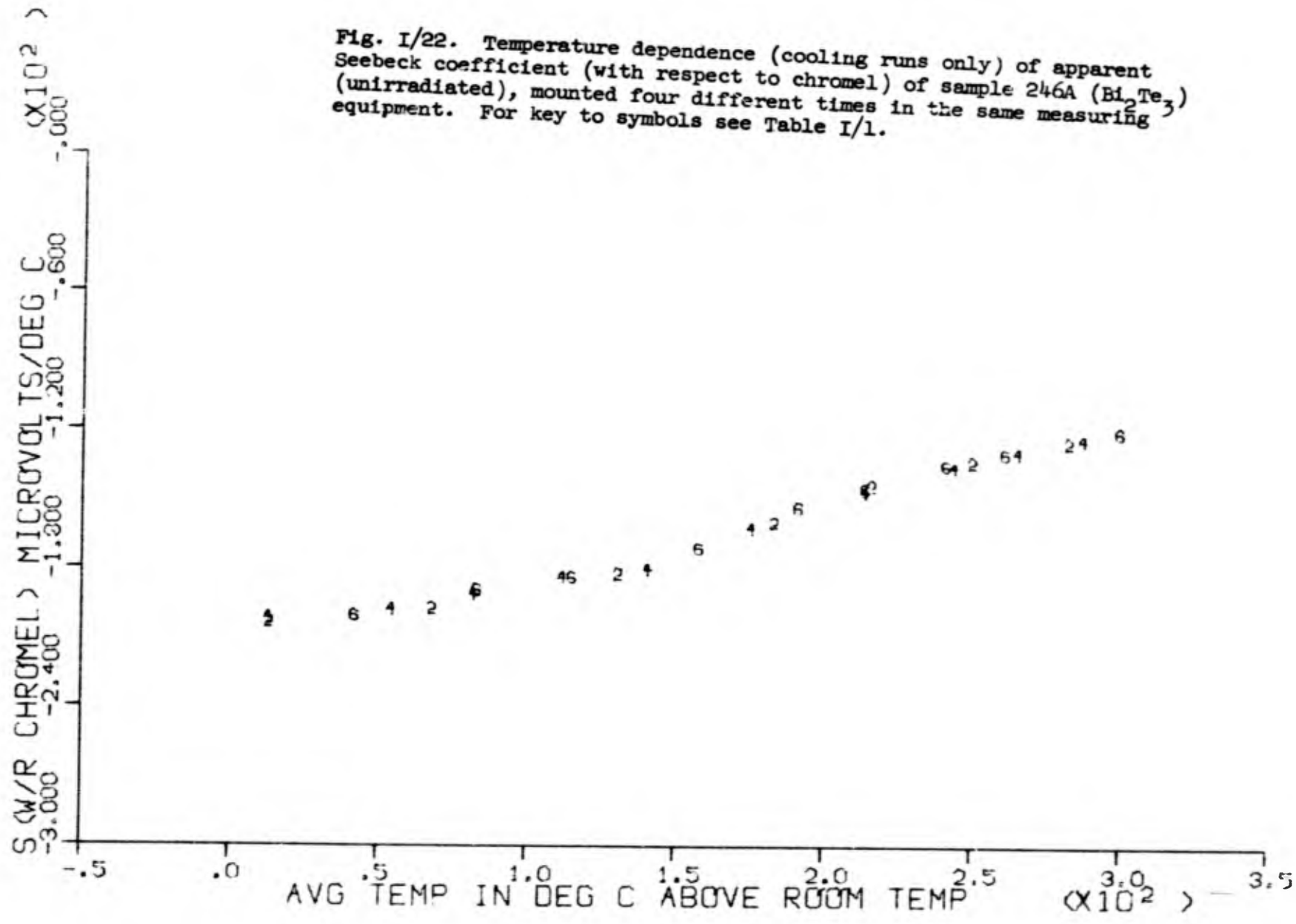

Fig. I/22. Temperature dependence (cooling runs only) of apparent Seebeck coefficient (with respect to chromel) of sample 246A (Bi_2Te_3) (unirradiated), mounted four different times in the same measuring equipment. For key to symbols see Table I/1.

Fig. I/23. Temperature dependence of electrical resistivity of sample 246A (Bi_2Te_3) (unirradiated), mounted four different times in the same measuring apparatus. For key to symbols see Table I/1.

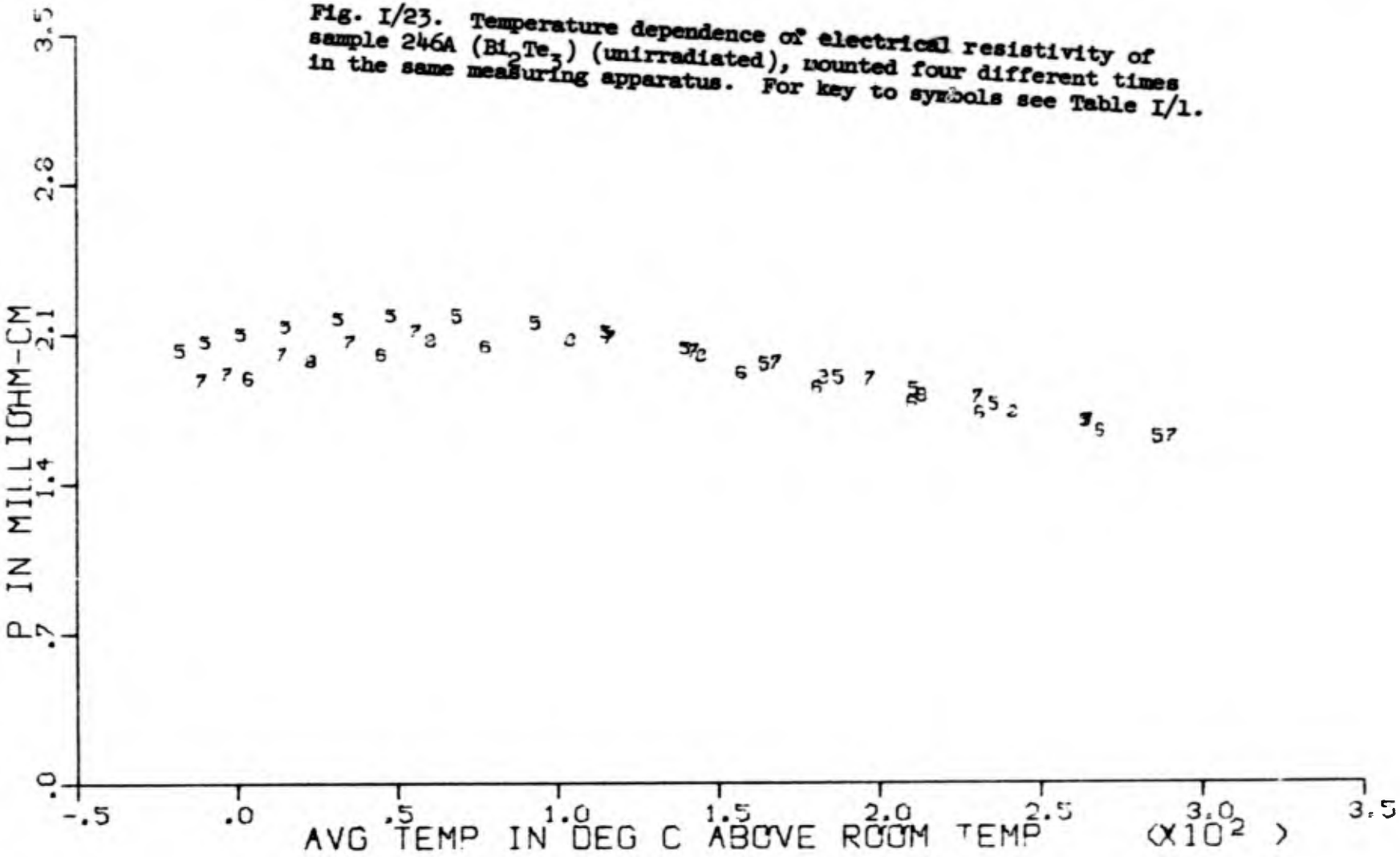

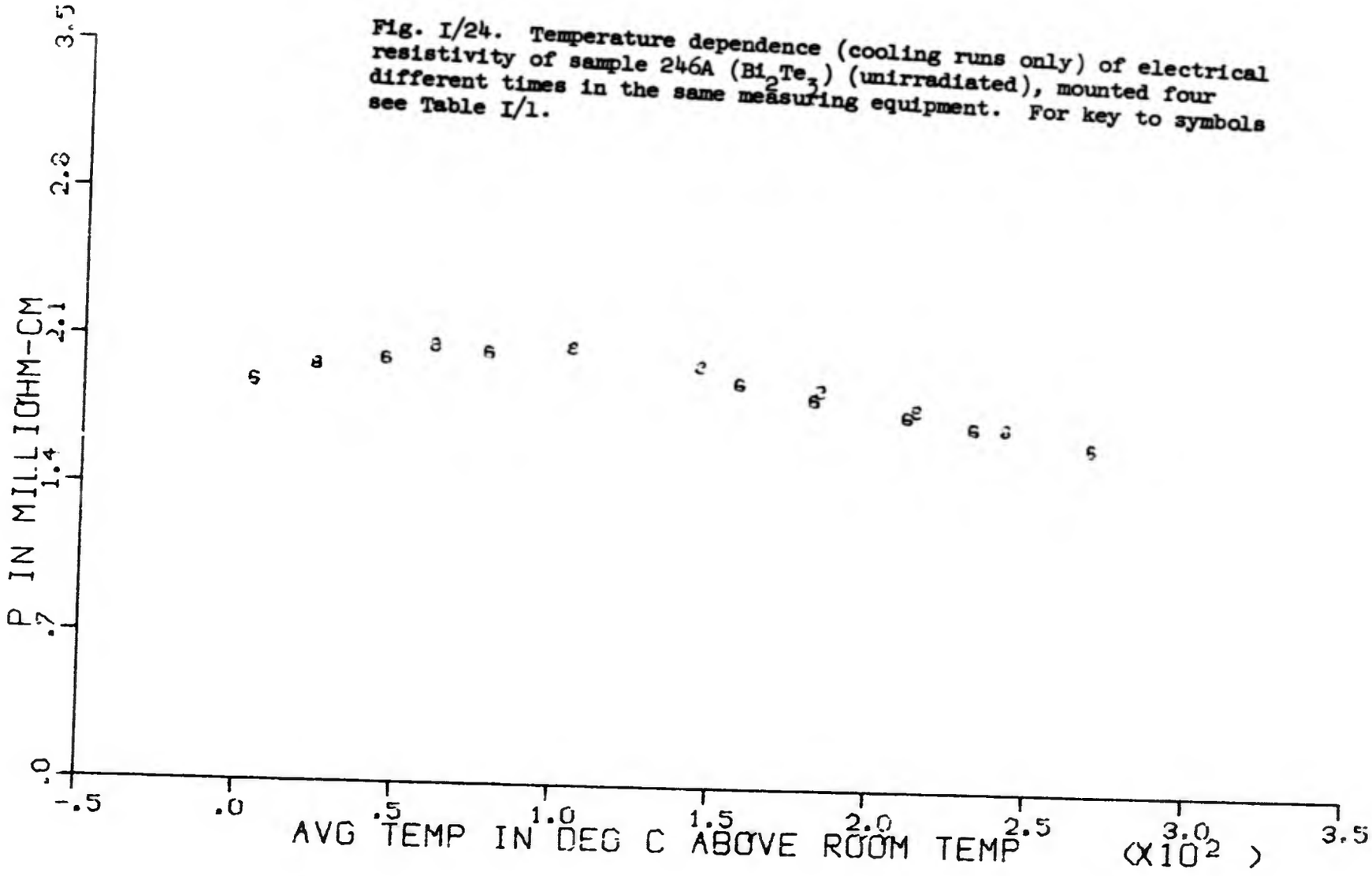

Fig. I/24. Temperature dependence (cooling runs only) of electrical resistivity of sample 246A (Bi_2Te_3) (unirradiated), mounted four different times in the same measuring equipment. For key to symbols see Table I/1.

Fig. I/25. Temperature dependence of apparent Seebeck coefficient (with respect to chromel) of sample 251E ($GeTe$-$AgSbTe_2$ alloy) (unirradiated), mounted three different times in the same measuring equipment. For key to symbols see Table I/1.

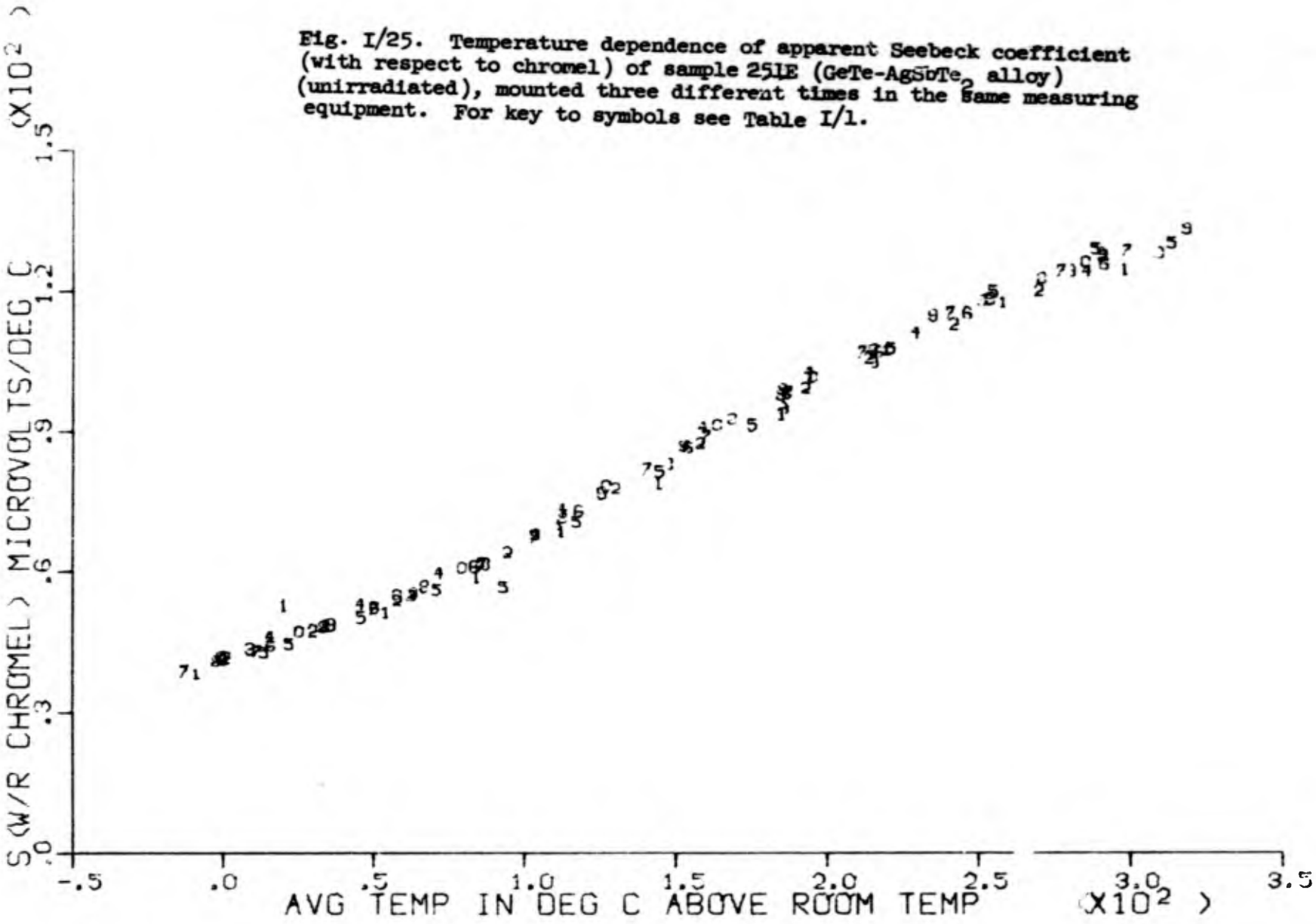

Fig. I/26. Temperature dependence (cooling runs only) of apparent Seebeck coefficient (with respect to chromel) of sample 251E ($GeTe-AgSbTe_2$ alloy) (unirradiated), mounted three different times in the same measuring equipment. For key to symbols see Table I/1.

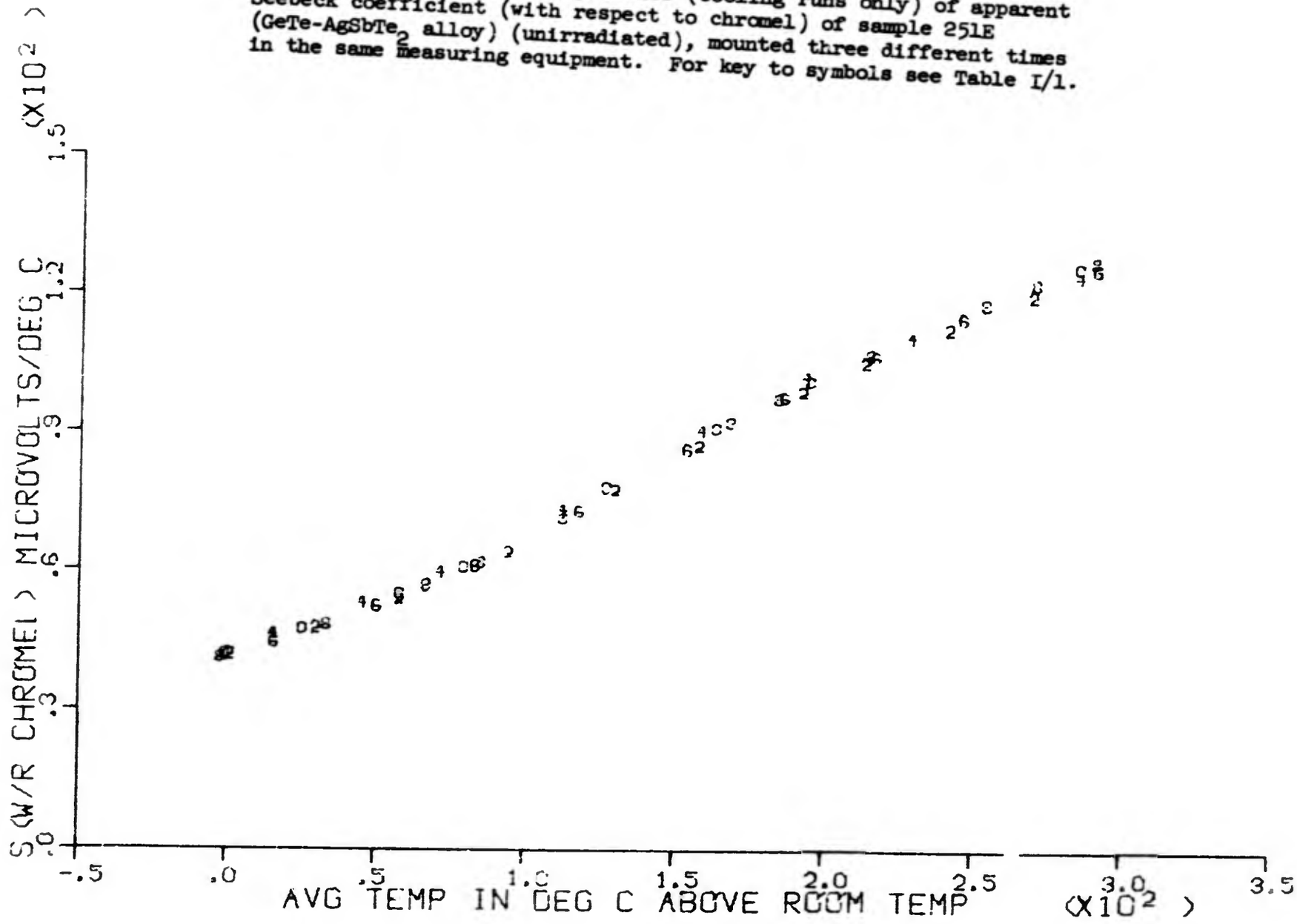

Fig. I/27. Temperature dependence of electrical resistivity of sample 251E ($GeTe-AgSbTe_2$ alloy) (unirradiated), mounted three different times in the same measuring equipment. For key to symbols see Table I/1.

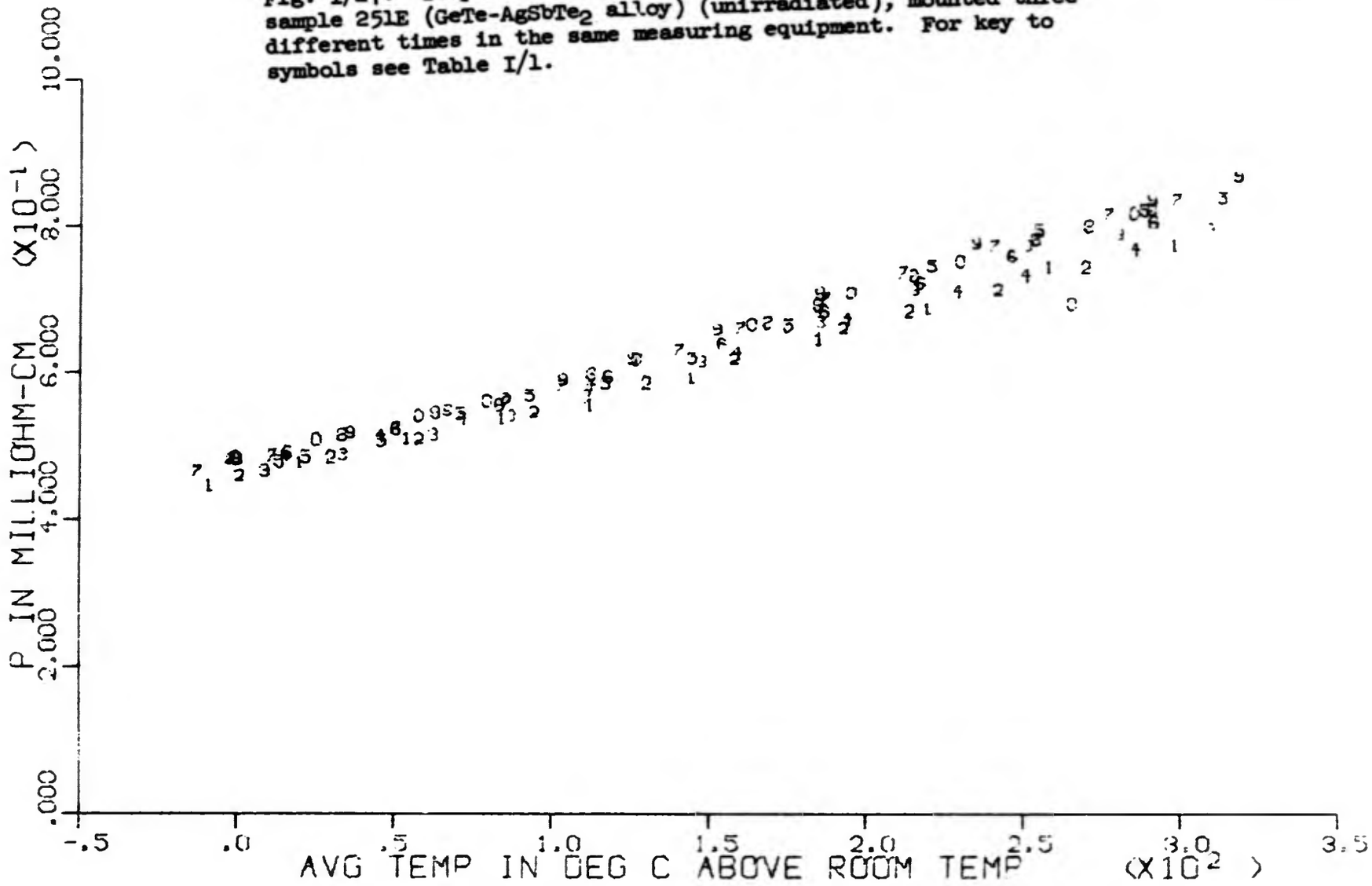

Fig. I/28. Temperature dependence (cooling runs only) of electrical resistivity of sample 251E ($GeTe-AgSbTe_2$ alloy) (unirradiated), mounted three different times in the same measuring equipment. For key to symbols see Table I/1.

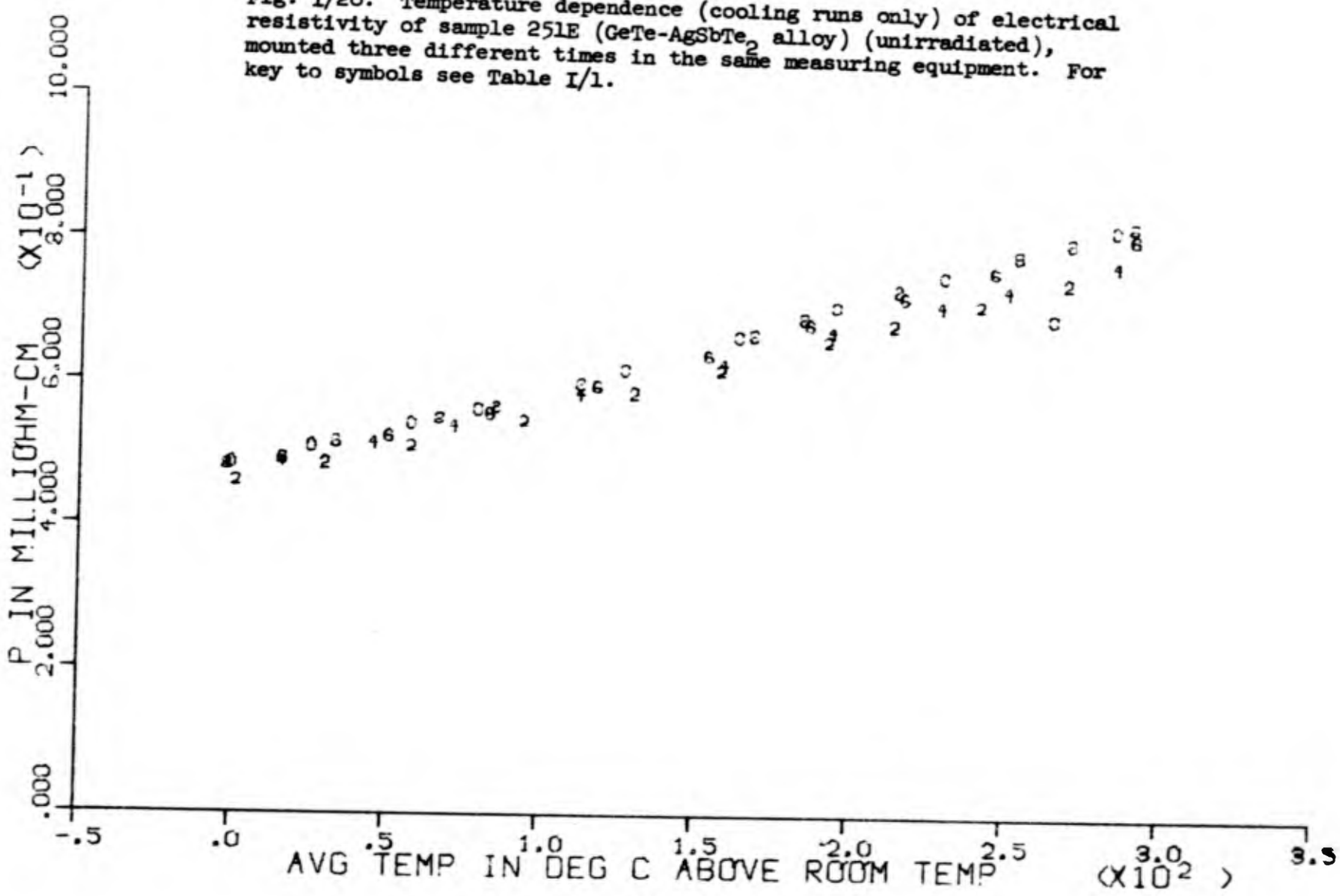

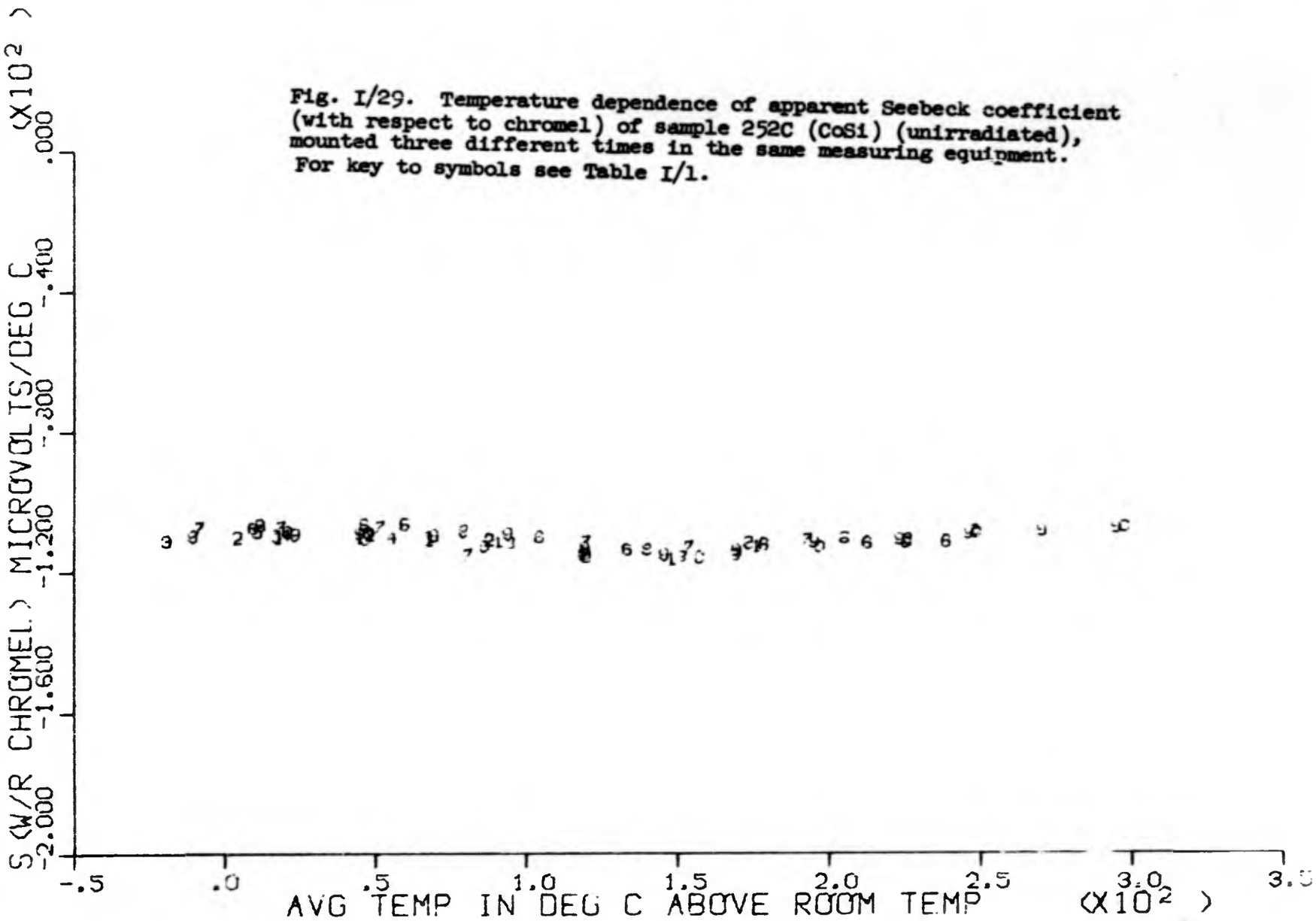

Fig. I/29. Temperature dependence of apparent Seebeck coefficient (with respect to chromel) of sample 252C (CoSi) (unirradiated), mounted three different times in the same measuring equipment. For key to symbols see Table I/1.

Fig. I/30. Temperature dependence (cooling runs only) of apparent Seebeck coefficient (with respect to chromel) of sample 252C (CoSi), (unirradiated), mounted three different times in the same measuring equipment. For key to symbols see Table I/1.

Fig. I/31. Temperature dependence of electrical resistivity of sample 252C (CoSi) (unirradiated), mounted three different times in the same measuring equipment. For key to symbols see Table I/1.

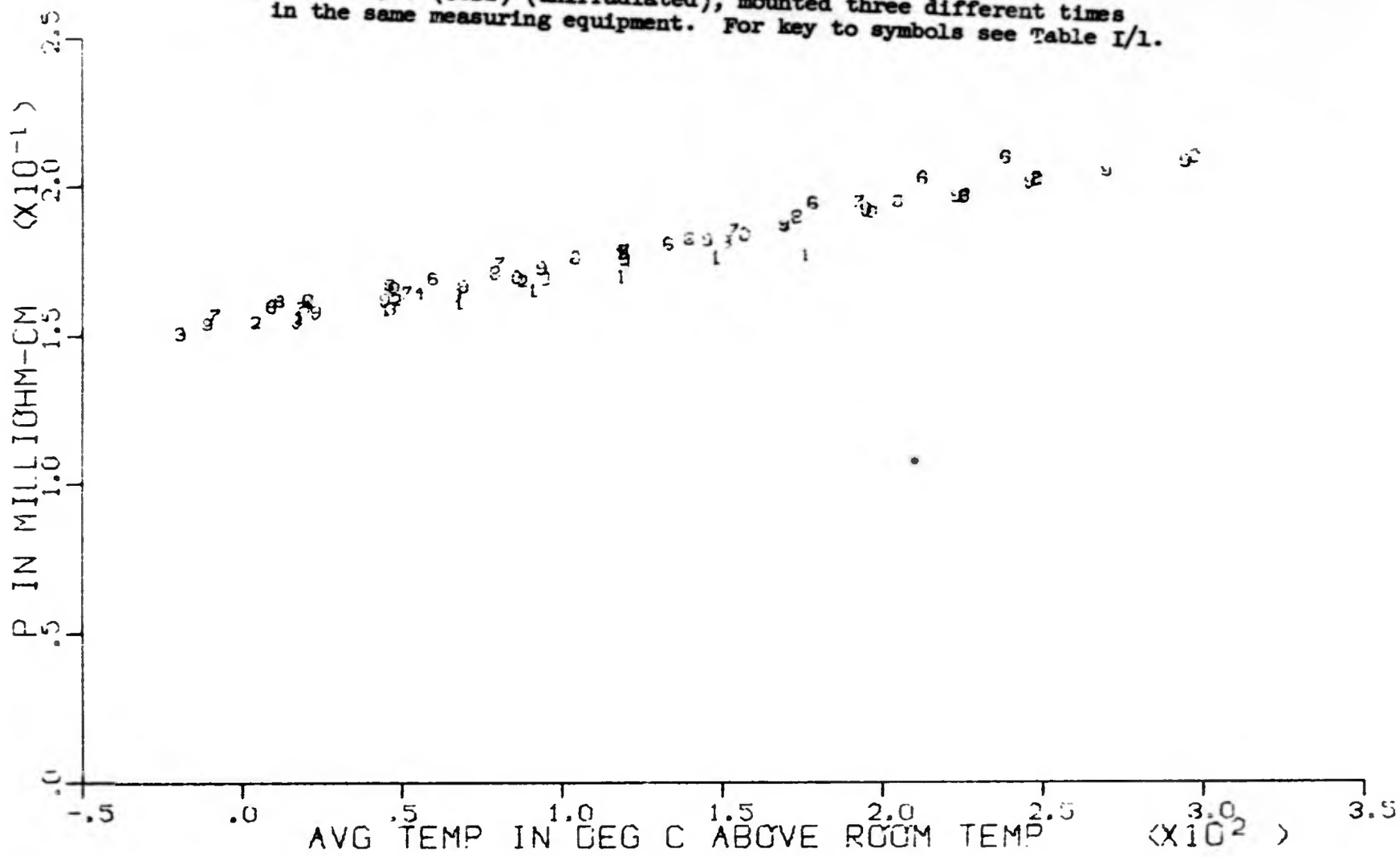

Fig. I/32. Temperature dependence (cooling runs only) of electrical resistivity of sample 252C (CoSi) (unirradiated), mounted three different times in the same measuring equipment. For key to symbols see Table I/1.

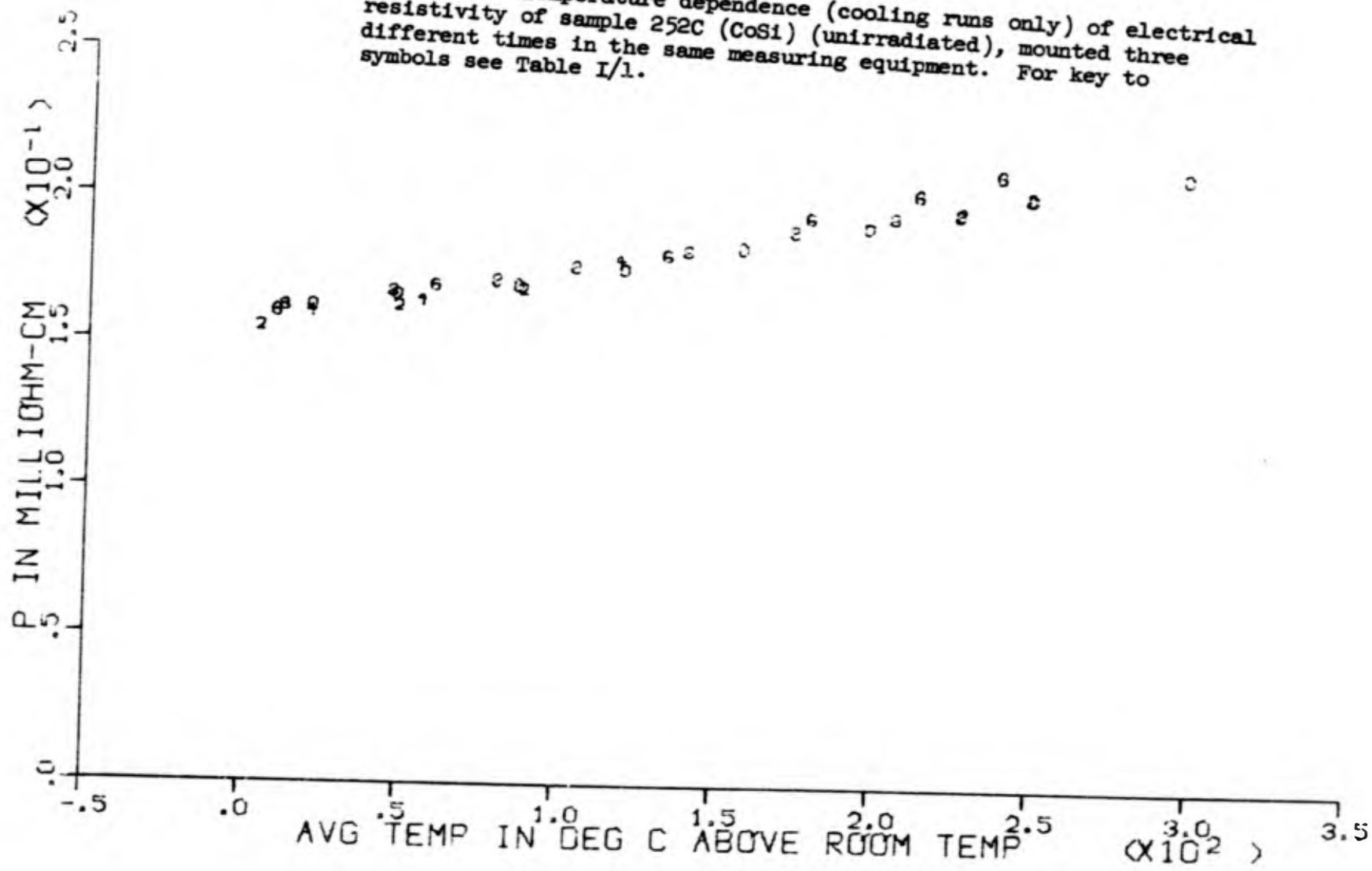

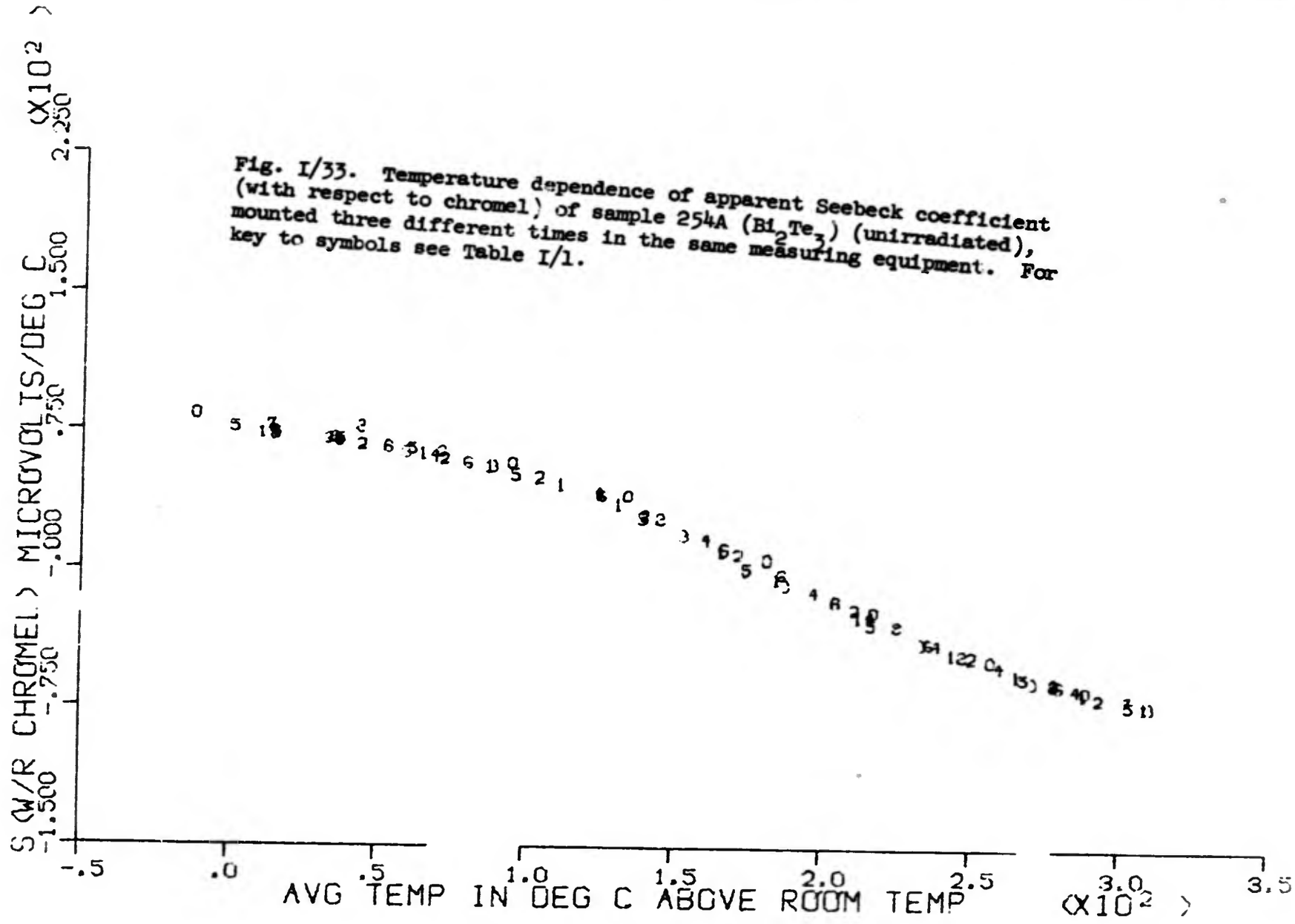

Fig. I/33. Temperature dependence of apparent Seebeck coefficient (with respect to chromel) of sample 254A (Bi_2Te_3) (unirradiated), mounted three different times in the same measuring equipment. For key to symbols see Table I/1.

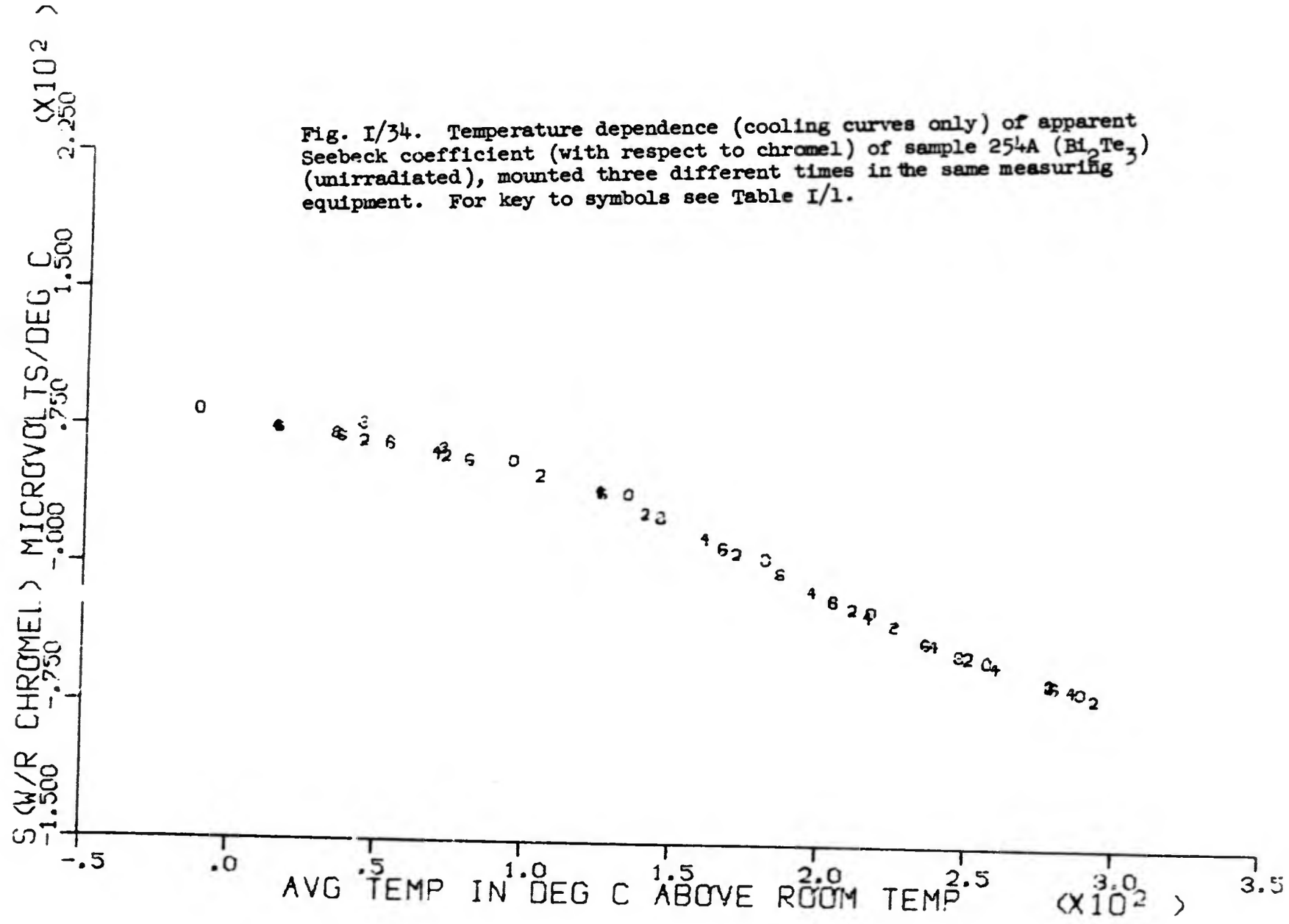

Fig. I/34. Temperature dependence (cooling curves only) of apparent Seebeck coefficient (with respect to chromel) of sample 254A (Bi_2Te_3) (unirradiated), mounted three different times in the same measuring equipment. For key to symbols see Table I/1.

Fig. I/35. Temperature dependence of electrical resistivity of sample 254A (Bi_2Te_3) (unirradiated), mounted three different times in the same measuring equipment. For key to symbols see Table I/1.

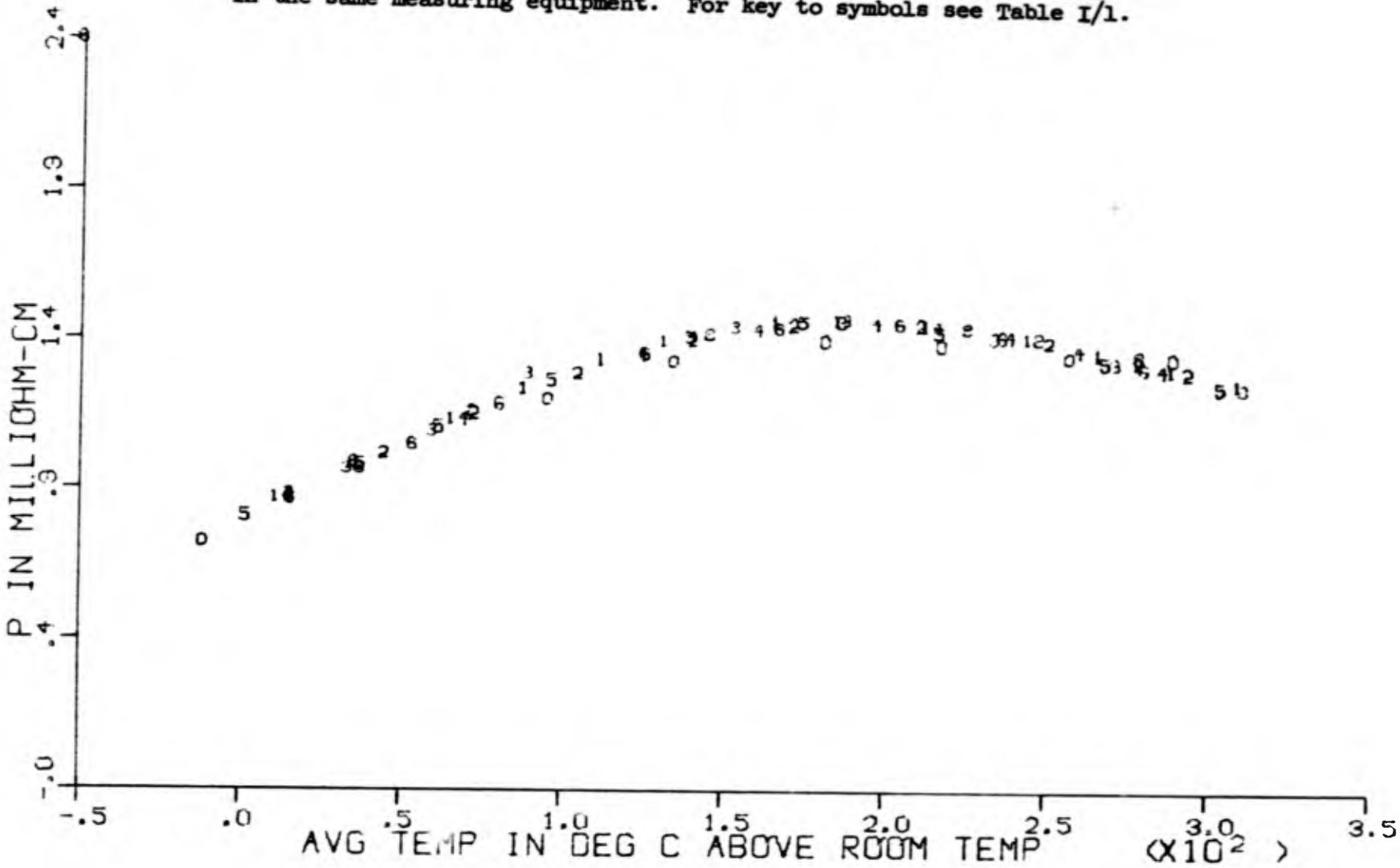

Fig. I/36 Temperature dependence (cooling runs only) of electrical resistivity of sample 254A (Bi_2Te_3) (unirradiated), mounted three different times in the same measuring equipment. For key to symbols see Table I/1.

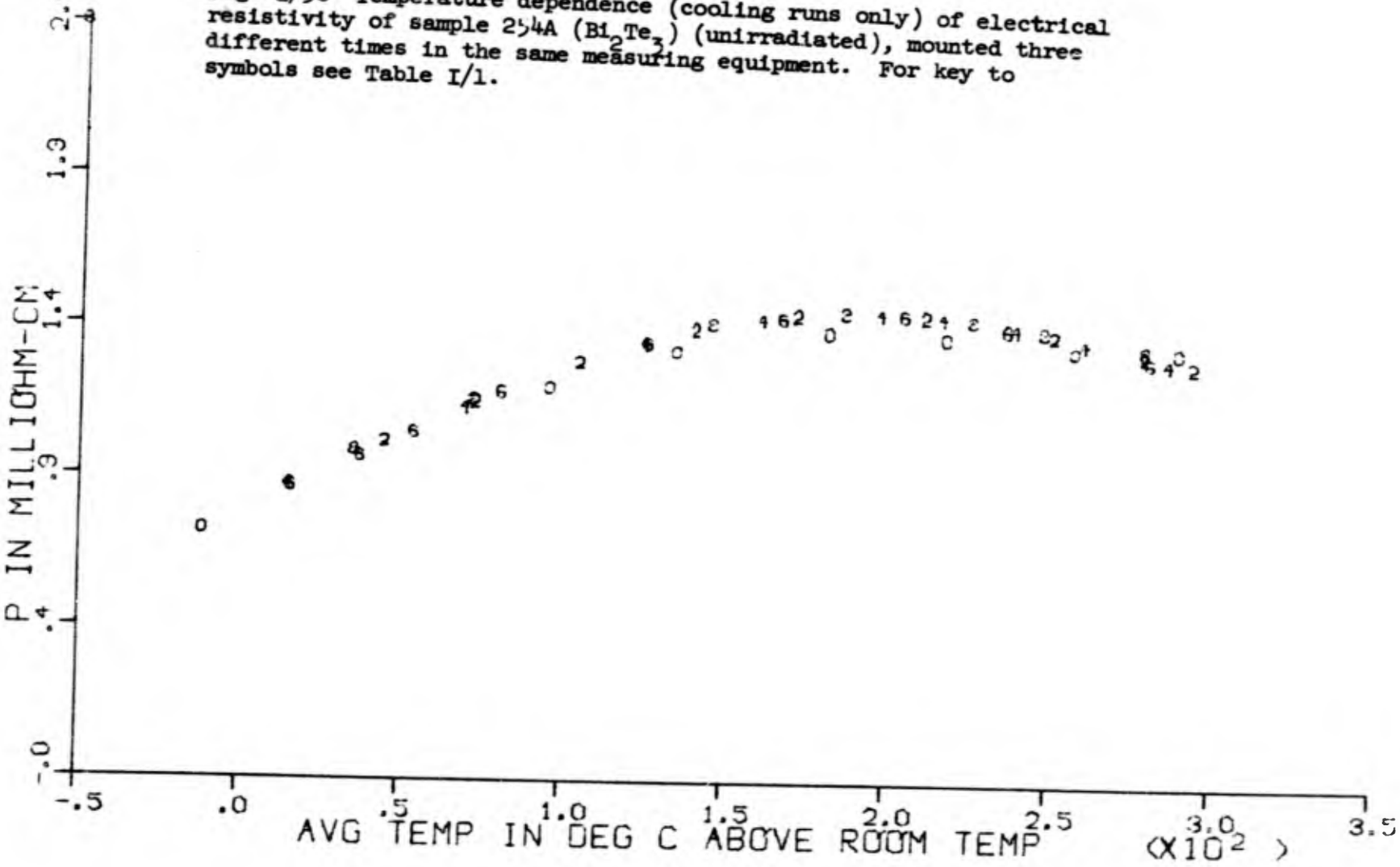

Fig. I/37. Temperature dependence of apparent Seebeck coefficient (with respect to chromel) of sample 255A (single crystal Bi_2Te_3) (unirradiated), mounted three different times in the same measuring equipment. For key to symbols see Table I/1.

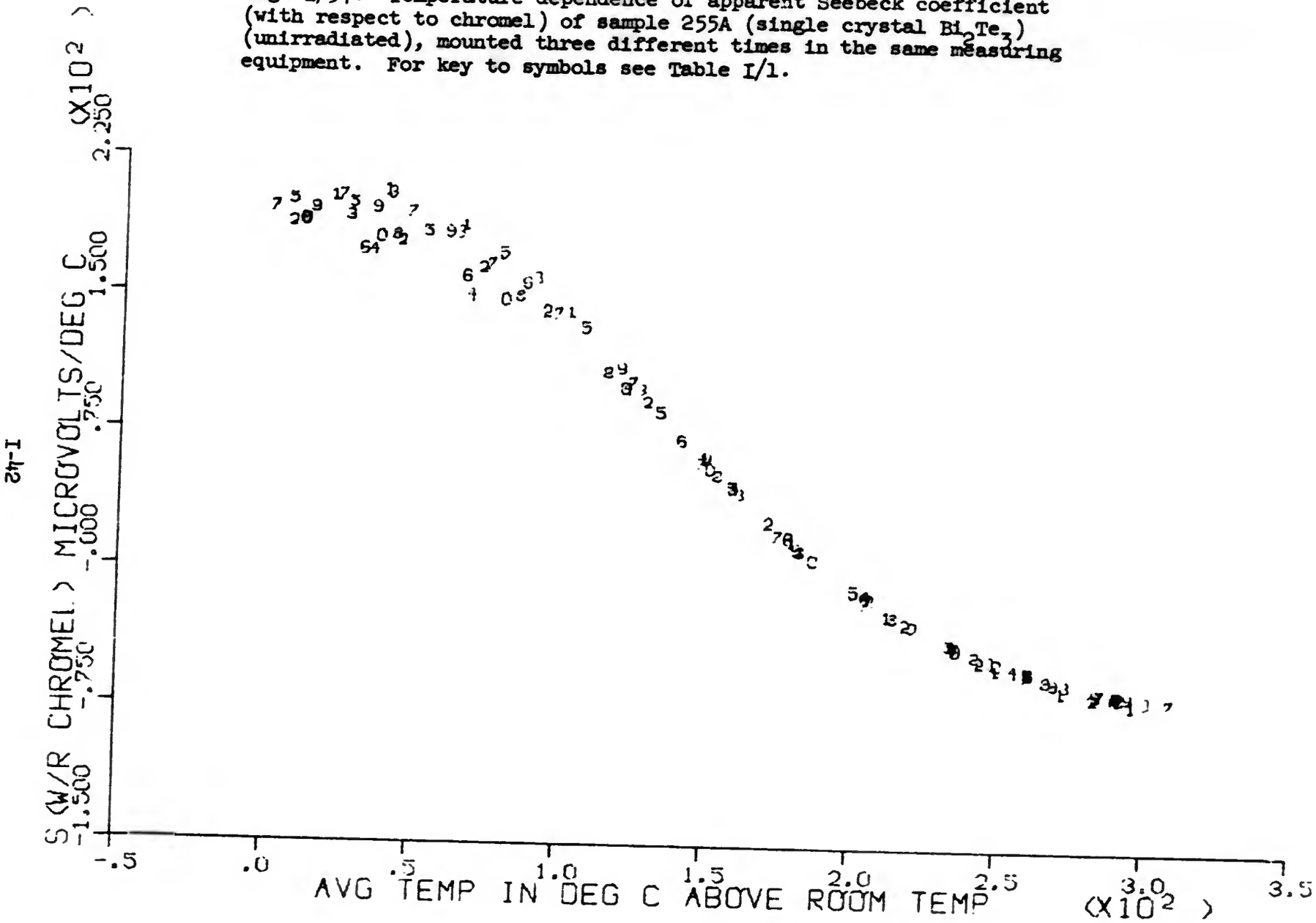

Fig. I/38. Temperature dependence (cooling runs only) of apparent Seebeck coefficient (with respect to chromel) of sample 255A (single crystal Bi_2Te_3) (unirradiated), mounted three different times in the same measuring equipment. For key to symbols see Table I.

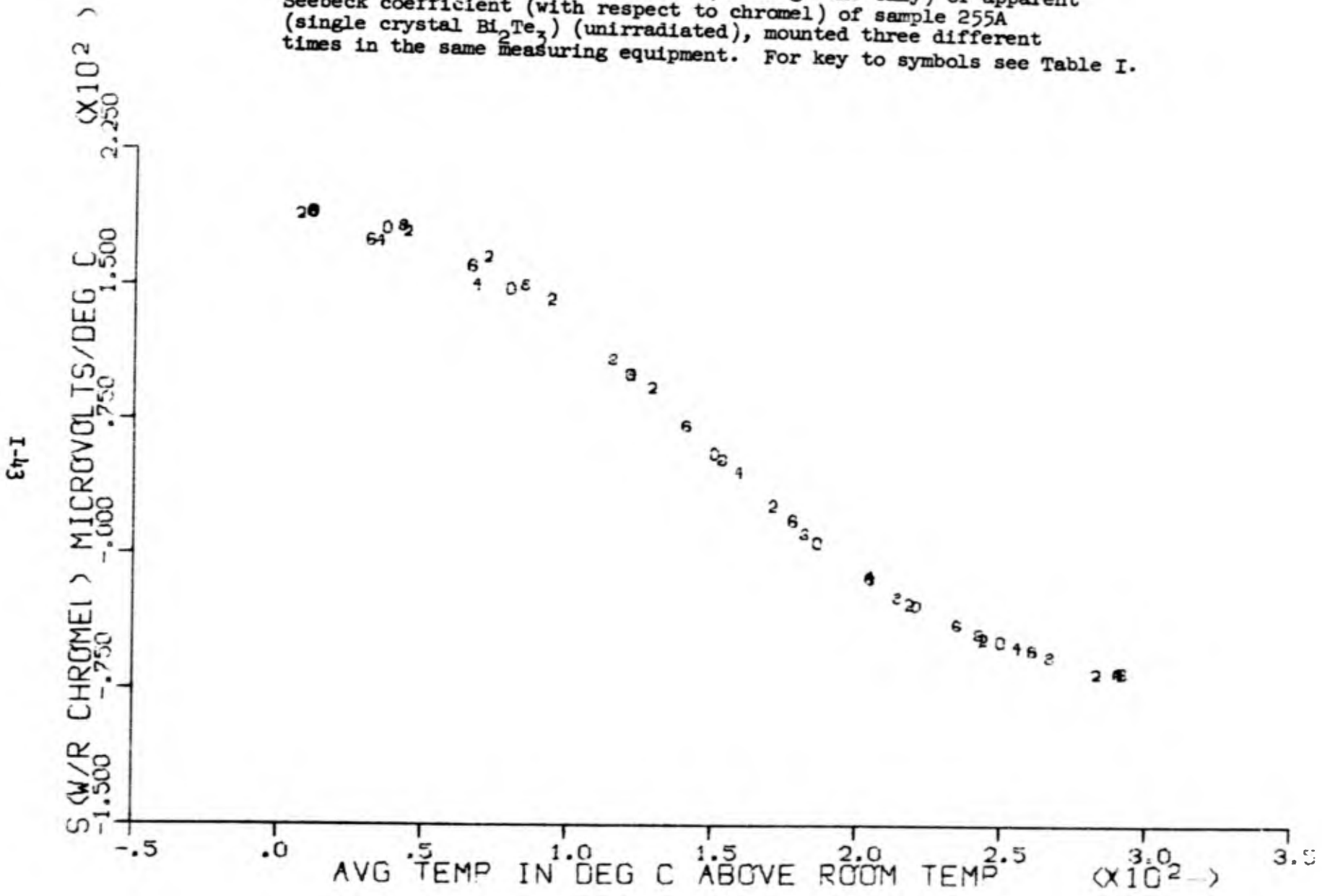

Fig. I/39. Temperature dependence of electrical resistivity of sample 255A (single crystal Bi_2Te_3) (unirradiated), mounted three different times in the same measuring equipment. For key to symbols see Table I/1.

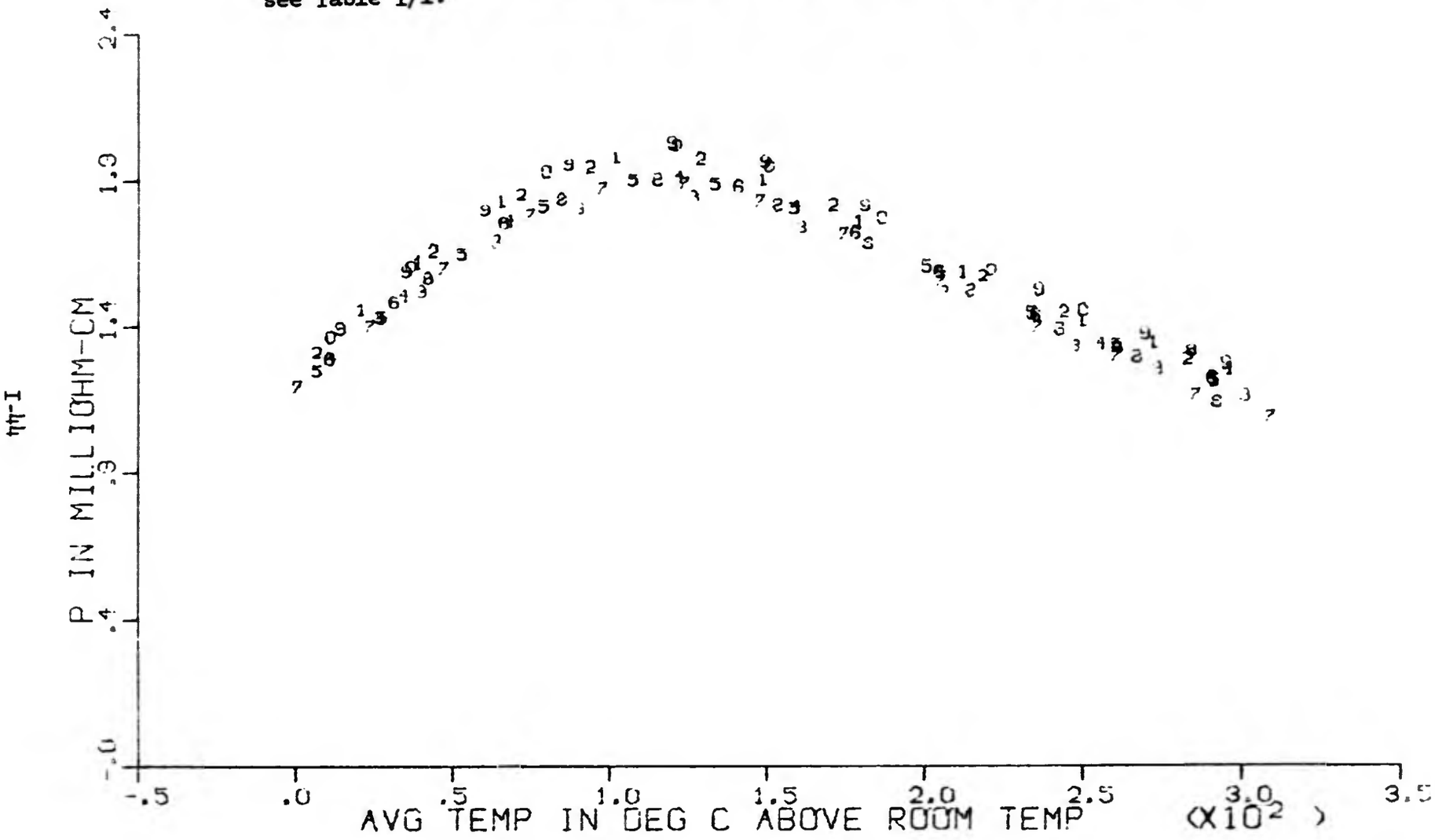

Fig. I/40. Temperature dependence (cooling runs only) of electrical reistivity of sample 255A (single crystal Bi_2Te_3) (unirradiated), mounted three different times in the same measuring equipment. For key to symbols see Table I/1.

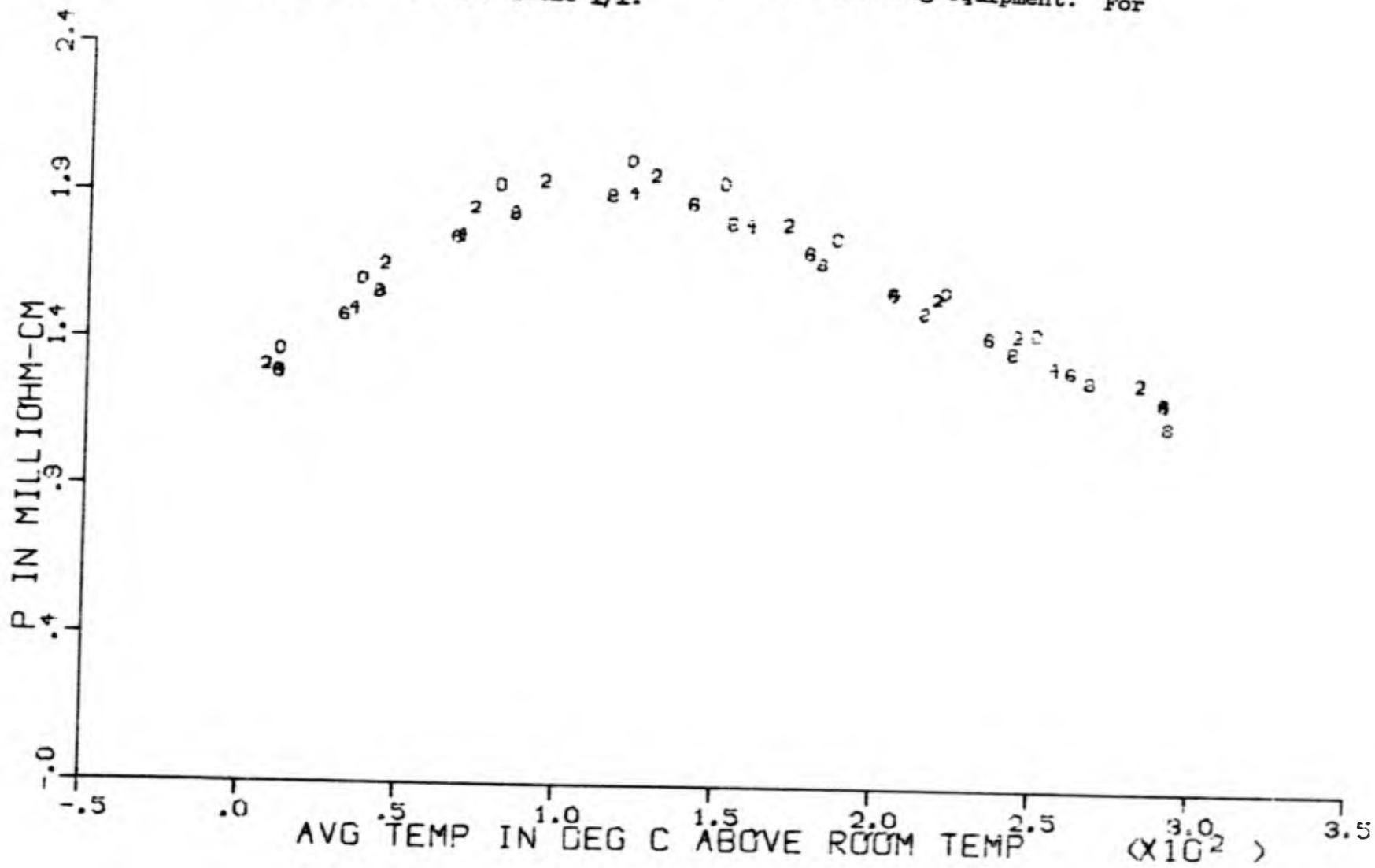

BLANK PAGE

APPENDIX II: PRE-, POST-IRRADIATION PLOTS

APPENDIX II: PRE-, POST-IRRADIATION PLOTS

APPENDIX II - PRE AND POST-IRRADIATION DATA

ORDER OF PRESENTATION

The general scheme followed in presenting the data of Appendix II has four main features. First, the data are grouped by material. Within these groups the machine-drawn plots are presented first, followed by the hand-drawn plots, i.e., the S and ρ plots precede the α plots within each material. Third, within the parametric subgroupings, the data are further grouped according to sample, in order of increasing total exposure dose. And, finally, in cases where the data were deemed sufficiently complicated, additional plots showing only the data taken while the sample was cooling, i.e., those from which the quantitative estimates were made, are presented following the corresponding complete plot.

COORDINATES

Seebeck coefficient data are presented in terms of the apparent Seebeck coefficient of the sample with respect to chromel, $S_{w/r\ chromel}$, as a function of the sample's average temperature, $\bar{T}$. The latter is calculated simply as the arithmetic mean of the temperatures indicated by the two chromel-alumel thermocouples shown in Fig. 2, using reference junctions at room temperature. The former is given by the equation

$$S_{w/r\ chromel} = V_s/\Delta T,$$

where ΔT is the difference between the temperatures indicated by the two thermocouples, and V_s is the current-independent part of V_+, also as shown in Fig. 2. During the measurements, ΔT was maintained in the neighborhood of 10°C. In view of the temperature dependences shown by the plots of this Appendix, this difference is amply small to make negligible errors due to such use of the secant as an approximation to the tangent.

If the samples were spatially homogeneous in S, the quantity so measured would indeed be the Seebeck coefficient with respect to chromel, and would depend upon only the values of T_1 and T_2. Since our samples generally are not so, the measured quantity depends somewhat upon the distribution of temperature between the points of measurement. Consequently, the measured quantity, strictly speaking, cannot be called simply the Seebeck coefficient. We choose to refer to this quality as the APPARENT SEEBECK COEFFICIENT, thus implying its dependence upon the measurement conditions.

The electrical resistivity is measured by a standard four-probe technique, based upon the current-dependent part of V_+, as shown in Fig. 2. Again speaking strictly, the quantity so measured is not true resistivity, since the sample is not in thermal equilibrium during the measurement. In this case, however, the distinction is more academic than practical, and we have chosen to ignore it.

AXIS LABELS

The parenthetical power of ten following some of the axis labels indicates that the numbers shown along that axis are to be multiplied by that power of ten. For example, the temperature range for Fig. II/1 is - 100 to + 400°C above room temperature.

SYMBOLS

Machine-Drawn Plots

Three different sets of symbols, namely numeric, alphabetic, and geometric, have been used to represent data-points in the machine-drawn plots of this Appendix. The numeric set, which includes the symbols - and + to represent 11 and 12, respectively, have been used for data taken from samples which eventually were exposed to the 2×10^{19} fluence. The alphabetic set is used for those which were exposed only to lesser fluences, and the geometric set for special cases.

In the alphabetic case, the conventional order of the symbols indicates the chronological order in which the respective data were taken. In the numeric set, the same is true except for the symbol 0, which is used to indicate the tenth in chronological order, and the symbols - and + which indicate the eleventh and twelfth, respectively.

In the geometric set, chronological distinctions are left unspecified.

In most cases where the calibration sample also was used for post-irradiation measurements, only the last of the several pre-irradiation runs is plotted. In all other complete plots, missing symbols indicate measurement runs that were made, but for one reason or another did not produce any usable data. In the incomplete plots, of course, existing data were omitted deliberately, in order to aid in the numerical estimation process.

In most cases, the "odd" symbols, i.e., 1, 3, 5, etc., and A, C, E, etc., indicate data taken while temperature was increasing, and "even" symbols indicate data taken while temperature was falling. A number of exceptions to this scheme were necessary, e.g., those cases in which the temperature was first lowered to liquid nitrogen temperature. These exceptions are identified as such in their captions.

Hand-Drawn Plots

The hand-drawn plots utilize geometric symbols. Their chronological order is indicated in their respective keys, and occassionally by arrows drawn between data-groups.

DATA ACCEPTANCE-REJECTION

The data presented are those which have survived only a gross editing. Points obviously falling many standard deviations outside the region established by the majority of the data have been rejected arbitrarily. Likewise, those taken during periods when the measuring equipment was known to have malfunctioned have been eliminated. The remaining data undoubtedly include many points which would be rejected by a more sophisticated editing process. Limitations on time available, however, have precluded application of such processes, and a number of questionable points are included.

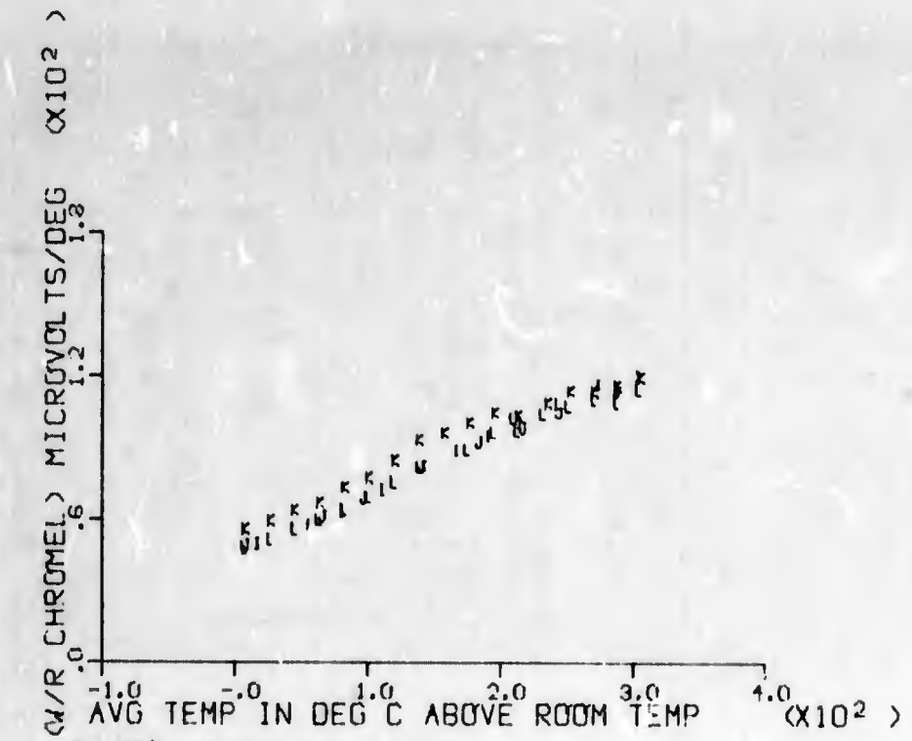

Fig. II/1. Temperature dependence of apparent Seebeck coefficient (with respect to chromel) of sample 136A (PbTe), before (I,J) and after (K,L) exposure to 1.6×10^{18} fast (E > 1 Mev) neutrons/cm^2. I, K = temperature increasing; J, L = temperature falling.

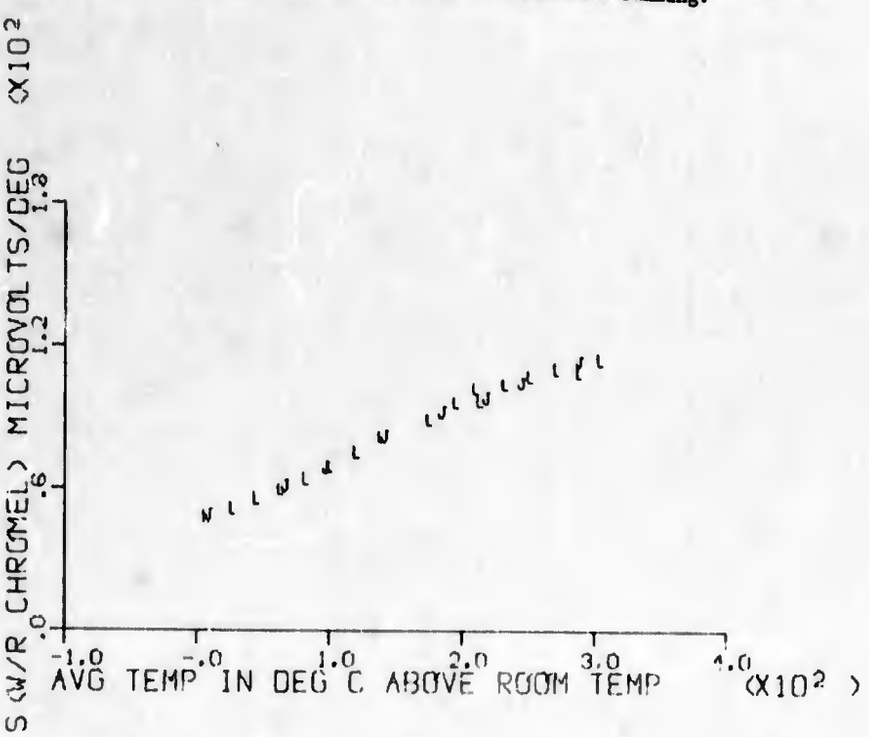

Fig. II/2. Temperature dependence of electrical resistivity of sample 136A (PbTe) before (I,J) and after (K,L) exposure to 1.6×10^{18} fast (E > 1 Mev) neutrons/cm². I,K = temperature increasing; J, L = temperature falling.

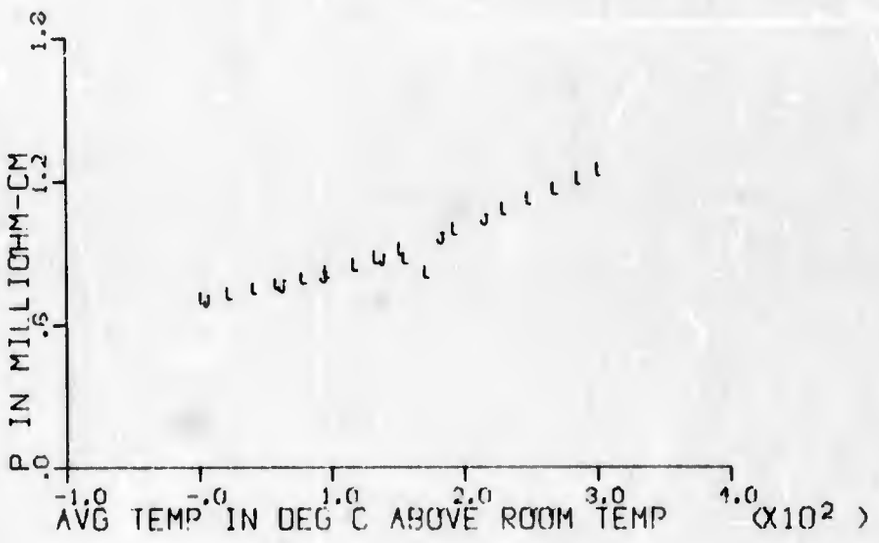

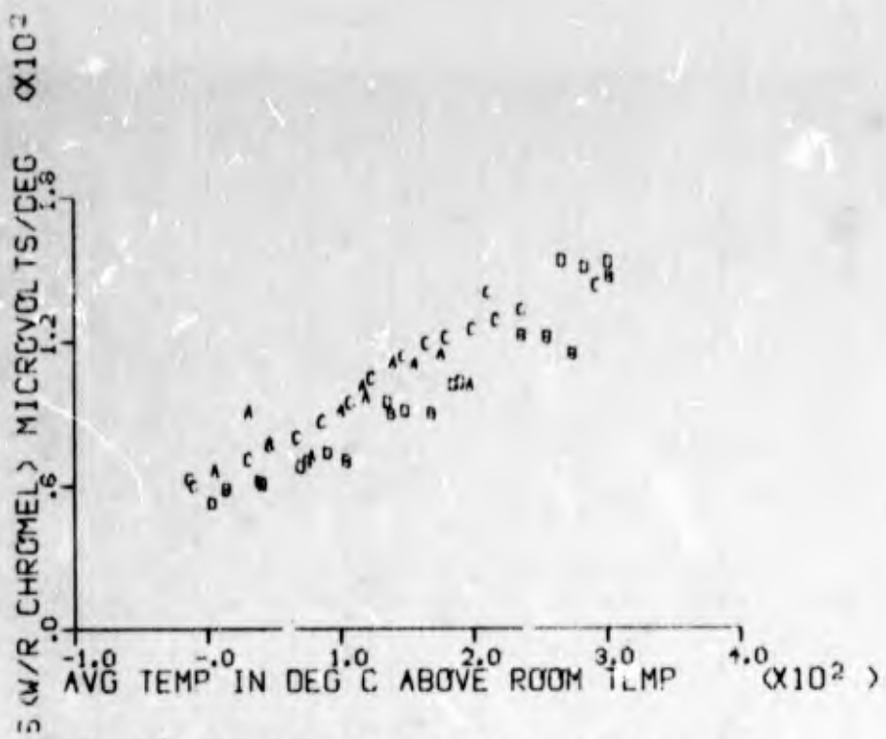

Fig. II/3. Temperature dependence of apparent Seebeck coefficient (with respect to chromel) of sample 136B (PbTe), before (A,B) and after (C,D) exposure to 1.6 x 10^{18} fast (E) 1 Mev) neutrons/cm^2. A,C = sample heating; B, D = sample cooling.

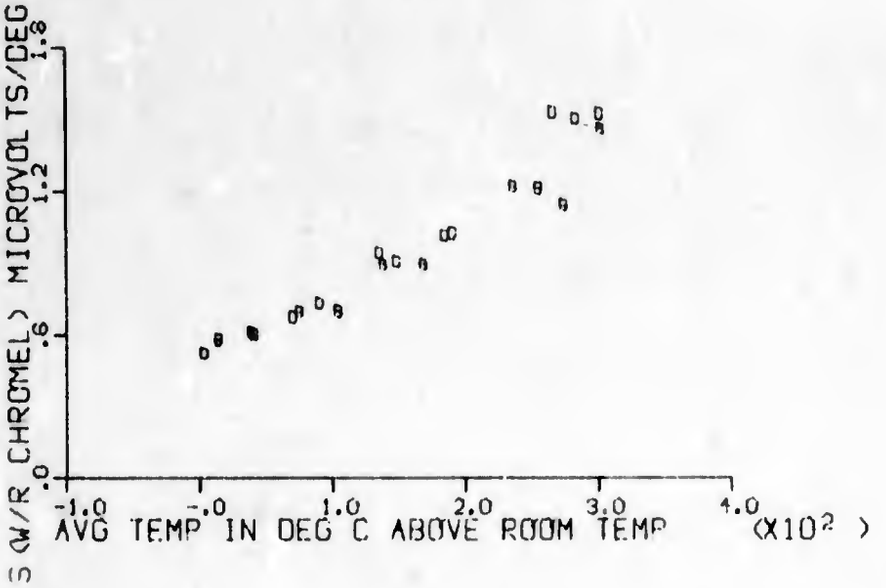

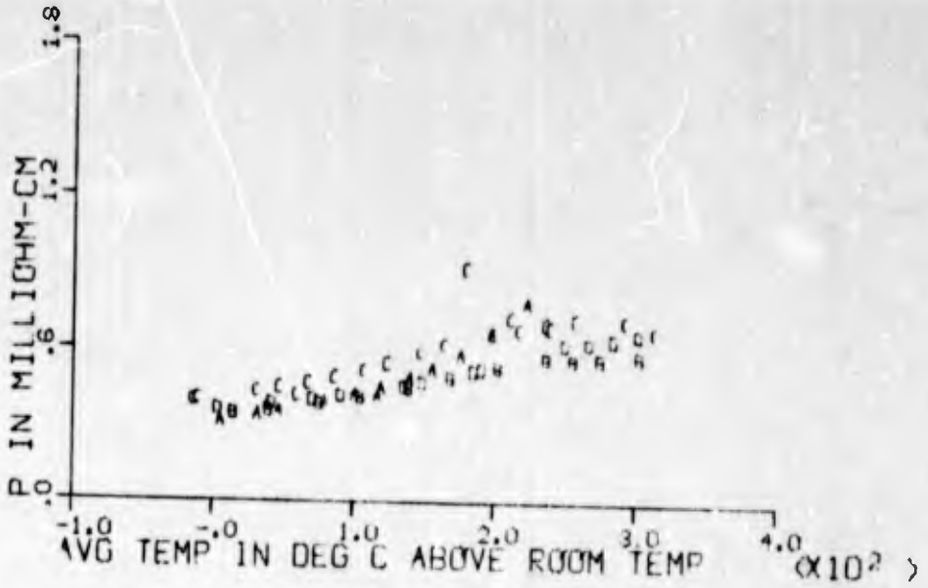

Fig. II/4. Temperature dependence of electrical resistivity of sample 136B (PbTe) before (A,B) and after (C,D) exposure to 1.6×10^{18} fast (E) 1 Mev) neutrons/cm^2. A,C = sample heating; B,D = sample cooling.

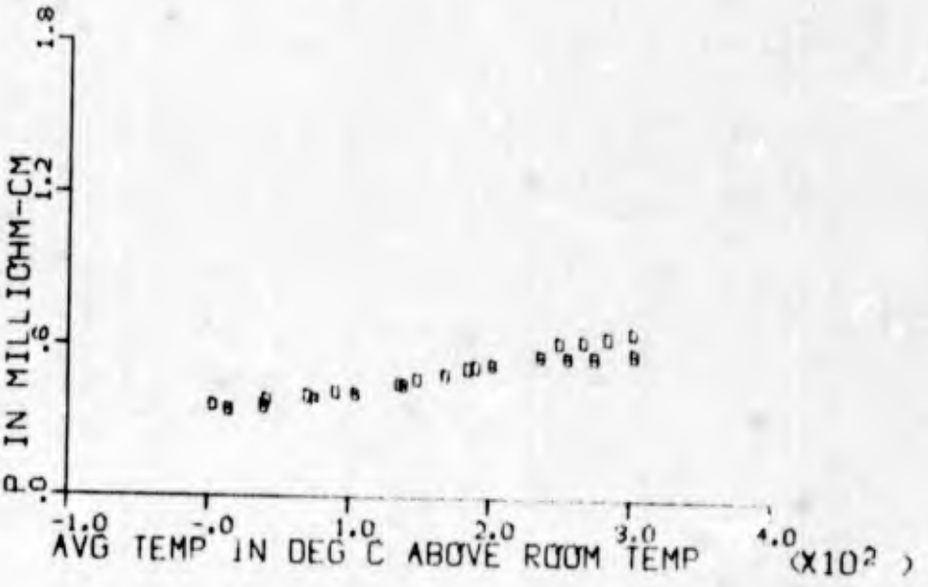

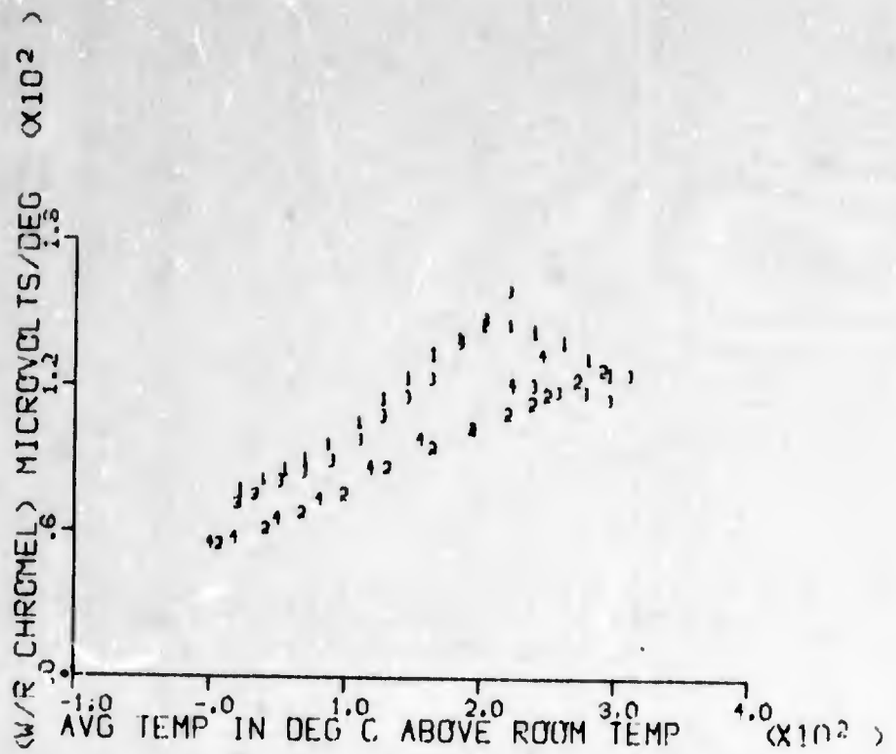

Fig. II/5. Temperature dependence of apparent Seebeck coefficient (with respect to chromel) of sample 130B (PbTe) before (1,2) and after (3,4) exposure to 2.3 x 10^{19} fast (E) 1 Mev) neutrons/cm^2. 1,3 = sample heating; 2,4, = sample cooling.

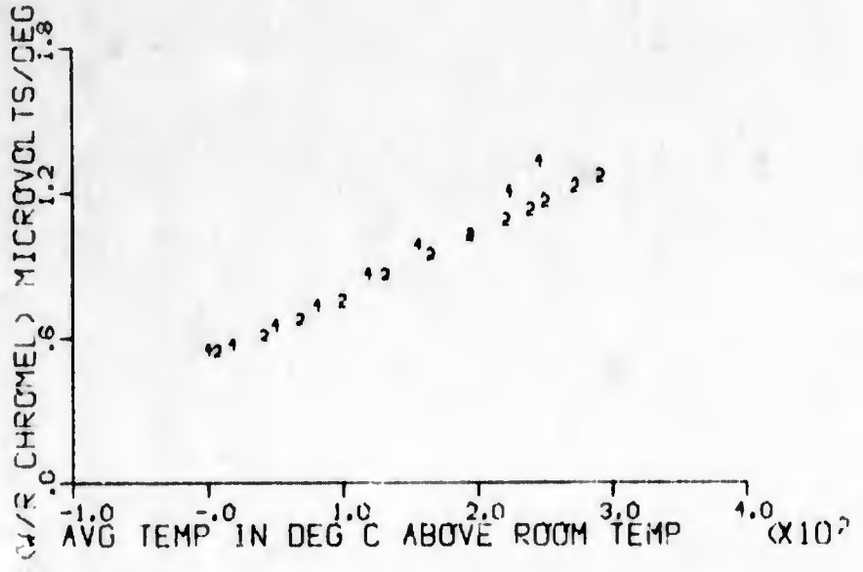

Fig. II/6. Temperature dependence of electrical resistivity of sample 130B (PbTe) before (1,2) and after (3,4) exposure to 2.3×10^{19} fast (E > 1 Mev) neutrons/cm². 1,3 = sample heating; 2,4 = sample cooling.

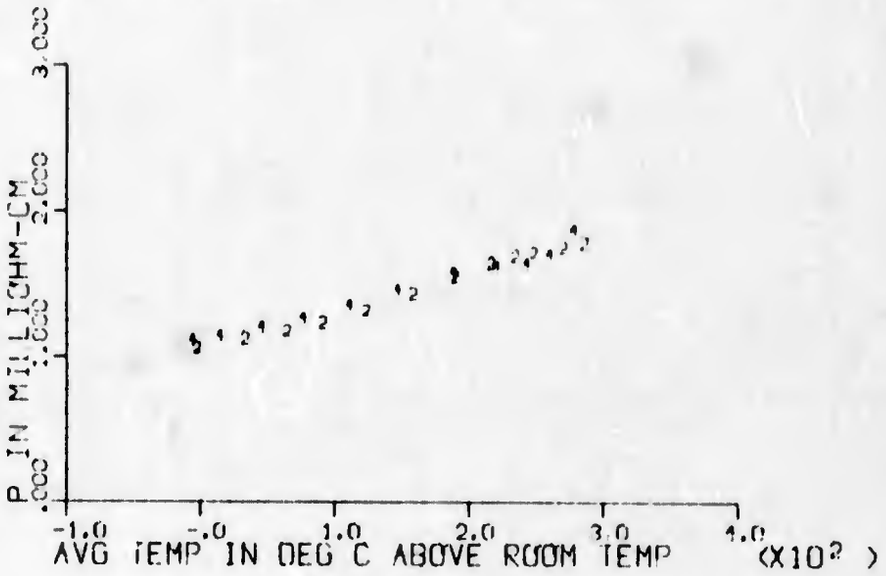

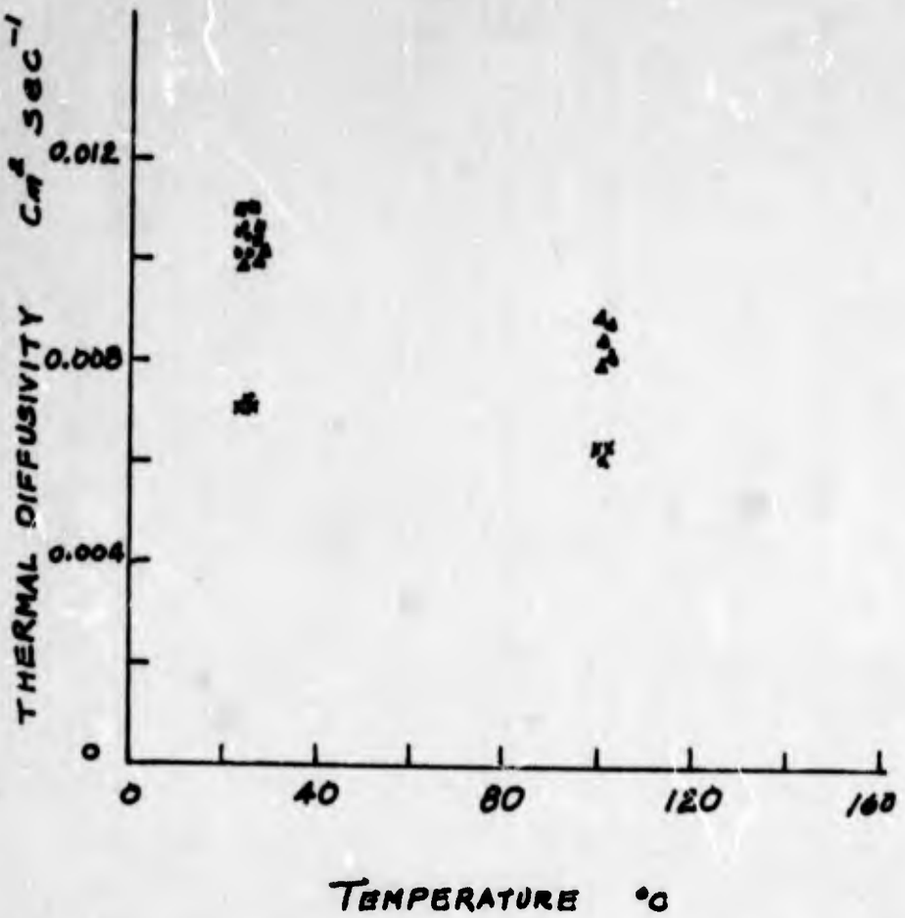

Fig. II/7. Thermal diffusivity of sample 135 (PbTe) at two temperatures before (□, Δ) and after exposure to 1.0 to 10^{17} (•) and 2.3 x 10^{19} (X) fast (E > 1 Mev) neutrons/cm².

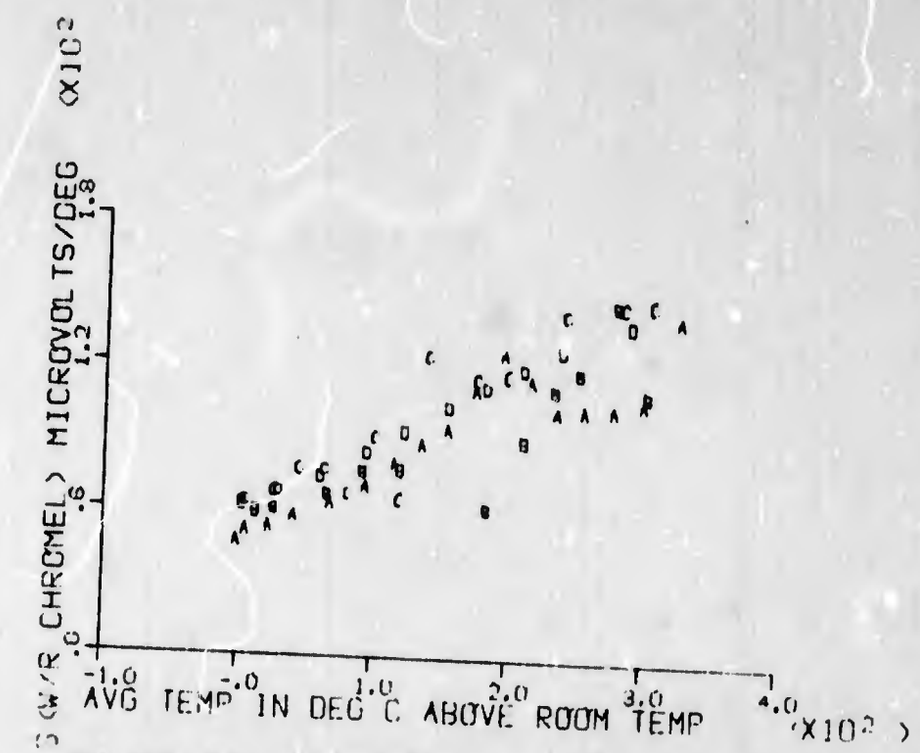

Fig. II/8. Temperature dependence of apparent Seebeck coefficient (with respect to chromel) of sample 145B ($Ge_{.95}Bi_{.05}Te$), before (A,B) and after (C,D) exposure to 1.6×10^{18} fast (E > 1 Mev) neutrons/cm². A, C = sample heating; B,D = sample cooling.

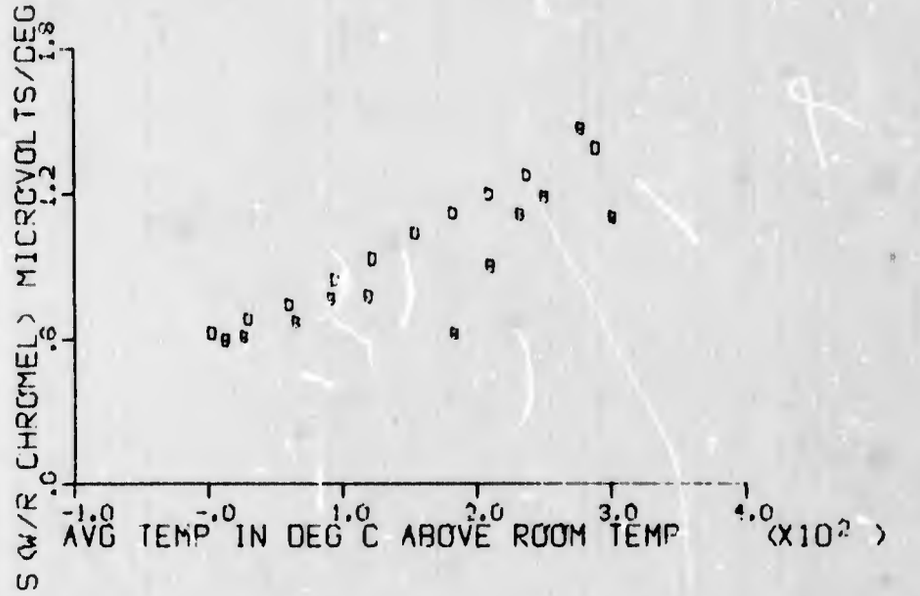

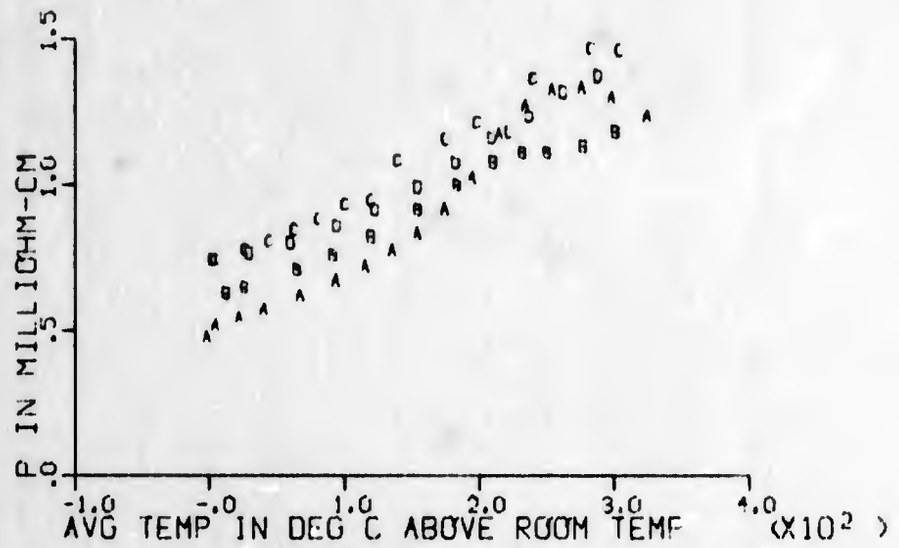

Fig. II/9 Temperature dependence of electrical resistivity of sample 145B ($Ge_{.95}Bi_{.05}Te$), before (A, B) and after (C,D) exposure to 1.6×10^{18} fast ($E > 1$ Mev) neutrons/cm^2. A,C = sample heating; B, D = sample cooling.

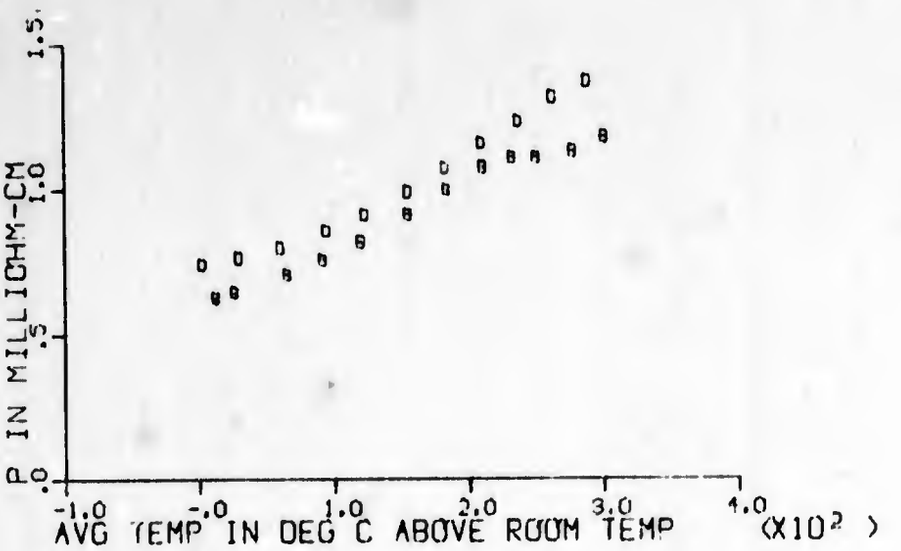

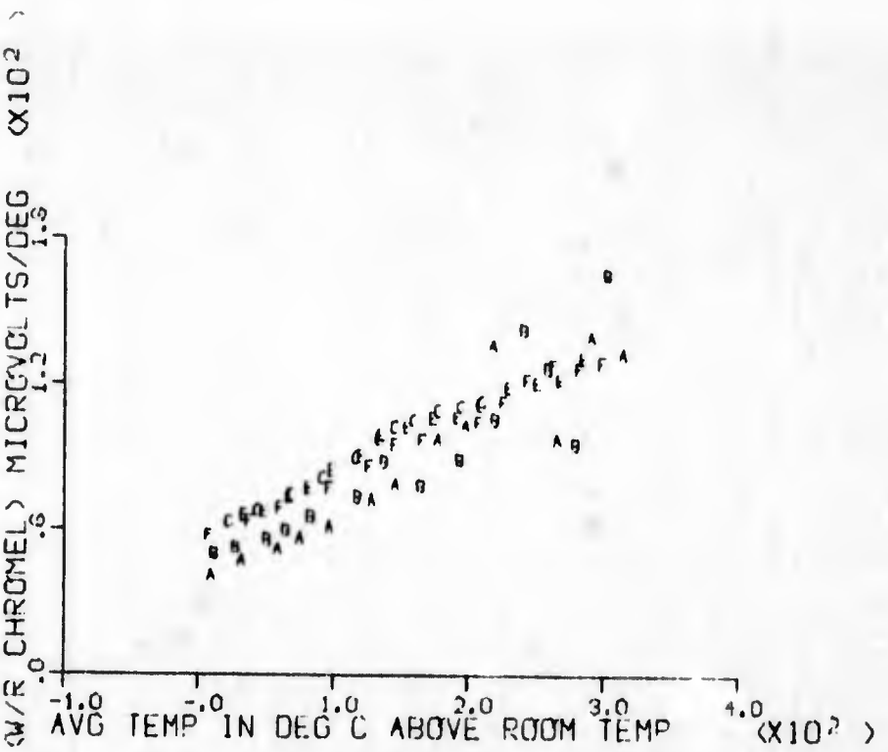

Fig. II/10. Temperature dependence of apparent Seebeck coefficient (with respect to chromel) of sample 147A ($Ge_{.95}Bi_{.05}Te$), before (A,B) and after (C,E,F) exposure to 1.6×10^{18} fast (E) 1 Mev) neutrons/cm^2. A,C,E = sample heating; B,F = sample cooling.

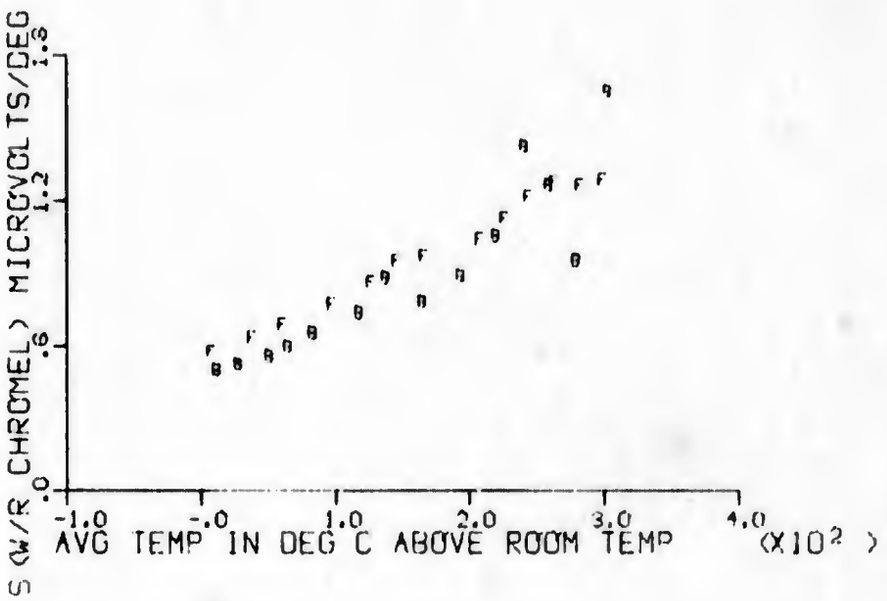

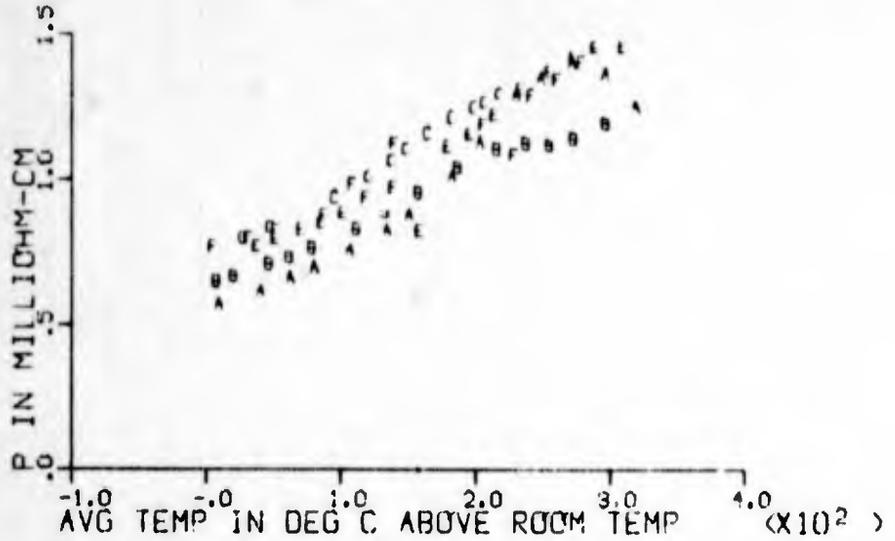

Fig. II/11. Temperature dependence of electrical resistivity of sample 147A ($Ge_{.95}Bi_{.05}Te$), before (A,B) and after (C,E,F) exposure to 1.6×10^{18} fast (E) 1 Mev) neutrons/cm^2. A,C,E = sample heating; B, F = sample cooling.

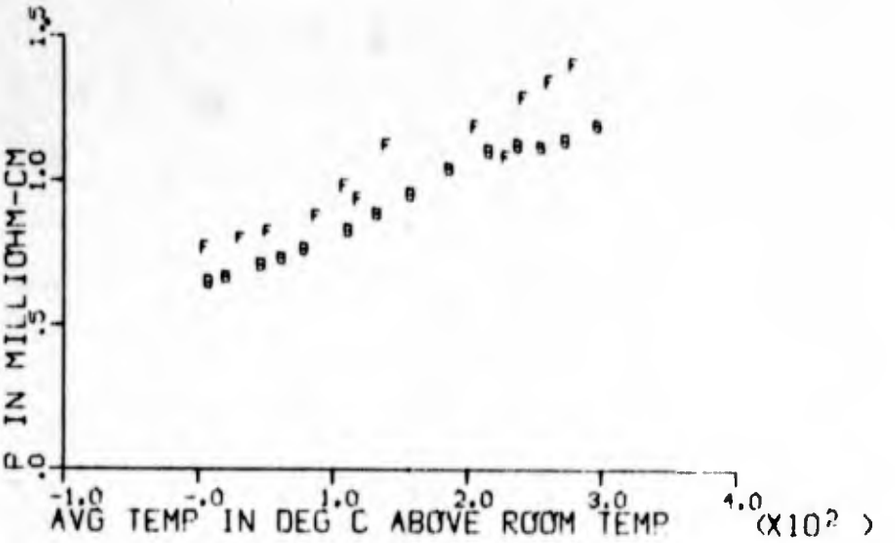

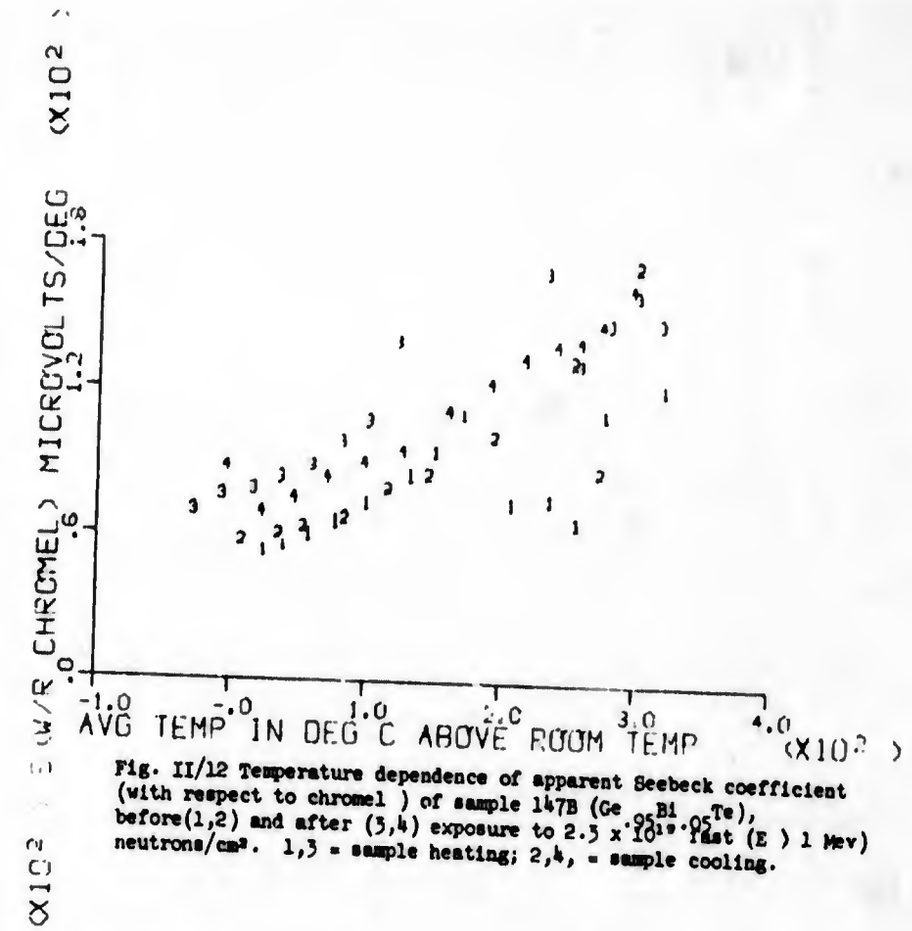

Fig. II/12 Temperature dependence of apparent Seebeck coefficient (with respect to chromel) of sample 147B ($Ge_{.95}Bi_{.05}Te$), before(1,2) and after (3,4) exposure to 2.5×10^{19} fast (E) 1 Mev) neutrons/cm². 1,3 = sample heating; 2,4, = sample cooling.

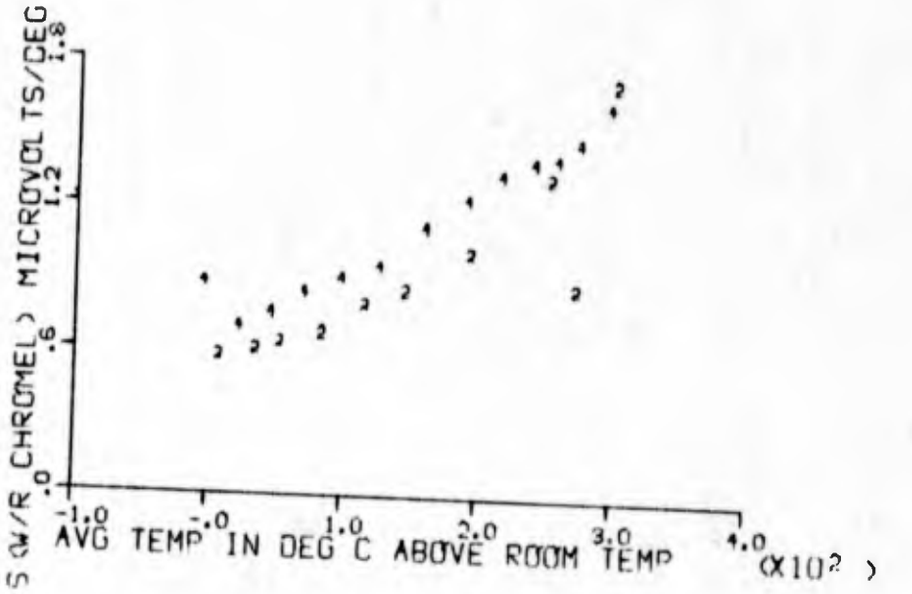

Fig. II/13. Temperature dependence of electrical resistivity of sample 147B ($Ge_{.95}Bi_{.05}Te$), before (1,2) and after (3,4) exposure to 2.3 x 10^{19} fast (E) 1 Mev) neutrons/cm^2. 1,3 = sample heating; 2.4 = sample cooling. The sharp peak around 200°C above room temperature is a typical example of measurement error arising from the combination of an annealing process with the dynamic measurement technique, as discussed in the Observations section of the main body of this report.

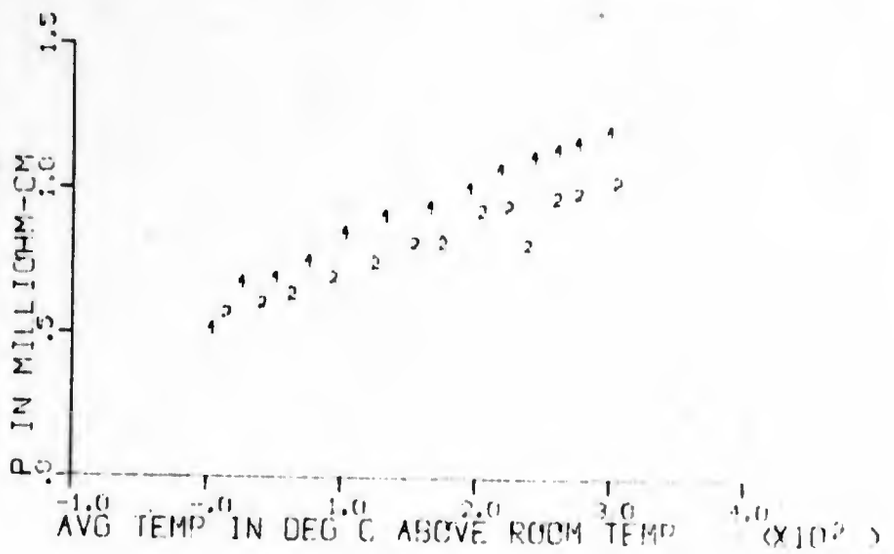

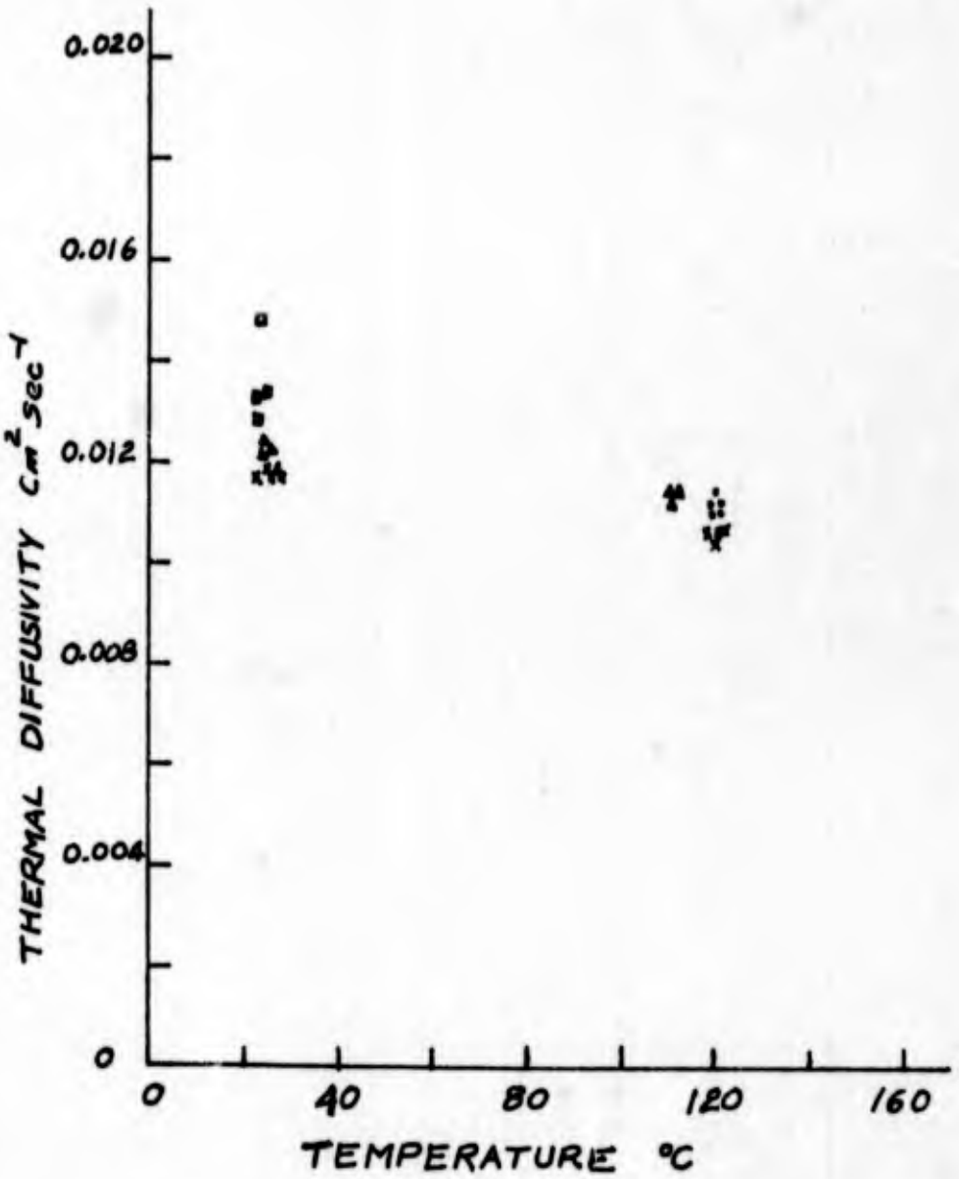

Fig. II/14. Thermal diffusivity of sample 148 ($Ge_{.95}Bi_{.05}Te$) at two temperatures before (□ , △) and after 1.0×10^{17} (●) and 1.6×10^{19} (X) fast (E > 1 Mev) neutrons/cm^2.

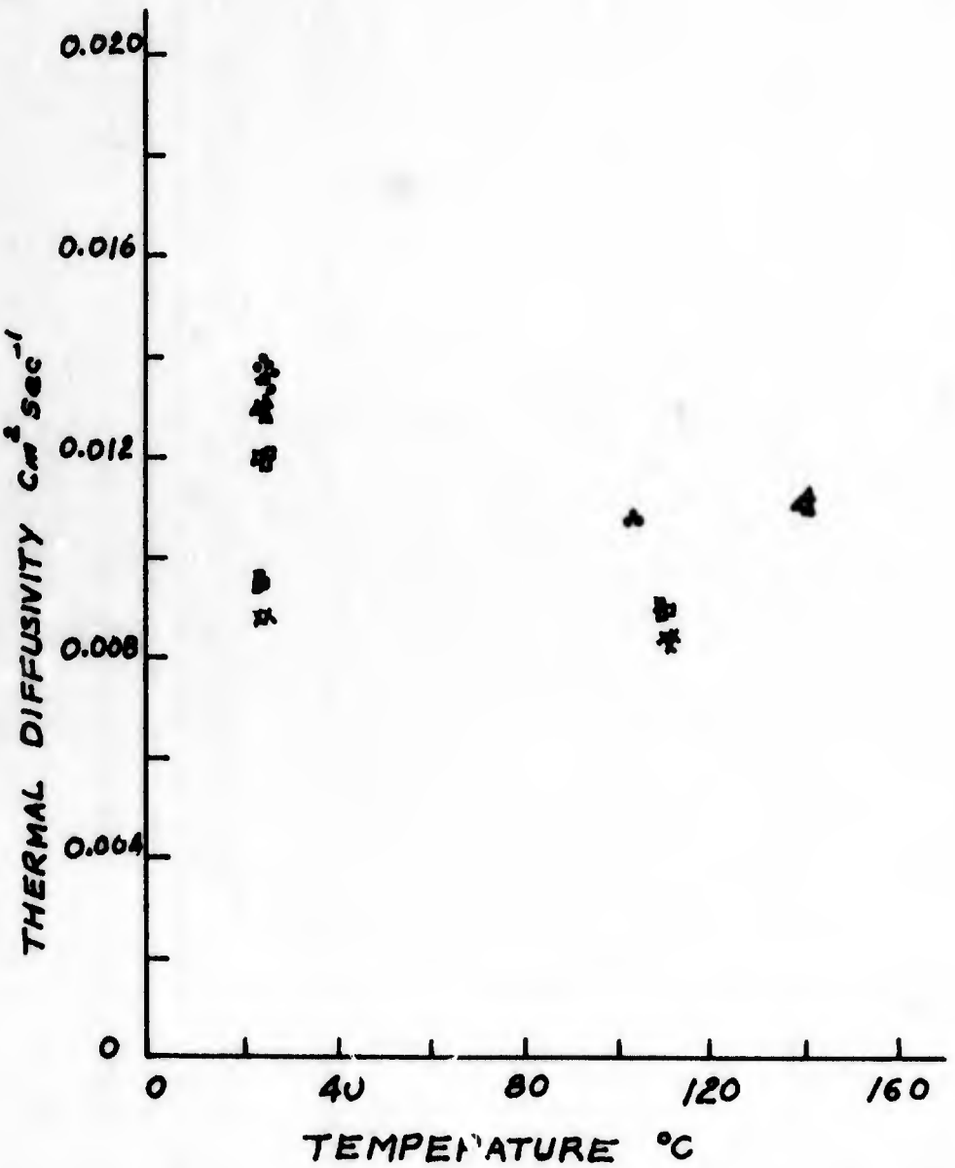

Fig. II/15. Thermal Diffusivity of sample 142 ($Ge_{.95}Bi_{.05}Te$) at various temperatures before (□ , △) and after 1.0×10^{19} (•) and 2.3×10^{19} (X) fast (E > 1 Mev) neutrons/cm².

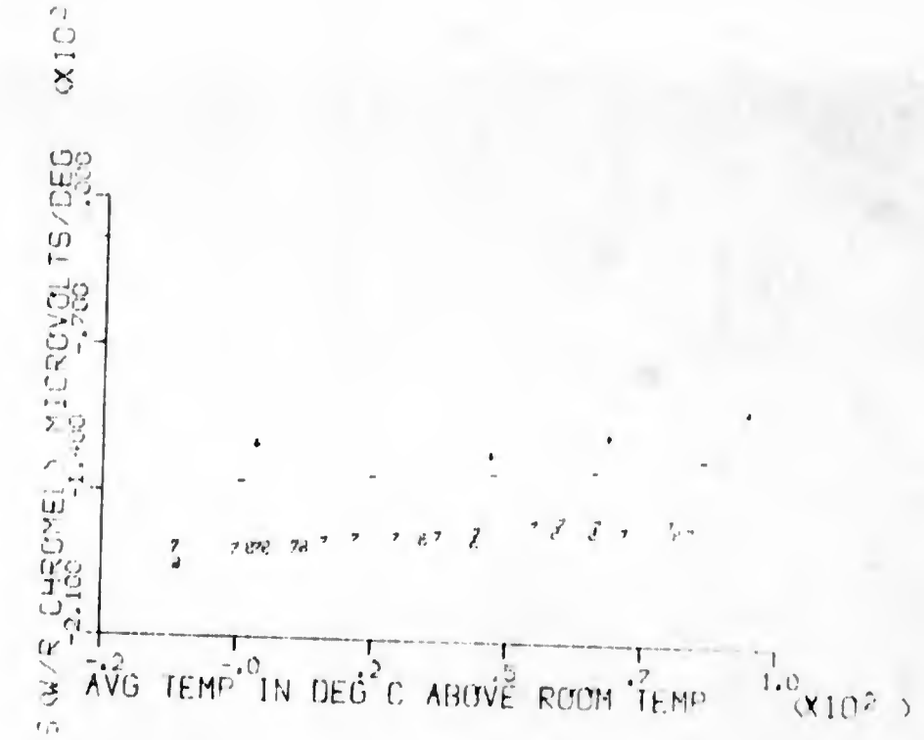

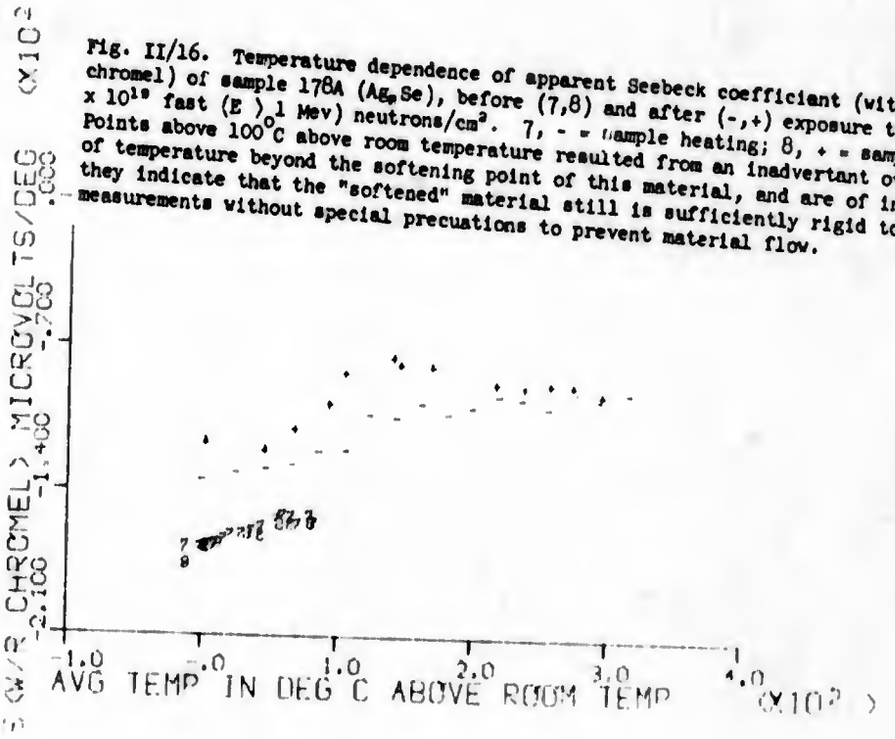

Fig. II/16. Temperature dependence of apparent Seebeck coefficient (with respect to chromel) of sample 178A (Ag_2Se), before (7,8) and after (-,+) exposure to 2.3 x 10^{19} fast (E_n 1 Mev) neutrons/cm^2. 7, - = sample heating; 8, + = sample cooling. Points above 100°C above room temperature resulted from an inadvertant over-run of temperature beyond the softening point of this material, and are of interest because they indicate that the "softened" material still is sufficiently rigid to permit measurements without special precautions to prevent material flow.

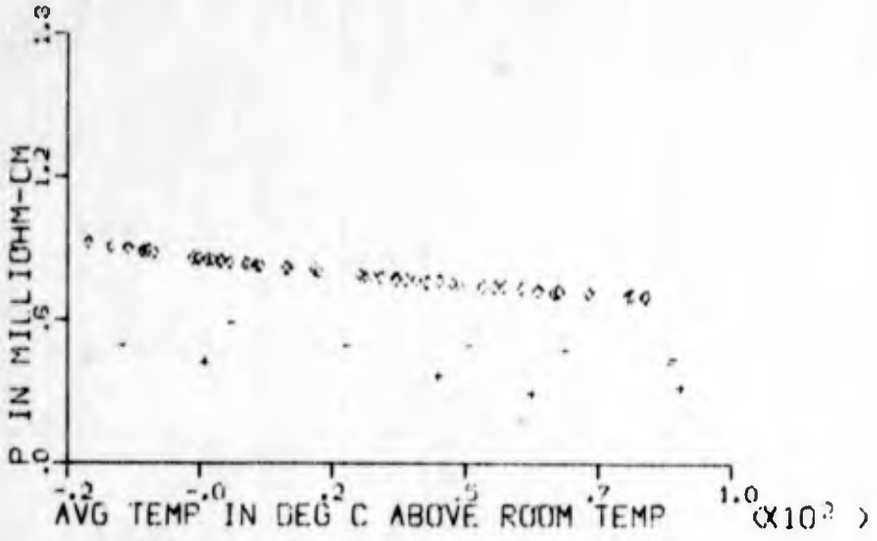

Fig. II/17. Temperature dependence of electrical resistivity of sample 178A (Ag_2Se), before (◊) and after (-,+) exposure to 2.3 x 10^{19} fast (E) 1 Mev) neutrons/cm^2. The discontinuity at about 100°C above room temperature corresponds to an observed "softening point" in this material. The points above this temperature resulted from an inadvertent over-run, and are of interest because they indicate that the "softened" material still is fairly rigid.

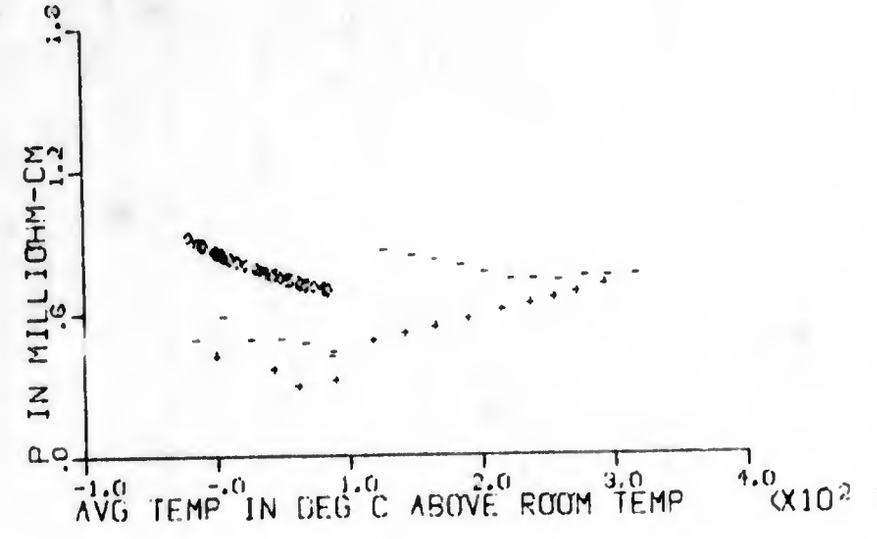

Fig. II/18. Temperature dependence of apparent Seebeck coefficient (with respect to chromel) of sample 181A (Ag_2Se) before (1,2) and after (3,4) exposure to 2.3×10^{18} fast (E) 1 Mev) neutrons/cm^2. 1,3 = sample heating; 2,4 = sample cooling.

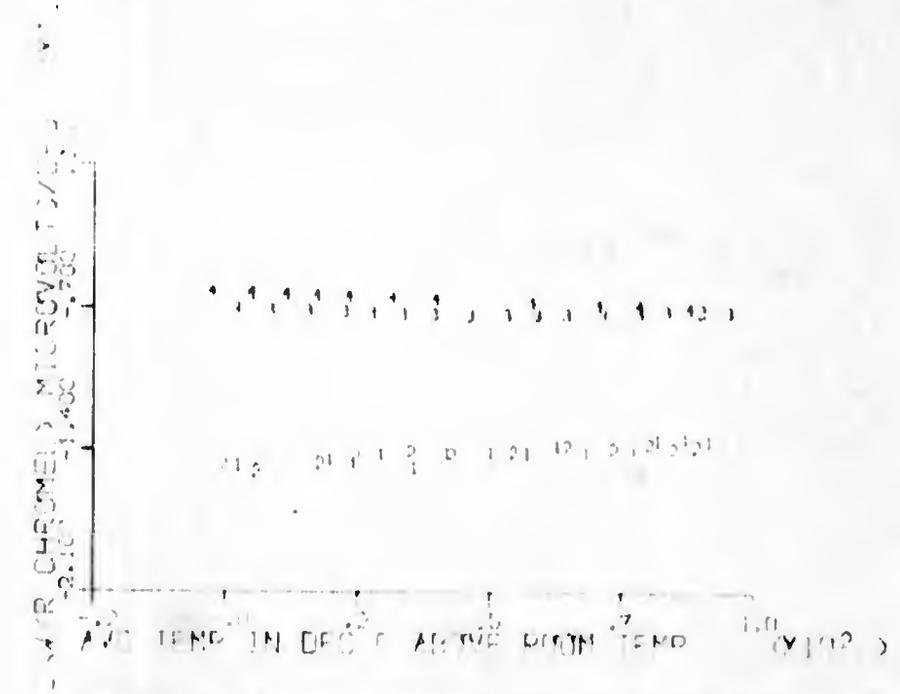

Fig. II/19. Temperature dependence of electrical resistivity of sample 181A (Ag_2Se), before (1,2) and after (3,4) exposure to 2.3×10^{18} fast (E) 1 Mev) neutrons/cm^2. 1,3 = sample heating; 2,4 = sample cooling.

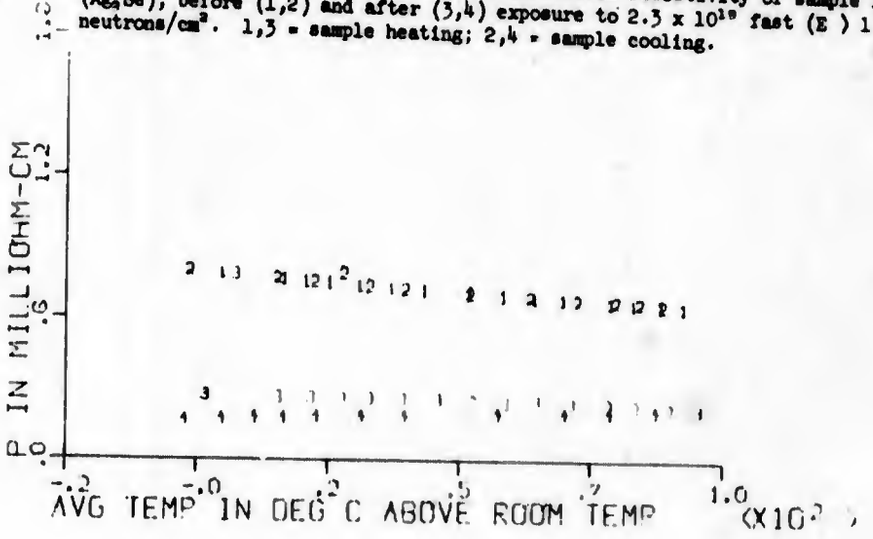

Fig. II/20. Temperature dependence of apparent Seebeck coefficient (with respect to chromel) of sample 181B (Ag_2Se), before (1,2) and after (3,4) exposure to 2.3×10^{19} fast (E) 1 Mev) neutrons/cm^2. 1,3 = sample heating; 2,4 = sample cooling.

Fig. II/21. Temperature dependence of electrical resistivity of sample 181B (Ag_2Se), before (1,2) and after (3,4) exposure to 2.3×10^{19} fast (E) 1 Mev) neutrons/cm^2. 1,3 = sample heating; 2,4 = sample cooling.

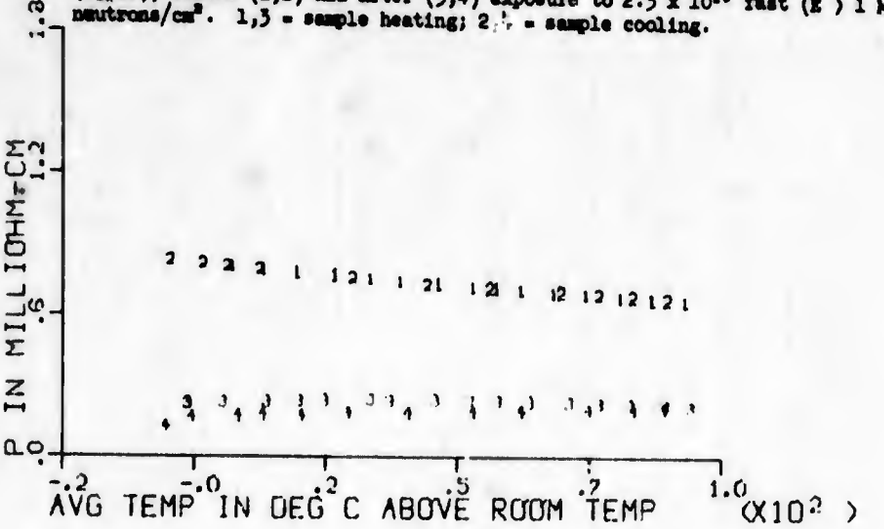

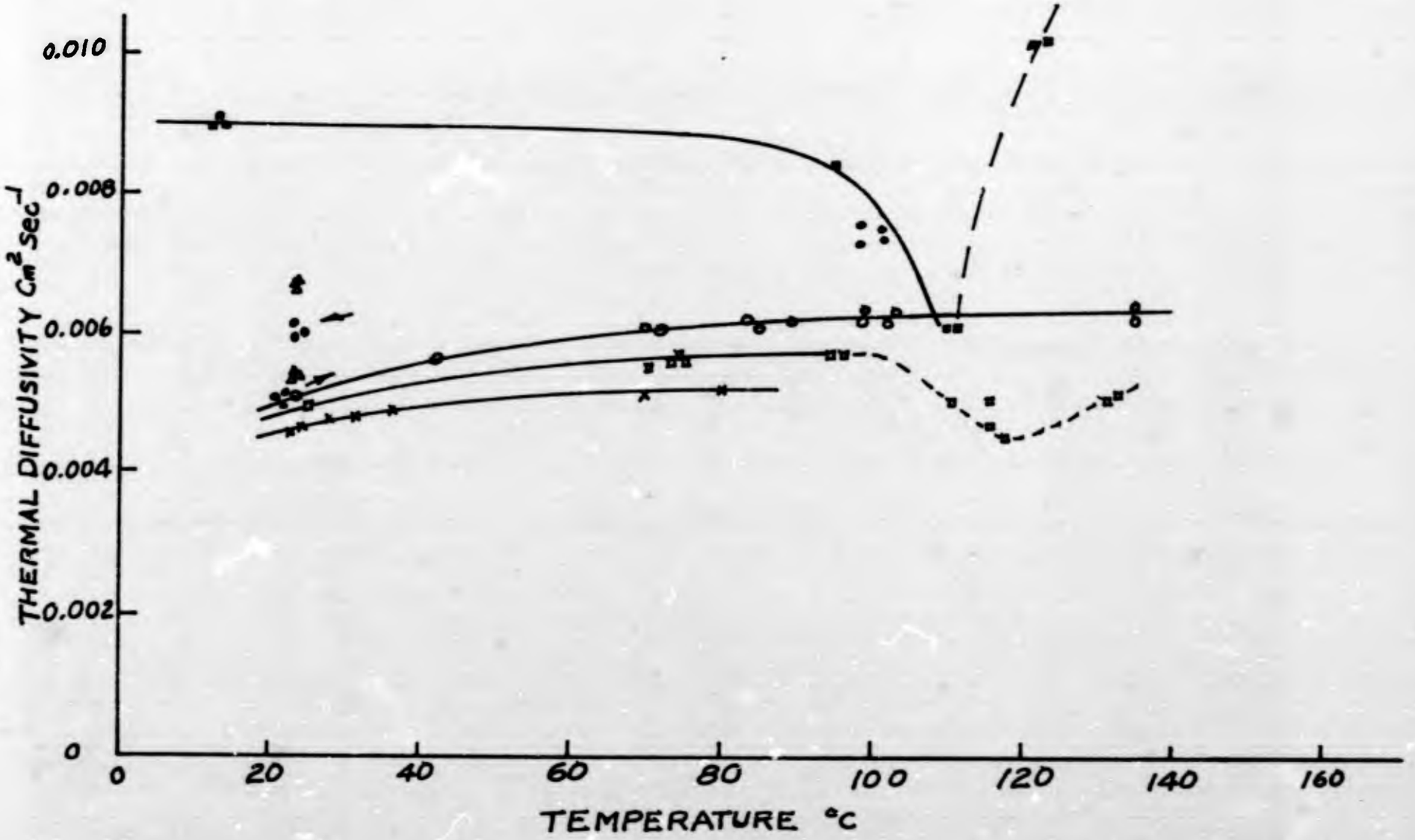

Fig. II/22. Temperature dependence of thermal diffusivity of sample 180 (Ag_2Se), before (○, □, X, Δ) and after exposure to 1.0×10^{17} (●) and 2.3×10^{19} (■) fast (E > 1 MeV) neutrons/cm^2.

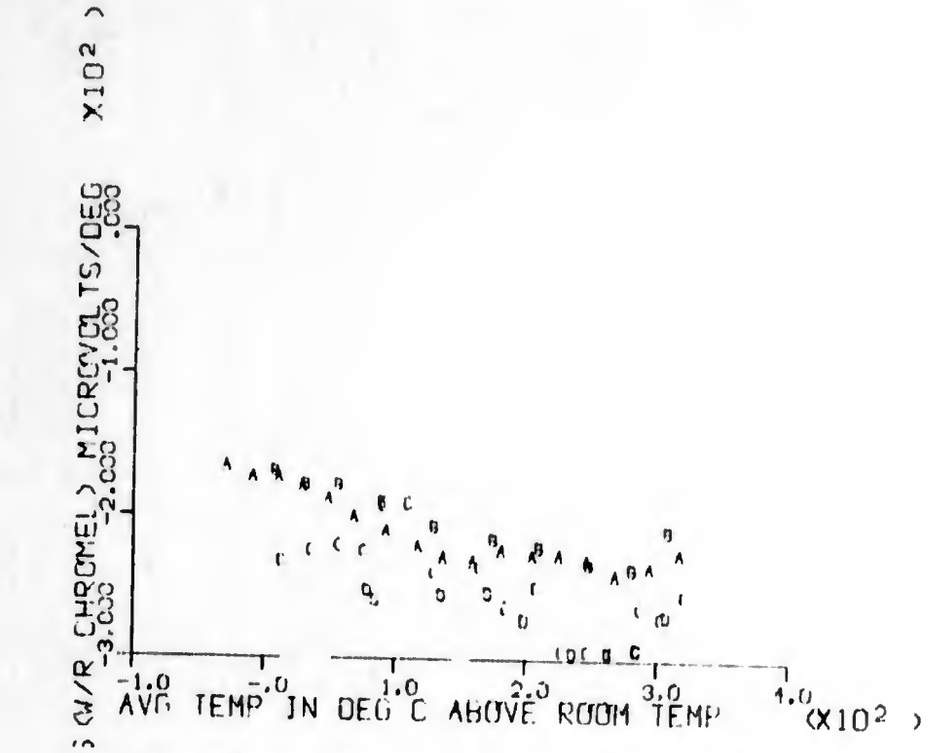

Fig. II/23. Temperature dependence of apparent Seebeck coefficient (with respect to chromel) of sample 224A (Ge-Si alloy), before (A,B) and after (C,D) exposure to 1.6 x 10^{18} fast (E > 1 Mev) neutrons/cm². A,C = sample heating; B,D = sample cooling.

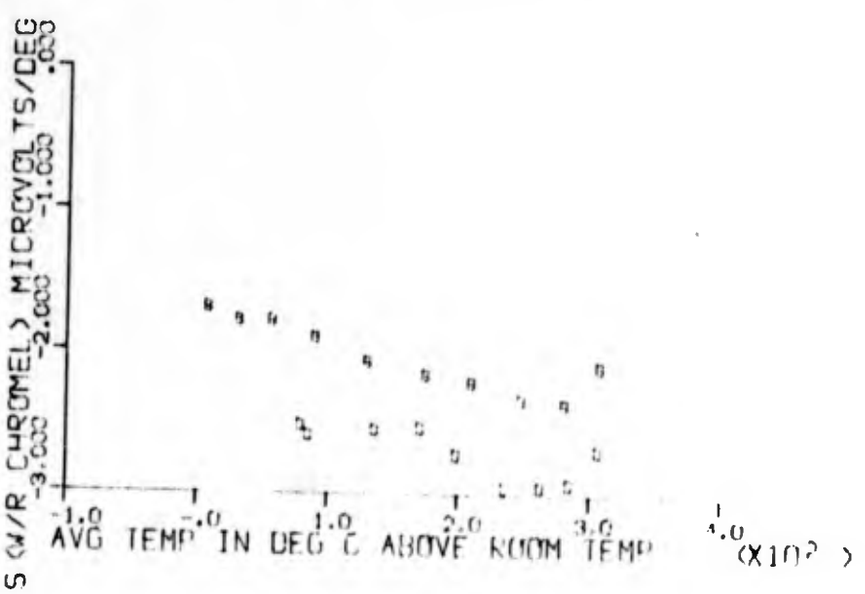

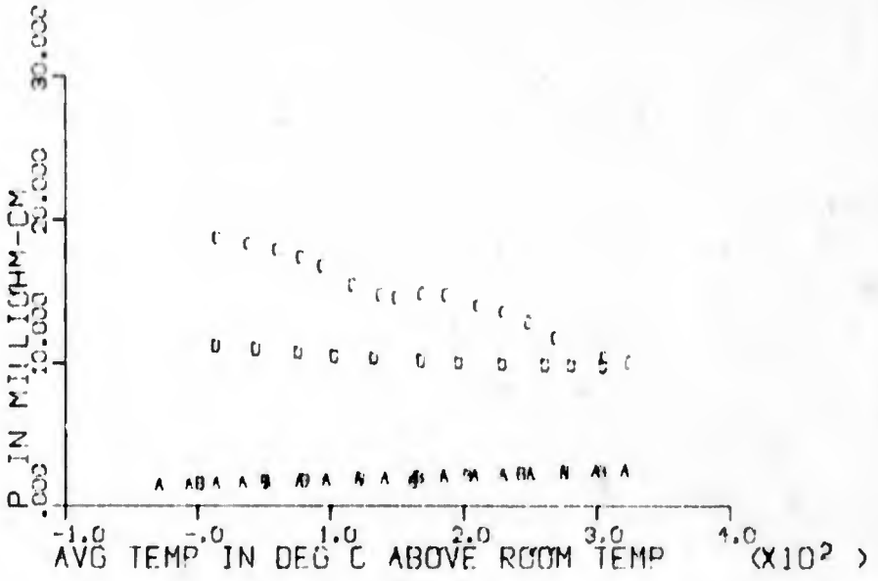

Fig. II/24. Temperature dependence of electrical resistivity of sample 124A (Ge-Si alloy), before (A, B) and after (C,D) exposure to 1.6 x 10^{18} fast (E) 1 Mev; neutrons/cm^2. A, C = sample heating; B, D = sample cooling.

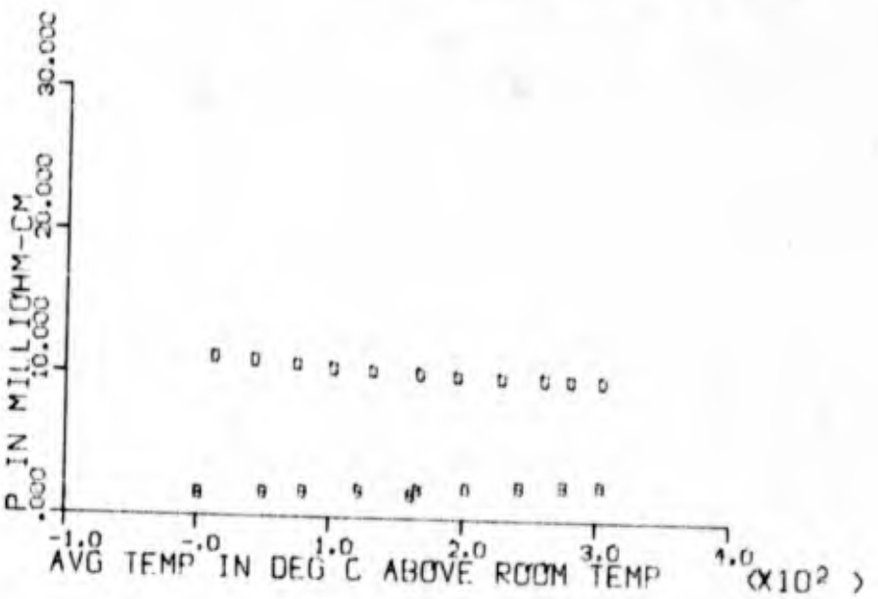

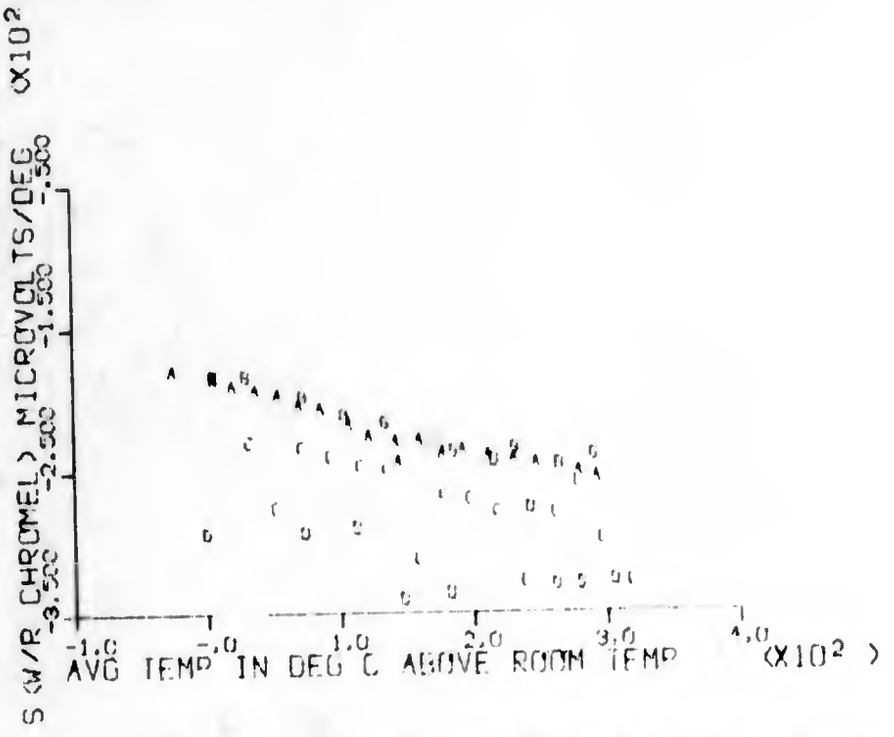

Fig. II/25. Temperature dependence of apparent Seebeck coefficient (with respect to chromel)of sample 224B (Ge-Si alloy), before (A,B) and after (C,D) exposure to 1.6×10^{18} fast (E > 1 Mev) neutrons/cm^2. A,C = sample heating; B,D = sample cooling.

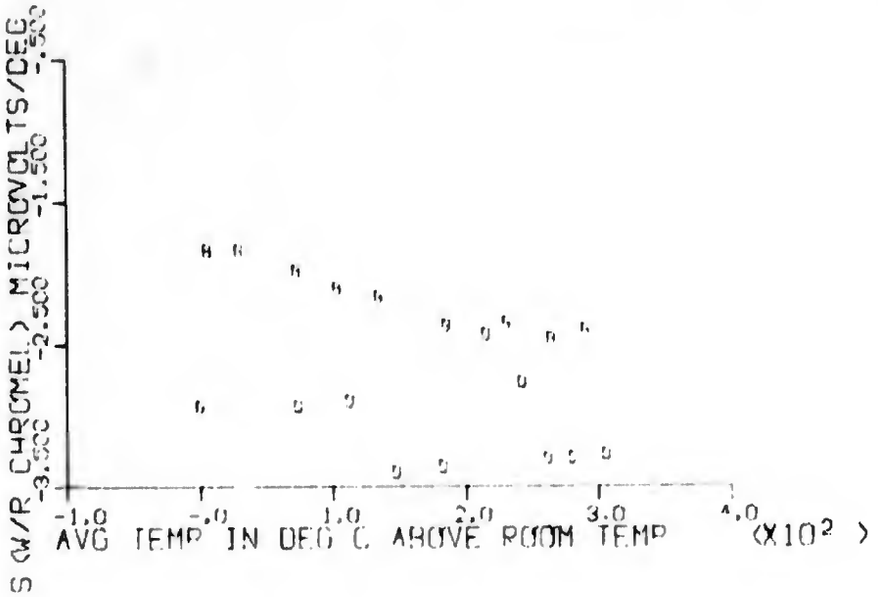

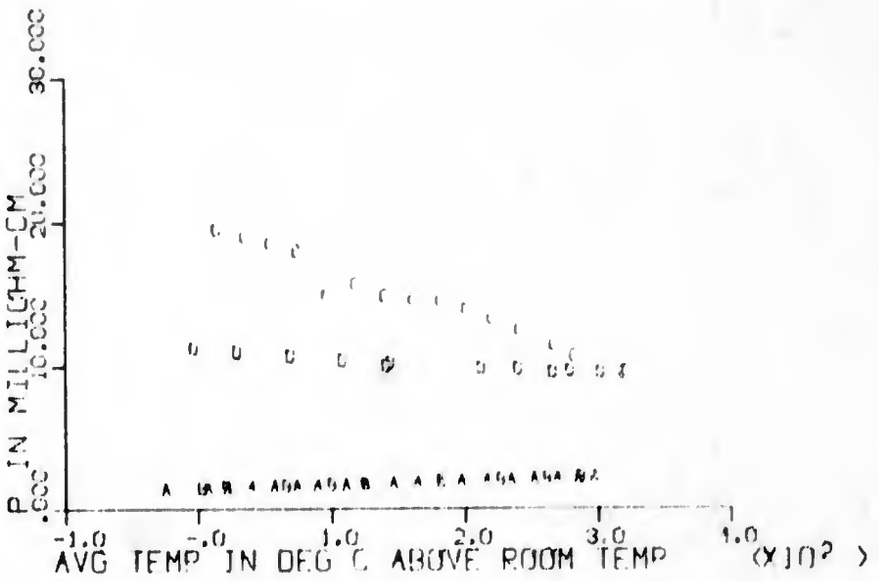

Fig. II/26. Temperature dependence of electrical resistivity of sample 224B (Ge-Si alloy), before (A,B) and after (C,D) exposure to 1.6 x 10^{18} fast (E > 1 Mev) neutrons/cm^2. A,C = sample heating; B,D = sample cooling.

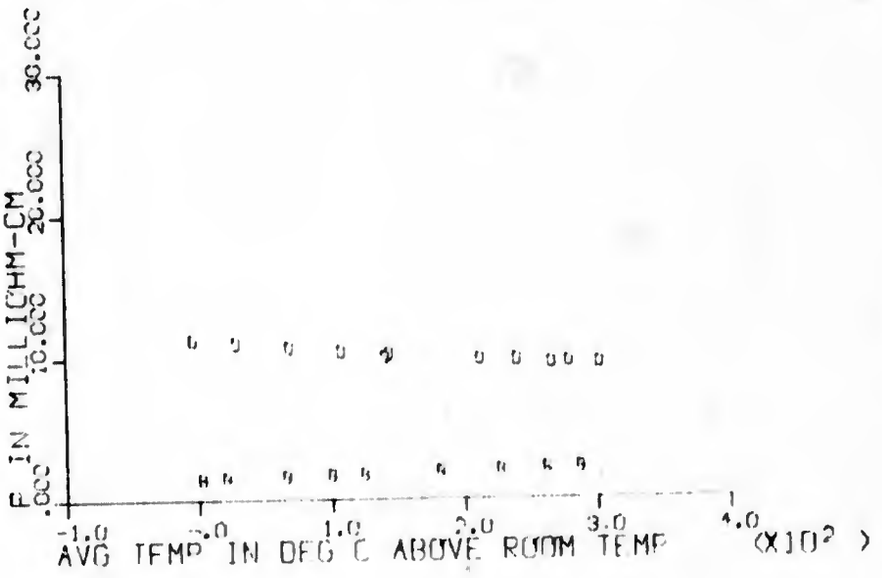

Fig. II/27. Temperature dependence of apparent Seebeck coefficient (with respect to chromel) of sample 224C (Os-Si alloy), before (1,2) (3,4) and after (5,6) exposure to 2.3 x 10^{19} fast (E > 1 Mev) neutrons/cm^2. 1,3,5 = sample heating; 2,4,6 = sample cooling.

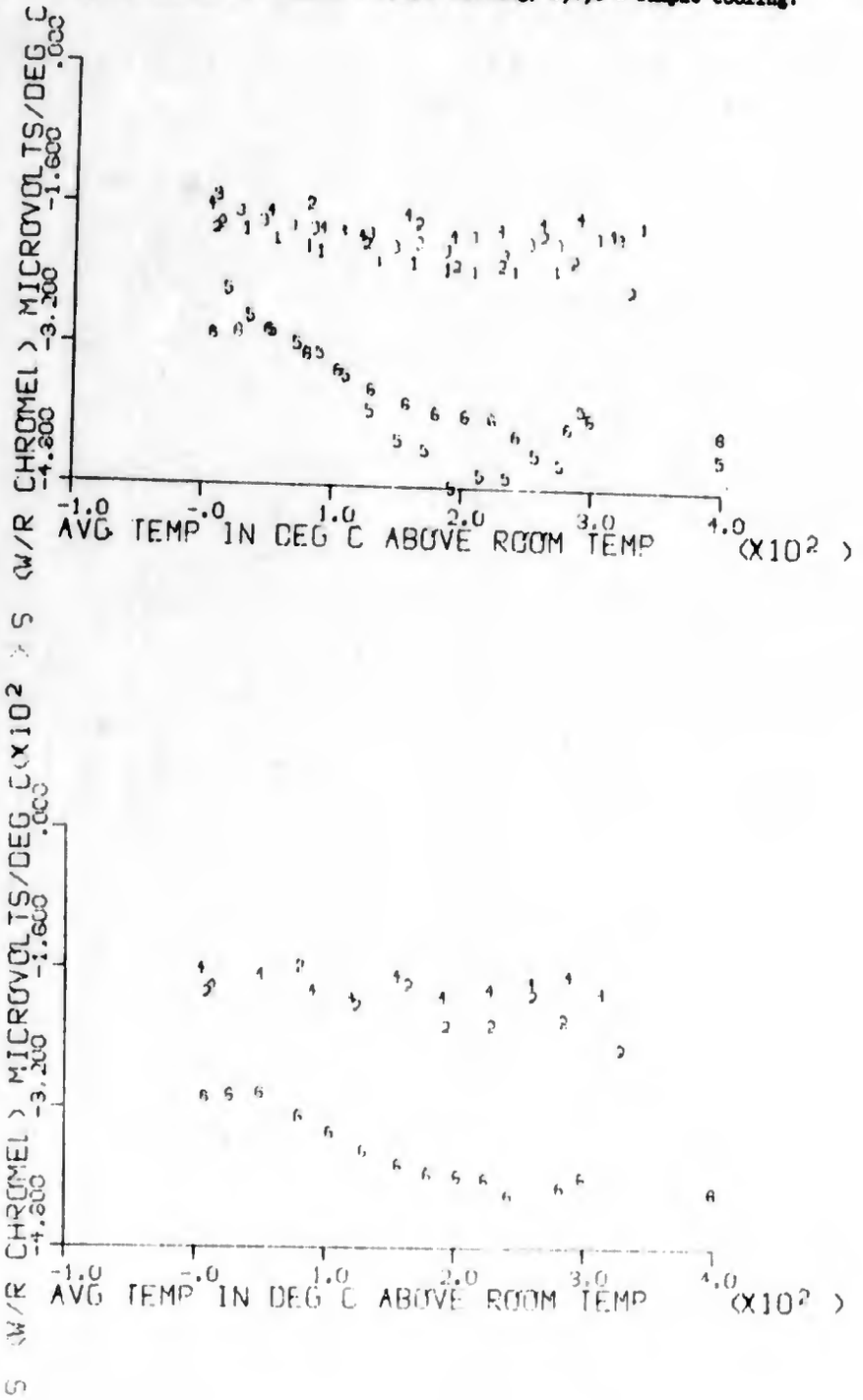

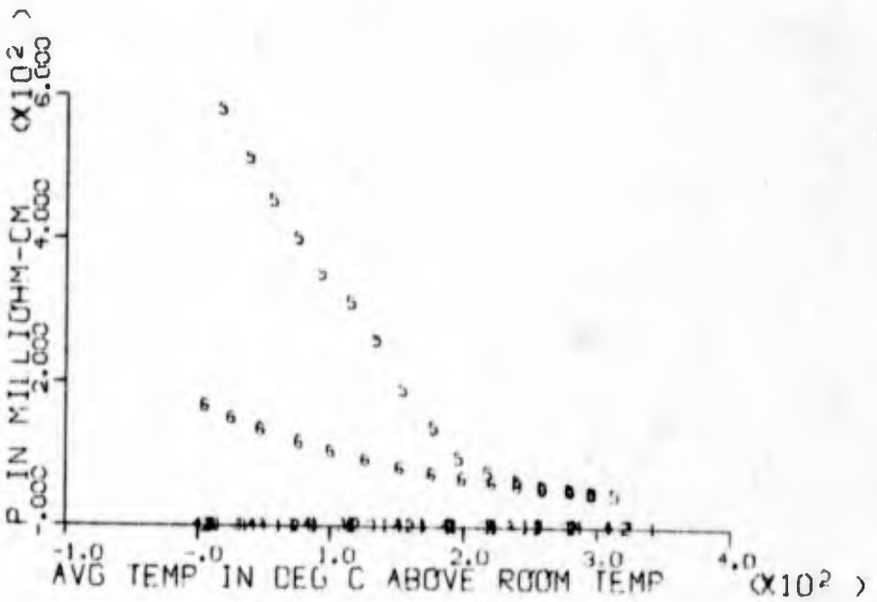

Fig. II/28. Temperature dependence of electrical resistivity of sample 224C (Ge-Si alloy) before (1,2,3,4) and after (5,6) exposure to 2.3 x 10^{19} fast (E > 1 Mev) neutrons/cm^2. 1,3,5 = sample heating; 2,4,6 = sample cooling.

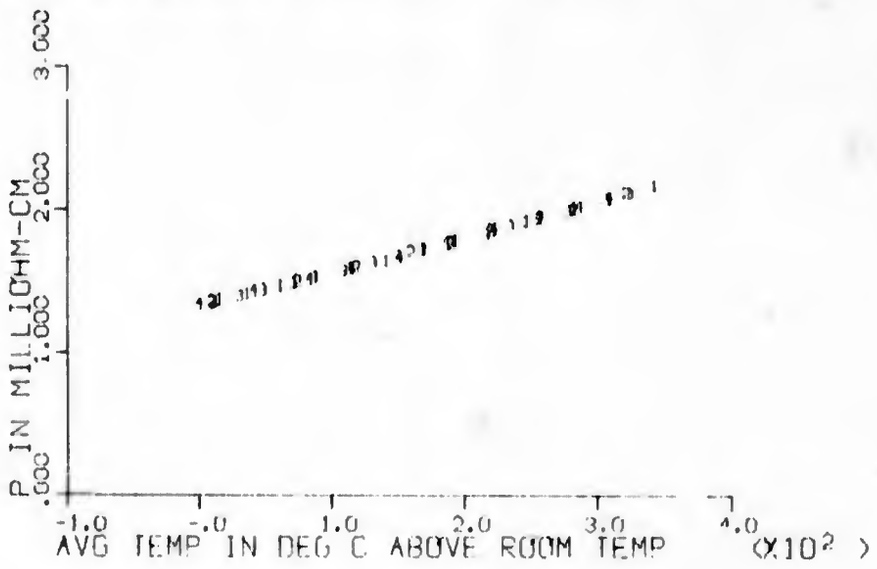

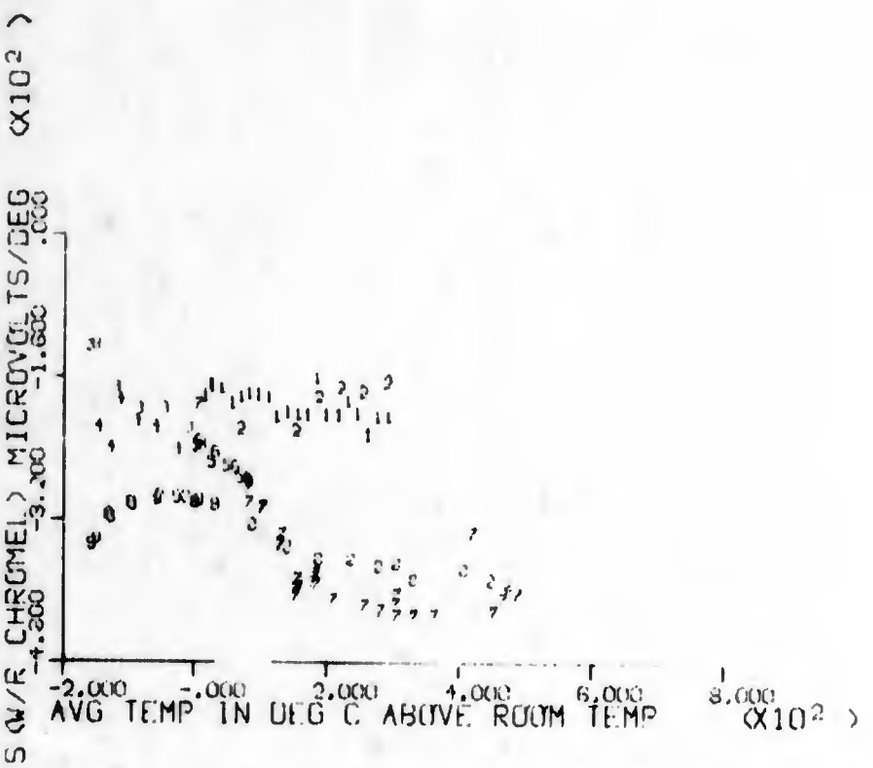

Fig. II/29. Temperature dependence of apparent Seebeck coefficient (with respect to chromel) of sample 224D (Ge-Si alloy), before (1,2) and after (3-0) exposure to 2.5 x 10^{19} fast (E > 1 Mev) neutrons/cm^2. Symbols 1,5 and 7 indicate data taken while heating the sample through the standard temperature range. Symbols 2 and 8 indicate data taken while the sample was cooling from room temperature down to about liquid nitrogen temperature, while 4 and 0 indicate data taken while the sample was warming through this range. Symbol 6 indicates a short cooling run made after partial warming into the standard temperature range.

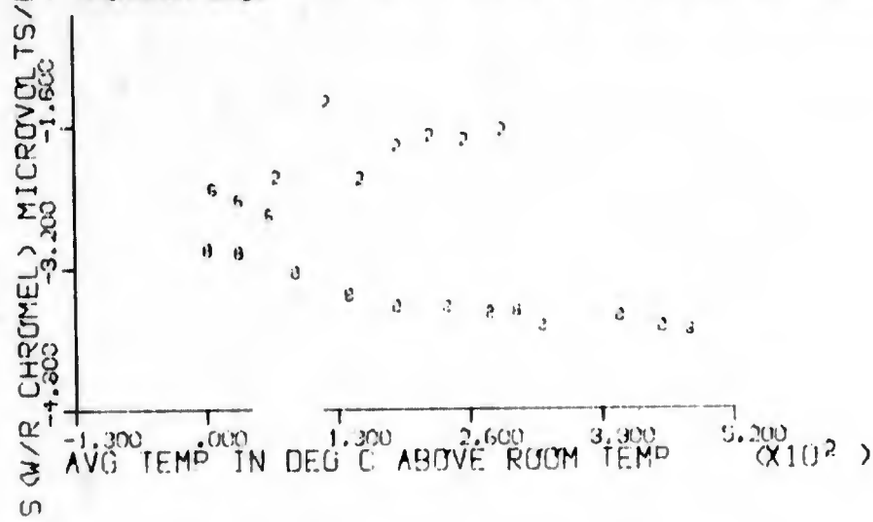

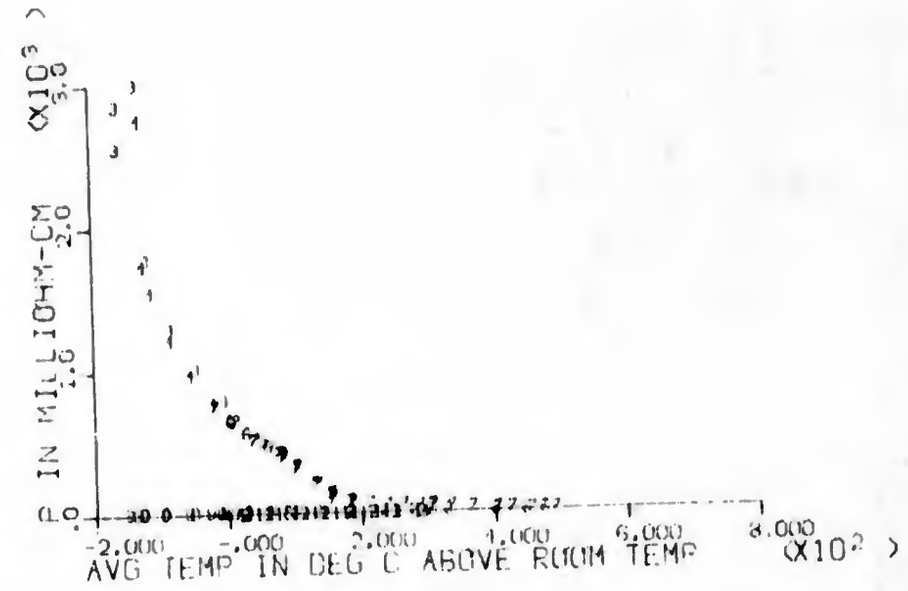

Fig. II/30. Temperature dependence of electrical resistivity of sample 224D (Ge-Si alloy), before (1,2) and after (3-0) exposure to 2.3×10^{19} fast (E) 1 Mev) neutrons/cm^2. For key to symbols see caption for Fig. II/29.

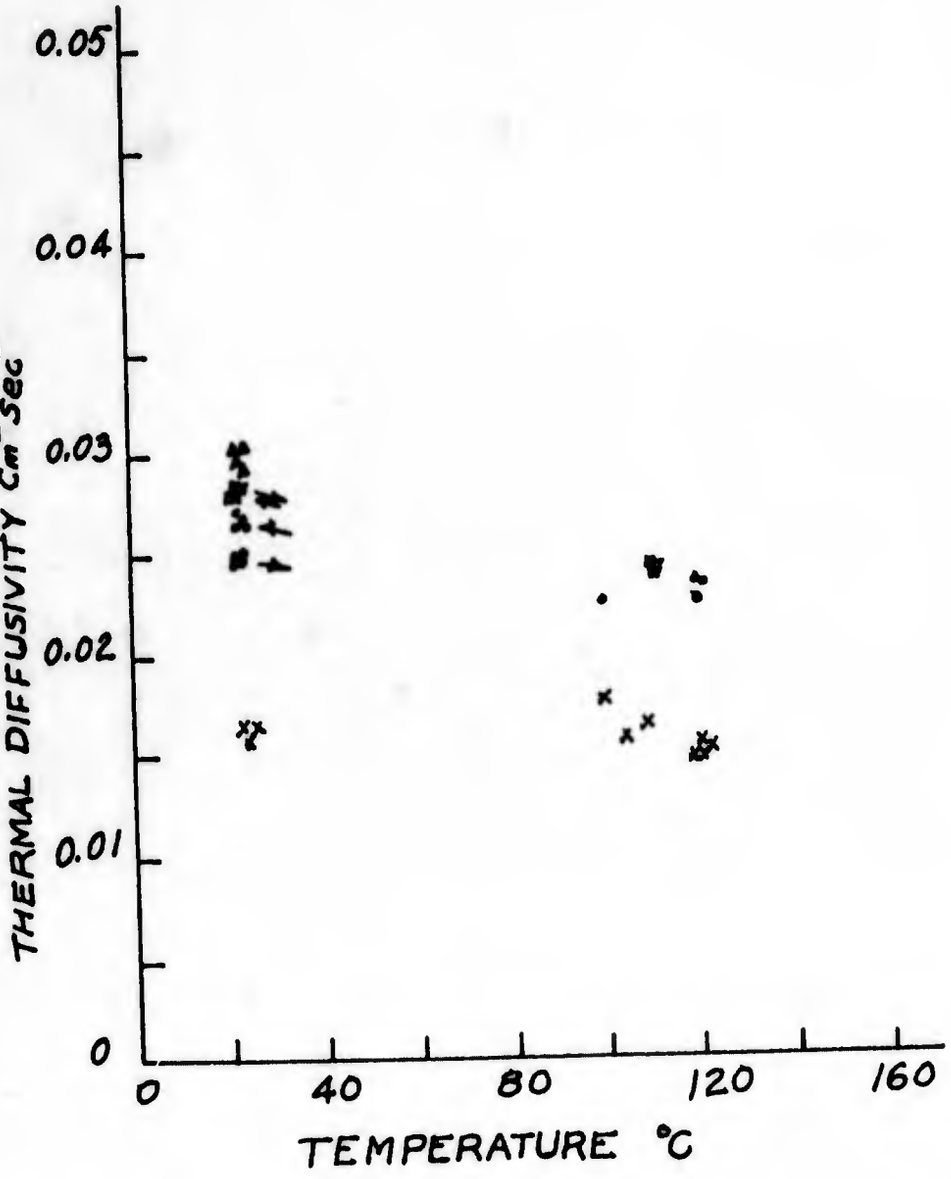

Fig. II/31. Thermal diffusivity of sample 225 (Ge-Si alloy) at two temperatures before (□, Δ) and after 1.0×10^{17} (•) and 1.6×10^{18} (X) fast (E > 1 MeV) neutrons/cm^2.

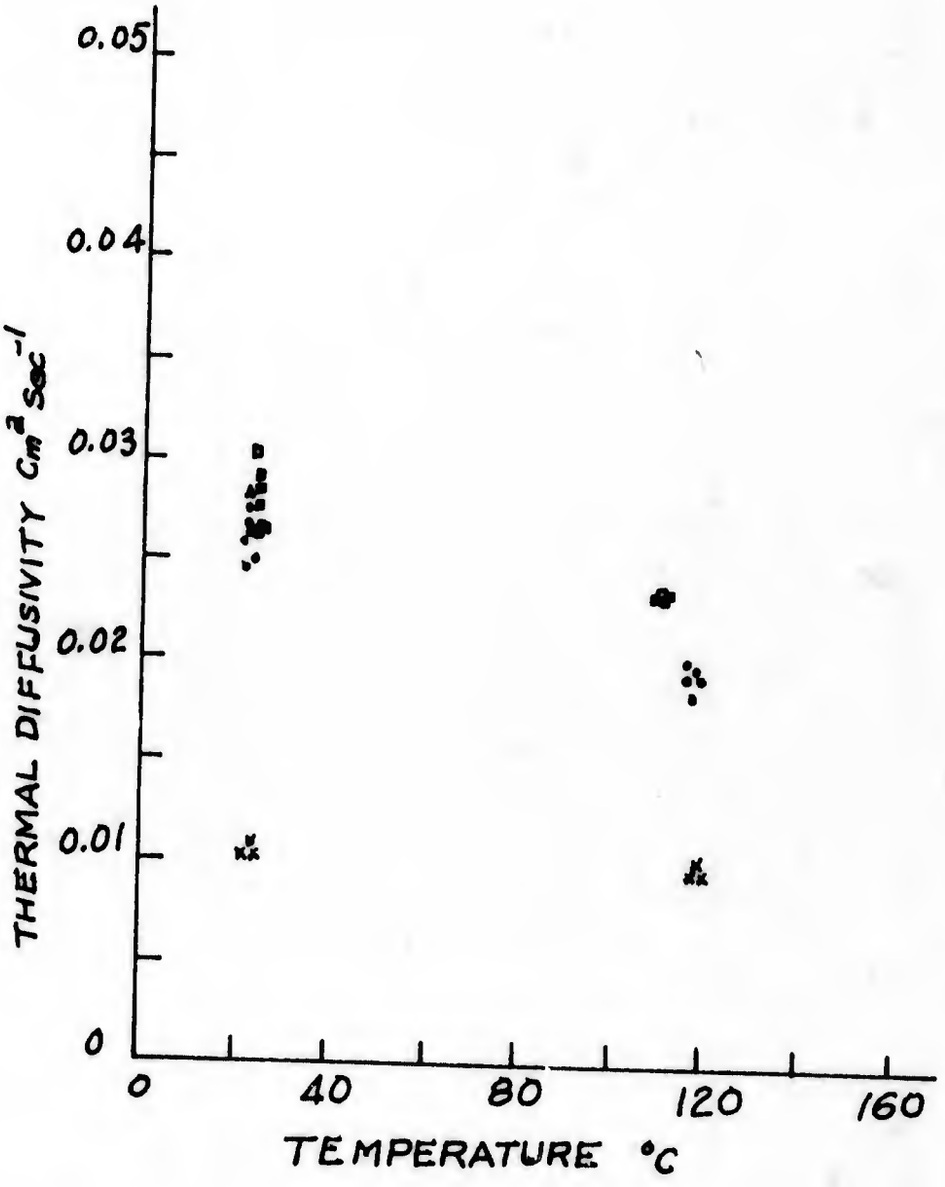

Fig. II/32. Thermal diffusivity of sample 226 (Ge-Si alloy) at two temperatures, before (□ , Δ) and after 1.0×10^{17} (•) and 2.3×10^{19} (X) fast (E > 1 MeV) neutrons/cm^2.

Fig. II/35. Temperature dependence of apparent Seebeck coefficient (with respect to chromel) of sample 230B (Ge-Si alloy), before (A,B) and after (C,D) exposure to 1.6 x 10^{18} fast (E) 1 Mev) neutrons/cm^2. A, C = sample heating; B, D = sample cooling.

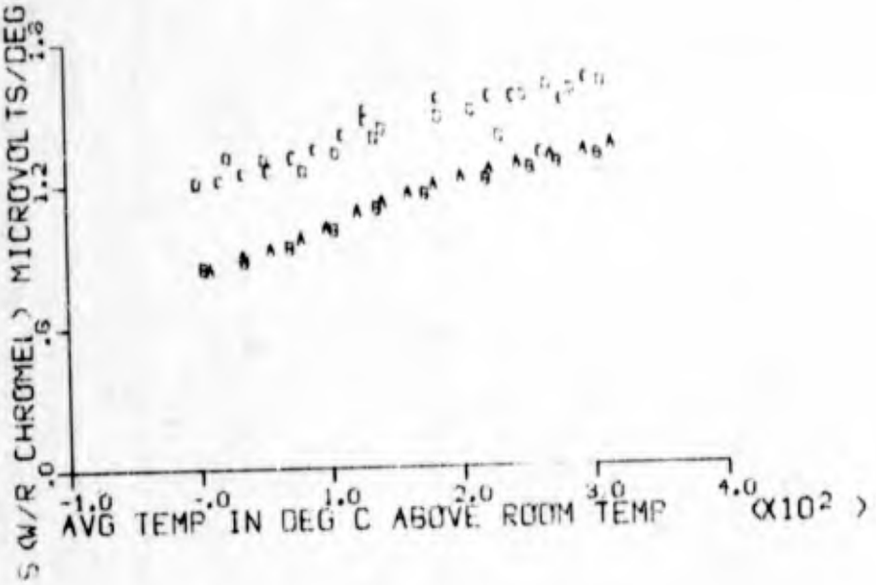

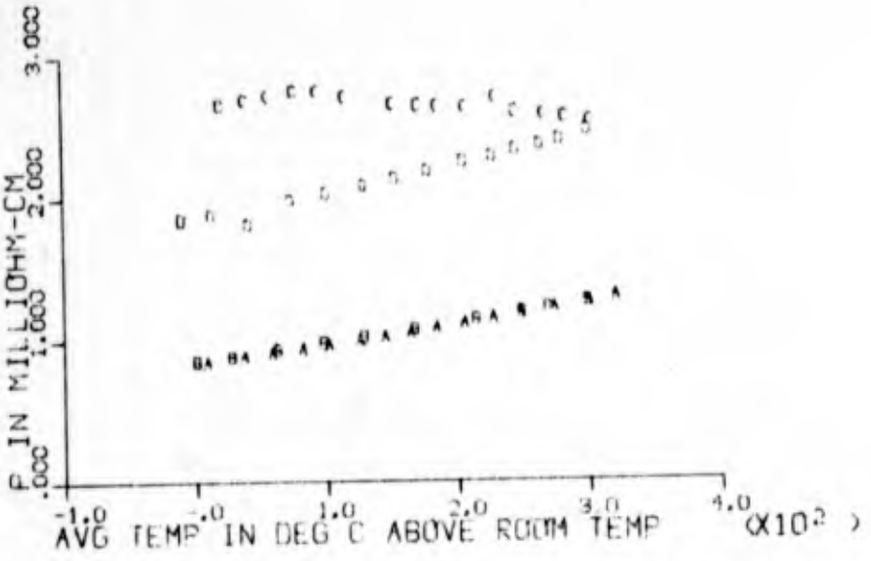

Fig. II/36. Temperature dependence of electrical resistivity of sample 230B (Ge-Si alloy), before (A,B) and after (C,D) exposure to 1.6 x 10^{18} fast (E) 1 Mev) neutrons/cm^2. A,C = sample heating; B,D = sample cooling.

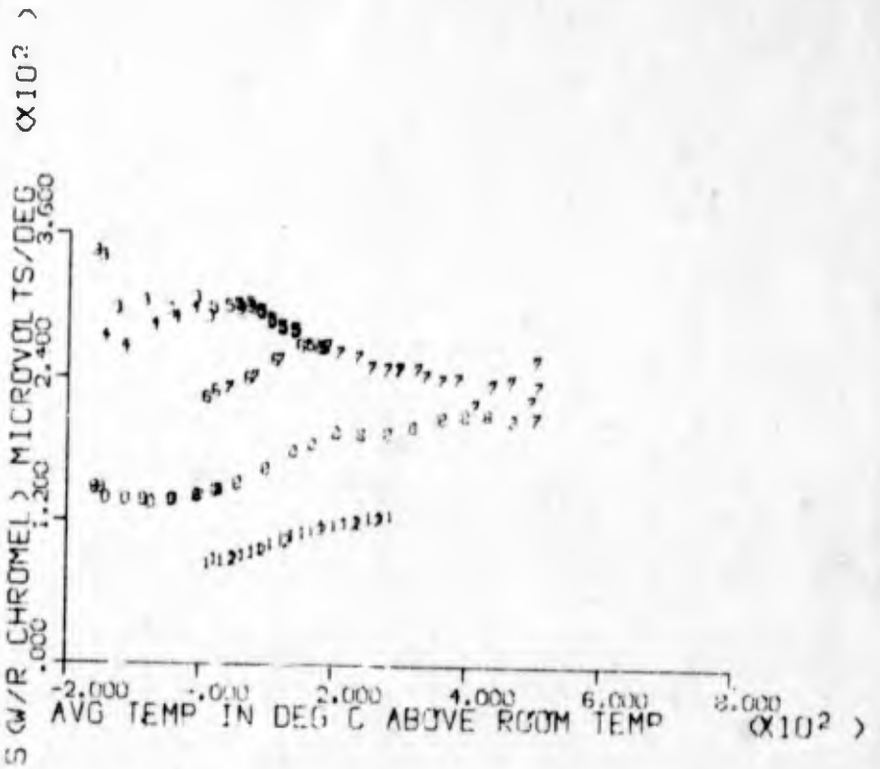

Fig. II/37. Temperature dependence of apparent Seebeck coefficient (with respect to chromel) of sample 232A (Ge-Si alloy), before (1,2) and after (3-0) exposure to 2.3×10^{19} fast (E) 1 Mev) neutrons/cm^2. 1,5 and 7 = sample heating (standard temperature range); 2,8 = sample cooling (standard range); 3,9 = sample cooling over range from room temperature to about liquid nitrogen temperature; 4.0 = sample warming over this low-temperature range; 6 = short cooling run made after partial warming into the standard temperature range.

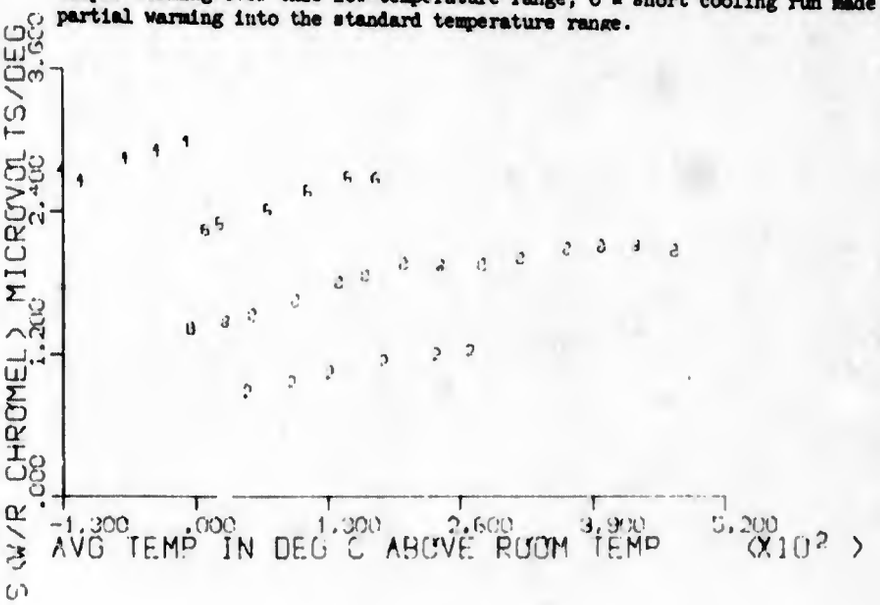

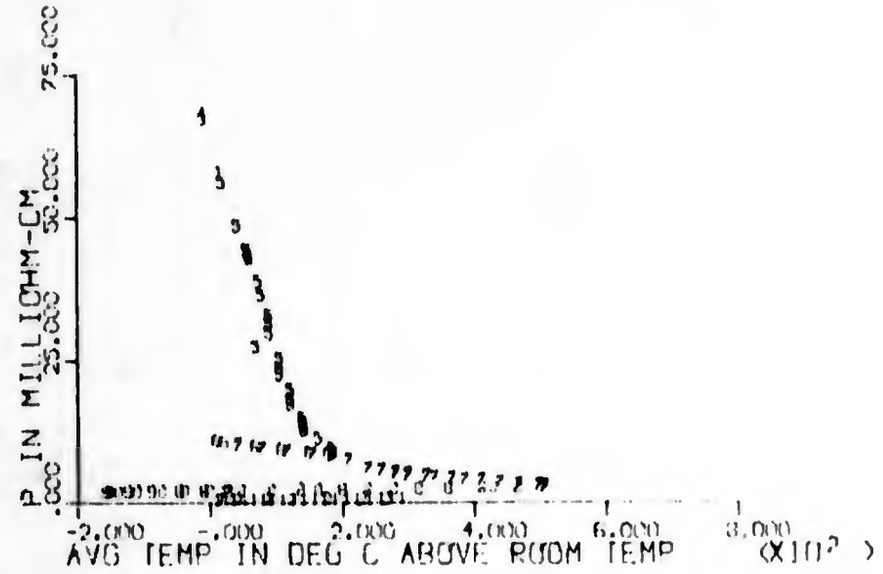

Fig. II/38. Temperature dependence of electrical resistivity of sample 232A (Ge-Si alloy), before (1,2) and after (5-0) exposure to 2.3 x 10^{19} fast (E > 1 Mev) neutrons/cm^2. For key to symbols see caption for Fig. II/37.

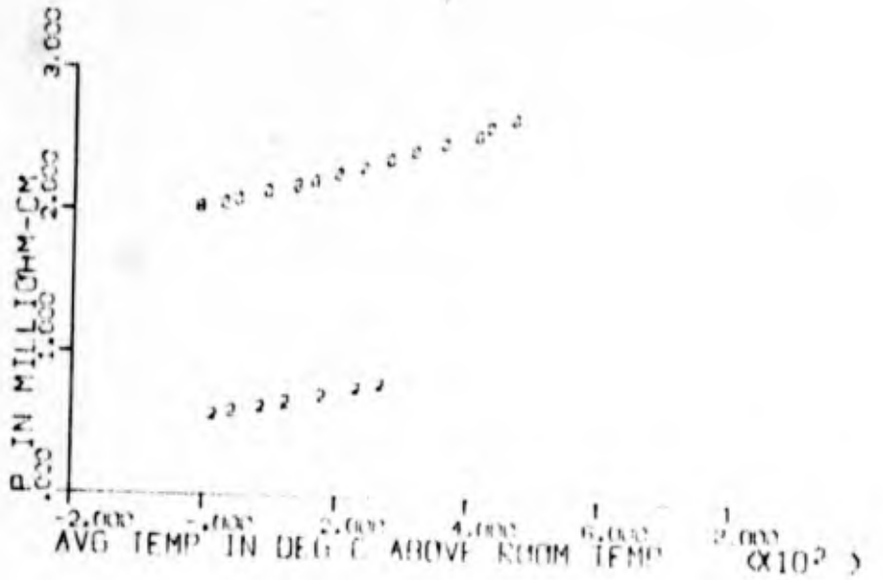

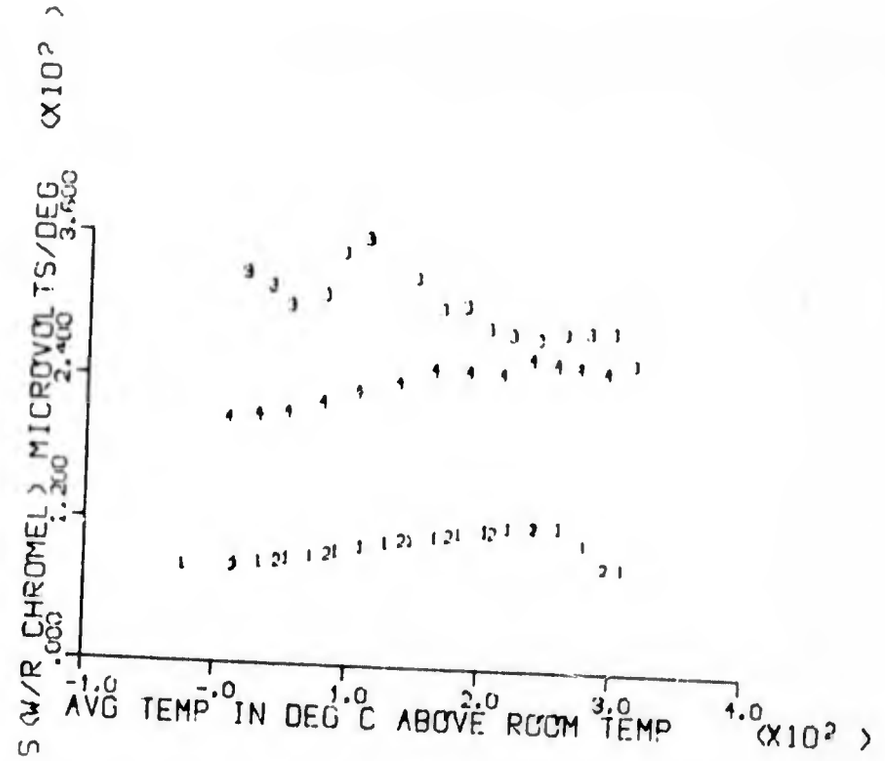

Fig. II/39. Temperature dependence of apparent Seebeck coefficient (with respect to chromel) of sample 232B (Ge-Si alloy), before (1,2) and after (3,4) exposure to 2.3 x 10^{19} fast (E) 1 Mev) neutrons/cm^2. 1,3 = sample heating; 2,4 = sample cooling.

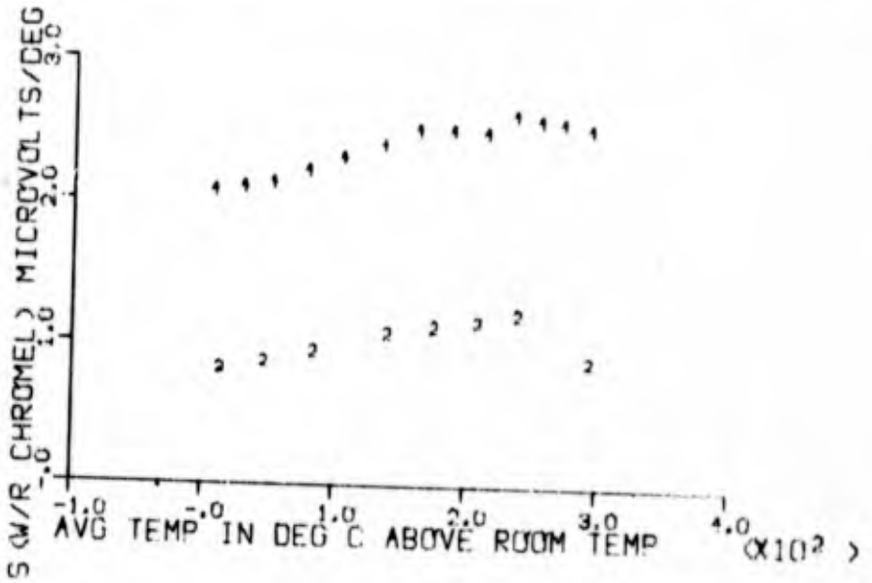

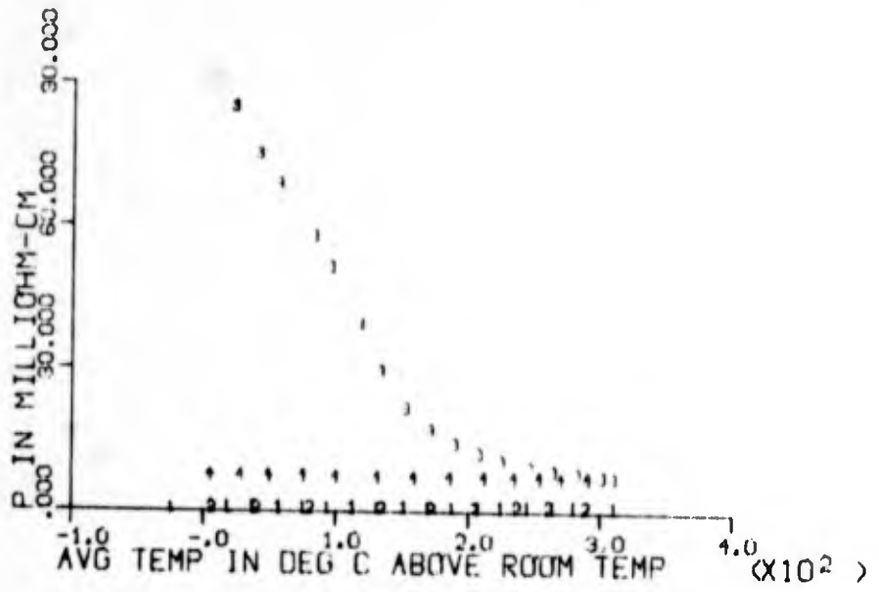

Fig. II/40. Temperature dependence of electrical resistivity of sample 232B (Ge-Si alloy), before (1,2) and after (3,4) exposure to 2.3 x 10^{19} fast (E > 1 Mev) neutrons/cm^2. 1,3 = sample heating; 2,4 = sample cooling.

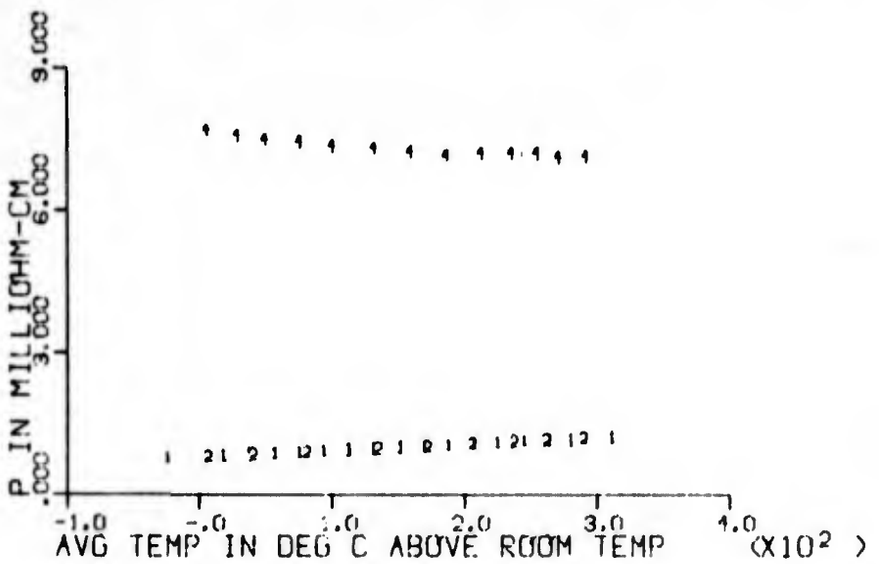

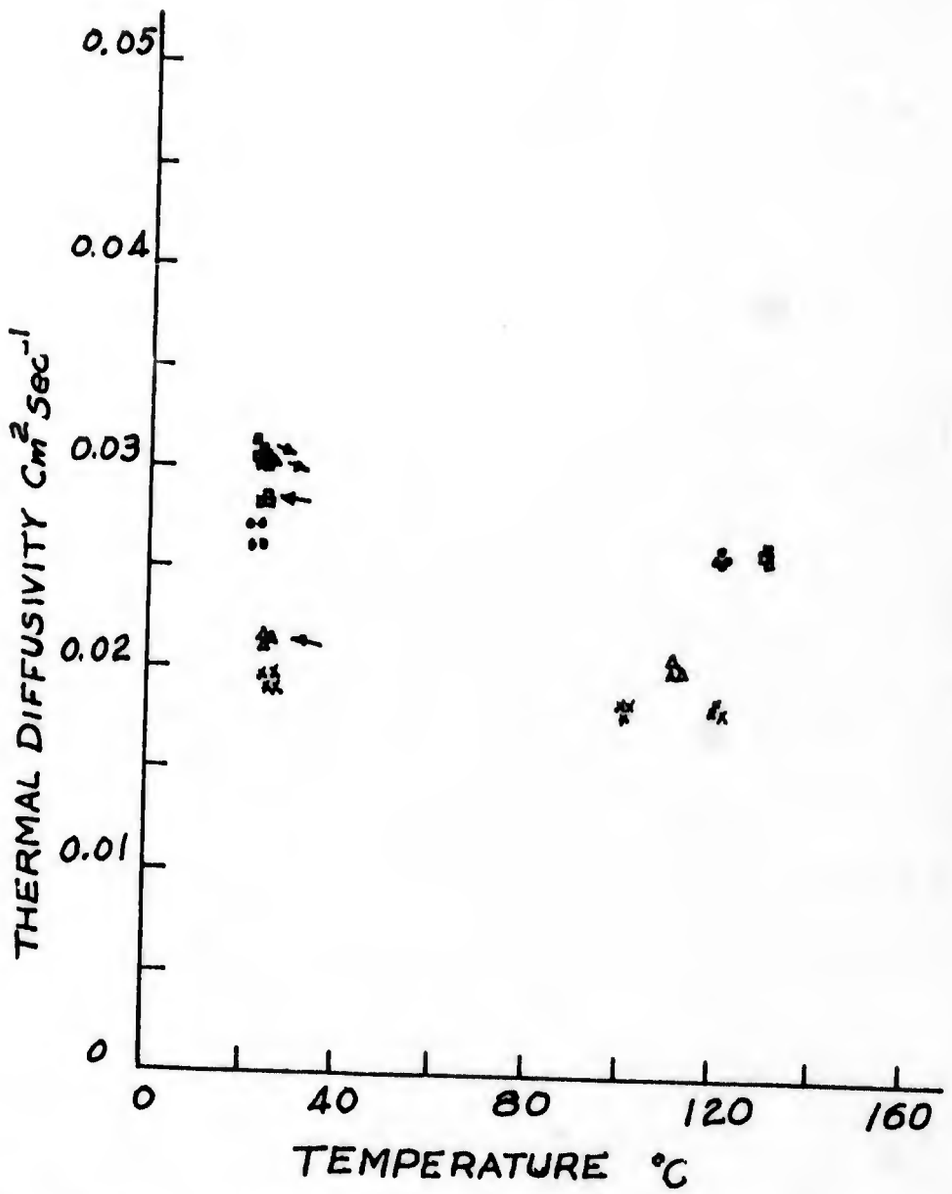

Fig. II/41. Thermal diffusivity of sample 234 (Ge-Si alloy) at two temperature, before (□, Δ) and after exposure to 1.0×10^{17} (•) and 1.6×10^{18} (X) fast (E > 1 Mev) neutrons/cm^2.

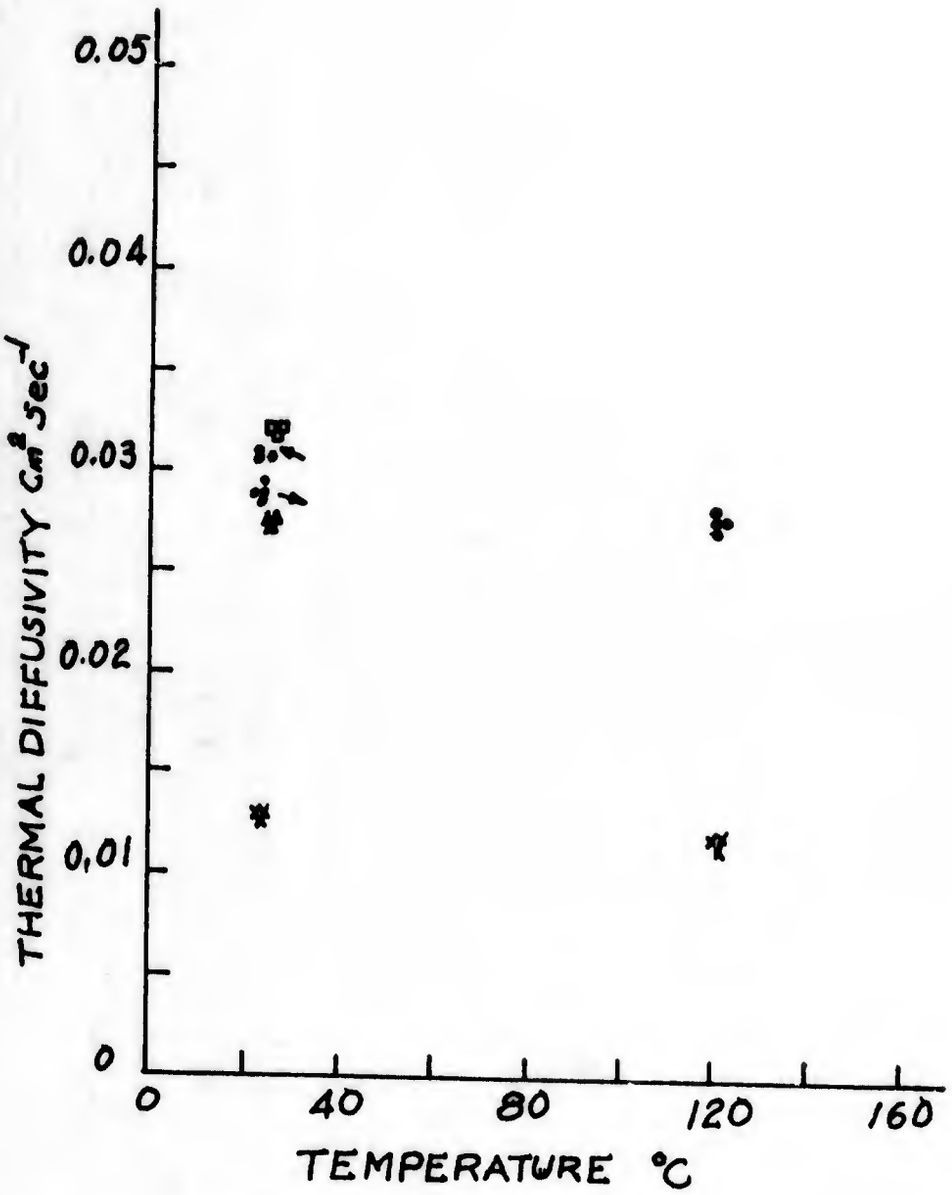

Fig. II/42. Thermal diffusivity of sample 236 (Ge-Si alloy) at two temperatures, before (□ , △) and after 1.0×10^{17} (●) and 2.3×10^{19} (X) fast (E > 1 Mev) neutrons/cm².

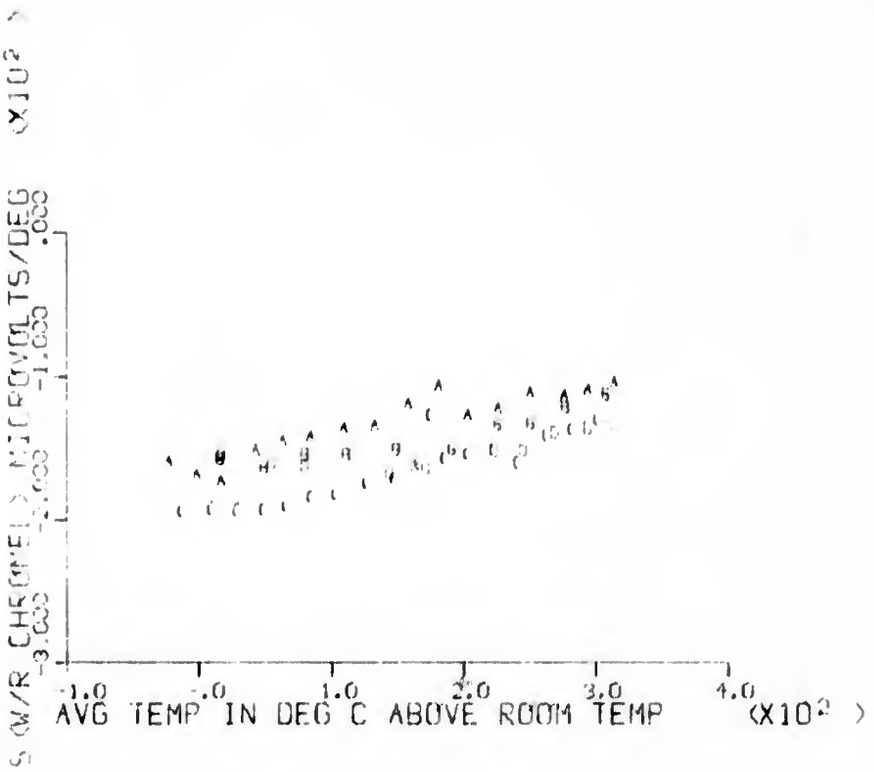

Fig. II/43. Temperature dependence of apparent Seebeck coefficient (with respect to chromel) of sample 245B (Bi_2Te_3), before (A,B) and after (C,D) exposure to 1.6 x 10^{18} fast (E) 1 Mev) neutrons/cm^2. A, C = sample heating; B, D = sample cooling.

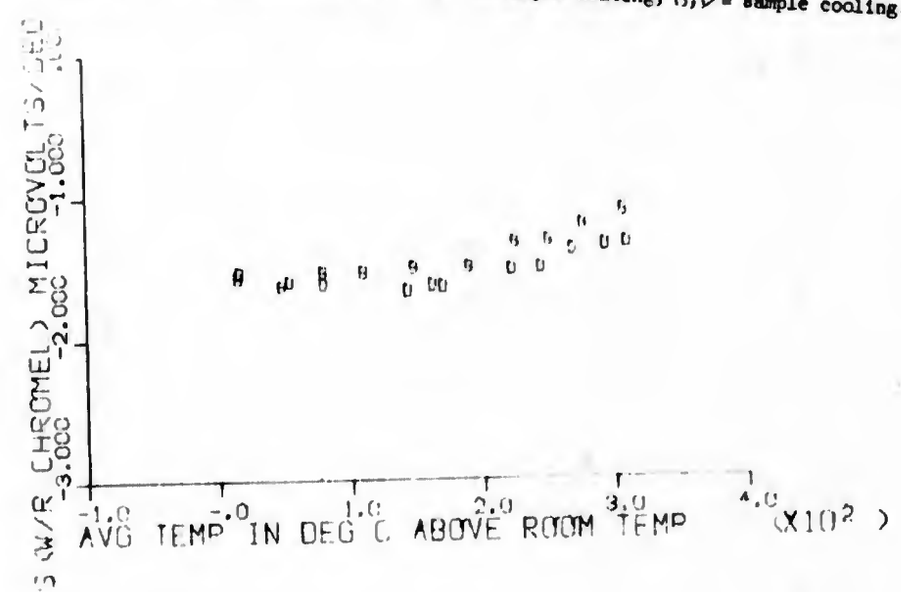

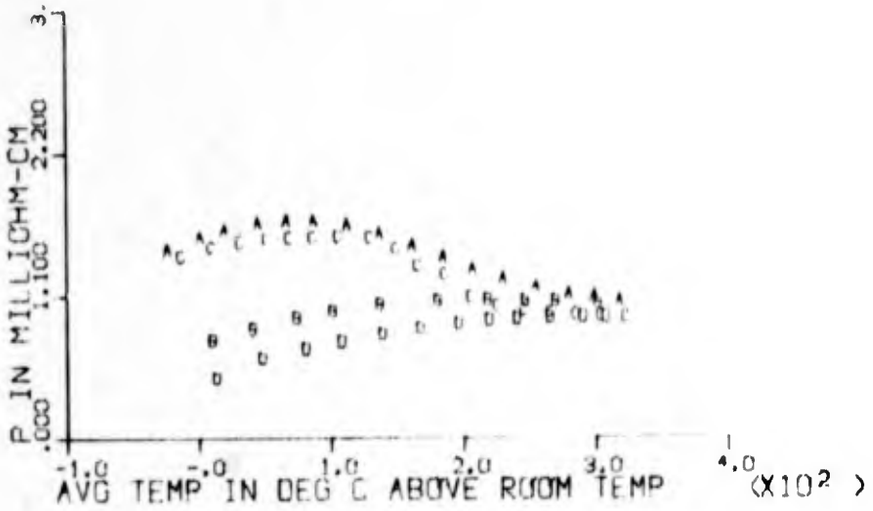

Fig. II/44. Temperature dependence of electrical resistivity of sample 245B (Bi_2Te_3), before (A,B) and after (C,D) exposure to 1.6 x 10^{18} fast (E) 1 Mev) neutrons/cm^2. A, C = sample heating; B, D = sample cooling.

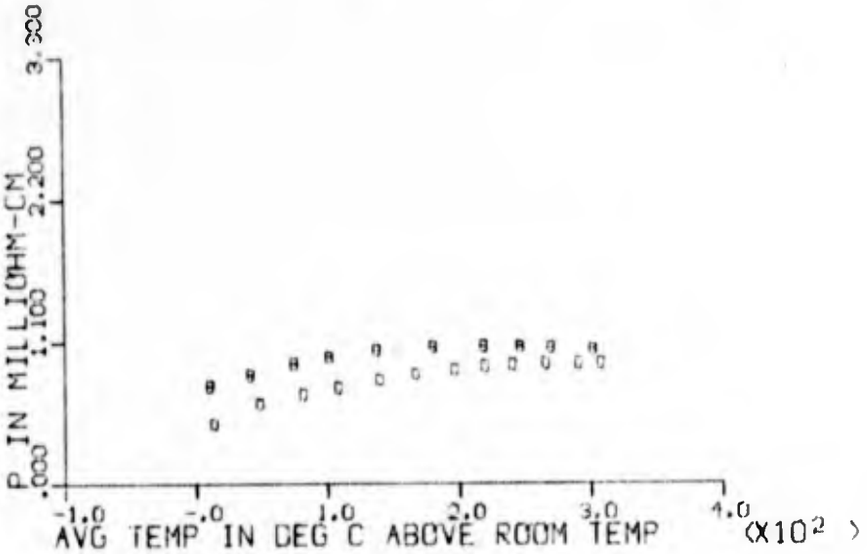

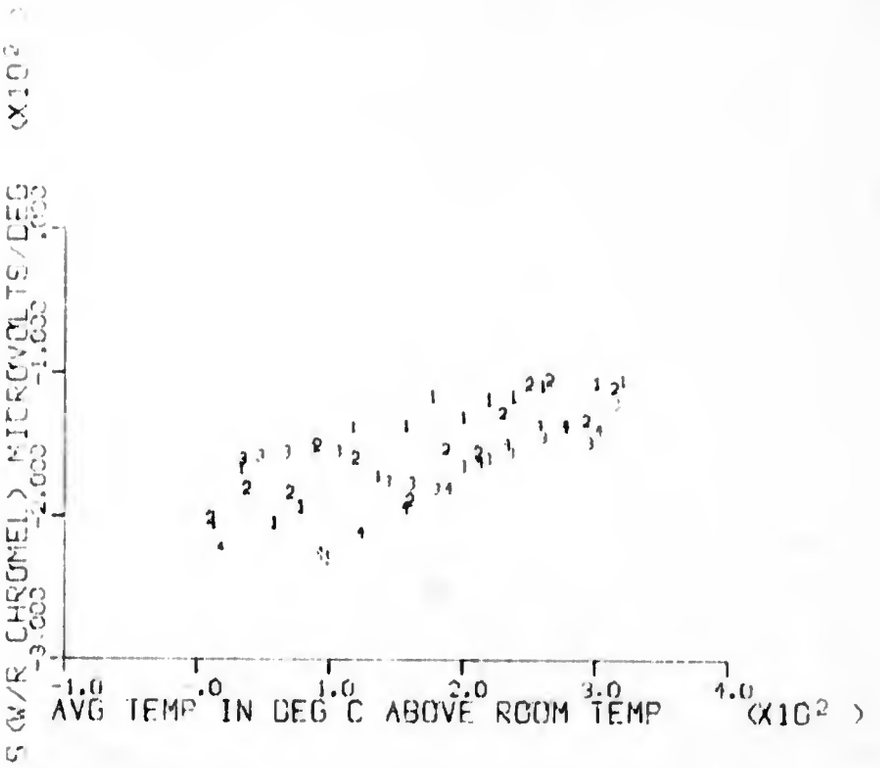

Fig. II/45. Temperature dependence of apparent Seebeck coefficient (with respect to chromel) of sample 245C(Bi_2Te_3), before (1,2) and after (3,4) exposure to 2.3×10^{19} fast (E) 1 Mev) neutrons/cm^2. 1,3 = sample heating; 2,4 = sample cooling.

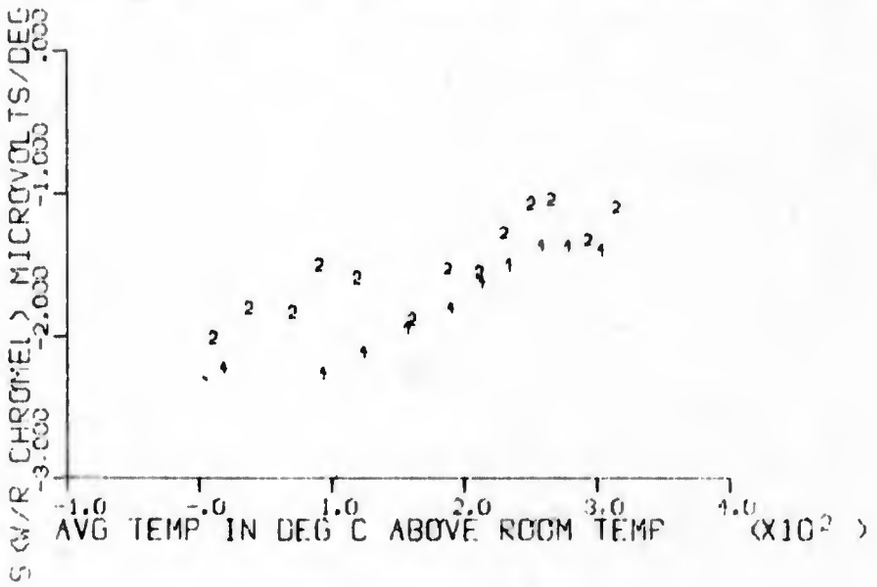

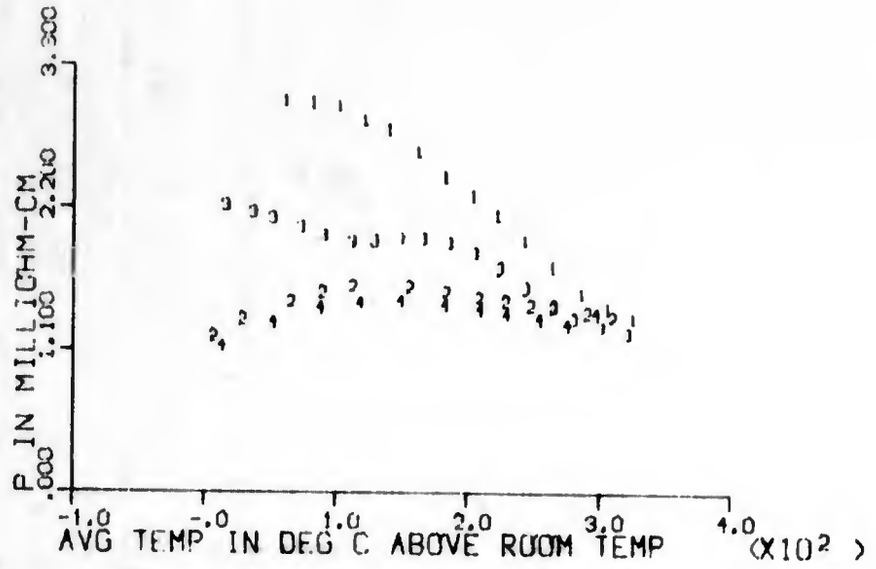

Fig. II/46. Temperature dependence of electrical resistivity of sample 245C (Bi_2Te_3), before (1,2) and after (3,4) exposure to 2.3 x 10^{18} fast (E) 1 Mev) neutrons/cm^2. 1,3 = sample heating; 2,4 = sample cooling.

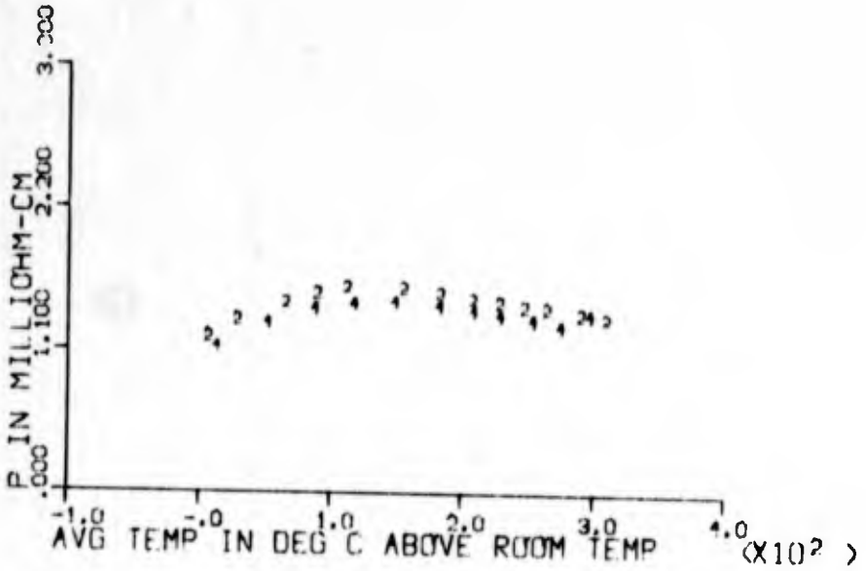

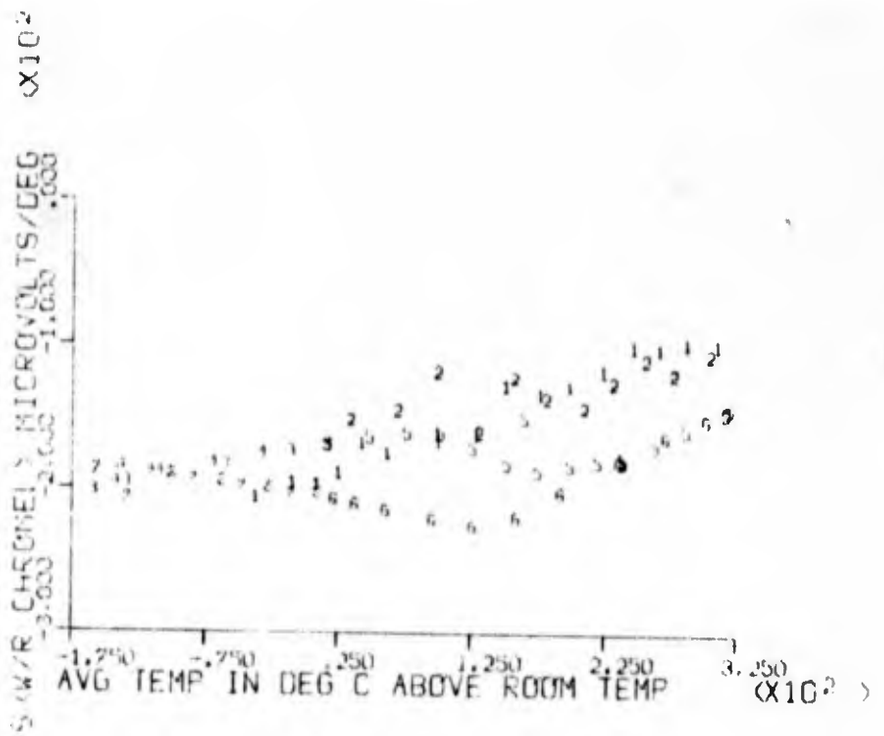

Fig. II/47. Temperature dependence of apparent Seebeck coefficient (with respect to chromel) of sample 245D (Bi_2Te_3), before (1,2) and after (3-8) exposure to 2.3 x 10^{19} fast (E) 1 Mev) neutrons/cm^2. 1,5 = sample heating through standard temperature range; 2,6 = sample cooling through same range; 3,7 = sample cooling from room temperature to liquid nitrogen region; 4,8 = sample warming through that region.

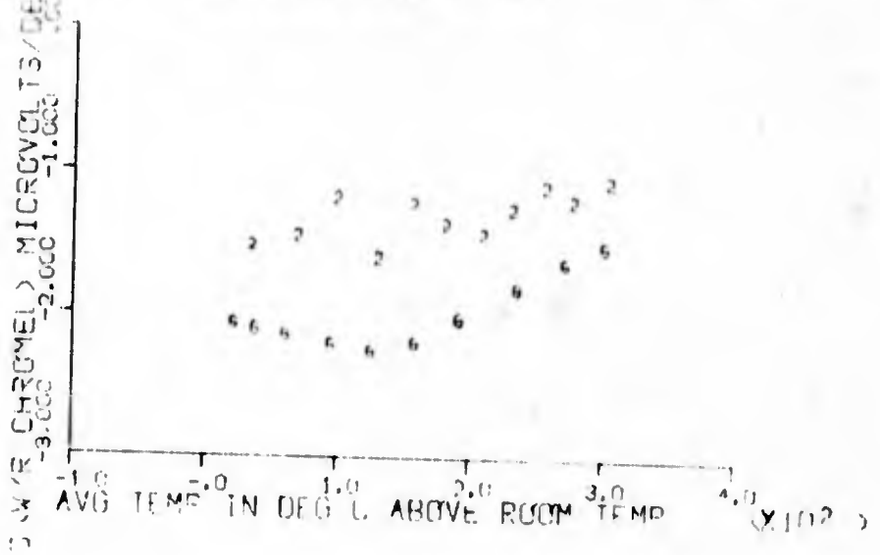

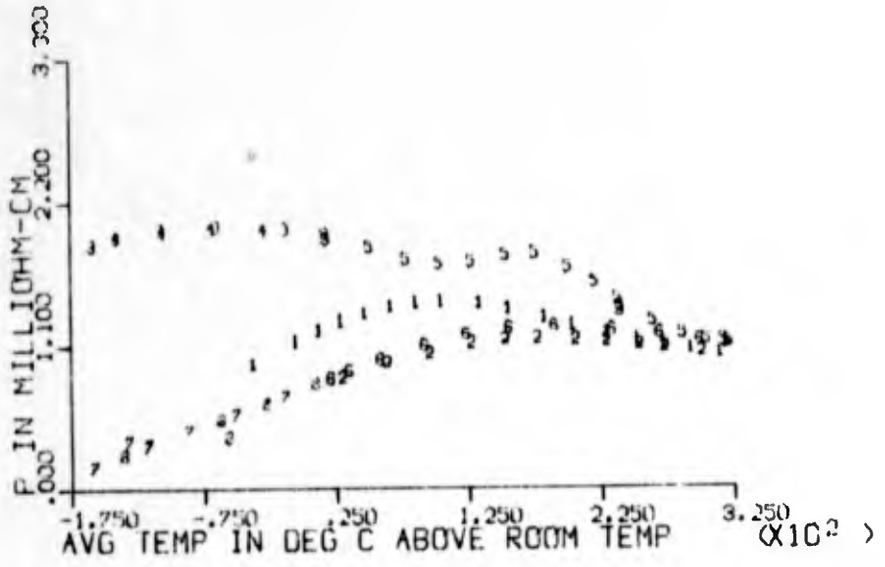

Fig. II/48. Temperature dependence of electrical resistivity of sample 245D (Bi_2Te_n), before (1,2) and after (3-8) exposure to 2.3 x 10^{18} fast (E) 1 Mev) neutrons/cm^2. For key to symbols see caption for Fig. II/47.

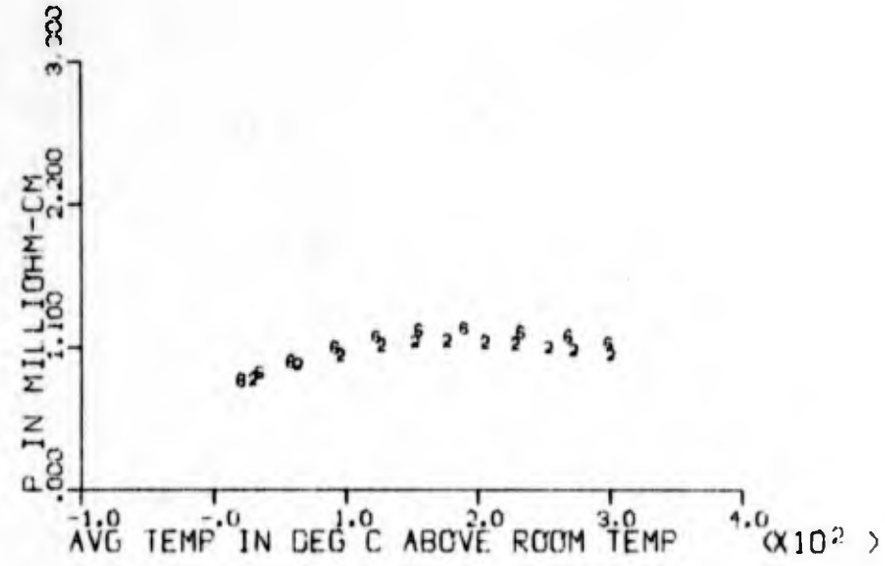

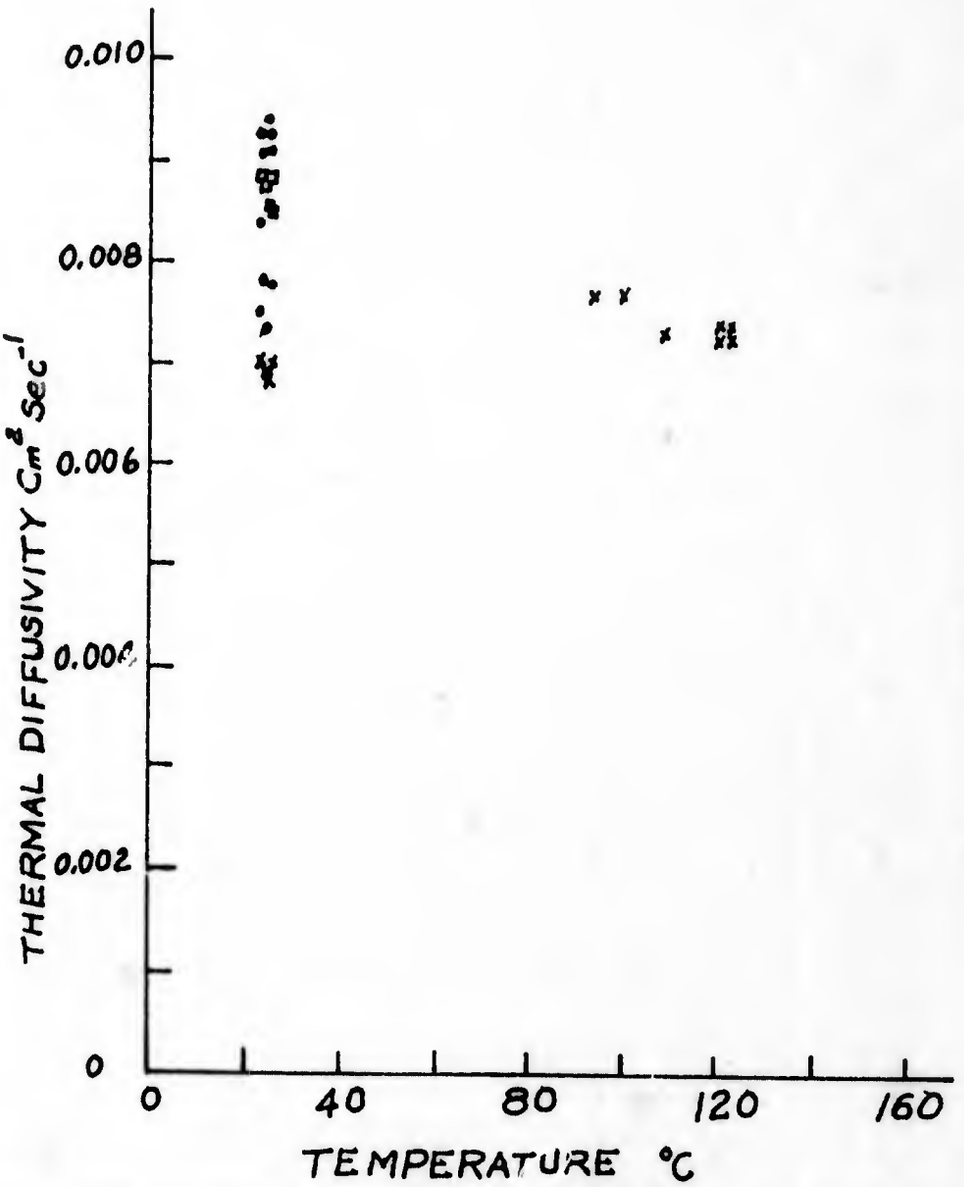

Fig. II/49. Thermal diffusivity of sample 239 (Bi_2Te_3) at several temperatures, before (□) and after exposure to 1.0×10^{17} (•) and 1.6×10^{18} (X) fast (E > 1 Mev) neutrons/cm^2.

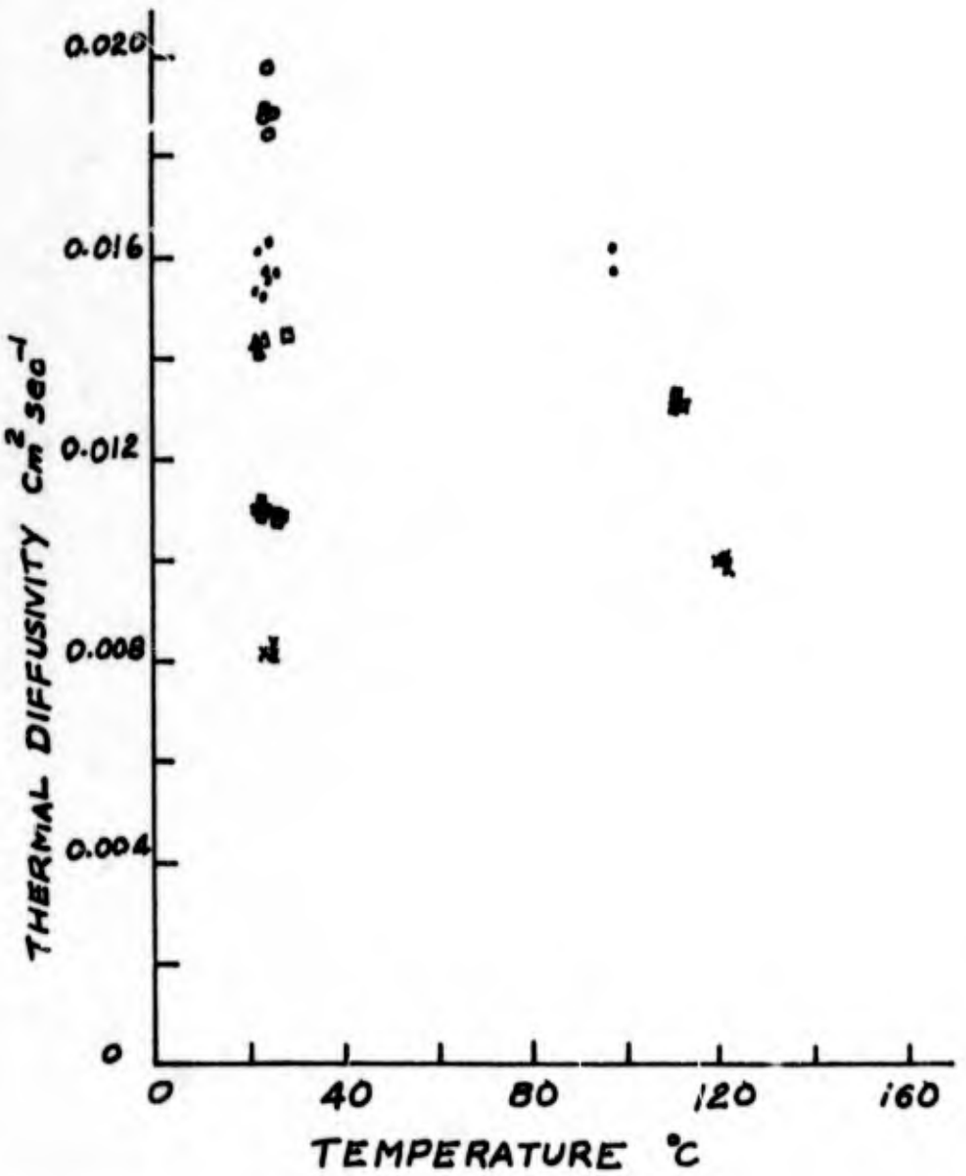

Fig. II/50. Thermal diffusivity of sample 206A (Bi_2Te_3) at several temperatures, before (□, Δ, ○) and after 1.0×10^{17} (●) and 2.3×10^{19} (X) fast (E 1 Mev) neutrons/cm^2.

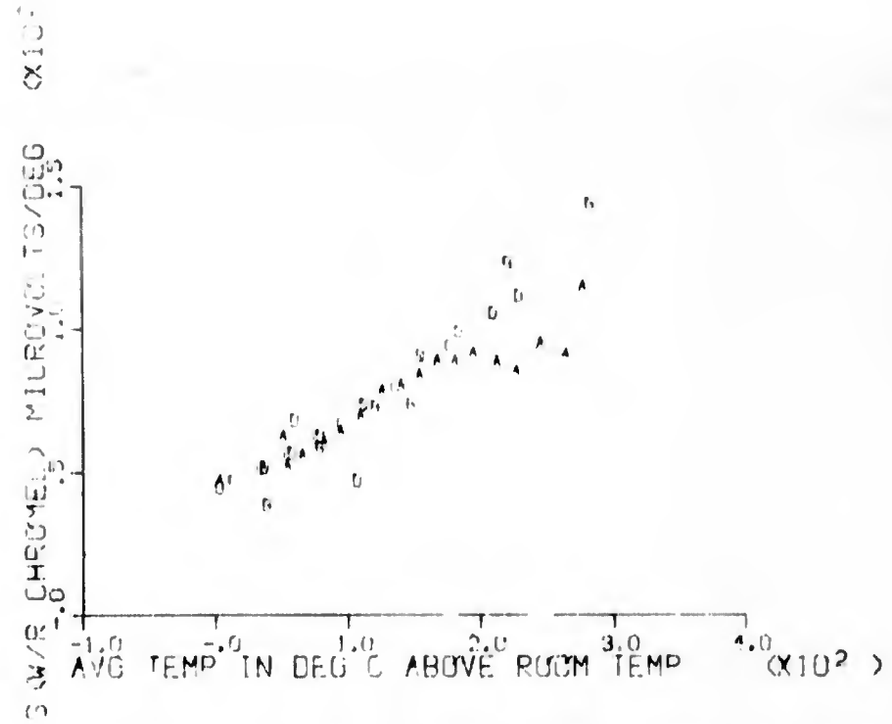

Fig. II/51. Temperature dependence of apparent Seebeck coefficient (with respect to chromel) of sample 251A ($GeTe$-$AgSbTe_2$ alloy), before (A,B) and after (C,D) exposure to 1.6×10^{18} fast (E) 1 Mev) neutrons/cm^2. A, C = sample heating; B, D = sample cooling.

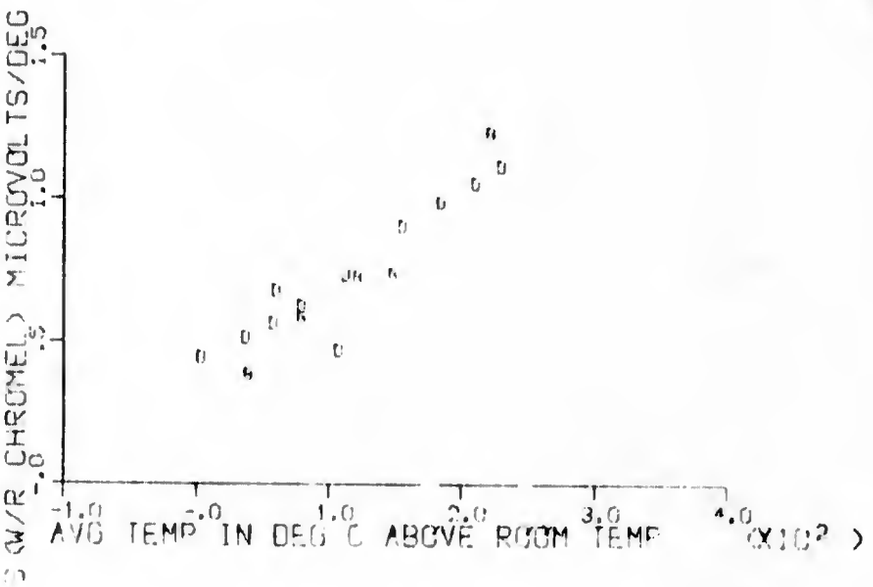

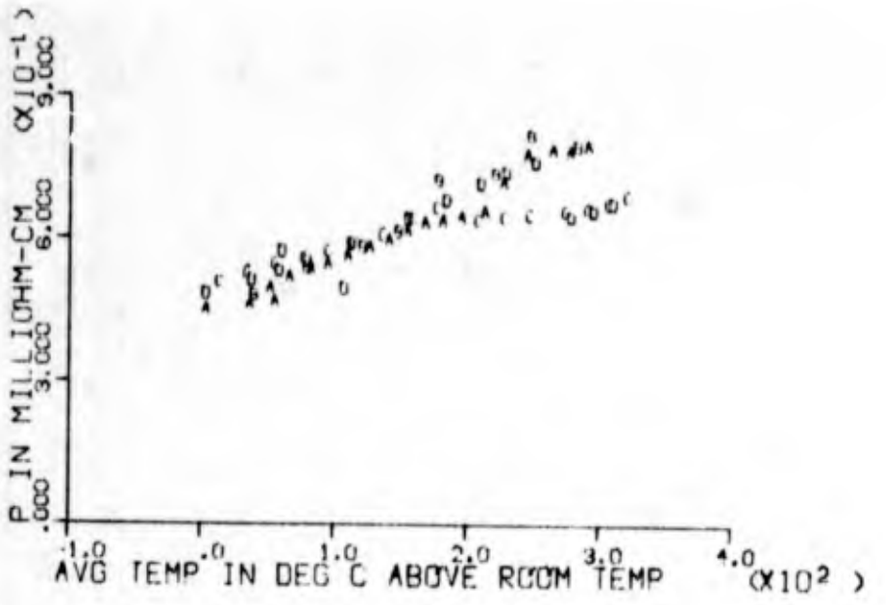

Fig. II/52 Temperature dependence of electrical resistivity of sample 251A (GeTe-$AgSbTe_2$ alloy), before (A,B) and after (C,D) exposure to 1.6 x 10^{18} fast (E > 1 Mev) neutrons/cm^2. A,C = sample heating; B, D = sample cooling.

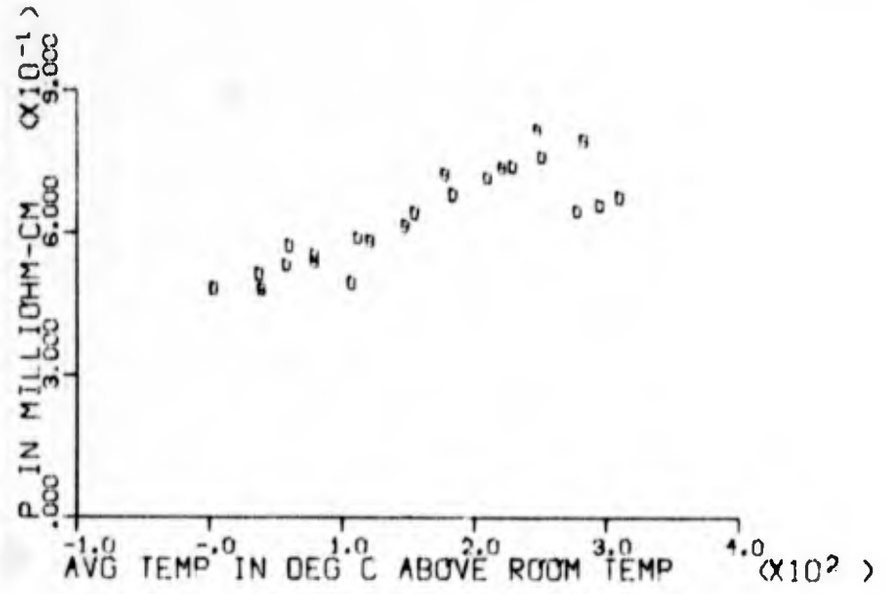

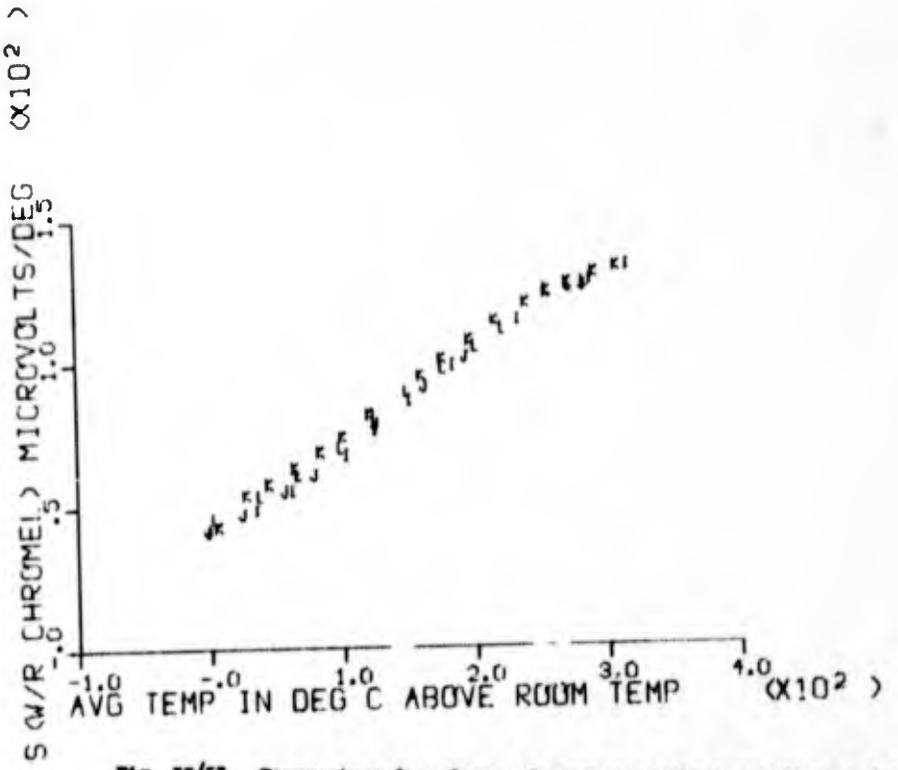

Fig. II/53. Temperature dependence of apparent Seebeck coefficient (with respect to chromel) of sample 251E (GeTe-$AgSbTe_2$ alloy), before (I,J) and after (K,L) exposure to 1.6×10^{18} fast (E > 1 Mev) neutrons/cm^2. I,K = sample heating; J, L = sample cooling.

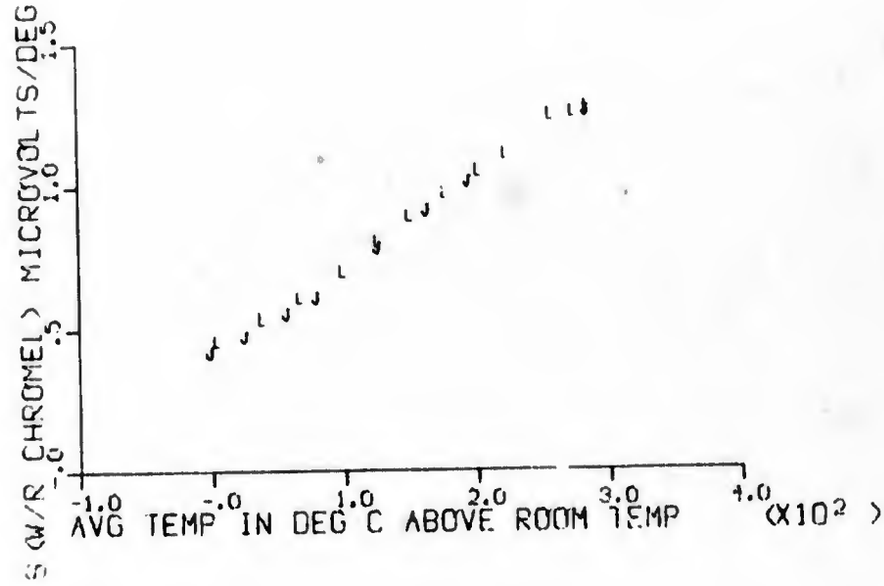

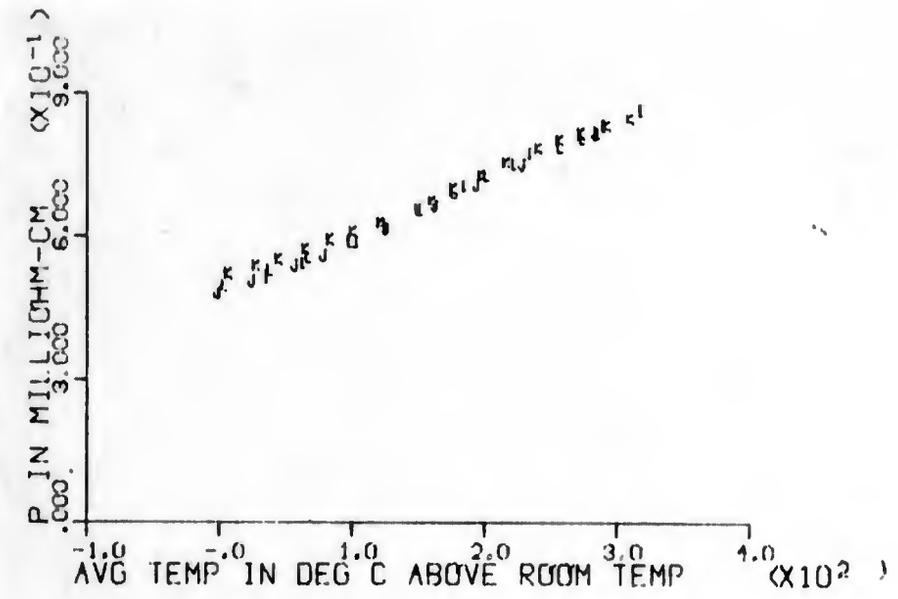

Fig. II/54 Temperature dependence of electrical resistivity of sample 251E (GeTe-$AgSbTe_2$ alloy), before (I,J) and after (K,L) exposure to 1.6×10^{18} fast (E) 1 Mev) neutrons/cm^2. I,K = sample heating; J, L = sample cooling.

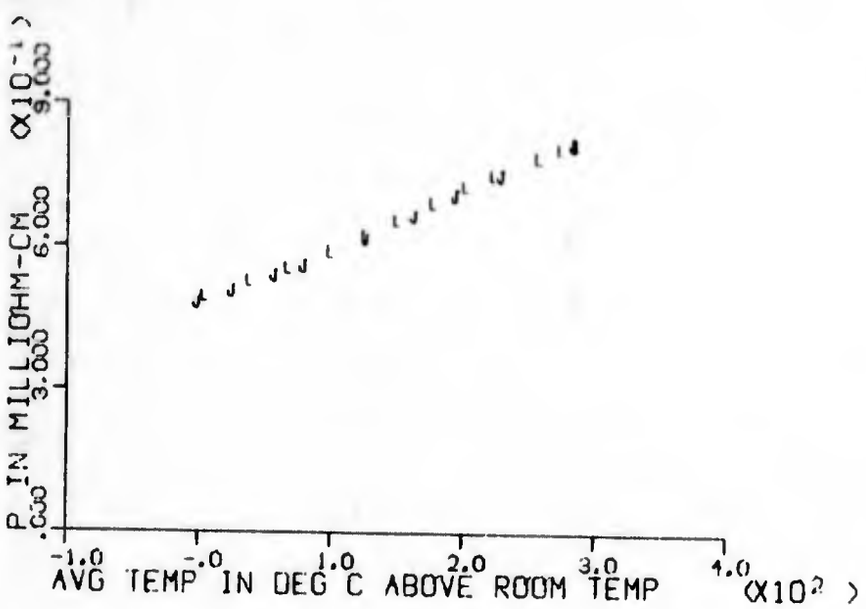

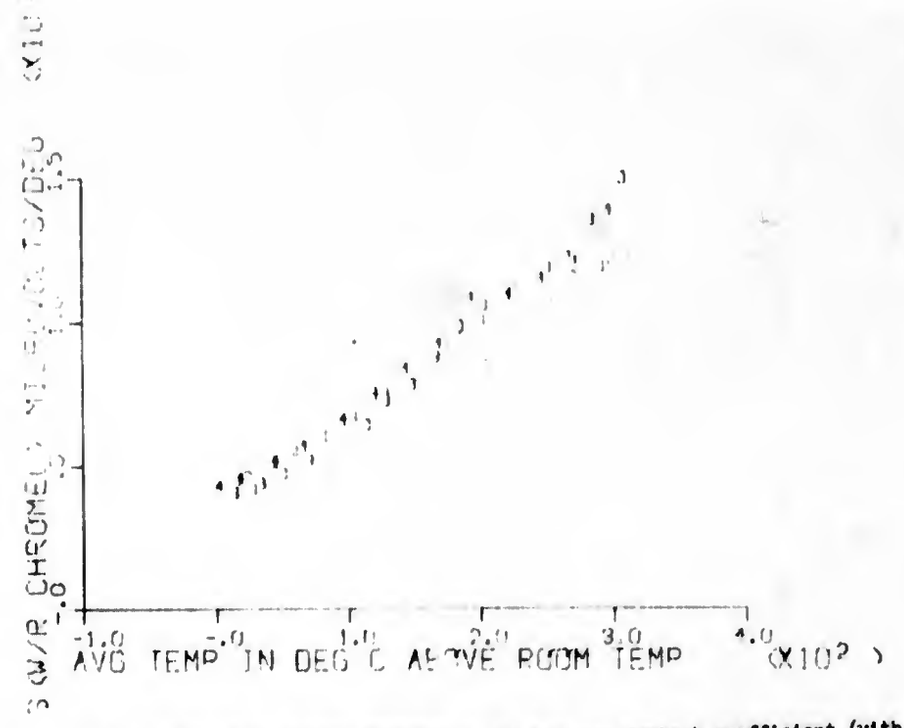

Fig. II/55. Temperature dependence of apparent Seebeck coefficient (with respect to chromel) of sample 251B ($GeTe-AgSbTe_2$ alloy), before (1,2) and after (3,4) exposure to 2.3×10^{19} fast (E > 1 Mev) neutrons/cm^2. 1,3 = sample heating; 2,4 = sample cooling.

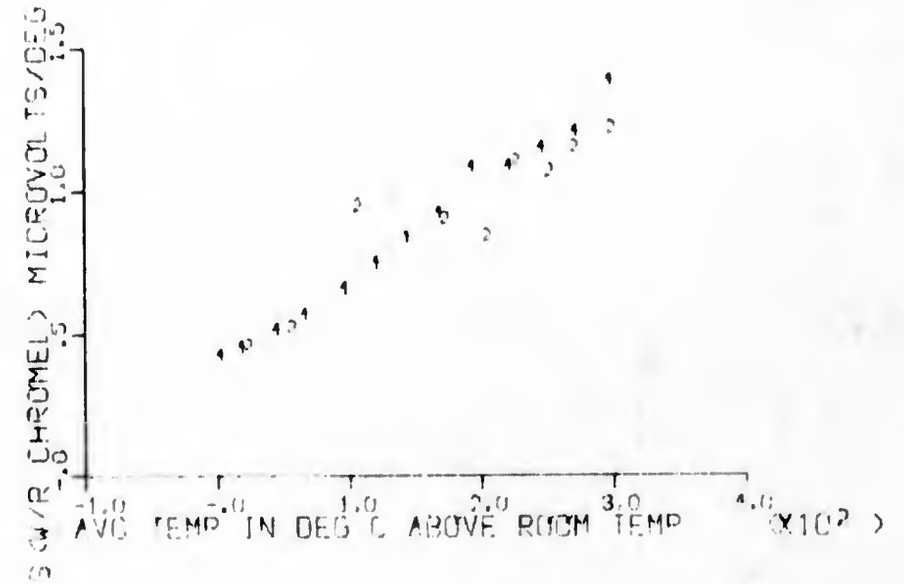

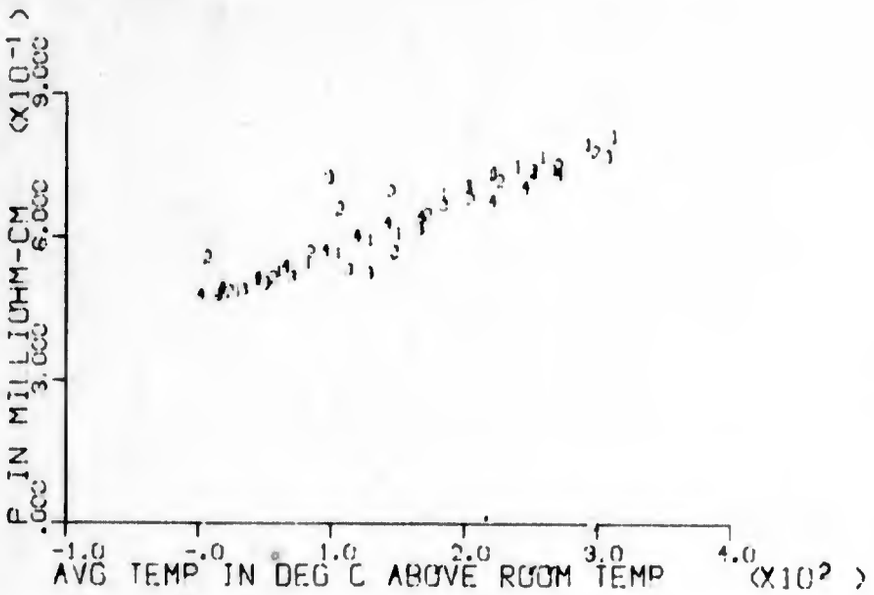

Fig. II/56. Temperature dependence of electrical resistivity of sample 251B ($GeTe$-Ag_5SbTe_8 alloy), before (1,2) and after (3,4) exposure to 2.5×10^{19} fast (E > 1 Mev) neutrons/cm^2. 1, 3 = sample heating; 2,4 = sample cooling.

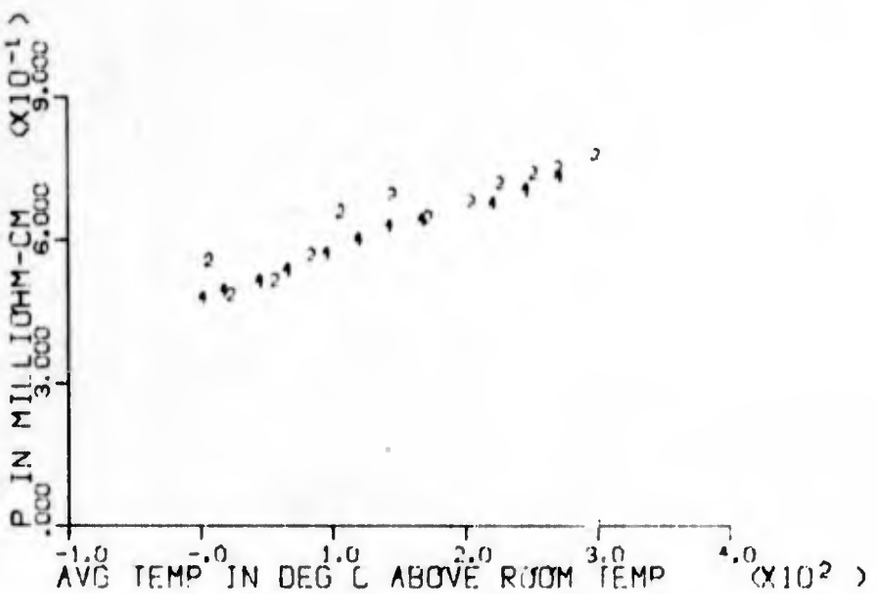

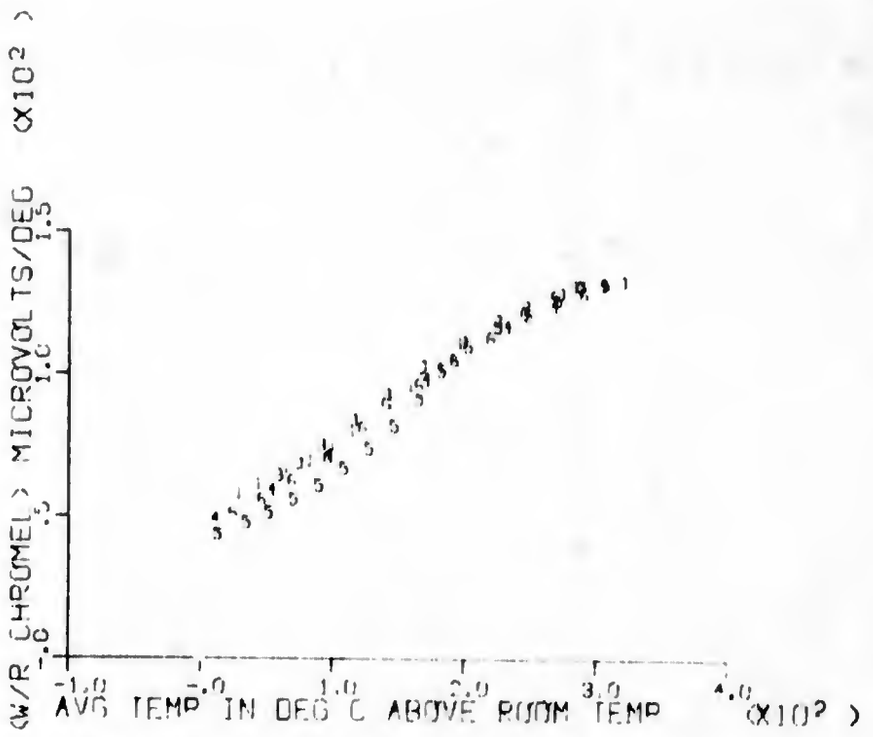

Fig. II/57. Temperature dependence of apparent Seebeck coefficient (with respect to chromel) of sample 251D ($GeTe$-$AgSbTe_2$ alloy), before (1,3,4) and after (5,6) exposure to 2.3×10^{19} fast ($E > 1$ Mev) neutrons/cm². 1,3,5= sample heating; 4,6 = sample cooling.

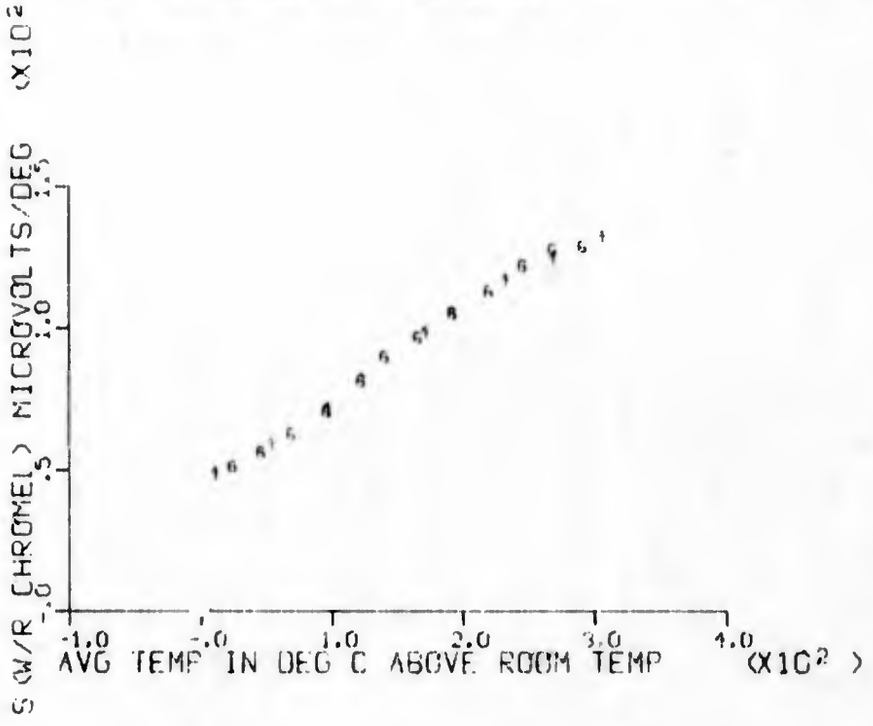

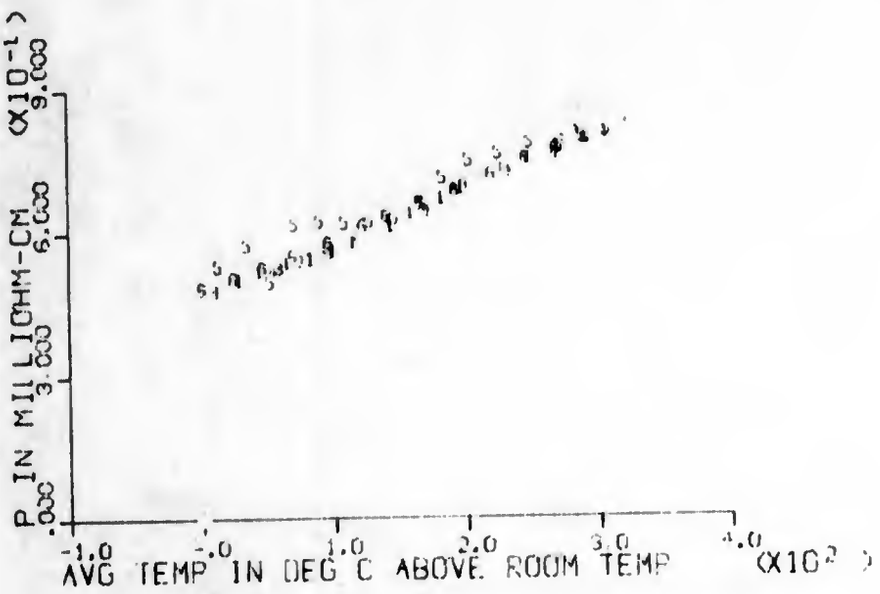

Fig. II/58. Temperature dependance of electrical resistivity of sample 251D (GeTe-$AgSbTe_2$ alloy), before (1,3,4) and after (5,6) exposure to 2.3 x 10^{19} fast (E > 1 Mev) neutrons/cm^2. 1,3,5 = sample heating; 4,6 = sample cooling.

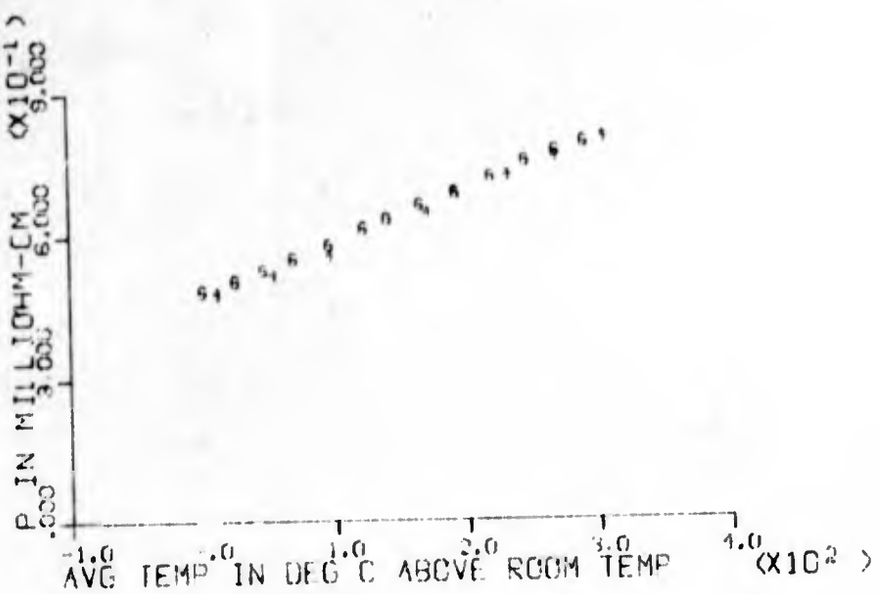

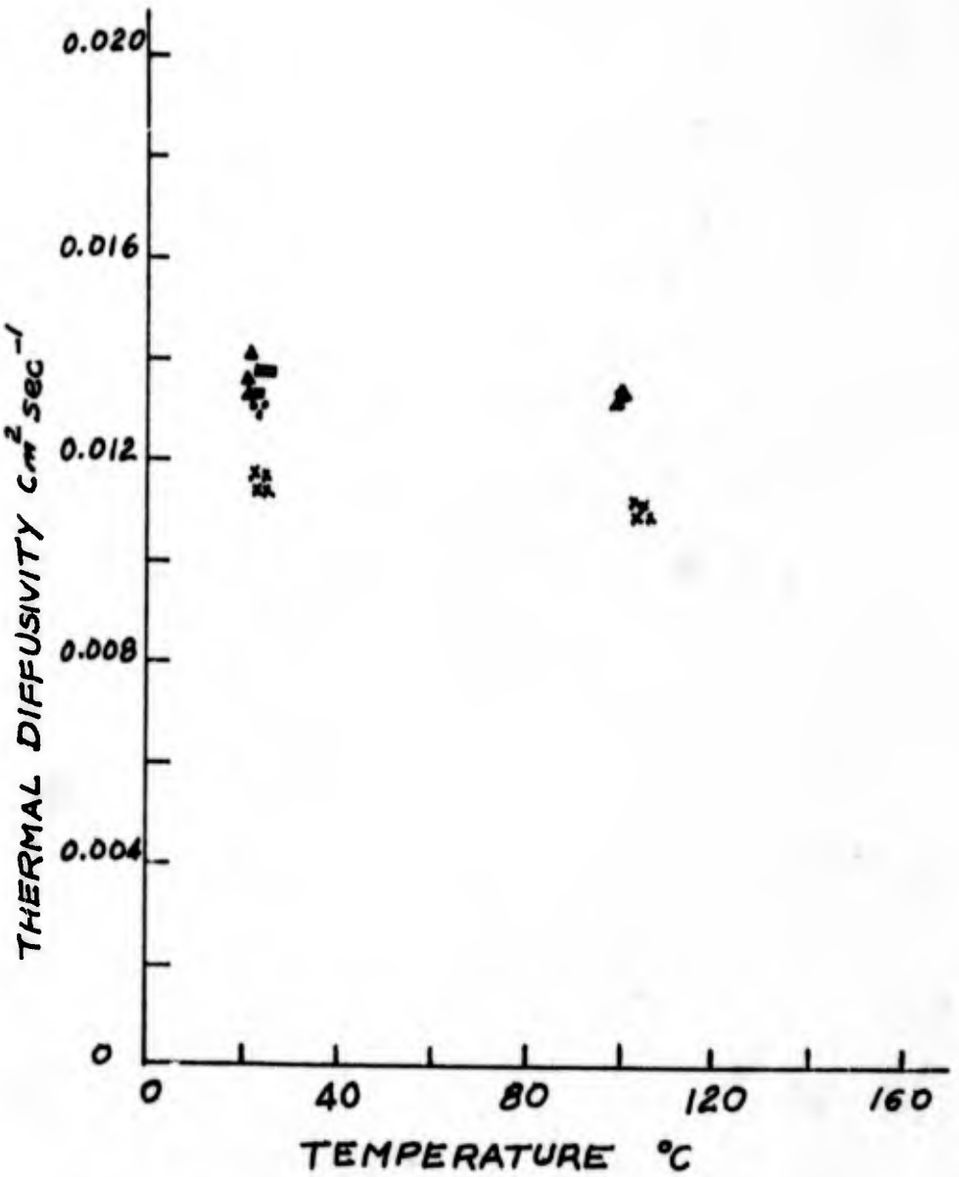

Fig. II/59. Thermal Diffusivity of Sample A (GeTe-AgSbTe$_2$ alloy) at two temperature, before (□ , △) and after 1.0 x 10^{17} (•), and 2.3 x 10^{19} (×) fast (E > 1 Mev) neutrons/cm^2.

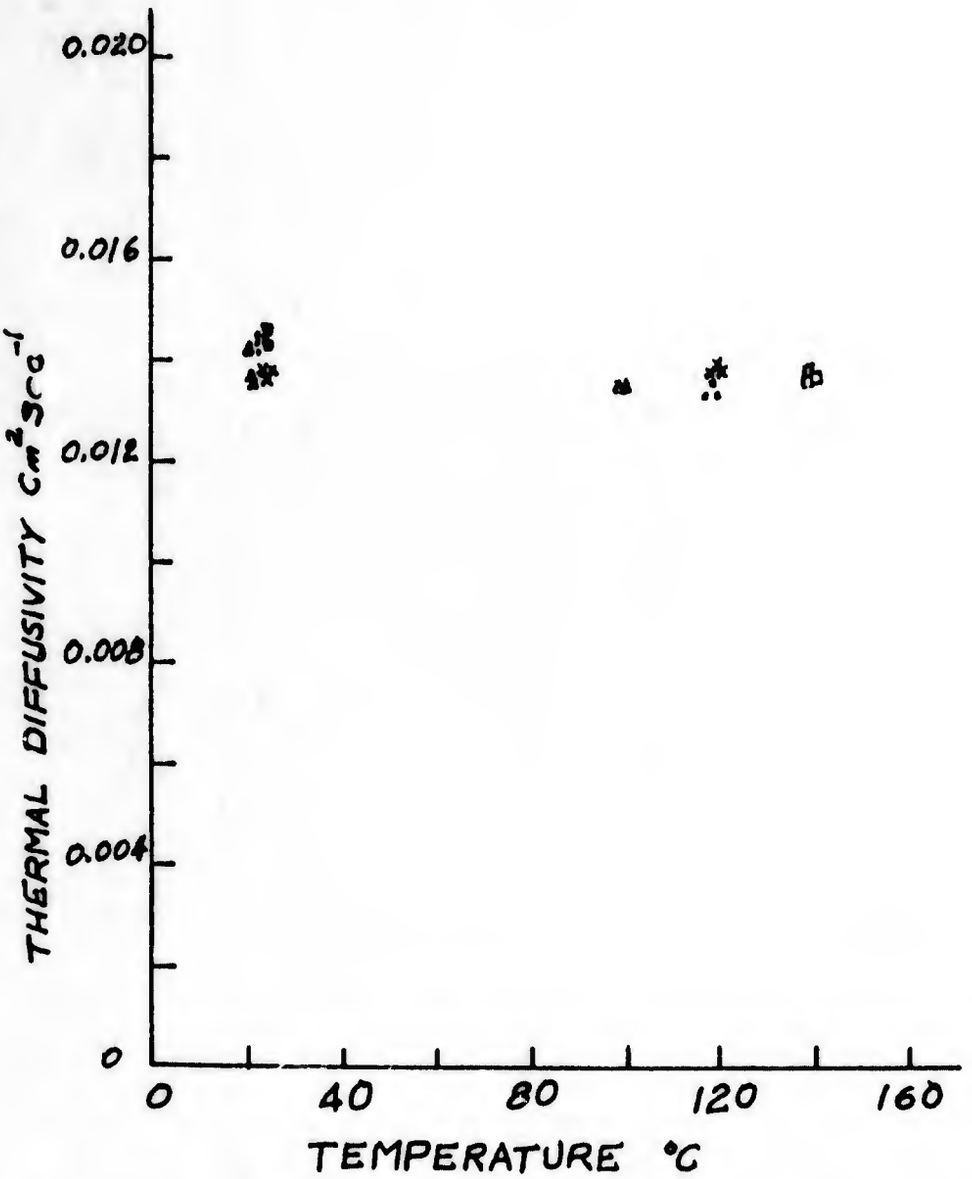

Fig. II/60 Thermal Diffusivity of sample C (GeTe-$AgSbTe_2$ alloy) at several temperatures, before (□, △) and after 1.0 x 10^{17} (•), and 2.3 x 10^{19} (X) fast (E > 1 Mev) neutrons/cm^2.

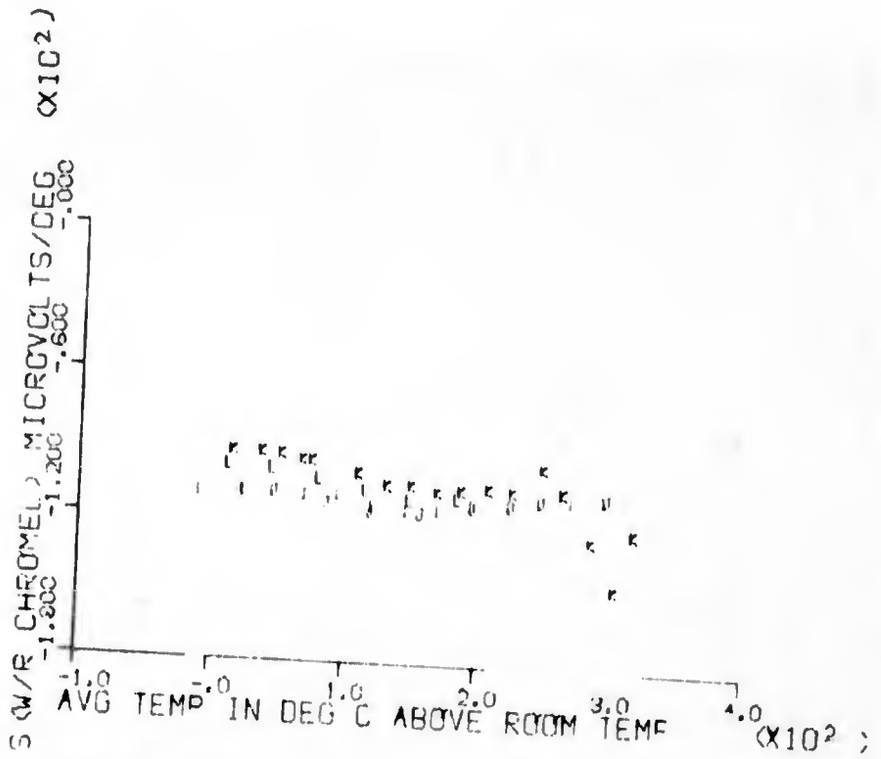

Fig. II/61. Temperature dependence of apparent Seebeck coefficient (with respect to chromel) to sample 252C(CoSi), before (I,J) and after (K,L) exposure to 1.6×10^{18} fast (E) 1 Mev) neutrons/cm^2. I,K = sample heating; J,L = sample cooling.

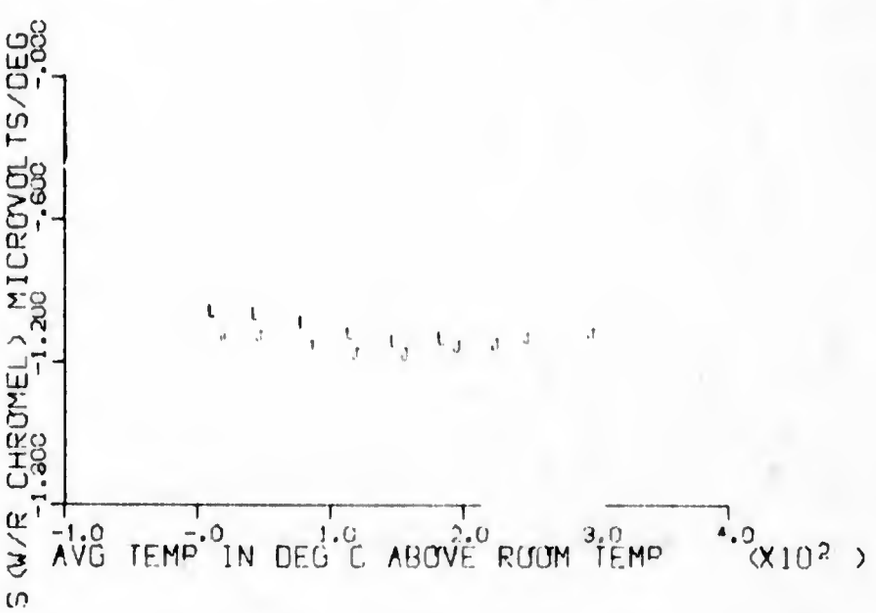

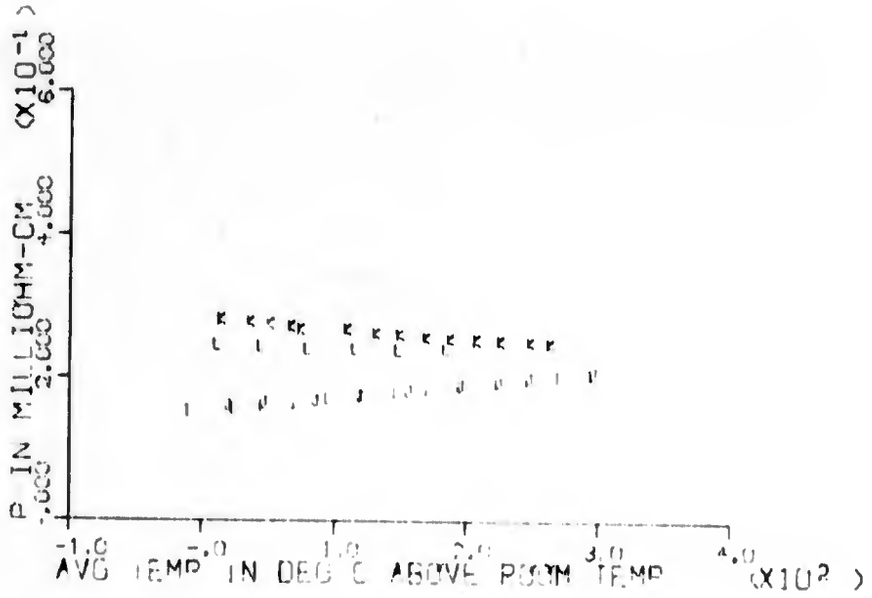

Fig. II/62. Temperature dependence of electrical resistivity of sample 252C (CoSi), before (I,J) and after (K,L) exposure to 1.6 x 10^{18} fast (E) 1 Mev) neutrons/cm^2. 1,3 = sample heating; 2,4 = sample cooling.

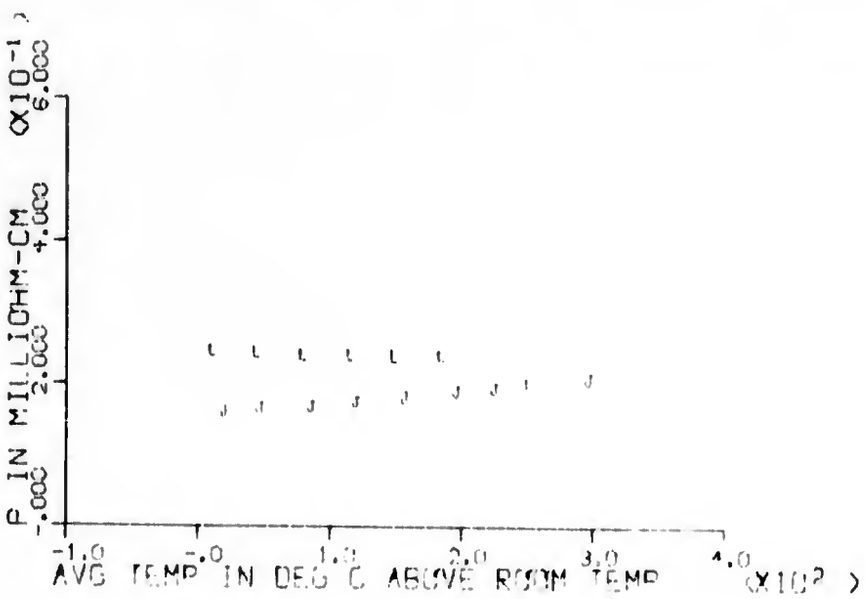

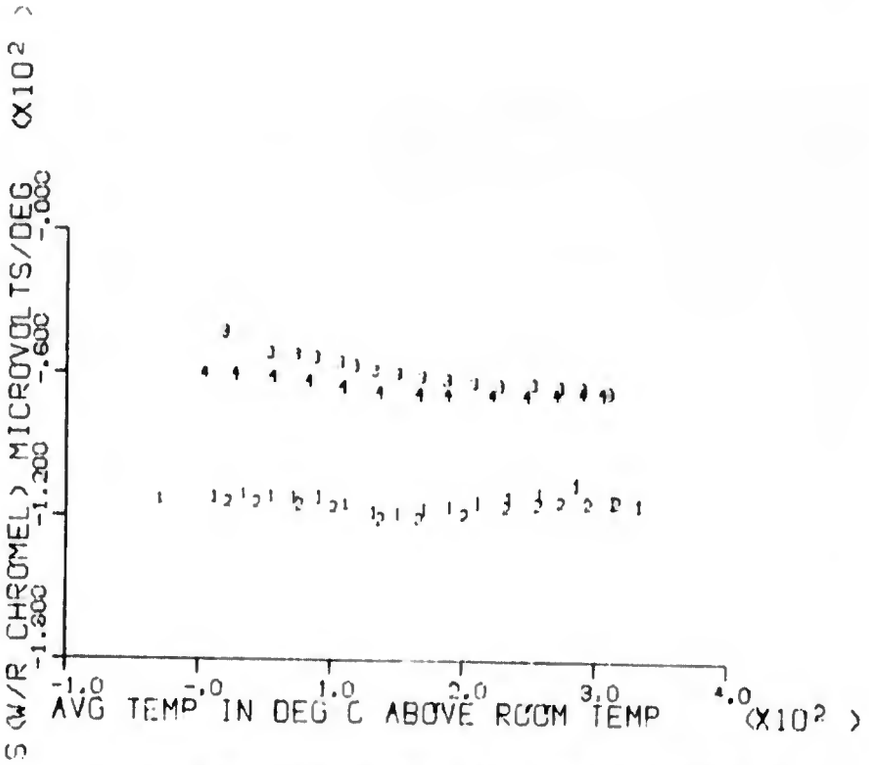

Fig. II/63. Temperature dependence of electrical resistivity of sample 252A (CoSi), before (1,2) and after (3,4) exposure to 2.3×10^{19} fast (E > 1 Mev) neutrons/cm^2. 1, 3 = sample heating; 2,4 = sample cooling.

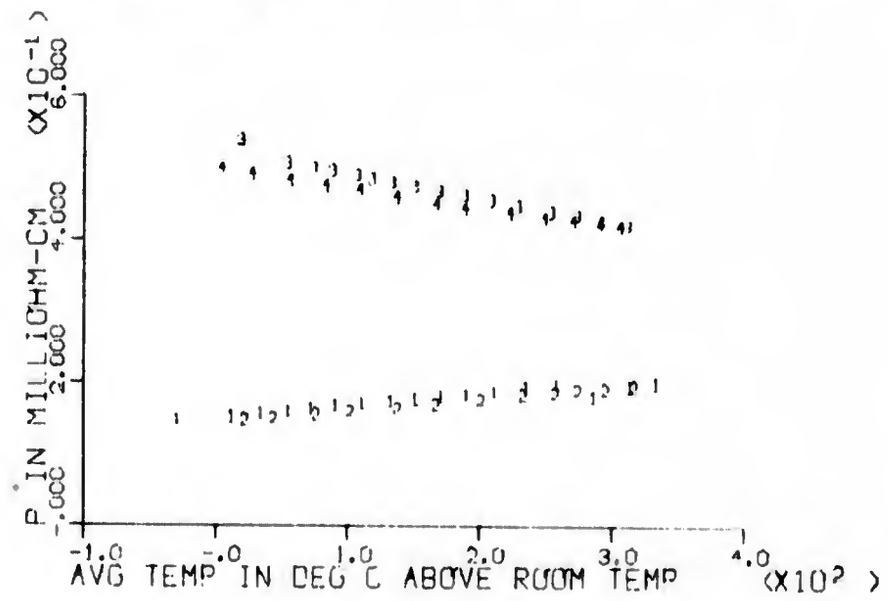

Fig. II/64. Temperature dependence of electrical resistivity of sample 252A (CoSi), before (1,2) and after (3,4) exposure to 2.3×10^{19} fast (E > 1 Mev) neutrons/cm^2. 1,3 = sample heating; 2,4 = sample cooling.

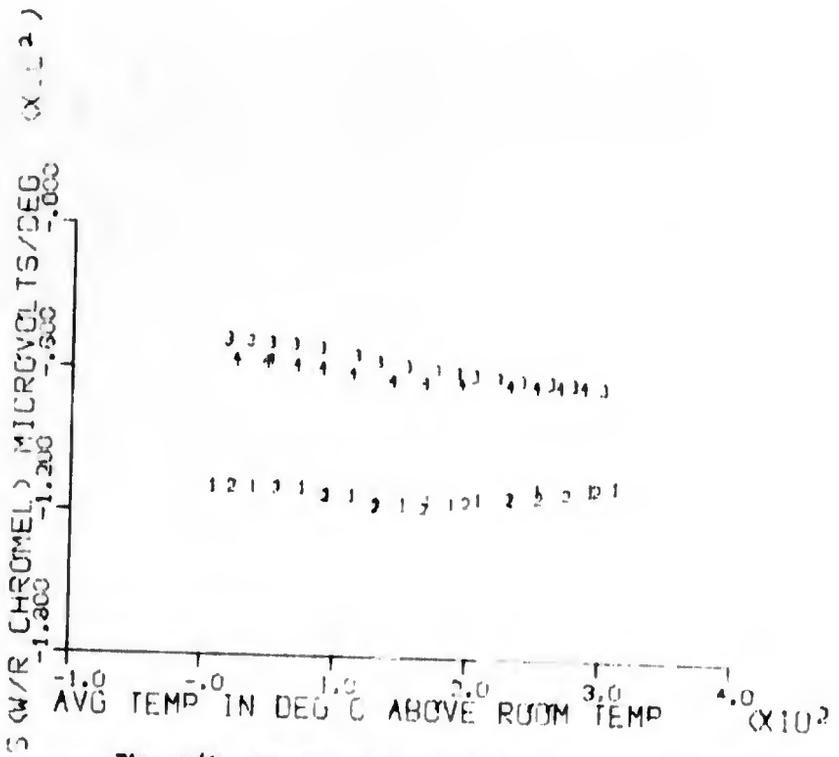

Fig. II/65. Temperature dependence of apparent seebeck coefficient (with respect to chromel) of sample 252B (CoSi), before (1,2) and after (3,4) exposure to 2.3×10^{19} fast (E) 1 Mev) neutrons/cm^2. 1,3 = sample heating; 2,4 = sample cooling.

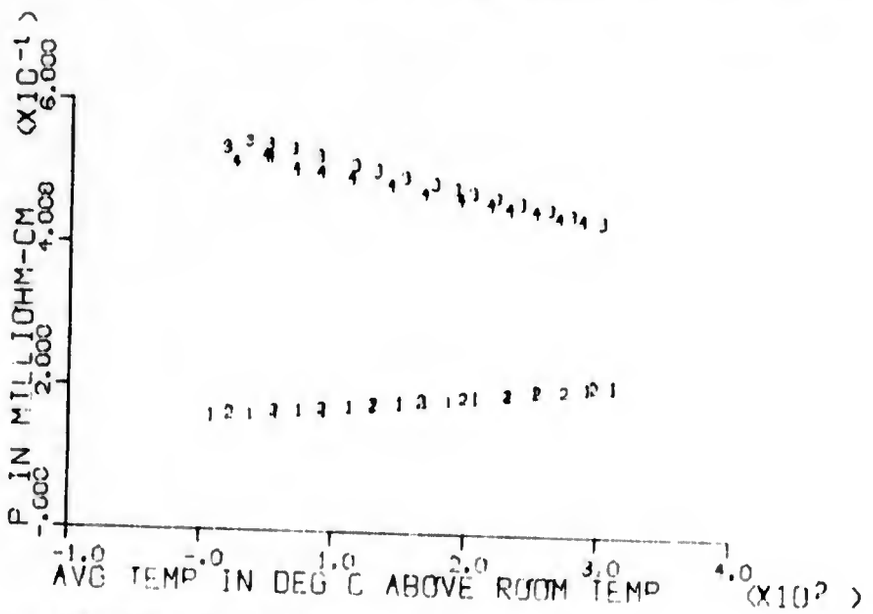

Fig. II/66. Temperature dependence of electrical resistivity of sample 252B (CoSi), before (1,2) and after (3,4) exposure to 2.3×10^{19} fast (E) 1 Mev) neutrons/cm^2. 1, 3 = sample heating; 2, 4 = sample cooling.

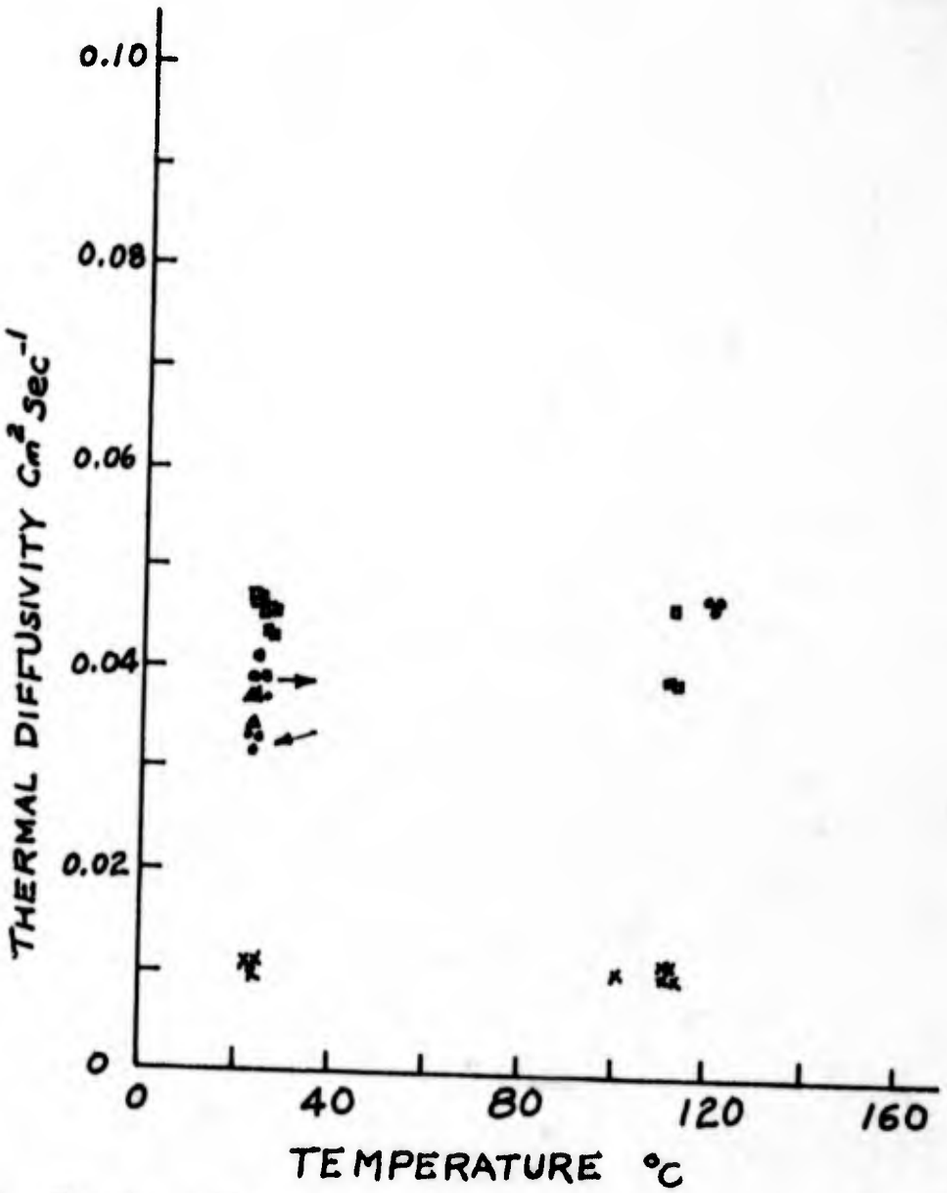

Fig. II/67. Thermal diffusivity of sample CoSi I (CoSi) at two temperatures, before (□, △) and after exposure to 1.0 x 10^{17} (•) and 2.3 x 10^{19} (X) fast (E > 1 Mev) neutrons/cm².

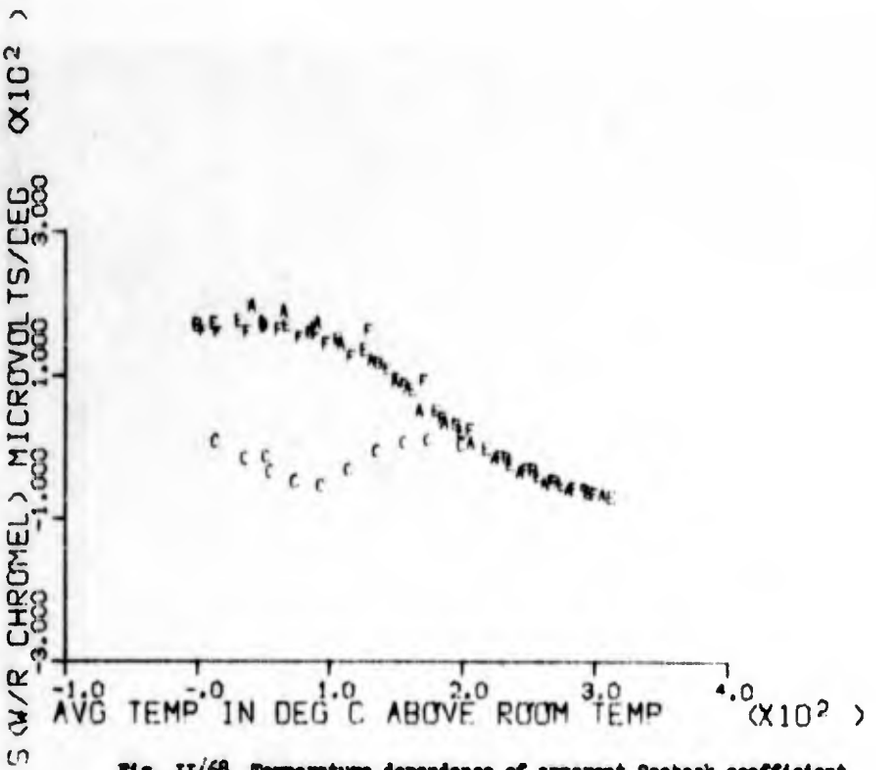

Fig. II/68 Temperature dependence of apparent Seebeck coefficient (with respect to chromel) of sample 254B (Bi_2Te_3), before (A,B) and after (C-F) exposure to 1.6×10^{18} fast (E > 1 Mev) neutrons/cm². A,C,E = sample heating; B, D, F = sample cooling.

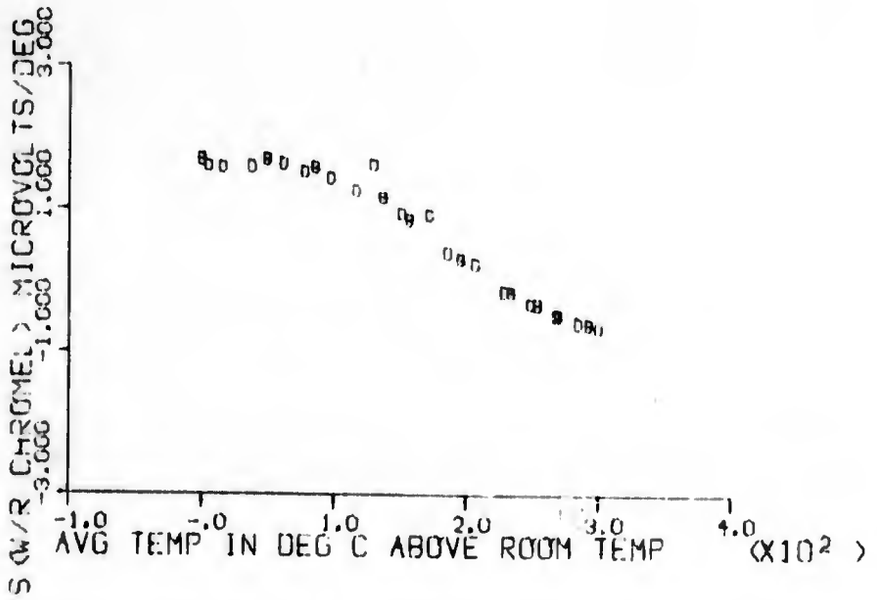

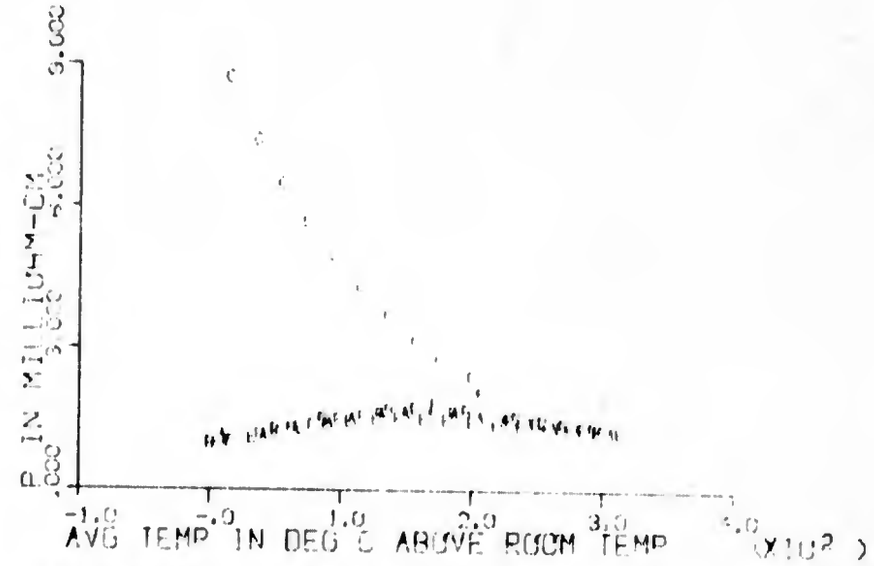

Fig. II/69. Temperature dependence of electrical resistivity of sample 254B(Bi_2Te_3), before (A,B) and after (C-F) exposure to 1.6×10^{18} fast (E > 1 Mev) neutrons/cm^2. A, C, E = sample heating; B, D, F = sample cooling.

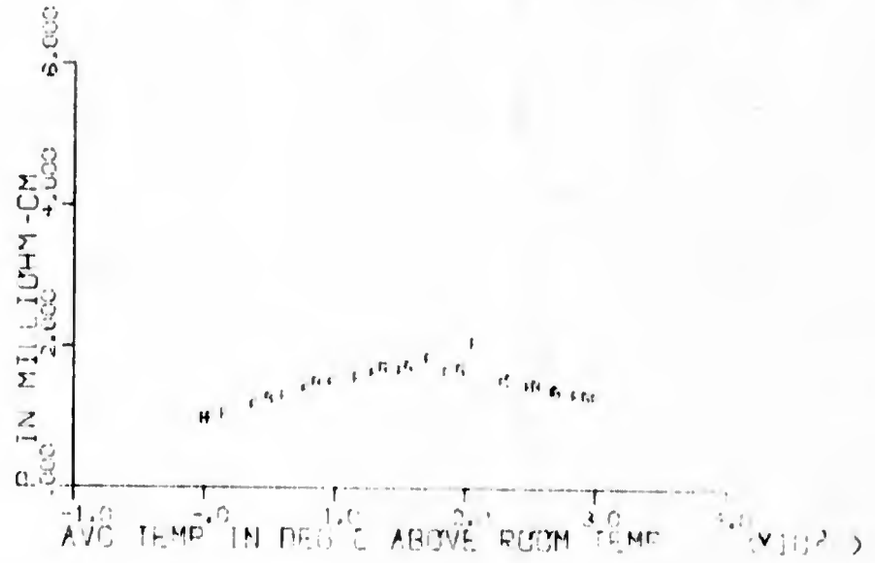

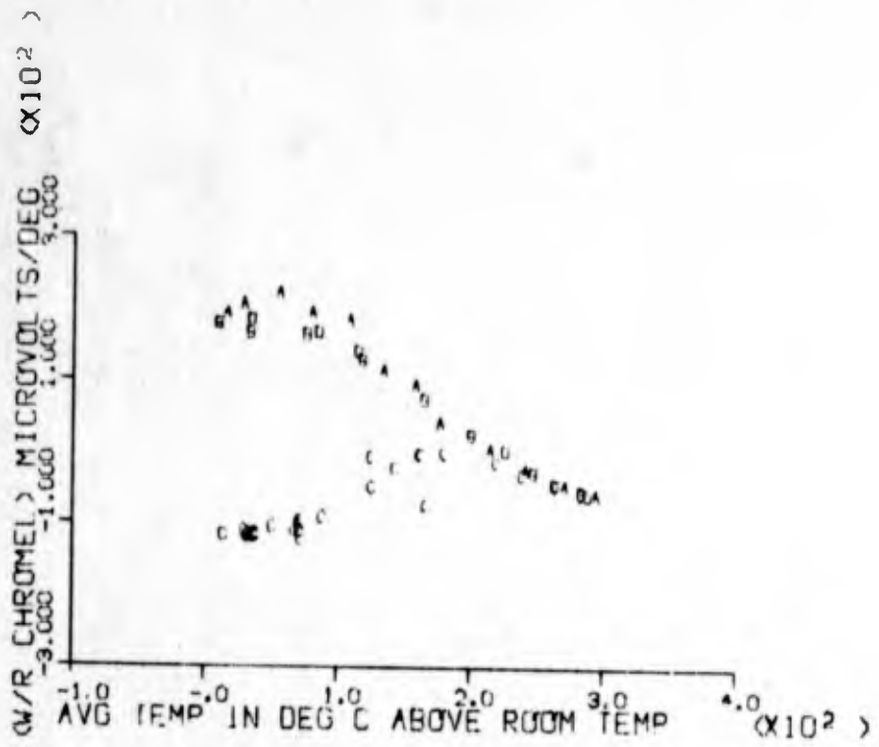

Fig. II/70. Temperature dependence of apparent Seebeck coefficient (with respect to chromel) of sample 254C (Bi_2Te_3), before (A,B) and after (C,D) exposure to 1.6 x 10^{18} fast (E > 1 Mev) neutrons/cm^2. A,C = sample heating; B, D = sample cooling.

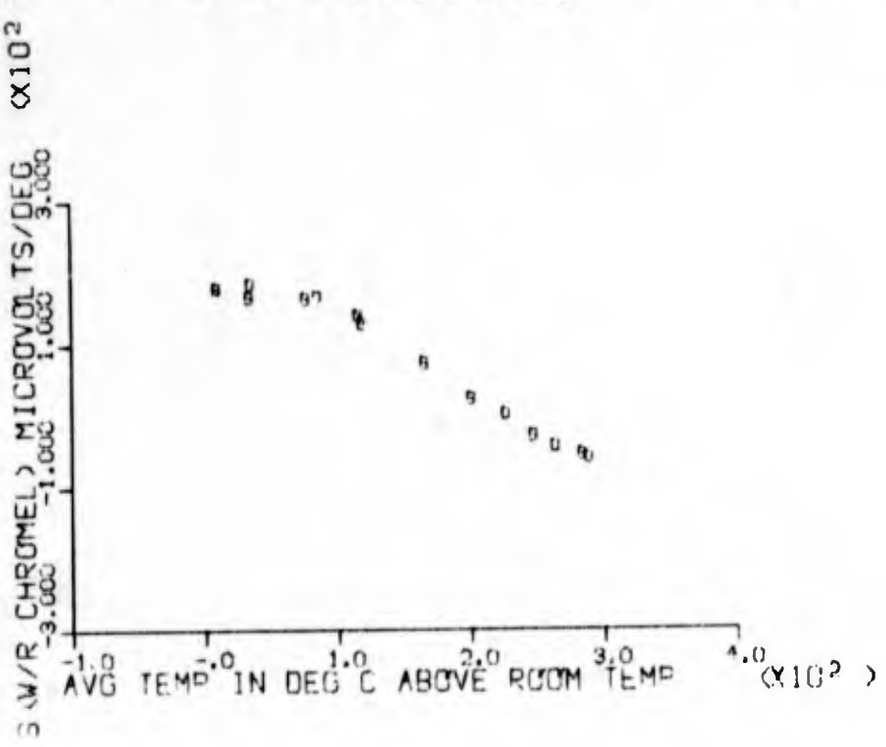

Fig. II/71. Temperature dependence of electrical resistivity of sample 254C (Bi_2Te_3), before (A,B) and after (C,D) exposure to 1.6×10^{18} fast ($E > 1$ Mev) neutrons/cm^2. A, C = sample heating; B, D = sample cooling.

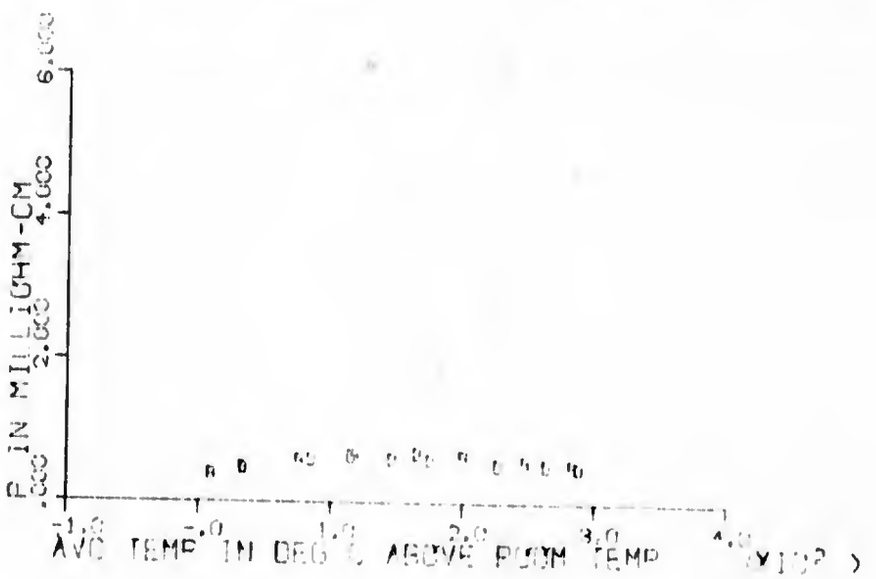

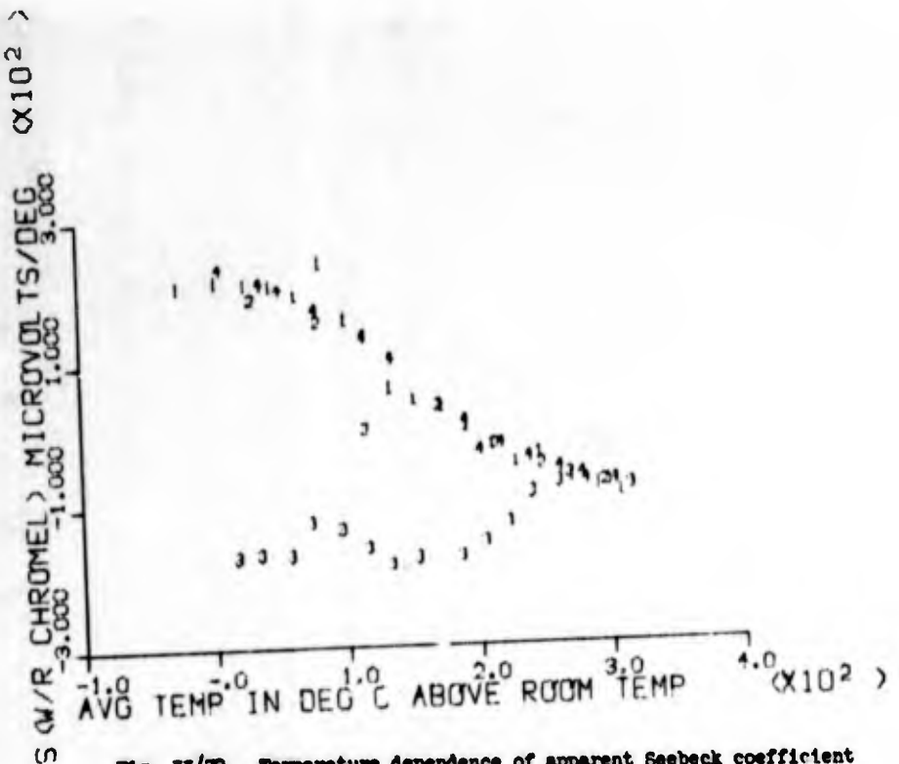

Fig. II/72. Temperature dependence of apparent Seebeck coefficient (with respect to chromel) of sample 254D (Bi_2Te_3), before (1,2) and after (3,4) exposure to 2.3 x 10^{18} fast (E) 1 Mev) neutrons/cm^2. 1, 3 = sample heating; 2, 4 = sample cooling.

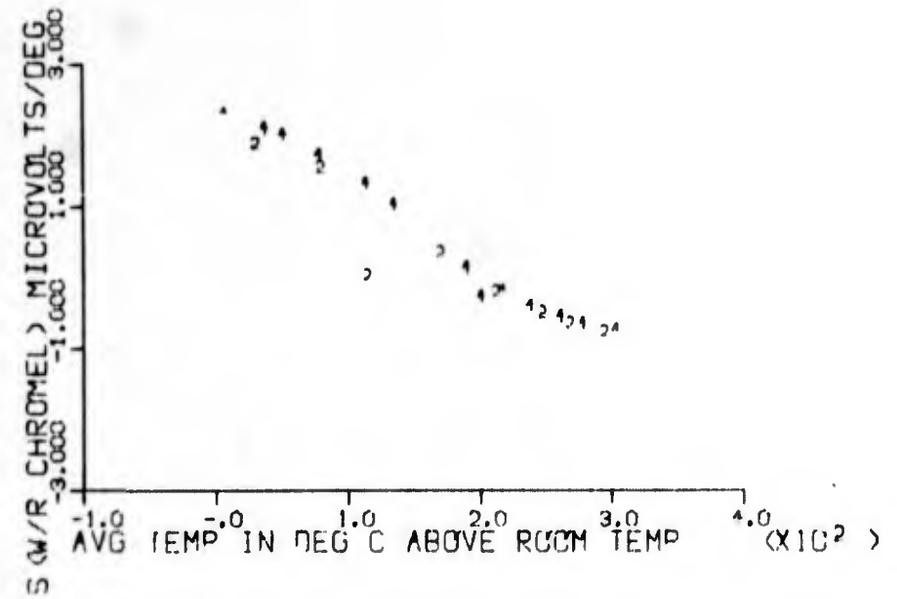

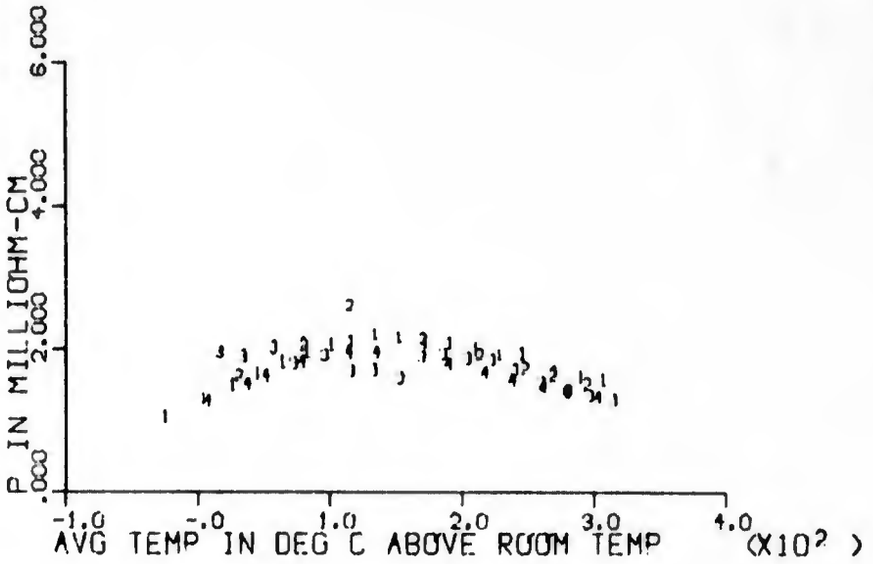

Fig. II/73. Temperature dependence of electrical resistivity of sample 254D (Bi_2Te_4), before (1,2) and after (3,4) exposure to 2.3×10^{19} fast (E > 1 Mev) neutrons/cm². 1, 3 = sample heating; 2,4 = sample cooling.

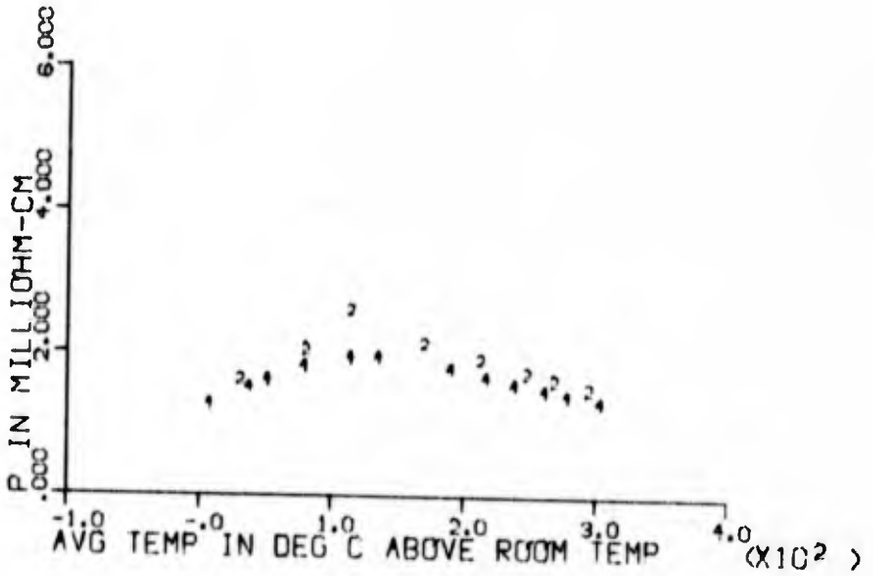

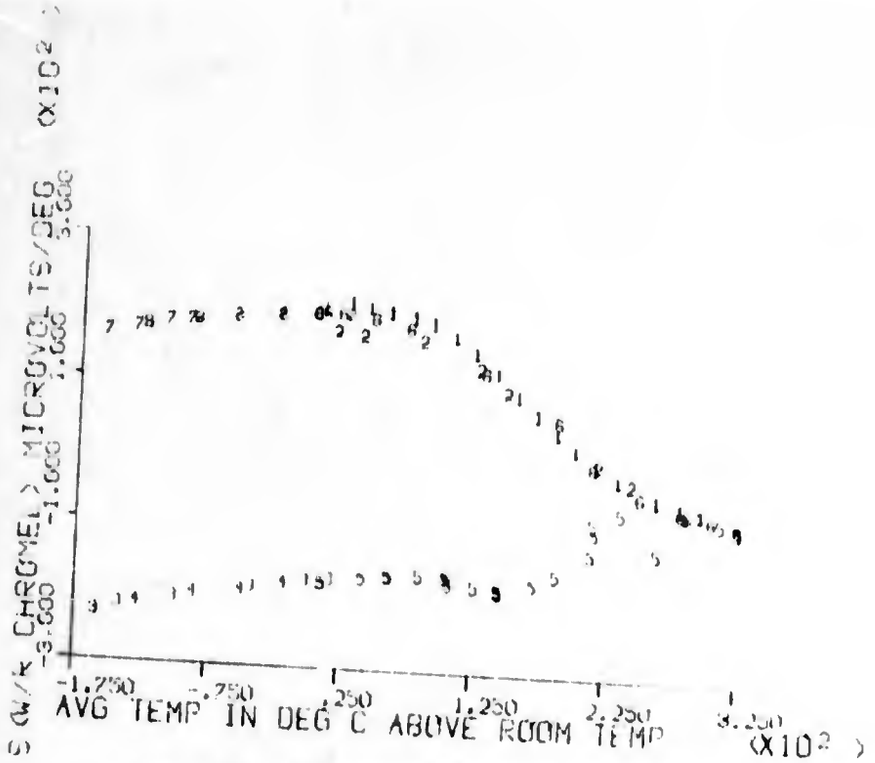

Fig. II/74. Temperature dependence of apparent Seebeck coefficient (with respect to chromel) of sample 254E (Bi_2Te_3), before (1,2) and after (3-8) exposure to 2.3 x 10^{19} fast (E > 1 Mev) neutrons/cm^2. 1, 5 = sample heating through standard temperature range; 2,6 = sample cooling through that range; 3,7 = sample cooling from room temperature to liquid nitrogen region; 4,8 = sample warming through that range.

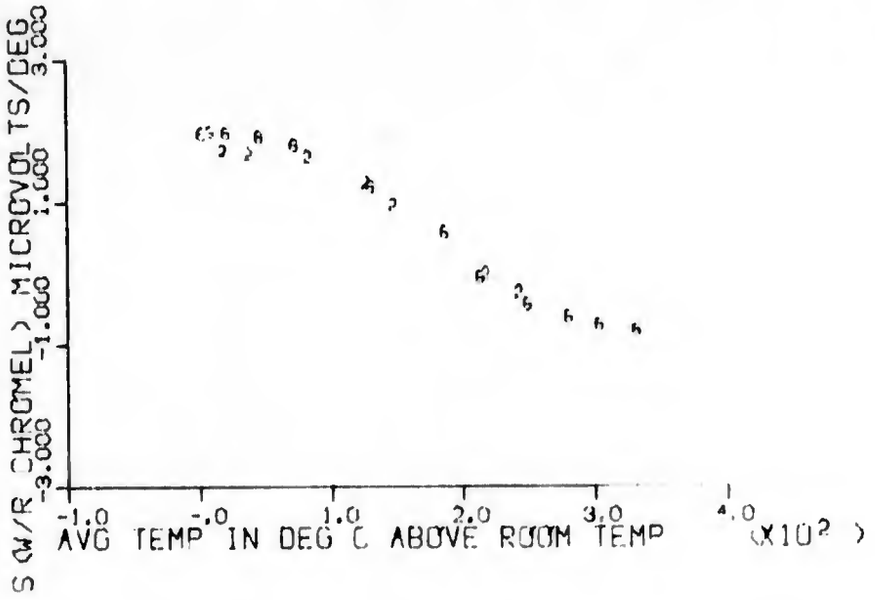

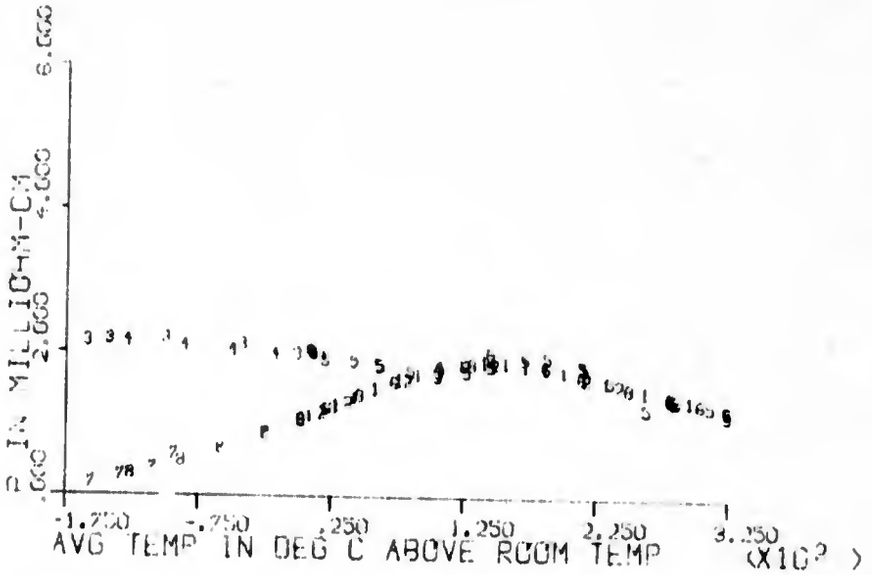

Fig. II/75. Temperature dependence of electrical resistivity of sample 254E (Bi_2Te_3), before (1,2) and after (3-8) exposure to 2.3 x 10^{19} fast (E) 1 Mev) neutrons/cm^2. For key to symbols see caption of Fig. II/74.

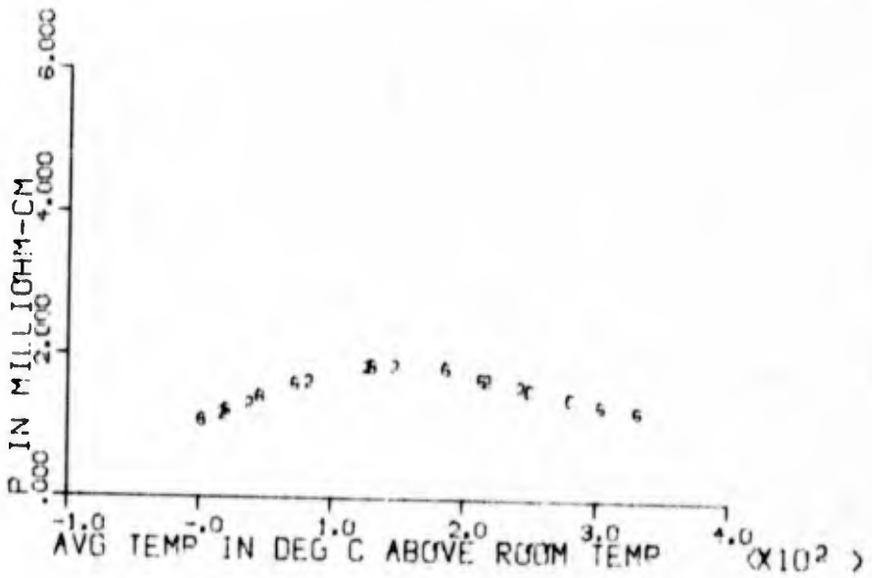

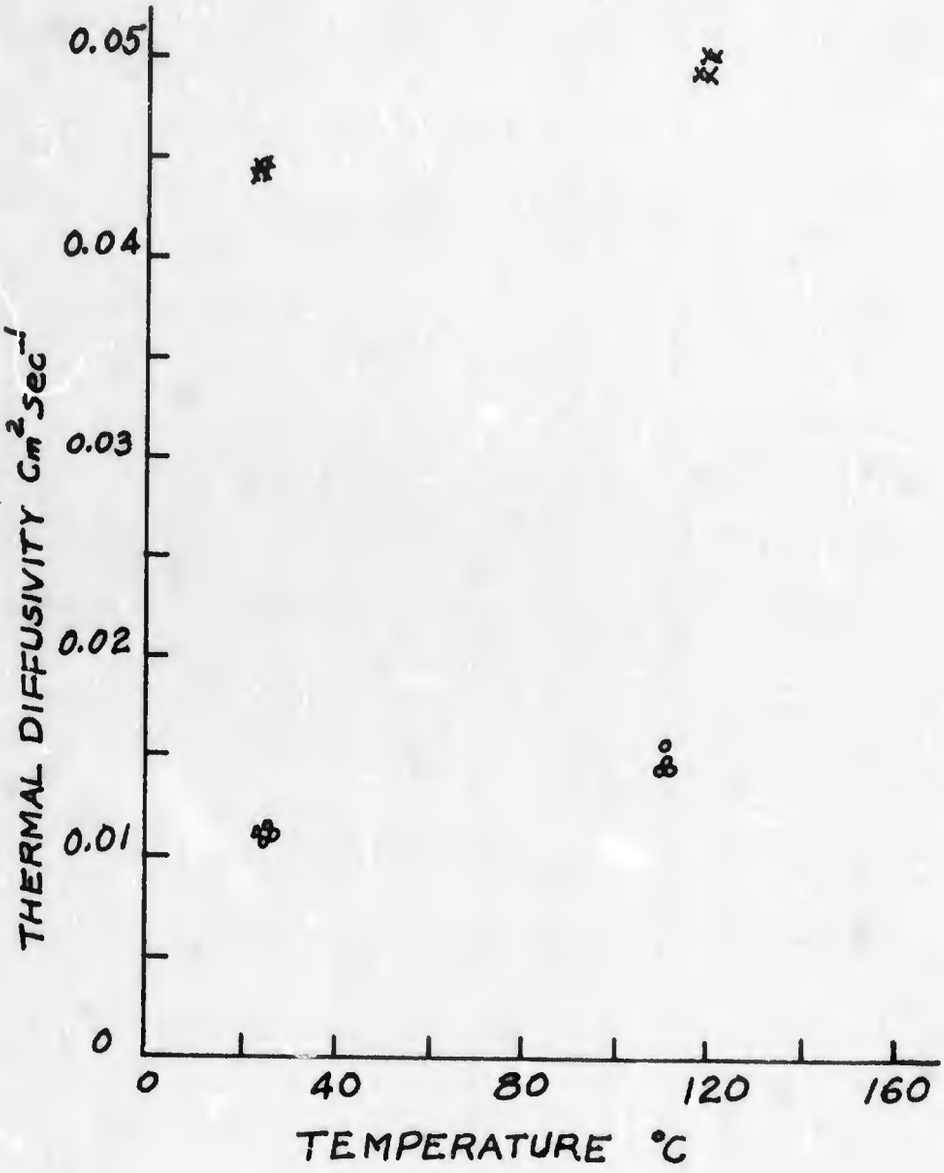

Fig. II/76. Thermal Diffusivity of sample 254 (Bi_2Te_3) at two temperatures, before (O) and after (X) exposure to 2.3 x 10^{19} fast (E 1 Mev) neutrons/cm^2.

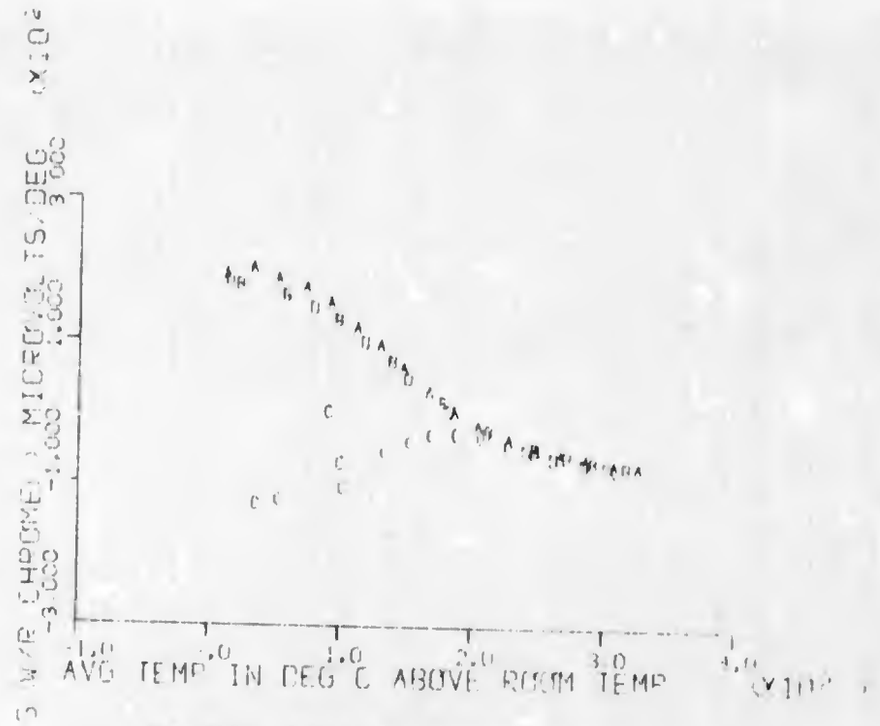

Fig. II/77. Temperature dependence of apparent Seebeck coefficient (with respect to chromel) of sample 255C (single crystal Bi_2Te_3), before (A,B) and after (C,D) exposure to 1.6×10^{18} fast (E > 1 Mev) neutrons/cm^2. 1,3 = sample heating; 2,4 = sample cooling.

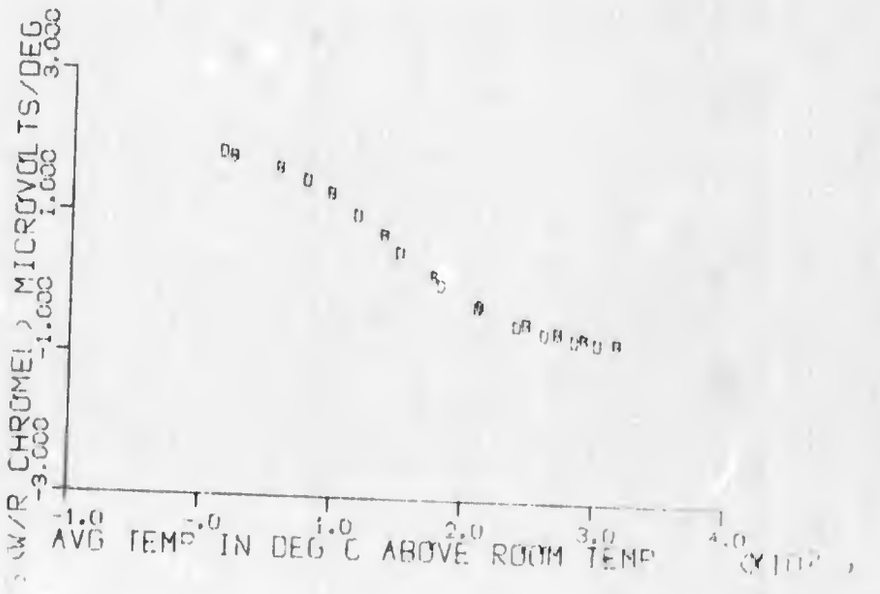

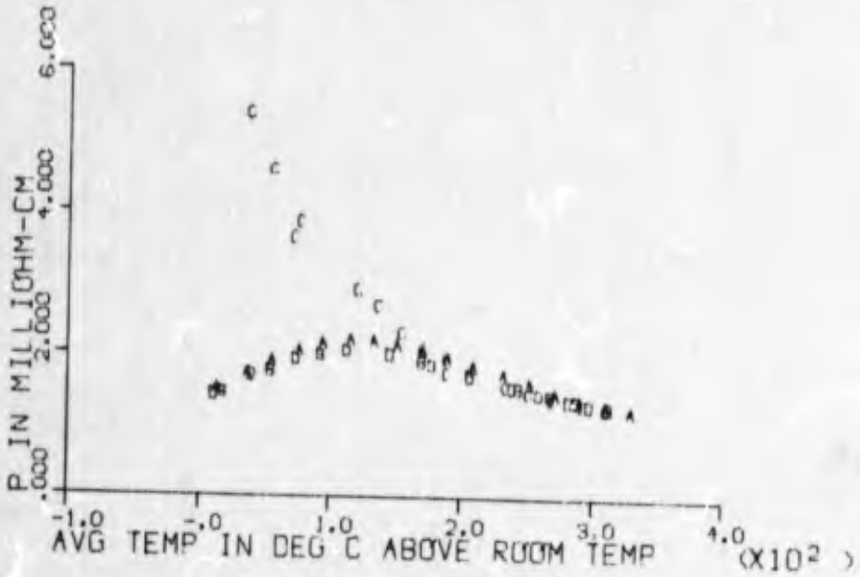

Fig. II/73. Temperature dependence of electrical resistivity of sample 255C (single crystal Bi_2Te_3), before (A,B) and after (C,D) exposure to 1.6×10^{18} fast (E) 1 Mev) neutrons/cm^2. A,C = sample heating; B, D = sample cooling.

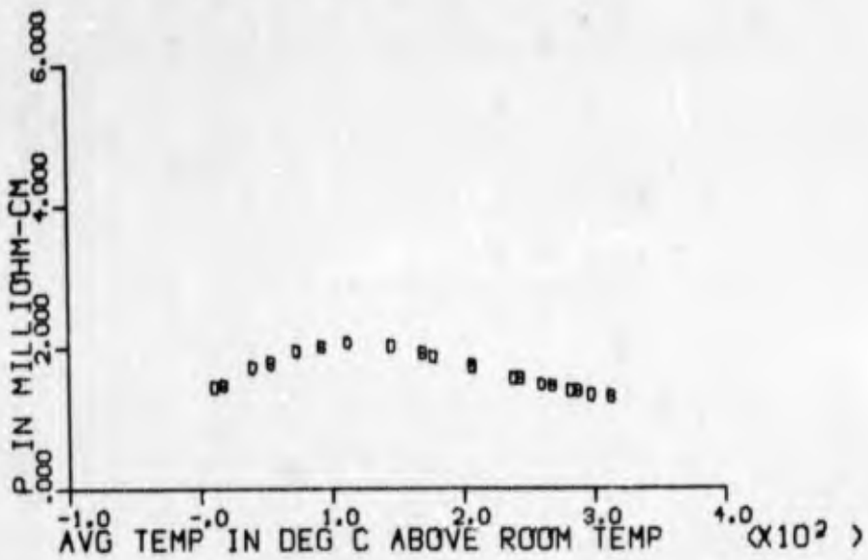

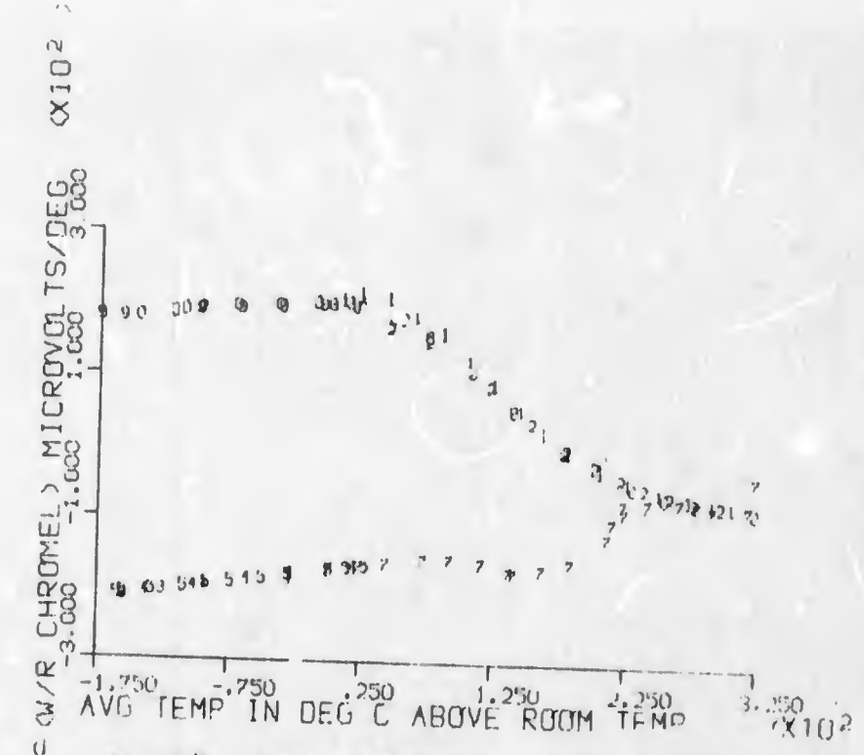

Fig. II/81. Temperature dependence of apparent Seebeck coefficient (with respect to chromel) of sample 255F (single crystal Bi_2Te_3), before (1,2) and after (3-0) exposure to 2.3 x 10^{19} fast (E) 1 Mev) neutrons/cm^2. 1,7 = sample heating through standard temperature range; 2,8 = sample cooling through same range; 3,5,9 = sample cooling from room temperature to liquid nitrogen region; 4,6,0 = sample warming through that range.

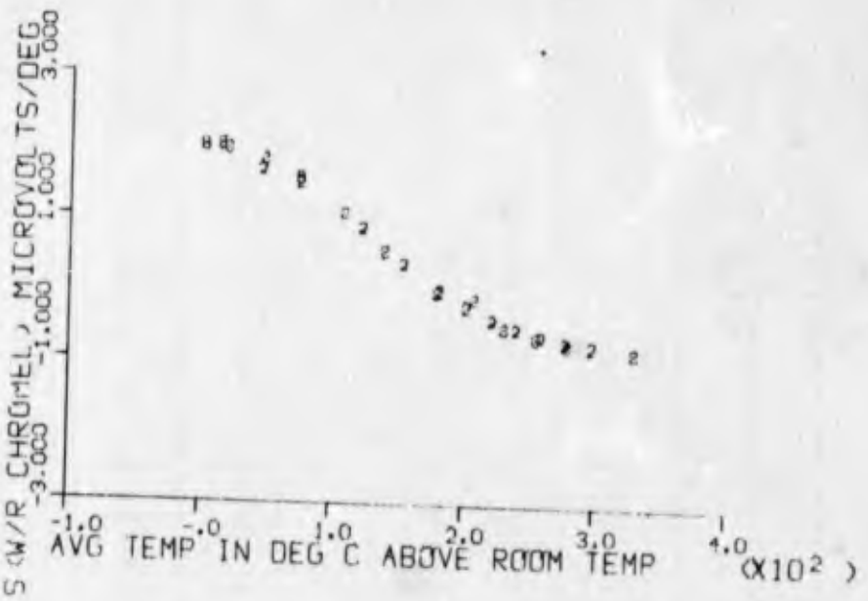

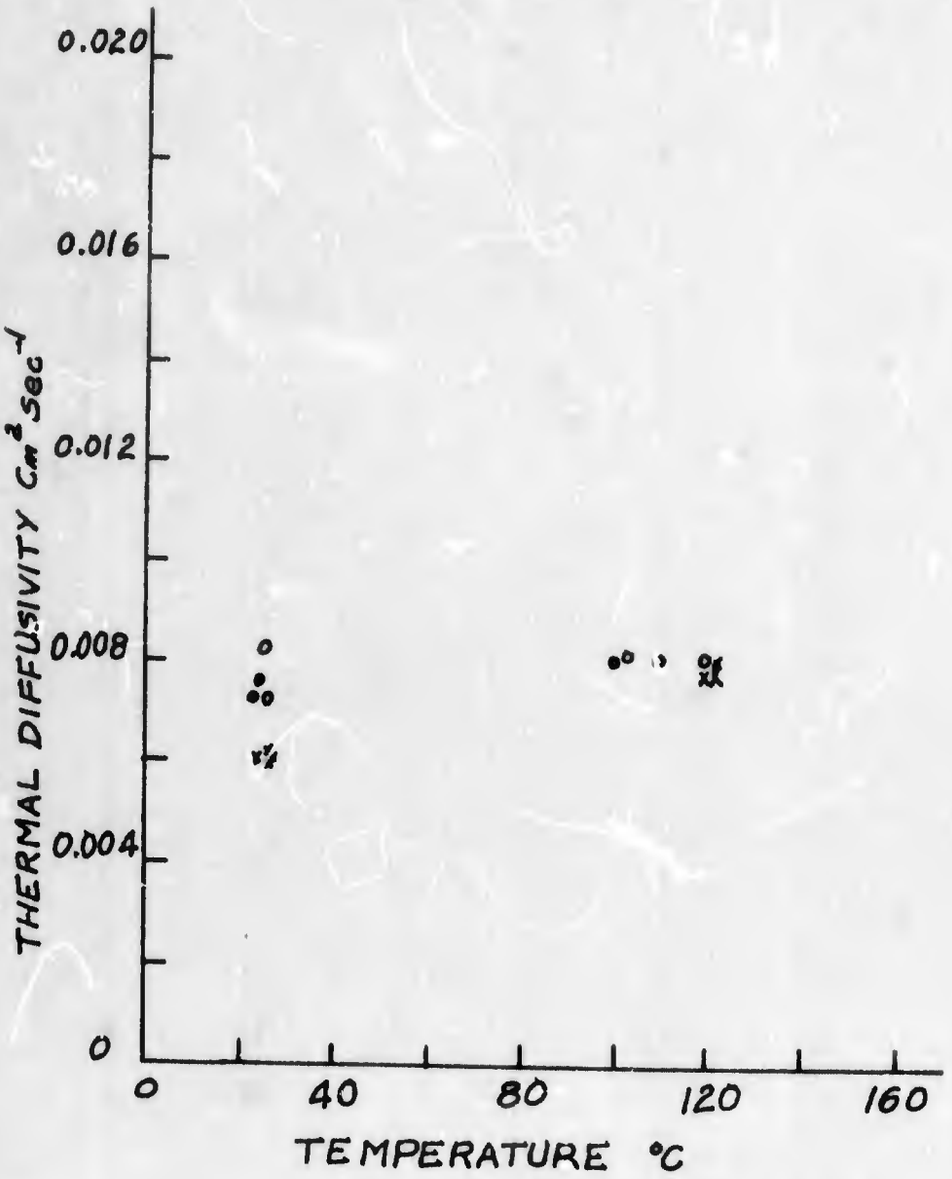

Fig. II/83. Thermal diffusivity of Sample 255 (single crystal Bi_2Te_3), before (0) and after (X) exposure to 2.3×10^{19} fast (E > 1 MeV) neutrons/cm^2.

UNCLASSIFIED

Security Classification

DOCUMENT CONTROL DATA - R & D

(Security classification of title, body of abstract and indexing annotation must be entered when the overall report is classified)

1. ORIGINATING ACTIVITY *(Corporate author)*
U. S. Naval Radiological Defense Laboratory
San Francisco, California 94135

2a. REPORT SECURITY CLASSIFICATION
UNCLASSIFIED

2b. GROUP

3. REPORT TITLE
RADIATION EFFECTS IN THERMOELECTRICS 2. PERMANENT AND QUASI-PERMANENT EFFECTS OF PILE BOMBARDMENT ON SEVERAL COMPOUND SEMICONDUCTORS

4. DESCRIPTIVE NOTES *(Type of report and inclusive dates)*

5. AUTHOR(S) *(First name, middle initial, last name)*
John W. Winslow

6. REPORT DATE	7a. TOTAL NO. OF PAGES	7b. NO. OF REFS
11 September 1967	107	8

8a. CONTRACT OR GRANT NO.	9a. ORIGINATOR'S REPORT NUMBER(S)
b. PROJECT NO.	USNRDL-TR-67-83
c. NSSC, Subproject SR007 1101, Task 10254	9b. OTHER REPORT NO(S) *(Any other numbers that may be assigned this report)*
d.	

10. DISTRIBUTION STATEMENT
This document has been approved for public release and sale; its distribution is unlimited.

11. SUPPLEMENTARY NOTES	12. SPONSORING MILITARY ACTIVITY
	Naval Ship Systems Command Washington, D. C. 20360

13. ABSTRACT

The effects of reactor bombardment on the thermoelectric properties of several compound semiconductors have been observed experimentally for exposure doses up to 2.3×10^{19} fast (E > 1 MeV) neutrons/cm^2. Results are reported for the following materials: PbTe; $Ge_{.95}Bi_{.05}Te$; Ag_2Se; n- and p-types of a Ge-Si alloy whose exact composition is classified; $(GeTe)_{90\%}(AgSbTe_2)_{10\%}$; CoSi; n- and p-types of commercial grade Bi_2Te_3; and single-crystal, stoichiometric Bi_2Te_3. Properties measured were Seebeck coefficient ($\mathcal{S}$), electrical resistivity (ρ), and thermal diffusivity (α). The effects observed ranged from an apparently simple case of change in majority charge carrier concentration due to transmutations, to rather complicated cases in which the behavior of the variables was strongly influenced, both for the better and for the worse, by post-irradiation, thermally activated processes, e.g., annealing. In some cases, no effects at all were found.

Post-annealing values of the radiation-induced changes found in the observed variables were used to calculate the corresponding changes to be expected in the thermoelectric figure of merit (z) of each material, using the relationship

$$Z = \frac{\mathcal{S}^2}{\rho\alpha\, c_p\, \delta} ,$$

where c_p is specific heat and δ is density, under the assumption that the product $c_p \delta$ remained constant. These changes in z ranged from a decrease of about an

(Abstract continued on another page)

DD FORM 1 NOV 65 1473 (PAGE 1)

S/N 0101-807-6801

UNCLASSIFIED

Security Classification

14. KEY WORDS	LINK A		LINK B		LINK C	
	ROLE	WT	ROLE	WT	ROLE	WT
Semiconductors - effects of radiation Thermoelectricity - effects of radiation Thermoelectric materials						

UNCLASSIFIED

Security Classification

DOCUMENT CONTROL DATA · R & D

(Security classification of title, body of abstract and indexing annotation must be entered when the overall report is classified)

1. ORIGINATING ACTIVITY *(Corporate author)*

2a. REPORT SECURITY CLASSIFICATION: UNCLASSIFIED

2b. GROUP

3. REPORT TITLE

RADIATION EFFECTS IN THERMOELECTRICS 2. PERMANENT AND QUASI-PERMANENT EFFECTS OF PILE BOMBARDMENT ON SEVERAL COMPOUND SEMICONDUCTORS

4. DESCRIPTIVE NOTES *(Type of report and inclusive dates)*

5. AUTHOR(S) *(First name, middle initial, last name)*

John W. Winslow

6. REPORT DATE

7a. TOTAL NO. OF PAGES

7b. NO. OF REFS

8a. CONTRACT OR GRANT NO.

b. PROJECT NO.

c.

d.

9a. ORIGINATOR'S REPORT NUMBER(S)

USNRDL-TR-67-83

9b. OTHER REPORT NO(S) *(Any other numbers that may be assigned this report)*

10. DISTRIBUTION STATEMENT

11. SUPPLEMENTARY NOTES

12. SPONSORING MILITARY ACTIVITY

13. ABSTRACT

(Abstract continued from another page)

order of magnitude, to about a four-fold increase in the pre-irradiation value of z.

Some indications that substantial improvements in z for the Ge-Si alloys may be possible through appropriate sequences of irradiation and post-irradiation thermal treatment, were seen. A brief review of the field, aimed at providing suitable background for non-specialist readers, and recommendations for future Navy activity in this technological area, are given.

DD FORM 1 NOV 65 1473 (PAGE 1)

S/N 0101-807-6801

UNCLASSIFIED

Security Classification